Non-equilibrium quantum field dynamics in the early Universe

by

Magdalena Eriksson

Thesis submitted in fulfilment of
the requirements for the degree of
PHILOSOPHIAE DOCTOR
(PhD)

University
of Stavanger

Faculty of Science and Technology
Department of Mathematics and Physics
2023

Acknowledgements

Table of Contents

1   Introduction

Inflation is the leading paradigm of early Universe cosmology. It provides compelling explanations of the observed near-homogeneity of the cosmic microwave background (CMB) radiation, the spatial flatness of the Universe and the generation of primordial density perturbations. The observed properties of the CMB, such as its isotropy, Gaussian distribution and specific temperature fluctuations, are in remarkable agreement with the predictions of inflationary models. The anisotropies in the CMB can be explained by vacuum fluctuations of light quantum fields during inflation. The spacetime expansion leads to an amplification of these quantum field fluctuations which seed classical matter density perturbations. The imprints of these perturbations are observed in the CMB and give rise to the formation of the large-scale distribution of matter in the Universe at later times.

The study of quantum fields on expanding spacetimes is a way of exploring the fundamental principles underlying inflationary cosmology. The inclusion of quantum effects modify the quantitative predictions of classical inflationary models, and investigating these corrections contributes to verifying the internal consistency and validity of various inflationary scenarios. Inflation sets the initial conditions for reheating [1, 2] and the subsequent cosmic evolution. The effective inflationary dynamics also influence symmetry-breaking processes during and after the inflationary phase. Future precision measurements of the CMB may in addition have the potential to reveal new physics beyond the Standard Model, which could be indicated by quantum corrections in inflationary models. The effect of quantum corrections on the inflationary evolution is one of the topics of investigation considered in this thesis.

The inflationary amplification of quantum modes give rise to non-perturbative phenomena. This is indicated for instance by the appearance of infrared and time-dependent (secular) divergences in quantum loop corrections to inflationary field dynamics. Secular divergences are general artefacts of usual perturbation theory applied to non-stationary, or

non-equilibrium, quantum field theory. This is due to time-translation non-invariance and the general lack of an obvious (small) expansion parameter in evolving systems, which apart from secular divergences also result in pinch singularities in certain correlation functions [3, 4]. As a consequence, in the sense of resumming perturbation theory, non-equilibrium processes are inherently non-perturbative.

A comprehensive understanding of non-equilibrium phenomena therefore necessitates the use of non-perturbative methods. Examples of such methods include resummation schemes based on Schwinger-Dyson equations [5–9], the large-N expansion [10] and non-perturbative renormalisation group techniques [11–17]. A more first-principles non-perturbative approach is lattice field theory. In thermal (equilibrium) field theory, non-perturbative physics can be captured by means of numerical Monte-Carlo integration of the path integral on a discretised Euclidean spacetime lattice. However, in the presence of a chemical potential or out of thermal equilibrium, the emergence of the sign problem [18] hinders the use of this approach. In the regime of large particle numbers, quantum dynamics can be approximated by its corresponding classical evolution equations. Classical-statistical simulations can accurately capture non-perturbative effects when statistical fluctuations dominate over quantum fluctuations. However, the presence of Reyleigh-Jeans divergences at high momenta restrict the momentum range applicable to the classical-statistical approximation. For this reason it should be viewed as an effective theory for highly-occupied, low-momentum modes.

Apart from inflation, resummed non-equilibrium field theory is an important tool for accurate descriptions of other early Universe phenomena, such as reheating, cosmological phase transitions, the generation of baryon assymmetry and dark matter production. See e.g. [19–23] for reviews. The same framework can also be used to capture non-perturbative effects in relativistic heavy-ion collisions [24–28] and the dynamics of Bose-Einstein condensates in condensed matter systems [29–31].

A well-established resummation scheme is based on the two-particle-irreducible (2PI) effective action [32–35]. The 2PI formalism has demonstrated great efficacy in exploring non-perturbative phenomena within

scalar and fermionic theories, but its application to gauge theories has been delayed due to the additional complexities that gauge symmetry presents, which poses challenges for its implementation. A central problem is that 2PI approximations are parametrically gauge-fixing dependent [36, 37] and it is unclear if or how gauge-invariant observable quantities can be constructed within a given truncation. The issue of gauge non-invariance in 2PI truncations is another subject of exploration in this work.

The resummation schemes mentioned above have also been applied to expanding spacetimes and reveal the generation of a non-perturbative effective mass proportional to the expansion rate which regulates infrared divergences. In the context of inflation, a popular alternative to the well-established resummation schemes is the stochastic inflation formalism [38, 39]. It is an effective theory for the long-wavelength modes of quantum fields that is based on modelling the influence of the short-wavelength modes as a stochastic noise. Interestingly, the stochastic inflation approach gives the same result for the effective mass as the resummation approaches. The stochastic formalism was originally derived as an approximation at the level of equations of motion for a light scalar field in (semi-)de Sitter spacetime, but its embedding in a first-principles quantum field theory remains only partly understood. For this reason it is not clear how it compares with the more theoretically rigorous resummation schemes. The region of validity of the stochastic inflation formalism is a third topic of investigation in the present work.

The goal of this thesis is to contribute to our understanding of quantum effective dynamics during inflation and the 2PI description for gauge theories far from equilibrium. The thesis is organised as follows. This introduction is followed by a review of inflationary cosmology with special emphasis on vacuum fluctuations in chapter 2. After this we present in chapter 3 an overview of the formulation of non-equilibrium quantum field theory in curved spacetime and discuss renormalisation. Chapter 4 contains an introduction of the 2PI formalism and the issues surrounding its formulation for gauge theories. In chapter 5 we investigate the influence of quantum field fluctuations, including also fluctuations of metric

degrees of freedom, on single-field inflationary dynamics. The quantum field-theoretical foundations of the stochastic inflation formalism are revisited in chapter 6 where we analyse the region of validity of this approach by investigating its parameter dependencies. In chapter 7 we formulate a two-loop truncation of the 2PI formulation of SU(2)-Higgs theory and set out to study its residual gauge dependence by performing comparisons with the classical-statistical approximation within its region of validity. Conclusions and future research directions are discussed in the final chapter 8 of this thesis.

Notation and conventions. Throughout this thesis we will use natural units, $c = \hbar = 1$, unless otherwise stated. The metric is $(3 + 1)$-dimensional with mostly positive signature $(-+++)$, and the spacetime indices are labelled by Greek letters $\mu, \nu, \ldots = 0, 1, 2, 3$. Latin letters $i, j, \ldots = 1, 2, 3$ label spatial indices and $a, b = 1, \ldots, N^2 - 1$ denote the different components of fields transforming under the adjoint representation of the SU(N) gauge group. Spacetime integrals are often abbreviated as $\int_x := \int \mathrm{d}^4 x \sqrt{-g}$.

4

2 Quantum fluctuations during inflation

Inflation was introduced as a complement to standard Big Bang cosmology as to provide an explanation for the observed near-homogeneity of the CMB and spatial flatness of the Universe. As a bonus it also provided an explanation of the origin of the small anisotropies in the CMB. The inflationary expansion of the Universe excited quantum fields and redshifted the wavelengths of the excitations from quantum to cosmological scales. On large scales these vacuum fluctuations became classical and induced perturbations in the energy density. Some time after inflation ended, these perturbations re-entered the observable Universe and were communicated to the primordial plasma, eventually giving rise to the temperature anisotropies in the CMB and the formation of large-scale structure.

Exhaustive reviews of inflation and the dynamics of cosmological perturbations can be found in e.g. [40–46]. In this chapter we will briefly introduce the calculational tool of cosmological perturbation theory and relevant concepts needed to study quantum corrections and large-scale inflationary dynamics in later chapters.

2.1 The expanding universe

Observations reveal that on large scales, above around 500 Mpc, the Universe appears homogeneous and isotropic. The cosmological principle postulates the Universe to be maximally symmetric, in which case it can be modelled with a flat Friedmann-Robertson-Walker (FRW) metric, with line element

$$\mathrm{d}s^2 := g_{\mu\nu}\mathrm{d}x^\mu\mathrm{d}x^\nu = -\mathrm{d}t^2 + a^2(t)\mathrm{d}\mathbf{x}^2, \tag{2.1}$$

for which the scale factor $a(t)$ evolves according to the Friedmann equations

$$H^2 = \frac{1}{3M_{\mathrm{Pl}}^2}\rho, \qquad \frac{\ddot{a}}{a} = -\frac{1}{6M_{\mathrm{Pl}}^2}(\rho + 3p). \tag{2.2}$$

Here $H := \dot{a}/a$ is the Hubble rate, which current value is given by $H_0 = 100h\,\mathrm{km\,s^{-1}\,Mpc^{-1}}$ with $h \approx 0.67 \pm 0.01$ [47]. The reduced Plank

5

mass is $M_{\text{Pl}} = (8\pi G)^{-1/2} \simeq 2.4 \times 10^{18}$ GeV. The energy density ρ and pressure p are the temporal and spatial components of the comoving energy-momentum tensor

$$T^{\mu\nu} = \text{diag}(\rho, p, p, p), \tag{2.3}$$

respectively. The Friedmann equations can be combined to recover the continuity equation

$$\dot{\rho} + 3H(\rho + p) = 0. \tag{2.4}$$

The energy density and pressure are both scalar functions of time and satisfy the equation of state

$$p(t) = \omega(t)\rho(t). \tag{2.5}$$

For $\omega = $ const, the continuity equation (2.4) can be solved as

$$\rho \propto a^{-3(1+\omega)}, \tag{2.6}$$

assuming $\omega \neq -1$. The dilution laws for radiation- and matter-dominated fluids are

$$
\begin{aligned}
\rho_{\text{rad}} \propto a^{-4} &\quad \Rightarrow \quad a(t) \propto t^{1/2}, \quad \omega = 1/3, \\
\rho_{\text{mat}} \propto a^{-3} &\quad \Rightarrow \quad a(t) \propto t^{2/3}, \quad \omega = 0,
\end{aligned}
\tag{2.7}
$$

which tell us how the energy densities for radiation and matter sources decrease with the growing scale factor.

2.1.1 Causality

As we seek an explanation of the observed homogeneity and isotropy of the Universe, we must first postulate a requirement for two points in space to be causally connected. This requirement is taken to be that a photon must be able to travel between them in a time less than the present age of the Universe. Points that are further apart than this are said to be causally disconnected. The boundary between causally connected and disconnected points is referred to as the particle horizon.

The current distance to the particle horizon is therefore the distance travelled by a photon over the course of the present age of the Universe.

This distance can be computed using the metric (2.1), and the fact that photons travel on the null geodesic $ds^2 = 0$, to

$$d_{\text{ph}}(t_0) = a(t_0) \int_0^{t_0} \frac{dt}{a(t)}, \tag{2.8}$$

where the initial time $t_i = 0$ denotes the origin of the Universe, or the Big Bang[1], and t_0 is the present age of the Universe.

Similarly, the comoving particle horizon $\Delta\tau_{\text{ph}}$ is the maximum distance that light can propagate between an initial time t_i and later time t,

$$\Delta\tau_{\text{ph}} := \int_{t_i}^t \frac{dt'}{a(t')} = \int_{\ln a_i}^{\ln a} (aH)^{-1} d\ln a. \tag{2.9}$$

The quantity $(aH)^{-1}$ is the comoving Hubble radius and corresponds to the distance a photon can travel during one expansion time $t_H = H^{-1} = dt/d\ln a$. It is therefore an instantaneous measure of causality between two particles within the next Hubble time.

A Universe modelled as a fluid with constant equation of state $\omega := p/\rho$ has comoving Hubble radius

$$(aH)^{-1} = H_0^{-1} a^{\frac{1}{2}(1+3\omega)}. \tag{2.10}$$

With the exception of dark energy, all known radiation and matter sources fulfil the strong energy condition (SEC) $1 + 3\omega > 0$, and so in a Universe dominated by these sources, the comoving Hubble radius is assumed to increase as the Universe expands. In this case the particle horizon is dominated by the present value of the comoving Hubble horizon, since for $a_i \to 0$ with $\omega > -1/3$, we have from (2.9),

$$\Delta\tau_{\text{ph}} = \frac{2H_0^{-1}}{1+3\omega} \left(a^{\frac{1}{2}(1+3\omega)} - a_i^{\frac{1}{2}(1+3\omega)} \right) \to \frac{2}{1+3\omega}(aH)^{-1}. \tag{2.11}$$

Around 380 000 years after the Big Bang, the Universe had cooled enough to allow for hydrogen to form and for photons to decouple from the primordial plasma. This event is known as recombination and the released radiation as the cosmic microwave background (CMB). The

---

[1]What is referred to as the Big Bang singularity is a moment in time, not a spatial point.
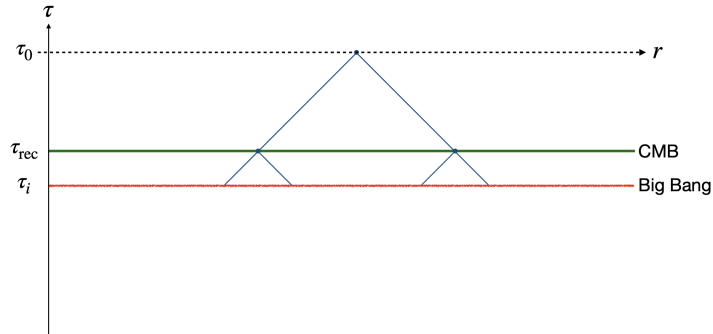
Figure 2.1: Conformal diagram illustrating the horizon problem in Big Bang cosmology. An observer at conformal time τ_0 observes two regions in the CMB which past light cones do not overlap at the time of the Big Bang singularity. The length scale r is measured in comoving coordinates.

CMB is almost perfectly isotropic, the temperature anisotropies of which are smaller than 10^{-5} compared to the average temperature. The fact that the time elapsed between the Big Bang and recombination is finite, $t_{\text{rec}} - t_i < \infty$, implies that the majority of the CMB anisotropies can not have overlapping past light cones, i.e. they could never have been in causal contact. See figure 2.1. The inability of the Big Bang model to explain the (near-)isotropy of the CMB is known as the horizon problem.

2.1.2 A decreasing Hubble sphere

The horizon problem can be said to be due to the growing Hubble horizon during Big Bang expansion. A straightforward solution is therefore to conjecture a phase of decreasing Hubble radius,

$$\frac{\mathrm{d}}{\mathrm{d}t}(aH)^{-1} < 0, \tag{2.12}$$

sometime in the early Universe. If this phase, known as inflation, lasts long enough for all energy sources to establish causal contact, the horizon problem can be resolved. Note that the degree(s) of freedom responsible for a decreasing Hubble sphere violates the SEC for a perfect fluid.

For a decreasing Hubble radius, the comoving particle horizon is instead dominated by the early time contribution in (2.11), since in this
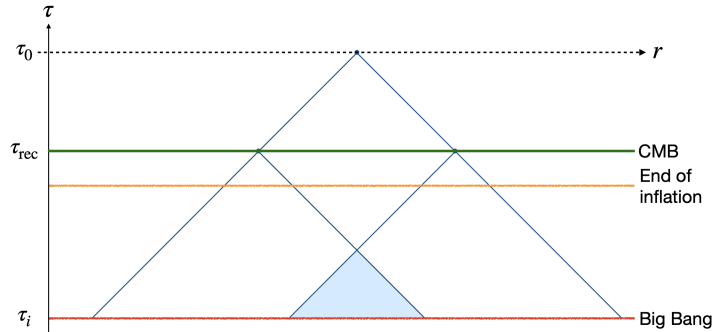
Figure 2.2: Conformal diagram illustrating how inflation resolves the horizon problem in Big Bang cosmology. A decreasing Hubble radius lead to an increased time interval between the Big Bang singularity and recombination. A sufficiently long period of inflation can ensure causal contact (shaded) between all points in the CMB at some point in the past.

case the Big Bang singularity goes to negative infinity as $a_i \to 0$ with $\omega < -1/3$,

$$\tau_i = \frac{2H_0^{-1}}{1 + 3\omega} a_i^{\frac{1}{2}(1+3\omega)} \to -\infty. \qquad (2.13)$$

This can be interpreted as a large increase in the time interval between the initial time and recombination. With this increase in elapsed time, also the most widely separated points in the CMB would have had time to establish causal contact. See figure 2.2. In inflationary cosmology it is common to define the initial time $t_i = 0$ to be the start of the era of Big Bang expansion, where $\omega > -1/3$, which follows an earlier inflationary era with $t_i < 0$ and $\omega < -1/3$.

Note that during Big Bang expansion, the particle horizon and Hubble radius are proportional, while inflation is constructed to realise the condition $\Delta\tau_{\mathrm{ph}} \gg (aH)^{-1}$.[2] Two particles that were in causal contact at the start of inflation will after some cease to be so when the distance d between them exceeds the comoving Hubble radius, i.e. $d > (aH)^{-1}$.

During inflation, spacetime expands faster than light can travel, which means that the Universe becomes larger than the particle horizon. As

---

[2]It is an unfortunate convention in the inflationary literature to refer to both the (comoving) particle horizon $\Delta\tau_{\mathrm{ph}}$ and the Hubble radius $(aH)^{-1}$ as simply "the horizon".

a consequence, there are past events that are unobservable to us in the present day. Analogously, there may be future event that will never be observable to us, or distant regions that we will never be able to influence. The maximum distance from which an observer in the future will receive signals emitted at some time t is

$$\Delta\tau_{\text{eh}} = \int_t^{t_f} \frac{\text{d}t'}{a(t')},$$

(2.14)

where t_f is a "final" moment of time, which may be finite or infinite. The time interval $\Delta\tau_{\text{eh}}$ is known as the (comoving) event horizon, and two points separated by $\Delta\tau > \Delta\tau_{\text{eh}}$ will never be perceived by one another.

2.1.3 Duration of inflation

To estimate how much inflation is needed to explain the uniformity of the largest observed scales in the CMB, we require that the present-day ($t = t_0$) observable Universe fitted inside the comoving Hubble radius at the start of inflation t_{s},

$$(a_0 H_0)^{-1} < (a_{\text{s}} H_{\text{s}})^{-1}.$$

(2.15)

If we for simplicity neglect the (relatively recent) matter- and dark energy-dominated eras, and assume that the Universe has been completely radiation dominated since the end of inflation t_{e}, then $H \propto a^{-2}$ and

$$\frac{a_0 H_0}{a_{\text{e}} H_{\text{e}}} \propto \frac{a_0}{a_{\text{e}}} \left(\frac{a_{\text{e}}}{a_0}\right)^2 = \frac{a_{\text{e}}}{a_0} \sim \frac{T_0}{T_{\text{e}}},$$

(2.16)

where T_{e} was the temperature at the end of inflation and the current temperature of the Universe is $T_0 \sim 2.7\,\text{K} \sim 10^{-3}\,\text{eV}$. At the end of inflation, it is commonly believed that the expansion left the Universe devoid of particles, such that $T = 0$.[3] The initiation of the reheating stage took place as the inflaton field, i.e. the field which held the dominant energy-density during inflation, started to transfer its energy to other particles through their interactions. The scatterings among these excited particles in turn eventually led to the thermalisation of the Universe to

---

[3]Alternative models include warm inflation scenarios [48–50].

some reheating temperature T_{rh}. The energy scale during inflation is often assumed to have been that of Grand Unified Theories (GUTs) at 10^{15} GeV, but the reheating temperature was likely less than this. Estimates of the reheating temperature depends on the details of the inflationary scenario at hand but most models not ruled out by data from the Planck mission [47] predict $T_{rh} \simeq 10^9 - 10^{10}$ GeV. Taking $T_e = T_{rh} = 10^9$ GeV, the condition (2.15) then says that $(a_s H_s)^{-1} > 10^{21}(a_e H_e)^{-1}$, i.e. that the comoving Hubble radius must have shrunk by a factor of 10^{21} during inflation.

The requirement (2.15) can be formulated in terms of a necessary duration of inflation. If the inflationary expansion rate is assumed to have been approximately constant, $H_s \sim H_e$, then

$$\frac{a_e}{a_s} > 10^{21} \quad \Leftrightarrow \quad \ln\left(\frac{a_e}{a_s}\right) > 48. \tag{2.17}$$

If we instead use the GUT scale as an upper estimate of T_e, the condition (2.17) gets modified to $a_e/a_s > 10^{27}$ for which $\ln(a_e/a_s) > 62$. Estimates from the Planck mission favours values between 50 and 60 e-folds [47]. Note that these values are estimates of the minimum duration of inflation necessary to account for the observed homogeneity of the CMB at its largest scales. However, at present the total duration of inflation remains unknown.

We have seen that the condition for inflation is that the comoving Hubble horizon is shrinking, i.e. (2.12). This requirement can be rewritten as

$$\frac{\mathrm{d}}{\mathrm{d}t}(aH)^{-1} \equiv -\frac{1}{a}\left(1 + \frac{\dot{H}}{H^2}\right) \equiv -\frac{\ddot{a}}{(aH)^2} < 0, \tag{2.18}$$

such that an equivalent condition is an accelerated expansion $\ddot{a} > 0$ or the smallness of the slow-roll parameter

$$\epsilon_H := -\frac{\dot{H}}{H^2} < 1. \tag{2.19}$$

In the case of $\epsilon_H = 0$, the scale factor is $a(t) = e^{Ht}$ with $H = $ const. This choice corresponds to a de Sitter spacetime. However, since inflation did not proceed indefinitely, $\epsilon_H \neq 0$ in general.

The requirement of a sufficiently long epoch of inflation can be formulated in terms of the number of e-folds as

$$N := \int_{a_\mathrm{s}}^{a_\mathrm{e}} \mathrm{d} \ln a = \int_{t_\mathrm{s}}^{t_\mathrm{e}} H(t) \mathrm{d} t, \tag{2.20}$$

so that the condition for inflation (2.19) can be written

$$\epsilon_H = -\frac{\mathrm{d} \ln H}{\mathrm{d} N} < 1. \tag{2.21}$$

This condition signifies that the fractional change of the Hubble radius per e-fold is small. The requirement that this condition for inflation persists for sufficiently long can be stated in terms of a second parameter

$$\eta_H := \frac{\mathrm{d} \ln \epsilon_H}{\mathrm{d} N} = \frac{\dot{\epsilon}_H}{H \epsilon_H}, \tag{2.22}$$

which states that for $|\eta_H| < 1$, the change of ϵ_H per Hubble time is small. A sustained period of inflation then corresponds to $\epsilon_H, |\eta_H| < 1$.

2.2 Scalar inflation and the slow-roll formalism

In its simplest realisation, inflation can be modelled with a single scalar field evolving in a potential $V(\phi)$,

$$\mathcal{L} = \tfrac{1}{2} M_\mathrm{Pl}^2 R + \tfrac{1}{2} \partial_\mu \phi \partial^\mu \phi - V(\phi), \tag{2.23}$$

where R is the Ricci curvature scalar. The energy and pressure densities are given by the diagonal components of the energy-momentum tensor, $T_{\mu\nu} = \partial_\mu \phi \partial_\nu \phi + g_{\mu\nu} \mathcal{L}$, as

$$\begin{aligned}
\rho &:= T_{00} = \frac{1}{2} \dot{\phi}^2 + V(\phi) + \frac{(\nabla \phi)^2}{2a^2}, \\
p &:= \frac{1}{3} T^i{}_i = \frac{1}{2} \dot{\phi}^2 - V(\phi) - \frac{(\nabla \phi)^2}{6a^2}.
\end{aligned} \tag{2.24}$$

As the large-scale Universe appears isotropic, the gradient terms in (2.24) are usually neglected. The inflaton field then evolves according to its equation of motion

$$\ddot{\phi} + 3H \dot{\phi} + V_{,\phi}(\phi) = 0, \tag{2.25}$$

along with the Friedmann equations

$$3H^2 = \frac{1}{M_{\mathrm{Pl}}^2}\left[\tfrac{1}{2}\dot\phi^2 + V(\phi)\right],$$

$$2\dot H + 3H^2 = -\frac{1}{M_{\mathrm{Pl}}^2}\left[\tfrac{1}{2}\dot\phi^2 - V(\phi)\right].$$

(2.26)

The inflaton field is assumed to be a (classical) background field in the evolution equations (2.26). The second Friedmann equation can be formulated using the first one as

$$\dot H = -\frac{1}{2M_{\mathrm{Pl}}^2}\dot\phi^2,$$

(2.27)

which makes no reference to the classical potential $V(\phi)$.

2.2.1 The slowly evolving inflaton

The slow-roll approximation amounts to assuming the potential energy to dominate over the kinetic, in which case $\omega \to -1$ so that the condition for inflation to hold is readily fulfilled. For inflation to be sustained for a long enough period of time, the acceleration term should be smaller than the friction and potential terms in the evolution equations. This constraint is usually quantified by the second slow-roll parameter η_H, which in terms of the inflaton field reads

$$\eta_H = 2(\epsilon_H - \delta_H) < 1, \quad \delta_H := -\frac{\ddot\phi}{H\dot\phi} < 1.$$

(2.28)

The slow-roll condition can also be formulated in terms of the potential, by defining the 'potential' slow-roll parameters[4]

$$\epsilon_V := \frac{M_{\mathrm{Pl}}^2}{2}\left(\frac{V'}{V}\right)^2 < 1, \quad |\eta_V| := M_{\mathrm{Pl}}^2\frac{|V''|}{V} < 1.$$

(2.29)

In terms of the above slow-roll parameters, the slow-roll approximation corresponds to assuming the conditions for inflation to be readily fulfilled,

---

[4]To distinguish between the two versions, the slow-roll parameters ϵ_H, η_H are often called the Hubble slow-roll parameters. During slow-roll inflation they are related to the potential-dependent versions as $\epsilon_V \simeq \epsilon_H$ and $\eta_V \simeq 2\epsilon_H - \tfrac{1}{2}\eta_H$.

i.e. $\epsilon_V, |\eta_V| \ll 1$, for which the the evolution equations (2.26) reduces to

$$3H\dot{\phi} + V'(\phi) = 0,$$
$$3M_{\text{Pl}}^2 H^2 = V(\phi). \tag{2.30}$$

The duration of inflation for a given (classical) potential can then be computed from (2.20) by

$$N = \int_{t_s}^{t_e} \mathrm{d}t\, H = \int_{\phi_s}^{\phi_e} \mathrm{d}\phi \frac{H}{\dot{\phi}} \approx \int_{\phi_s}^{\phi_e} \mathrm{d}\phi \frac{V(\phi)}{M_{\text{Pl}}^2 V'(\phi)}. \tag{2.31}$$

While CMB observations put tight constraints on the slow-roll parameters and their interrelations, there is still a rather large number of inflationary potentials that are consistent with these constraints, see e.g. [47].

2.2.2 Field quantisation

Having discussed how a single scalar field is sufficient to model the inflationary expansion, in this section we turn to the mechanisms behind the generation of the CMB anisotropies. The origin of these inhomogeneities is currently understood to have been originated from small "seed" perturbations that grew over time. Ultimately, the inflaton is a quantum field, and as we will see, the seed perturbations can be understood as quantum fluctuations of the inflaton.

The inflaton field fluctuations back-react on the background metric, so it is necessary to also consider metric perturbations in order to make observable predictions. However, it is instructive to first consider the dynamics of the fluctuations of a generic scalar field on a classical, unperturbed, FRW background. Quantising the matter sector while keeping the gravitational sector classical is referred to as the semi-classical approximation.

To study the inflaton dynamics in within the semi-classical approximation, we promote the inflaton field to a quantum operator $\hat{\varphi}(x)$ and express it in terms of a small spacetime-dependent perturbation $\delta\hat{\phi}(x)$ around a homogeneous background field $\phi(t)$, i.e.,

$$\hat{\varphi}(t, \mathbf{x}) = \phi(t) + \delta\hat{\phi}(t, \mathbf{x}). \tag{2.32}$$

Here the hatted quantities $\hat{\varphi}(x)$ and $\delta\hat{\phi}(x)$ should be understood as being operator-valued. The quantum field fluctuation can be expanded in time-dependent mode functions,

$$\delta\hat{\phi}(t, \mathbf{x}) = \int \frac{\mathrm{d}^3 k}{(2\pi)^3} \delta\hat{\phi}_{\mathbf{k}}(t) e^{i\mathbf{k}\cdot\mathbf{x}},$$
$$\delta\hat{\phi}_{\mathbf{k}}(t) = a_{\mathbf{k}}\delta\phi_k(t) + a_{\mathbf{k}}^{\dagger}\delta\phi_k^*(t), \tag{2.33}$$

where $a_{\mathbf{k}}$, $a_{\mathbf{k}}^{\dagger}$ are the creation and annihilation operators and the mode functions satisfy the Wronskian

$$\delta\phi_k\delta\dot{\phi}_k^* - \delta\dot{\phi}_k\delta\phi_k^* = i. \tag{2.34}$$

We remark that the mode decomposition (2.33) is not unique. For a second decomposition in terms of modes $\hat{u}_{\mathbf{k}}(t)$ with corresponding set of operators $b_{\mathbf{k}}$, $b_{\mathbf{k}}^{\dagger}$, the two mode solutions are related via the complex and time-independent Bogolyubov coefficients α_k and β_k,

$$u_k(t) = \alpha_k\delta\phi_k(t) + \beta_k\delta\phi_k^*(t), \tag{2.35}$$

where the coefficients satisfy the Wronskian normalisation (2.34) by

$$|\alpha_k|^2 - |\beta_k|^2 = 1. \tag{2.36}$$

On an FRW background, the mean field evolves according to (2.25), while the mode solutions of the quantum fluctuation in (2.32) evolve according to

$$\delta\ddot{\phi}_k + 3H\delta\dot{\phi}_k + \left(\frac{k^2}{a^2} + V_{,\phi\phi}\right)\delta\phi_k = 0. \tag{2.37}$$

It is useful to rewrite (2.37) by rescaling the field

$$\delta\tilde{\phi}_k := \frac{\delta\phi_k}{a}, \tag{2.38}$$

and proceed in conformal time,

$$\mathrm{d}\tau := \frac{\mathrm{d}t}{a(t)}, \quad \tau \simeq -\frac{1}{aH}\frac{1}{1 - \epsilon_H}, \tag{2.39}$$

where the Hubble rate and slow-roll parameters ϵ_H, δ_H are given by

$$\mathcal{H} := \frac{a'}{a}, \quad \epsilon_H = 1 - \frac{\mathcal{H}'}{\mathcal{H}}, \quad \delta_H = 1 - \frac{\phi''}{\mathcal{H}\phi'}, \tag{2.40}$$

15

and prime denotes $d/d\tau$. In terms of the rescaled field (2.38), the evolution equation (2.37) then becomes

$$\delta\tilde{\phi}_k'' + [k^2 + M^2(\tau)]\delta\tilde{\phi}_k = 0, \tag{2.41}$$

where the effective mass[5] is given by

$$M^2(\tau) = a^2 V_{,\phi\phi} - \frac{a''}{a}. \tag{2.42}$$

To first order in slow-roll the acceleration term on the right-hand side in (2.42) is given by

$$\frac{a''}{a} \simeq \frac{1}{\tau^2}(2 + 3\epsilon_H), \tag{2.43}$$

for which the equation of motion (2.41) reduces to

$$\delta\tilde{\phi}_k'' + \left[k^2 - \frac{1}{\tau^2}\left(\nu^2 - \frac{1}{4}\right)\right]\delta\tilde{\phi}_k = 0. \tag{2.44}$$

For example in the case of a massive free field with $V(\phi) = \frac{1}{2}m^2\phi^2$, the index ν is given by

$$\nu^2 = \frac{9}{4} + 3\epsilon_H - 3\epsilon_M, \quad \epsilon_M := \frac{m^2}{3H^2}. \tag{2.45}$$

The solution to (2.44) is given by

$$\delta\tilde{\phi}_k(\tau) = \sqrt{-\tau}[c_1 H_\nu^{(1)}(-k\tau) + c_2 H_\nu^{(2)}(-k\tau)], \tag{2.46}$$

where $H^{(1,2)}(x)$ are the Hankel functions of first and second kind.

2.2.3 The Bunch-Davies vacuum

The coefficients c_1 and c_2 in (2.46) satisfy the Wronskian normalisation condition (2.34), but are fixed only by the choice of vacuum state. Time-dependent Hamiltonians have different corresponding vacuum states at each point in time, yet for inflation there exists a preferred choice of

---

[5]The effective mass term during the different expansive epochs can be parameterised in terms of the equation of state as $\frac{a''}{a} = \frac{1}{2}(aH)^2(1 - 3\omega)$.

vacuum state. In particular, in the early time limit, we see from (2.44) that all modes have time-independent frequencies,

$$\omega_k^2 = k^2 - \frac{1}{\tau^2}\left(v^2 - \frac{1}{4}\right) \to k^2, \quad \tau \to -\infty. \tag{2.47}$$

In this case the equation of motion (2.44) reduces to that of a free field in Minkowski spacetime,

$$\delta\tilde{\phi}_k'' + k^2\delta\tilde{\phi}_k = 0, \tag{2.48}$$

with plane-wave solutions $\delta\phi_k \propto e^{\pm ik\tau}$. The Wronskian normalisation condition (2.34) then chooses the positive-frequency solution. Hence, the initial inflationary vacuum mode functions are given by their Minkowski space counterparts,

$$\lim_{\tau \to -\infty} \delta\tilde{\phi}_k(\tau) = \frac{1}{\sqrt{2k}}e^{-ik\tau}, \tag{2.49}$$

and define a unique vacuum, known as the Bunch-Davies vacuum. Requiring that the general solution (2.46) matches the Bunch-Davies solution in the early-time limit, for which

$$H_\nu^{(1)}(x \gg 1) \simeq \sqrt{\frac{2}{\pi x}}e^{i(x - \frac{\pi}{2}\nu - \frac{\pi}{4})},$$
$$H_\nu^{(2)}(x \gg 1) \simeq H_\nu^{(1)}(x \gg 1)^*, \tag{2.50}$$

determines the coefficients in (2.46) to

$$c_1 = \frac{\sqrt{\pi}}{2}e^{i\frac{\pi}{2}(\nu + \frac{1}{2})}, \quad c_2 = 0. \tag{2.51}$$

2.2.4 Sub- and super-horizon modes

It is useful to consider the asymptotic behaviours of the mode solution (2.46). In particular, we see that the asymptotic forms of the mode functions depend on the value of $k|\tau|$. The quantity $k|\tau|$ can be interpreted in terms of the mode wavelengths relative to the Hubble horizon. A mode of comoving wavenumber k has comoving wavelength $\lambda = 2\pi/k$ and
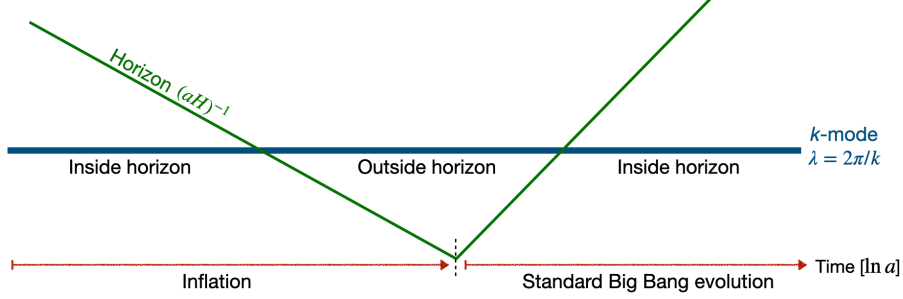
Figure 2.3: The time dependence of the comoving Hubble horizon and a comoving wavelength $\lambda = \lambda_{\text{phys}}/a$ during inflation and subsequent Big Bang expansion.

physical wavelength $\lambda_{\text{phys}} = a(\tau)\lambda$, and so

$$k|\tau| \sim \frac{(aH)^{-1}}{\lambda} = \frac{H^{-1}}{\lambda_{\text{phys}}}. \tag{2.52}$$

Large values of $k|\tau|$ correspond to wavelengths that are much shorter than the horizon radius H^{-1} at time τ, and the modes with such wavelengths are referred to as sub-horizon modes. The super-horizon modes have small values of $k|\tau|$ and physical wavelengths much larger than the Hubble horizon $\lambda_{\text{phys}} \gg H^{-1}$. A mode with wavenumber k is sub-horizon at early times, and transitions to being super-horizon at a k-dependent time $\tau_*(k)$, at which the wavelength is equal to the horizon, i.e. $k|\tau_*| = 1$. The time τ_* is known as the moment of horizon crossing for the mode ϕ_k. The notion of horizon crossing is a consequence of the decreasing Hubble horizon during inflation, see figure 2.3. For an increasing Hubble horizon during inflation, corresponding to a decelerating spacetime, there would not be any horizon crossing for any length scales λ.

Using the concept of sub- and super-horizon modes, we see e.g. from (2.44) that sub-horizon modes are essentially unaffected by the curvature of spacetime. For these modes, the equation of motion (2.44) reduces to that of an harmonic oscillator. In contrast, on super-horizon scales the equation of motion reduces to

$$\delta\tilde{\phi}_k'' + M^2(\tau)\delta\tilde{\phi}_k = 0, \tag{2.53}$$

which tells us that the super-horizon modes remain essentially constant. Indeed, on these scales the asymptotic mode solution to (2.46) is[6]

$$\lim_{k|\tau|\to 0}\delta\tilde{\phi}_k(\tau) = e^{i\frac{\pi}{2}(\nu-\frac{1}{2})}2^{\nu-\frac{3}{2}}\frac{\Gamma(\nu)}{\Gamma(3/2)}\frac{1}{\sqrt{2k}}(-k\tau)^{\frac{1}{2}-\nu}, \qquad (2.54)$$

which in terms of the original variable $\delta\phi_k$ becomes

$$|\delta\phi_k| \simeq \frac{H}{\sqrt{2k^3}}\left(\frac{k}{aH}\right)^{\frac{3}{2}-\nu}, \qquad \frac{k}{aH} \ll 1. \qquad (2.55)$$

In the above equation we see that the time-dependence entering in the last factor is highly suppressed due to the smallness of the slow-roll parameters.

2.2.5 Emergence of classical behaviour for super-horizon modes

The fact that the super-horizon modes eventually stop evolving in time is the key ingredient to generating the cosmological anisotropies. In particular, it results in that super-horizon modes undergo a quantum-to-classical transition. This can be seen for instance from the canonical commutation relations, where the solution (2.55) implies that $\delta\hat{\pi}_{\mathbf{k}} \propto \delta\hat{\phi}_{\mathbf{k}} \propto \delta\hat{\phi}_{\mathbf{k}}$, such that

$$[\delta\hat{\phi}_{\mathbf{k}}(x), \delta\hat{\pi}_{\mathbf{k}}(x')] \simeq 0, \qquad \frac{k}{aH} \ll 1, \qquad (2.56)$$

for $\nu \simeq 3/2$. Alternatively, computing the particle number density n_k from the Hamiltonian $H_k = \omega_k(n_k + 1/2)$ corresponding to the Lagrangian

$$\mathcal{L}(k) = \tfrac{1}{2}\left(\delta\phi_k'^2 + \left[k^2 - M^2(\tau)\right]\delta\phi_k^2\right), \qquad (2.57)$$

one finds that on super-horizon scales,

$$n_k \simeq \frac{\delta\phi_k'^2}{\omega_k} \simeq \left(\frac{H}{\sqrt{k^3}}\right)^2\frac{a'^2}{k} \sim \left(\frac{k}{aH}\right)^{-4} \gg 1. \qquad (2.58)$$

Therefore, some time after the modes have crossed the horizon, they can be modelled as classical stochastic variables, and their expectation values by classical ensemble averages.

---

[6] $H_\nu^{(1)}(x \ll 1) \simeq \sqrt{2/\pi}e^{-i\pi/2}2^{\nu-3/2}x^{-\nu}\Gamma(\nu)/\Gamma(3/2)$.

From the super-horizon asymptotic solution (2.55) we can compute the power spectrum of the scalar field fluctuations. Assuming that the fluctuations $\delta\hat{\phi}$ are real random fields,

$$\delta\hat{\phi}(t,\mathbf{x}) = \int \frac{\mathrm{d}^3 k}{(2\pi)^3} \delta\hat{\phi}_{\mathbf{k}}(t) e^{i\mathbf{k}\cdot\mathbf{x}}, \quad \delta\hat{\phi}_{\mathbf{k}} = \hat{c}_{\mathbf{k}} + i\hat{d}_{\mathbf{k}}, \tag{2.59}$$

then they are in addition Gaussian if $\hat{c}_{\mathbf{k}}$ and $\hat{d}_{\mathbf{k}} = -\hat{d}_{-\mathbf{k}}$ are uncorrelated and normal-distributed random numbers. The vacuum expectation value of a two-point correlation function can then be defined as

$$\langle 0|\delta\hat{\phi}_{\mathbf{k}}\delta\hat{\phi}_{\mathbf{k}'}|0\rangle := (2\pi)^3 \delta(\mathbf{k}+\mathbf{k}')|\delta\phi_k|^2, \tag{2.60}$$

where $|0\rangle$ is the vacuum state of the system and spatial isotropy is assumed. From this relation we can define the power spectrum $\mathcal{P}_{\delta\phi}$ of the fluctuations as

$$\begin{aligned}
\langle 0|\delta\hat{\phi}(t,\mathbf{x})\delta\hat{\phi}(t,\mathbf{x}')|0\rangle &= \int \frac{\mathrm{d}^3 k}{(2\pi)^3} e^{i\mathbf{k}\cdot(\mathbf{x}-\mathbf{x}')}|\delta\phi_k(t)|^2 \\
&:= \int_0^\infty \frac{\mathrm{d}k}{k}\frac{\sin(kr)}{kr}\mathcal{P}_{\delta\phi}(t,k),
\end{aligned} \tag{2.61}$$

with $r := |\mathbf{x}-\mathbf{x}'|$. Using (2.55) we see that the power spectrum on super-horizon scales is indeed nearly constant,

$$\mathcal{P}_{\delta\phi}(t,k) := \frac{k^3}{2\pi^2}|\delta\phi_k(t)|^2 = \left(\frac{H}{2\pi}\right)^2\left(\frac{k}{aH}\right)^{3-2\nu}, \tag{2.62}$$

since the spectral index $n_{\delta\phi}$ is small:

$$n_{\delta\phi} - 1 := \frac{\mathrm{d}\ln P_{\delta\phi}}{\mathrm{d}\ln k} = 3 - 2\nu = 2\epsilon_M - 2\epsilon_H. \tag{2.63}$$

To make observable predictions for the cosmological perturbations, it is necessary to consider also metric fluctuations. Their account is the topic of the next section.

2.3 Vacuum fluctuations as seeds of large-scale structure

The observable anisotropies in the CMB arise from combinations of both field and metric quantum fluctuations. As long as the inflationary

fluctuations remain relatively small, their dynamics can be studied per-turbatively. To this end we now write both the metric and inflaton field in terms of homogeneous background fields and small perturbations,

$$\hat{g}_{\mu\nu}(\tau, \mathbf{x}) = \bar{g}_{\mu\nu}(\tau) + \delta\hat{g}_{\mu\nu}(\tau, \mathbf{x}), \quad \hat{\varphi}(\tau, \mathbf{x}) = \phi(\tau) + \delta\hat{\phi}(\tau, \mathbf{x}), \quad (2.64)$$

where $\bar{g}_{\mu\nu}$ denotes the background metric. In the following we will suppress the hat notation and let the perturbations be implicitly operator-valued. The metric has 10 degrees of freedom and its perturbations can be decomposed into scalar-vector-tensor (SVT) degrees of freedom:

$$\delta g_{00} = -2\Phi,$$
$$\delta g_{i0} = \partial_i B + B_i, \quad (2.65)$$
$$\delta g_{ij} = -2\Psi\delta_{ij} + (\partial_i\partial_j - \tfrac{1}{3}\delta_{ij}\nabla^2)E + \partial_i E_j + \partial_j E_i + E_{ij},$$

where the vector and tensor perturbations are divergenceless and the tensor perturbation is also traceless,

$$\partial^i B_i = \partial^i E_i = 0, \quad \partial^i E_{ij} = \partial^i E_{ji} = 0, \quad E^i{}_i = 0. \quad (2.66)$$

The scalars Φ, B, Ψ, E account for four degrees of freedom and the two vectors B_i and E_i for $2 \times 2 = 4$ since $B_i = B_i^\perp + B_i^\parallel$ where $\nabla \times \mathbf{B}^\parallel = 0$ and $\nabla \cdot \mathbf{B}^\perp = 0$. The final two degrees of freedom come from the two polarisations of the traceless transverse tensor E_{ij}. In four dimensions, the physical degrees of freedom is six, where each of the scalar, vector and tensor sectors contribute with two degrees of freedom.

The SVT decomposition proves to be valuable because scalars, vectors and tensors do not mix at linear order in the Einstein equations, and they can therefore be treated separately.

2.3.1 Gauge-invariant perturbations

The metric perturbations in (2.65) are not uniquely defined under co-ordinate transformations and to proceed it is necessary to either fix the gauge or work in terms of gauge-invariant quantities. Predictions for observables must regardless consist of gauge-invariant quantities. There are gauge-invariant combinations of the metric perturbations in (2.65),

known as the Bardeen variables, which consist of the scalar potentials

$$\Phi_B := \Phi + \mathcal{H}(B - \tfrac{1}{2}E') + (B - \tfrac{1}{2}E')', \qquad (2.67)$$

$$\Psi_B := \Psi + \tfrac{1}{6}\nabla^2 E - \mathcal{H}(B - \tfrac{1}{2}E'), \qquad (2.68)$$

together with $\Psi_i := E_i' - B_i$ and E_{ij} for vector and tensor perturbations. Vector perturbations are predicted to decay with the expansion during inflation [42, 51]. This can be attributed to the absence of anisotropic stress in a perfect fluid, which in combination with the momentum conservation of the energy-momentum tensor leads to a suppression of linear vector perturbations as $1/a^2(t)$ during inflation. Because of this decay of vector fluctuations we will analyse only the generation of classical scalar and tensor modes in the following.

There are also gauge-invariant combinations which contain both metric and field perturbations. One important such combination is the comoving curvature perturbation

$$\mathcal{R} := \Psi - \frac{1}{3}\nabla^2 E + \mathcal{H}\left(B + \frac{\delta\phi}{\phi'}\right), \qquad (2.69)$$

which is the curvature perturbation $(\Psi - \tfrac{1}{3}\nabla^2 E)$ evaluated on comoving hypersurfaces, where observers see $T_{0i} \propto \partial_i \delta\phi\phi' = 0$ and $B_i = 0$. It is the comoving curvature perturbations that can be related to the density perturbations $\delta\rho$ during the later matter-dominated eras after inflation, which in turn translates into the temperature anisotropies δT in the CMB. The path from density perturbations to the resulting temperature anisotropies observed in the CMB is an intricate process that extends beyond the scope of this thesis. For a detailed exploration of this topic, we kindly direct the reader to e.g. [52–54].

2.3.2 Evolution of primordial perturbations in Newtonian gauge

In general there is no preferred choice of gauge for the metric perturbations in (2.65) but depending on the object of interest, some are more convenient than others. For example, the spatially flat gauge $\Psi = E = 0$ allows one to focus more directly on the inflaton perturbations $\delta\phi$. We will proceed in the Newtonian (longitudinal) gauge $B = E = 0$, which is suitable to

compute observable cosmological perturbations. In this gauge the metric scalar degrees of freedom are reduced to the two perturbations $\Phi \equiv \Phi_B$ and $\Psi \equiv \Psi_B$. Neglecting vector perturbations, the metric is then given by

$$\mathrm{d}s^2 = a^2(\tau)\left\{-(1 + 2\Phi)\mathrm{d}\tau^2 + [(1 - 2\Psi)\delta_{ij} + E_{ij}]\mathrm{d}x^i \mathrm{d}x^j\right\}, \quad (2.70)$$

and resembles that of the weak-field limit of general relativity (GR) around Minkowski space, with Φ corresponding to the gravitational potential. The linearised Einstein equations are

$$\bar{G}_{\mu\nu} + \delta G_{\mu\nu} = 8\pi G[\bar{T}_{\mu\nu} + \delta T_{\mu\nu}], \quad (2.71)$$

where the (barred) zeroth order equations are given by the Friedmann equations in (2.26). The components of the perturbed energy momentum tensor are given by

$$\begin{aligned}
\delta T^0{}_0 &= \Phi\phi'^2 - \delta\phi'\phi' - a^2 V_{,\phi}\delta\phi, \\
\delta T^i{}_0 &= \phi'\partial^i\delta\phi, \\
\delta T^i{}_j &= \left[-\Phi\phi'^2 + \delta\phi'\phi' - a^2 V_{,\phi}\delta\phi\right]\delta^i_j.
\end{aligned} \quad (2.72)$$

The absence of anisotropic stress in the energy-momentum tensor offers additional simplification of the Einstein equations, since in this gauge the off-diagonal ($i \neq j$) part of the equations for the scalar perturbations reads

$$\partial^i\partial_j(\Psi - \Phi) = 0, \quad (2.73)$$

which sets $\Phi = \Psi$. The (00)-, (0i)- and (ii)-components of the scalar sector of the Einstein equations are then reduced to

$$3\mathcal{H}(\Psi' + \mathcal{H}\Psi) - \nabla^2\Psi = -4\pi G[\phi'\delta\phi' \\
- \phi'^2\Psi + a^2 V'\delta\phi], \quad (2.74)$$

$$\Psi' + \mathcal{H}\Psi = 4\pi G\phi'\delta\phi, \quad (2.75)$$

$$\Psi'' + 3\mathcal{H}\Psi' + \left[2\frac{a''}{a} - \left(\frac{a'}{a}\right)^2\right]\Psi = -4\pi G[\phi'\delta\phi' \\
- \phi'^2\Psi + a^2 V'\delta\phi]. \quad (2.76)$$

23

The tensor part of the Einstein equation is given by

$$E_{ij}'' + 2\mathcal{H}E_{ij} - \nabla^2 E_{ij} = 0. \tag{2.77}$$

Combining equations (2.74) and (2.76) and eliminating $V_{,\phi}$ via the inflaton equation of motion, we find for the gravitational potential,

$$\Psi_k'' + 2\mathcal{H}\delta_H\Psi_k' + [k^2 + 2\mathcal{H}^2(\delta_H - \epsilon_H)]\Psi_k = 0. \tag{2.78}$$

The above equation has a similar form to that of the scalar field evolving in a classical FRW background in (2.37). Because of this we may use the same arguments for the super-horizon modes leading up to (2.53). That is, we can infer that Ψ, too, is almost constant on super-horizon scales. This allows us to approximate (2.75) to

$$\Psi \simeq \epsilon_H \mathcal{H}^2 \frac{\delta\phi}{\phi'}, \quad k\tau \ll 1, \tag{2.79}$$

where we have used the Friedmann equation (2.27), which in conformal time reads $\mathcal{H}^2 - \mathcal{H}' = 4\pi G\phi'^2$.

2.3.3 The curvature perturbation power spectrum

On super-horizon scales, the comoving curvature perturbation can be computed solely from the field perturbation by using the approximate solution (2.79),

$$\mathcal{R} = \Psi + \mathcal{H}\frac{\delta\phi}{\phi'} \simeq (1 + \epsilon_H)\mathcal{H}^2\frac{\delta\phi}{\phi'}, \quad k\tau \ll 1. \tag{2.80}$$

The power spectrum of the comoving curvature perturbation then reads, to leading order in slow-roll,

$$\mathcal{P_R}(t,k) \simeq \frac{k^3}{2\pi^2}\left(\frac{H}{\dot\phi}\right)^2 |\delta\phi_k(t)|^2 = \frac{k^3}{4\pi^2 M_{\text{pl}}^2 \epsilon_H}|\delta\phi_k(t)|^2, \tag{2.81}$$

where we have restored cosmic time. To obtain an explicit expression, the next step is to solve for the evolution of the modes $\delta\phi_k$ of the matter field fluctuation.

With the metric (2.70) set in Newtonian gauge, the Klein-Gordon equation of motion for the scalar perturbation is given by

$$\delta\phi'' + 2\mathcal{H}\delta\phi - \nabla^2\delta\phi + a^2 V_{,\phi\phi}\delta\phi = 4\Psi'\phi' - 2\Psi V_{,\phi}. \tag{2.82}$$

24

The right-hand side can be simplified using that on super-horizon scales $|\Psi'\phi'| \ll |\Psi V_{,\phi}|$, along with the slow-roll condition $V_{,\phi} \simeq -2\mathcal{H}\phi'$ and (2.79), to

$$\delta\phi'' + 2\mathcal{H}\delta\phi' + (a^2 V_{,\phi\phi} - 4\epsilon_H\mathcal{H}^2)\delta\phi = 0. \qquad (2.83)$$

Rescaling the field $\delta\tilde{\phi} = \delta\phi/a$, this equation can be written

$$\delta\tilde{\phi}_k'' - \frac{1}{\tau^2}\left(\nu^2 - \frac{1}{4}\right)\delta\tilde{\phi}_k = 0, \quad \nu^2 = \frac{9}{4} + 9\epsilon_H - 3\eta_V. \qquad (2.84)$$

The solution on super-horizon scales then has the same form as in (2.46) with $\nu \simeq 3/2 + 3\epsilon_H - \eta_V$, and the power spectrum of the comoving curvature perturbation is then

$$\mathcal{P}_\mathcal{R}(t, k) = \frac{4\pi G}{\epsilon_H}\left(\frac{H}{2\pi}\right)^2\left(\frac{k}{aH}\right)^{n_s-1} := A_\mathcal{R}^2\left(\frac{k}{aH}\right)^{n_s-1}, \qquad (2.85)$$

where the spectral index of the comoving curvature perturbation is

$$n_s - 1 := \left.\frac{\mathrm{d}\ln\mathcal{P}_\mathcal{R}}{\mathrm{d}\ln k}\right|_{k=k_*} = 3 - 2\nu \simeq 2\eta_V - 6\epsilon_H. \qquad (2.86)$$

The spectrum of the curvature perturbation in (2.85) is almost scale invariant. This means that, on super-horizon scales, the amplitude of the fluctuation is almost independent of the time that it crossed the horizon before it became frozen in after some Hubble times. The small deviance from scale invariance, quantified by the slow-roll parameters, is due to the effective mass of the inflaton. It can be shown using energy-momentum conservation that with only adiabatic[7] modes present, the comoving curvature perturbation is exactly conserved on super-horizon scales, see e.g. [42].

2.3.4 The tensor perturbation power spectrum

Finally, we consider the tensor fluctuations. The tensor perturbations have two physical degrees of freedom, which are referred to as polarisations (labelled $+$ and $\times$). These degrees of freedom can be expressed as two

---

[7]Adiabatic, or curvature, perturbations are characterised by uniform changes in the energy density of different components, such as radiation or matter, while maintaining the same overall entropy.

independent polarisation tensors, e_{ij}^{λ}, such that the tensor fluctuations can be written

$$\hat{E}_{ij}(\tau, \mathbf{x}) = \int \frac{\mathrm{d}^3 k}{(2\pi)^3} \sum_{\lambda=\times,+} e_{ij}^{\lambda}(\mathbf{k}) \hat{E}_{\mathbf{k}}(\tau) e^{i\mathbf{k}\cdot\mathbf{x}}, \qquad (2.87)$$

where the polarisation tensors satisfy

$$\begin{aligned} e_{ij}^{\lambda} &= e_{ji}^{\lambda}, \quad k^i e_{ij}^{\lambda} = 0, \quad e_{ii}^{\lambda} = 0, \\ e_{ij}^{\lambda}(\mathbf{k})^* &= e_{ij}^{\lambda}(-\mathbf{k}), \quad (e_{ij}^{\lambda})^* e_{ij}^{\lambda'} = \delta^{\lambda\lambda'}. \end{aligned} \qquad (2.88)$$

As mentioned earlier, the tensor E_{ij} is gauge-invariant and therefore represents physical degrees of freedom. The equation of motion for the tensor perturbations is given by (2.77), and with the usual procedure of rescaling the modes,

$$\tilde{E}_k = \frac{M_{\text{Pl}}}{2} a E_k, \qquad (2.89)$$

the equation of motion can be recast into the form

$$\tilde{E}_k'' + \left(k^2 - \frac{a''}{a} \right) \tilde{E}_k = 0. \qquad (2.90)$$

The solution is the same as for the scalar perturbation on a background FRW metric (2.41) but with vanishing mass. On super-horizon scales, the tensor perturbation power spectrum is then given by

$$\mathcal{P}_T(t, k) = \frac{8}{M_{\text{Pl}}^2} \left(\frac{H}{2\pi} \right)^2 \left(\frac{k}{aH} \right)^{n_T} := A_T^2 \left(\frac{k}{aH} \right)^{n_T}, \qquad (2.91)$$

with tensor spectral index defined as[8]

$$n_T := \left. \frac{\mathrm{d}\ln\mathcal{P}_T}{\mathrm{d}\ln k} \right|_{k=k_*} = 3 - 2\nu_T = -2\epsilon_H. \qquad (2.92)$$

The tensor fluctuations are, like the scalar fluctuations, nearly scale invariant. However, the tensor perturbations depend only on the inflationary Hubble rate, which in turn is related to the energy scale associated to the inflaton potential. A detection of primordial gravitational waves would

---

[8]The spectral index convention for scalar and tensor modes differ due to historical reasons.

therefore provide a direct measurement of the energy scale linked to the inflationary epoch.

The relative dependence of the scalar and tensor perturbations to the energy scale of inflation can be quantified with the tensor-to-scalar amplitude ratio

$$r := \frac{A_T^2}{A_{\mathcal{R}}^2} = 16\epsilon_H, \tag{2.93}$$

which implies that $r = -8n_T$. Combined measurements of CMB temperature anisotropies and polarisation therefore provide constraints on the energy scale of inflation. Note that this relation is a prediction of single-field inflationary models. If this relation were to be falsified by future CMB measurements, then inflation must have been driven by more than one field. Inflationary models are often classified by their predictions for the parameters n_s and r, or alternatively, by the relation between the slow-roll parameters. These values are estimated to $n_s \approx 0.9649$ and $r < 0.056$ by the 2018 Planck data [47]. See also [47] for constraints on viable inflationary potentials resulting from these estimates of n_s and r.

2.4 Quantum corrections to inflation

So far we have considered cosmological perturbations at linear level, i.e. without assuming any self-interactions in the inflaton or metric fields. CMB observations have established this assumption to be a good approximation, since the CMB anisotropies appear Gaussian to a high degree [55]. This means that the statistical information of the fluctuations appear to be primarily collected in their variance. A non-Gaussian distribution receives contributions from higher order n-point functions, information of which can only be obtained beyond linear order in perturbation theory. Since the inflaton is expected to be coupled to Standard Model fields, and because of the non-linear properties of general relativity, some degree of non-Gaussianity is expected.

The literature on computing quantum corrections to observable n-point functions due to gravitational- and matter self-interactions is vast. In addition to field loop corrections to the CMB power spectrum, significant

27

attention has been paid to the appearance of non-Gaussianity in CMB observables due to metric self-interactions [56, 57] as well as multiple matter fields [57–59]. Matter-field loop corrections to the quantum effective potential [60–65] (more recently [66–68]) and the inflaton equation of motion and Friedmann equations [69] have also been considered. On expanding backgrounds, infrared (IR) divergences arise as consequence of their dependence on the scale factor. In particular, the variance $\langle \phi^2 \rangle$ of a generic scalar field on a (semi-)de Sitter spacetime contains a term $\propto \ln a(t)$ which results in a logarithmic divergence that originates from the IR part of the integration over loop momentum. Since it is the large-scale, or infrared dynamics of the fluctuations that enter into observables, the use of cut-off procedures is inappropriate in this context. To address this issue, resummation schemes have been applied to (semi-)de Sitter backgrounds [69–75], and reveal that an effective mass is generated that regularises the IR divergences.

What many of the studies concerning inflationary loop corrections have in common is the use of the semi-classical approximation. That is, metric loop corrections are neglected. The matter loop corrections are instead computed on a homogeneous background, aided by the standard slow-roll relations (2.29), to some order in slow-roll parameters. The argument for the use of the semi-classical approximation is that far below the Planck scale, metric perturbations are anyway suppressed by H/M_{Pl}, where the Hubble rate H sets the typical energy scale of matter fluctuations on an FRW background.

A complete treatment nevertheless requires the inclusion of metric fluctuations, and the question remains whether or within which limits the semi-classical approximation is a good approximation for a given inflationary scenario. The inclusion of metric loop corrections breaks the standard slow-roll relations. They also introduce the issue of consistent renormalisation, which may threaten the utility of the resummed computations. It is therefore desirable to establish a framework in which the range of validity of the semi-classical approximation for a given inflationary setup can be verified. This issue has been addressed previously in [76] and a continuation of this work is the topic of chapter 5, where we

compute the quantum corrected field and Friedmann equations of motion, including both field and metric fluctuations.

3 Quantum field theory on curved backgrounds

In non-equilibrium field theory, the observables of a system are time-dependent. The lack of time-translation invariance leaves the standard LZH (in-out) formalism [77, 78] inapplicable, as it relies on the assumption that the asymptotic initial (in) and final (out) states surrounding a scattering process are the same. While this is a valid assumption for processes on short time scales that are not significantly affected by medium-induced effects like temperature fluctuations, as in high-energy particle collisions at accelerators, this is not the case for thermal or evolving systems. For systems with time-dependent Hamiltonians, the energy-minimising state of the system (the vacuum state) is different at each point in time. Similarly, if the energy of some particles of interest are comparable to the temperature of a surrounding medium, the temperature fluctuations need to be accounted for.

The appropriate framework to describe the time evolution of quantum expectation values is the Schwinger-Keldysh formalism [79, 80].[1] For thermal (finite temperature) theories, the closely related imaginary-time formalism [81] enables perturbative calculations applicable to systems in thermal equilibrium. Reviews of these frameworks can be found e.g. in the textbooks [82–85]. In this chapter we introduce the main ingredients of non-equilibrium quantum field theory on curved spacetimes and discuss the most common renormalisation procedures in this context.

3.1 Schwinger-Keldysh formalism

Correlation functions can be expressed as expectation values in terms of the density matrix ρ, which contains all the quantum and statistical information of a system. The expectation value of an operator O is given

---

[1]Also known as the closed time-path, in-in or real-time formalism.

by

$$\langle O(t,\mathbf{x})\rangle = Z^{-1}\operatorname{Tr}[\rho O(t,\mathbf{x})], \quad Z[\rho] := \operatorname{Tr}\rho \equiv \sum_{\varphi}\langle\varphi|\rho|\varphi\rangle, \quad (3.1)$$

where $Z[\rho]$ is the partition function and the Heisenberg states $|\varphi\rangle$ form a complete set, or basis, of field eigenstates spanning the Hilbert space of the physical system. In non-equilibrium situations we are interested in the time evolution of the system and therefore seek a time-dependent generalisation of the states in (3.1). In the Schrödinger picture the time-dependence of a state is introduced by the unitary time evolution operator $U(t,t_i)$ as

$$|\varphi(t)\rangle := U(t,t_i)|\varphi(t_i)\rangle, \quad (3.2)$$

where t_i denotes an initial time. In the presence of a source $J(x)$, the time-evolution operator can be written schematically as

$$U(t,t_i)|\varphi(t_i)\rangle := T\exp\left[-i\int_{t_i}^{t}\mathrm{d}t'\int\mathrm{d}^3\mathbf{x}\sqrt{-g}J(t',\mathbf{x})\hat{\varphi}(t',\mathbf{x})\right]|\varphi(t_i)\rangle, \quad (3.3)$$

where T denotes time ordering and $\hat{\varphi}(t,\mathbf{x})|\varphi(t_i)\rangle = \varphi(t_i,\mathbf{x})|\varphi(t_i)\rangle$ is a Heisenberg field operator that couples to the source. The time-dependent density matrix can then be expressed as

$$\rho(t) := U(t,t_i)\rho(t_i)U^{\dagger}(t,t_i), \quad (3.4)$$

where $U^{\dagger}(t,t_i) \equiv U(t_i,t)$ is the anti-time ordering operator which evolves backward in time. The density matrix evolves according to the Liouville equation

$$i\partial_t\rho(t) = [H(t),\rho(t)], \quad (3.5)$$

where $H(t)$ is the Hamiltonian of the system. In thermal equilibrium the commutator vanishes and the thermal density matrix is given by $\rho_{\mathrm{eq}} \sim e^{-\beta H}$ with β being the inverse temperature and we assume vanishing chemical potential.

The form of the time-dependent density matrix (3.4) is a generalisation of its time-independent counterpart in (3.1). However, the evolution operators in (3.4) suggest a forward time evolution of $\rho(t_i)$ from t_i to

t, followed by a backward time evolution from t to t_i. There appears to be no net time evolution gained, and this is a consequence of the forward and backward evolution operators being complex conjugates of each other. To obtain a concrete time evolution, the idea behind the Schwinger-Keldysh formalism is to separate the time path for forward and backward evolution by assuming that the field, rather than coupling to only one external source, couples to two different sources $J^+(x)$ and $J^-(x)$. The forward and backward time evolution operators $U_{J^+}(t, t_i)$ and $U_{J^-}^\dagger(t_i, t)$ are then defined in terms of J^+ and J^- respectively.

The time evolution is defined relative to the time interval $[t_i, t]$, where the forward time path is defined as $C^+ : t_i \to t$ and the backward one as $C^- : t \to t_i$. The merging of these paths at t results in a closed time-path known as the Keldysh contour C, whose time-evolution operator is given by

$$U_J := U_{J^-}^\dagger(t, t_i) U_{J^+}(t_i, t) = T_C \exp\left[i \int_C dt d^3\mathbf{x} \sqrt{-g} J(x) \hat{\varphi}(x) \right]. \quad (3.6)$$

The initial time is usually taken to be located in the infinite past relative to the time t, and the initial source terms $J^\pm(x)$ are separated by a small shift in the imaginary time direction. The contour C can then be set to run from $t_i = -\infty + i\epsilon$ to t and then back to $t_i = -\infty - i\epsilon$. This choice aligns with the Wick-rotated pole structures of various propagators, such as the $-i\epsilon$-prescription for the Feynman propagator, which is necessary for the convergence of the path integral and a proper time-ordering that ensures causality.

With the separation of the source and coupled field into $J^\pm(x)$ and $\varphi^\pm(x)$, the partition function takes the form

$$Z[\rho, J^\pm] = \int \mathcal{D}\varphi^+ \mathcal{D}\varphi^- \langle \varphi^+(t_i) | \rho | \varphi^-(t_i) \rangle \quad (3.7)$$

$$\times \exp\left[i \int dt \int d^3\mathbf{x} \sqrt{-g} \left[(\mathcal{L}[\varphi^+] + \varphi^+ J^+) - (\mathcal{L}[\varphi^-] + \varphi^- J^-) \right] \right].$$

Here the expectation value of the exponential term has been evaluated using $\hat{\varphi}(t, \mathbf{x}) | \varphi^\pm(t_i) \rangle = \varphi^\pm(t_i, \mathbf{x}) | \varphi^\pm(t_i) \rangle$. In terms of the closed-path-
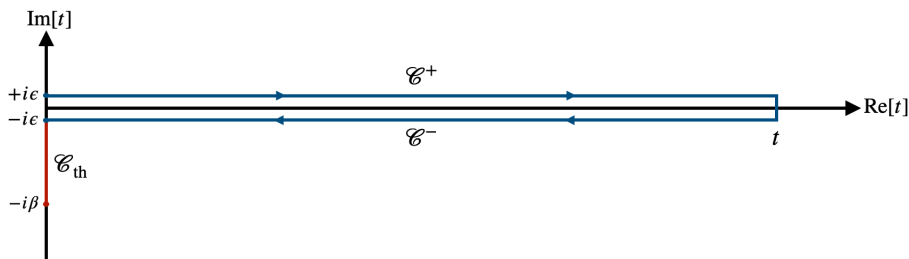
Figure 3.1: The Schwinger-Keldysh closed time contour for real-time evolution (blue) running from $t_i + i\epsilon$ to t and back to $t_i - i\epsilon$ with $t_i = 0$. In thermal equilibrium (red) the closed time path runs from $t_i = 0$ to $t = -i\beta$ and back.

ordering T_C, (3.7) can be written

$$Z[\rho, J] = \text{Tr}\left\{\rho(t_i)T_C \exp\left[i \int_{x,C} [\mathcal{L}[\varphi] + J(x)\varphi(x)]\right]\right\}, \qquad (3.8)$$

where $\int_{C,x} := \int_C dt \int d^3\mathbf{x}\sqrt{-g}$ and we have defined the initial density matrix $\rho(t_i) := \langle\varphi^+(t_i)|\rho|\varphi^-(t_i)\rangle$. The factorisation of $Z[\rho, J]$ into an expectation value of the initial density matrix and exponential in (3.7) and (3.8) implies a factorisation between the statistical and quantum fluctuations of the system. Here the statistical fluctuations are encoded in the averaging procedure of the initial density matrix elements and the functional integral carries the information about the quantum fluctuations.

As a final remark, we note that in the case of thermal equilibrium the partition function $Z = \text{Tr}\, e^{-\beta H}$ can be evaluated formally in terms of an imaginary time evolution operator, $U = \exp[-iHt]$ with $t = -i\beta$. The Keldysh contour in the imaginary time formalism is then given by $C_{\text{th}} = [0, -i\beta]$. For a non-equilibrium system with a thermal initial density matrix, the resulting Keldysh contour is given by the thermal contour C_{th} at the initial (imaginary) time coupled to the real-time contour C at the point $t = 0 - i\epsilon$, see figure 3.1.

3.1.1 The initial density matrix

For a given choice of initial density matrix, n-point correlation functions are obtained by n functional variations of $Z[\rho, J]$ with respect to the

source J. The initial density matrix can be parametrised as an exponentiated polynomial P in the initial field variables [29, 86],

$$\rho(t_i) = N \exp[iP[\varphi(t_i)]], \qquad (3.9)$$

where N is a normalisation factor and

$$
\begin{aligned}
P[\varphi(t_i)] = c_0 &+ \int_{\mathbf{x}} c_1^+(\mathbf{x})\varphi_{t_i}^+(\mathbf{x}) - \int_{\mathbf{x}} c_1^-(\mathbf{x})\varphi_{t_i}^-(\mathbf{x}) \\
&+ \frac{1}{2}\int_{\mathbf{xy}} c_2^{++}(\mathbf{x},\mathbf{y})\varphi_{t_i}^+(\mathbf{x})\varphi_{t_i}^+(\mathbf{y}) + \frac{1}{2}\int_{\mathbf{xy}} c_2^{--}(\mathbf{x},\mathbf{y})\varphi_{t_i}^-(\mathbf{x})\varphi_{t_i}^-(\mathbf{y}) \\
&- \frac{1}{2}\int_{\mathbf{xy}} c_2^{+-}(\mathbf{x},\mathbf{y})\varphi_{t_i}^+(\mathbf{x})\varphi_{t_i}^-(\mathbf{y}) - \frac{1}{2}\int_{\mathbf{xy}} c_2^{-+}(\mathbf{x},\mathbf{y})\varphi_{t_i}^-(\mathbf{x})\varphi_{t_i}^+(\mathbf{y}) \\
&+ \frac{1}{3!}\int_{\mathbf{xyz}} c_3^{+++}(\mathbf{x},\mathbf{y},\mathbf{z})\varphi_{t_i}^+(\mathbf{x})\varphi_{t_i}^+(\mathbf{y})\varphi_{t_i}^+(\mathbf{z}) + \dots, \qquad (3.10)
\end{aligned}
$$

with $\int_{\mathbf{xy}} := \int d^3\mathbf{x} \int d^3\mathbf{y}$, etc. The coefficients $c_0, c_1(x), \dots$ can be interpreted as initial-time source terms. Choosing only c_0 and $c_1(x)$ to be non-vanishing in the initial density matrix, they can be absorbed into the source term $J(x)$ in (3.8), so that $Z[\rho(t_i), J] \to Z[J]$.

3.1.2 Time-ordered correlation functions

Given a specified initial state, the one-point function, or mean field, is obtained by functional variation with respect to the source:

$$\left.\frac{\delta Z[J]}{i\delta J(x)}\right|_{J=0} = \text{Tr}[\rho(t_i)\hat{\varphi}(x)] = \langle\hat{\varphi}(x)\rangle := \phi(x). \qquad (3.11)$$

The mean field is the same regardless if it is obtained by differentiation with respect to $J^+(x)$ or $J^-(x)$. Similarly for the two-point function, a second functional derivative gives

$$\left.\frac{\delta Z[J]}{i\delta J(x)i\delta J(y)}\right|_{J=0} = \text{Tr}[\rho(t_i)T_C\hat{\varphi}(x)\hat{\varphi}(y)] = \langle T_C\hat{\varphi}(x)\hat{\varphi}(y)\rangle, \qquad (3.12)$$

from which the connected two-point function, or propagator, is defined by

$$G(x,y) := \langle T_C\hat{\varphi}(x)\hat{\varphi}(y)\rangle - \phi(x)\phi(y). \qquad (3.13)$$

In the above relations, the time-ordering T_C is explicitly given by [86]

$$T_C \hat{\varphi}(x)\hat{\varphi}(y) = \begin{cases} \hat{\varphi}(x)\hat{\varphi}(y)\Theta(x^0 - y^0) + \hat{\varphi}(y)\hat{\varphi}(x)\Theta(y^0 - x^0), & x^0, y^0 \in C^+, \\ \hat{\varphi}(x)\hat{\varphi}(y)\Theta(y^0 - x^0) + \hat{\varphi}(y)\hat{\varphi}(x)\Theta(x^0 - y^0), & x^0, y^0 \in C^-, \\ \hat{\varphi}(y)\hat{\varphi}(x), & x^0 \in C^+, y^0 \in C^-, \\ \hat{\varphi}(x)\hat{\varphi}(y), & x^0 \in C^-, y^0 \in C^+, \end{cases}$$
$$:= \hat{\varphi}(x)\hat{\varphi}(y)\Theta_C(x^0 - y^0) + \hat{\varphi}(y)\hat{\varphi}(x)\Theta_C(y^0 - x^0),$$

$$(3.14)$$

where we have defined the Keldysh contour step function $\Theta_C(x^0 - y^0)$ on the last line. The time-ordered two-point functions can be expressed in terms of the contour sources $J^{\pm}(x)$ as

$$\frac{\delta^2 Z[\rho, J]}{i\delta J^+(x) i\delta J^+(y)}\bigg|_{J=0} = \langle \hat{\varphi}(x)\hat{\varphi}(y)\Theta(x^0 - y^0) + \hat{\varphi}(y)\hat{\varphi}(x)\Theta(y^0 - x^0)\rangle$$
$$:= G^{++}(x, y) + \phi(x)\phi(y), \qquad (3.15)$$

$$\frac{\delta^2 Z[\rho, J]}{i\delta J^-(x) i\delta J^-(y)}\bigg|_{J=0} = \langle \hat{\varphi}(x)\hat{\varphi}(y)\Theta(y^0 - x^0) + \hat{\varphi}(y)\hat{\varphi}(x)\Theta(x^0 - y^0)\rangle$$
$$:= G^{--}(x, y) + \phi(x)\phi(y), \qquad (3.16)$$

$$\frac{\delta^2 Z[\rho, J]}{i\delta J^+(x) i\delta J^-(y)}\bigg|_{J=0} = \langle \hat{\varphi}(y)\hat{\varphi}(x)\rangle := G^{+-}(x, y) + \phi(x)\phi(y), \qquad (3.17)$$

$$\frac{\delta^2 Z[\rho, J]}{i\delta J^-(x) i\delta J^+(y)}\bigg|_{J=0} = \langle \hat{\varphi}(x)\hat{\varphi}(y)\rangle := G^{-+}(x, y) + \phi(x)\phi(y). \qquad (3.18)$$

We remark that the two-point correlation functions in (3.15)–(3.18) are not independent, since $\Theta(x^0 - y^0) + \Theta(y^0 - x^0) = 1$, we have

$$G^{++}(x, y) + G^{--}(x, y) = G^{+-}(x, y) + G^{-+}(x, y). \qquad (3.19)$$

In following chapters, the Keldysh time-ordering will be implicit if not otherwise stated.

3.2 Effective equations of motion

The functional $Z[\rho, J]$ in (3.8) is the time-dependent generalisation of the thermodynamic partition function in the presence of a source J.

Similar to thermodynamics, the physics of the system can be equivalently described in terms of the Legendre transformation of the logarithm of Z with respect to source terms. The procedure of Legendre transforming leads to different parametrisations of the free energy functional Γ. The logarithm of the generating functional is referred to as the effective action W, defined as

$$
\begin{aligned}
Z[\rho, J] &:= \exp[iW[\rho, J]] \\
&= \mathrm{Tr}\left\{\rho(t_i)T_C \exp\left[i \int_{x,C} [\mathcal{L}[\varphi] + J(x)\varphi(x)]\right]\right\},
\end{aligned}
\tag{3.20}
$$

from which the mean field ϕ is obtained by functional variation with respect to the source as

$$
\frac{\delta W[J]}{\delta J(x)} = \frac{1}{Z[J]}\frac{\delta Z[J]}{i\delta J(x)} := \phi(x).
\tag{3.21}
$$

The one-particle irreducible (1PI) effective action $\Gamma[\phi]$ is defined from a Legendre transformation of $Z[J, \rho_0]$ with respect to the one-point source $J(x)$,

$$
\Gamma[\phi] = W[J] - \int_x \frac{\delta W[J]}{\delta J(x)}J(x) \equiv W[J] - \int_x J(x)\phi(x),
\tag{3.22}
$$

and generates all 1PI diagrams of the theory. Successive Legendre transformations with respect to higher-point source terms generalise the concept to nPI effective actions. From (3.22) we can obtain an expression for the source as

$$
\frac{\delta \Gamma[\phi]}{\delta \phi(x)} = -J(x).
\tag{3.23}
$$

In the case of $J = 0$, the mean field extremizes the effective action, and the corresponding field solution, i.e. the solution $\bar{\phi}$ to the stationarity condition

$$
\left.\frac{\delta \Gamma[\phi]}{\delta \phi(x)}\right|_{\phi=\bar{\phi}} = 0,
\tag{3.24}
$$

is referred to as the classical mean field.[2]

---

[2]It is also known as the physical, on-shell field or order parameter.

In the previous chapter we derived equations of motion for the field perturbations of the inflaton field and metric by perturbing the Einstein equations to linear order in perturbations. From these equations the power spectra of fluctuations can be determined and related to observable quantities in the CMB. However, the field perturbations also enter into the classical Friedmann and mean field equations of motion. For example, assuming only the inflaton to be quantised, the effective evolution equations can be obtained by inserting $\hat{\varphi} = \phi + \delta\hat{\phi}$ into the classical evolution equations resulting from the Lagrangian density (2.23) and thereafter evaluating the expectation value of these equations of motion. This procedure leads to the same effective mean field equations obtained from expanding instead the action in perturbations $\delta\hat{\phi}$. Expanding the equations of motion to quadratic order in perturbations, the effective mean field equation of motion reads

$$-\Box\phi + V_{,\phi}(\phi) + \tfrac{1}{2}V_{,\phi\phi\phi}(\phi)\langle\delta\hat{\phi}^2\rangle = 0, \qquad (3.25)$$

where the d'Alembertian operator is defined as

$$\Box_x := \frac{1}{\sqrt{-g(x)}}\partial_\mu\left(\sqrt{-g(x)}g^{\mu\nu}(x)\partial_\nu\right). \qquad (3.26)$$

At quadratic order in perturbations, the quantum fluctuation evolves as a free field,

$$\left[-\Box + M^2(\phi)\right]\delta\hat{\phi} = 0, \quad M^2(\phi) := V_{,\phi\phi}(\phi). \qquad (3.27)$$

A quantum action in which the quantum fluctuations are freely evolving corresponds to a perturbative one-loop approximation of the effective action (3.22). This can be inferred from writing $\hat{\varphi} = \phi + \sqrt{\hbar}\delta\hat{\phi}$ and expanding to linear order in $\hbar$.

The corrections to the mean field ϕ enter indirectly into the power spectrum of perturbations by changing the relation between the slow-roll parameters, which are defined in terms of the inflaton potential $V(\phi)$. Importantly, albeit rather unsurprisingly, the resulting corrections enter the mean field and Friedmann equations differently. The effective potentials in these equations are therefore different, and as a result the slow-roll relations (2.29) based on the classical equations (2.26) do no longer hold.

In a similar manner, a quantised metric $\hat{g}^{\mu\nu} = \bar{g}^{\mu\nu} + \delta\hat{g}^{\mu\nu}$ will result in metric quantum corrections to (3.25). The above general procedure to obtain quantum-corrected equations of motion can then be expressed as

$$\left\langle \left. \frac{\delta S[\phi, g^{\mu\nu}]}{\delta\phi} \right|_{\phi \to \phi + \delta\phi} \right\rangle = 0, \quad \left\langle \left. \frac{\delta S[\phi, g^{\mu\nu}]}{\delta g^{\mu\nu}} \right|_{g \to \bar{g} + \delta g} \right\rangle = 0. \quad (3.28)$$

The advantage of quantising at the level of the equations of motion is that it is straightforward to include metric perturbations. This is in contrast to effective action descriptions, since a quantum theory of gravity has yet to be established. One reason for this is that the non-linear nature of general relativity does not lend itself to a straightforward construction of a consistent renormalisation scheme.

As mentioned in the previous chapter, and which we will see explicitly in chapter 5, one-loop metric corrections are proportional to $(H/M_{\text{Pl}})^2$. They are therefore parametrically suppressed far below the Planck scale. Due to this parametric suppression of metric quantum corrections and the difficulties associated with renormalisation, quantum field theory on curved spacetimes is typically formulated using a semi-classical description.

In the semi-classical approximation, the effective action (3.22) applied to curved spacetimes $g^{\mu\nu} \neq \eta^{\mu\nu}$ provides an alternative route to the effective equations of motion, via

$$\frac{\delta\Gamma[\phi, g^{\mu\nu}]}{\delta\phi} = 0, \quad \frac{\delta\Gamma[\phi, g^{\mu\nu}]}{\delta g^{\mu\nu}} = 0. \quad (3.29)$$

Note here that the effective action is formulated in terms of the mean field ϕ. In a single scalar model with classical action

$$S[\phi, g^{\mu\nu}] = \int_x \left[\Lambda_{\text{cc}} + c_1 R - \tfrac{1}{2}\partial_\mu\phi\partial^\mu\phi - V(\phi, g^{\mu\nu}) \right], \quad (3.30)$$

where Λ_{cc} represents the cosmological constant and c_1 is an arbitrary (bare) constant, the second equation in (3.29) is given by

$$2c_1 G_{\mu\nu} - g_{\mu\nu}\Lambda_{\text{cc}} = \langle T_{\mu\nu} \rangle := -\frac{2}{\sqrt{-g}} \frac{\delta\Gamma[\phi, g^{\mu\nu}]}{\delta g^{\mu\nu}}, \quad (3.31)$$

where $G_{\mu\nu} := R_{\mu\nu} - \frac{1}{2}g_{\mu\nu}R$. In a one-loop approximation the effective action can be expressed as[3]

$$\Gamma[\phi, g^{\mu\nu}] = S[\phi, g^{\mu\nu}] + \frac{i}{2}\operatorname{Tr}\ln G^{-1}(x, y) := \int_x \mathcal{L}_{\text{eff}}[\phi, g^{\mu\nu}], \quad (3.32)$$

where $G(x, y)$ is the time-ordered Feynman propagator (3.13) and satisfies the equations of motion

$$\left[-\Box_x + M^2(\phi)\right] G(x, y) = -i[-g(x)]^{-1/2}\delta(x - y). \quad (3.33)$$

For a general curved background metric $g_{\mu\nu}(x)$, it is difficult to find explicit forms of the one-loop term in (3.32) and often necessary to resort to approximation schemes suitable to the applications in mind. The most widely used method to obtain explicit expressions of the effective action in curved spacetime is the Schwinger-DeWitt expansion[4] [6, 87]. The Schwinger-DeWitt representation of the propagator may also be used to renormalise the action (3.32), which we will turn to next.

3.3 Renormalisation in curved spacetime

The use of the effective action (3.32) in the semi-classical approximation allows for consistent renormalisation of the effective equations of motion (3.29). On curved backgrounds it is not possible to resort to normal-ordering or vacuum subtraction since in this case the vacuum expectation values are ambiguous.

3.3.1 Renormalisation of the effective action

To illustrate the renormalisation procedure at the level of the effective action, we consider the scalar model (3.30) with the potential

$$V(\phi, g^{\mu\nu}) = \frac{1}{2}(m^2 + \xi R)\phi^2 + \frac{1}{4!}\lambda\phi^4. \quad (3.34)$$

The Schwinger-DeWitt expansion allows one to express the one-loop term in (3.32) as a sum over all possible paths connecting the points x

---

[3]This can be seen using the identities $(\det A)^{-1/2} = \int \mathcal{D}\phi \exp[-\frac{1}{2}\phi A\phi]$ and $\det A = \exp[\operatorname{Tr}\ln A]$ together with (3.33) for a square matrix A.

[4]Also known in this context as the gradient-, derivative- or heat-kernel-expansion.

and y, weighted by a series of coefficients that depend on the space-time curvature. The starting point is the proper-time Schwinger-DeWitt representation of the Feynman propagator

$$G(x, y) = \Delta^{1/2}(x, y) \int_0^\infty \frac{\mathrm{d}s}{(4\pi i s)^{\frac{d}{2}}} \exp\left[\frac{\sigma(x, y)}{2is} - iM^2 s\right] \sum_{n=0}^\infty \tilde{a}_n(x, y)(is)^n,$$
(3.35)

with $M^2 := V_{,\phi\phi}$ and where

$$\Delta(x, y) = [-g(x)]^{-1/2} \det\left[-\partial_\mu^x \partial_\nu^y \sigma(x, y)\right] [-g(y)]^{-1/2},$$
(3.36)

is the Van Vleck-Morette determinant and

$$\sigma^2(x, y) = \tfrac{1}{2} l(x, y)^2,$$
(3.37)

where $l(x, y)$ is the proper geodesic distance between x and y. The first three coefficients in the sum in (3.35) are given by [87] (see also [88–90]):

$$\begin{aligned}
\lim_{x \to y} \tilde{a}_0(x, y) &= 1, \\
\lim_{x \to y} \tilde{a}_2(x, y) &= \left(\tfrac{1}{6} - \xi\right) R, \\
\lim_{x \to y} \tilde{a}_3(x, y) &= \tfrac{1}{180} R_{\mu\nu\rho\sigma} R^{\mu\nu\rho\sigma} - \tfrac{1}{180} R_{\mu\nu} R^{\mu\nu} \\
&\quad - \tfrac{1}{6}\left(\tfrac{1}{5} - \xi\right) \Box R + \tfrac{1}{2}\left(\tfrac{1}{6} - \xi\right)^2 R^2,
\end{aligned}$$
(3.38)

and become increasingly complicated at higher orders. An alternative form of (3.35) was proposed in [91] which sums the contributions from the curvature R. In this form, the propagator is expressed (implicitly) as a sum over modes that are solutions of the Klein-Gordon equation, where each mode is weighted by a factor that depends on the Ricci curvature. This representation can be written as in (3.35) but with the effective mass M^2 replaced by

$$M_{\text{SDW}}^2(\phi) := M^2(\phi) - \tfrac{1}{6} R,$$
(3.39)

41

and the first three coefficients in (3.38) exchanged in favour of

$$\lim_{x \to y} a_0(x, y) = 1,$$

$$\lim_{x \to y} a_2(x, y) = 0,$$

$$\lim_{x \to y} a_3(x, y) = \tfrac{1}{180} R_{\mu\nu\rho\sigma} R^{\mu\nu\rho\sigma} - \tfrac{1}{180} R_{\mu\nu} R^{\mu\nu} - \tfrac{1}{6} \left(\tfrac{1}{5} - \xi \right) \Box R.$$

(3.40)

The first term in the expansion (3.35) corresponds to the free propagator, and which describes the behaviour of the field in flat spacetime. Higher order terms with $n \geq 3$ involve integrals over the curvature tensor and its derivatives, and become increasingly complicated as the order of the expansion increases.

With dimensional regularisation we are free to take the coincidence limit, and using the representation (3.35), the one-loop contribution in (3.32) can be expressed as[5]

$$\frac{i}{2} \operatorname{Tr} \ln G^{-1}(x, x) = -\frac{i}{2} \mu^{4-d} \int \mathrm{d}^d x \sqrt{-g} \int_0^\infty \frac{\mathrm{d}s}{s} K(s; x, x), \quad (3.41)$$

where the coefficients of (3.35) defines the kernel function K by

$$K(s; x, x) = \frac{i}{(4\pi i s)^{d/2}} \exp\left[-i M_{\mathrm{SDW}}^2 s \right] \sum_{n=0}^\infty a_n(x, x)(is)^n, \quad (3.42)$$

and the integral is regularised with $d = 4 - \epsilon$ and the scale μ ensures the correct dimension of the action. Since the expansion (3.35) is an expansion in small proper time argument, the divergences in the integral (3.41) arise at $s = 0$ for $d = 4$. The ultraviolet (UV) sector of the theory therefore corresponds to the $s \simeq 0$ region. Note that the expansion (3.35) serves as the starting point of other regularisation schemes, besides dimensional regularisation. Namely, it is possible to regularise (3.32) by ζ-function regularisation set in Euclidean spacetime, as well as by point-splitting regularisation, in which x and y are kept separated. The point-splitting procedure was first used to renormalise the two-point function in de Sitter spacetime in [92].

---

[5]This can be seen from a variation of the one-loop contribution, namely

$$\delta \frac{i}{2} \operatorname{Tr} \ln G^{-1} = \frac{i}{2} \delta G^{-1} G = -\frac{1}{2} \int_0^\infty \mathrm{d}s \, \delta G^{-1} \exp[-is G^{-1}] = \delta \left[-\frac{i}{2} \int_0^\infty \frac{\mathrm{d}s}{s} \operatorname{Tr} \exp[-is G^{-1}] \right].$$

With the ansatz (3.41), the resulting one-loop term in the effective action (3.32) becomes

$$-\frac{i}{2}\operatorname{Tr}\ln G(x,x) = \int \mathrm{d}^d x \sqrt{-g}\, \frac{(M_{\text{\tiny SDW}}^2/\mu)^{d-4}}{2(4\pi)^{d/2}} \sum_{n=0}^{\infty} M_{\text{\tiny SDW}}^{4-2n} a_n(x,x)\Gamma\left(n-\frac{d}{2}\right),$$
(3.43)

which generalises the Coleman-Weinberg result [93] in flat spacetime.

In (3.43) the gamma function diverges for the first three terms in the sum over n. These divergences are geometrical, and appear as coefficients of the Ricci curvature and higher-order gravitational tensors. This is expected since the divergences originate from the UV behaviour of the modes, which is only sensitive to the local spacetime features. For this reason, in order to renormalise the one-loop effective action, the divergences are better regarded as contributions to the gravitational sector of the theory. To accommodate the counterterms needed to cancel the divergent coefficients in (3.43), the gravitational sector is extended to

$$S_{\text{g}}[g^{\mu\nu}] = \int_x \left[\Lambda_{\text{cc}} + c_1^{\text{b}} R + c_2^{\text{b}} R^2 + c_3^{\text{b}} R_{\mu\nu} R^{\nu\mu} + c_4^{\text{b}} R_{\mu\nu\rho\sigma} R^{\sigma\rho\nu\mu}\right],$$
(3.44)

where the $c_1^{\text{b}}, \ldots, c_4^{\text{b}}$ are unrenormalised constants. By reparametrising all the constants c of the theory as $c^{\text{b}} = c + \delta c$ in the usual manner, the renormalisation conditions are then analogous to the ones of perturbative renormalisation in flat spacetime. The renormalised parameters in the one-loop effective potential are required to match the ones of the classical action at some scale μ, i.e., with (3.32), we impose

$$\mathcal{L}_{\text{eff}}[\phi, g^{\mu\nu}]\big|_{X_\mu} = \mathcal{L}[\phi, g^{\mu\nu}]\big|_{X_\mu},$$
$$\frac{\partial \mathcal{L}_{\text{eff}}[\phi, g^{\mu\nu}]}{\partial X}\bigg|_{X_\mu} = \frac{\partial \mathcal{L}[\phi, g^{\mu\nu}]}{\partial X}\bigg|_{X_\mu},$$
(3.45)

for

$$X = \{\dot{\phi}^2,\ \phi^2,\ \phi^2 R,\ R^2,\ R_{\alpha\beta} R^{\beta\alpha},\ R_{\mu\nu\rho\sigma} R^{\sigma\rho\nu\mu}\}.$$
(3.46)

The quantum-corrected Einstein- and field equations of motion can then be obtained by functional variations of the renormalised effective Lagrangian (3.32). The renormalisation conditions provide well-defined

43

finite physical constants of the theory at the renormalisation scale. However, due to the expansion in (3.42), the conditions (3.45) fixes the physical values of the parameters in Minkowski spacetime. This limits the range of applicability of the Schwinger-DeWitt effective action in physical phenomena.

3.3.2 Adiabatic subtraction

An alternative route to obtaining renormalised effective equations of motion is via adiabatic subtraction. In this scheme, the subtraction terms correspond to the divergent quantities of interest expanded to nth order around the adiabatic vacuum. For the variance and energy-momentum tensor, this can be written schematically as

$$
\begin{aligned}
\langle \hat{\varphi}^2(x) \rangle_{\text{finite}} &= \langle \hat{\varphi}^2(x) \rangle_{\text{bare}} - \langle 0^{(n)} | \hat{\varphi}^2(x) | 0^{(n)} \rangle_{n=2}, \\
\langle \hat{T}_{\mu\nu}(x) \rangle_{\text{finite}} &= \langle \hat{T}_{\mu\nu}(x) \rangle_{\text{bare}} - \langle 0^{(n)} | \hat{T}_{\mu\nu}(x) | 0^{(n)} \rangle_{n=4},
\end{aligned}
\tag{3.47}
$$

where $\langle \hat{\varphi}^2(x) \rangle := \lim_{y \to x} \langle \hat{\varphi}(x) \hat{\varphi}(y) \rangle$. With adiabatic subtraction finite quantities can therefore be obtained directly at the level of the equations of motion, where the metric can be fixed. This circumvents the necessary approximations needed to obtain an explicit expression of the one-loop effective potential in the case of a general metric.

The adiabatic quantities are found using the WKB approximation which assumes slowly-varying mode functions. In this approximation, the mode solution to the free equation of motion (3.27) is often represented using the WKB ansatz

$$
\varphi_k(t) = \frac{1}{\sqrt{2a^3 \Omega_k(t)}} \exp\left[-i \int_0^t dt' \Omega_k(t') \right].
\tag{3.48}
$$

On an FRW background, the adiabatic expansion can be written

$$
\Omega_k^2(t) = \omega_k^2(t) - \frac{3}{2}\dot{H} - \frac{9}{4}H^2 - \frac{1}{2}\frac{\ddot{\Omega}_k}{\Omega_k} + \frac{3}{4}\left(\frac{\dot{\Omega}_k}{\Omega_k}\right)^2,
\tag{3.49}
$$

where $\omega_k^2(t) := k^2/a^2 + M^2(\phi)$. By iteratively solving for (3.49), the mode functions $\varphi_k(t)$ are approximated to adiabatic order n by keeping terms containing n time derivatives, and the operator $a_{\mathbf{k}}$ can be chosen

to annihilate the nth order adiabatic vacuum $\left|0^{(n)}\right\rangle$. These approximate mode functions are then used in the expressions (3.47). In this way, the subtraction takes place at the level of the mode integrand, so that (would-be) divergences are cancelled before evaluating the mode integral. As a consequence, the coincide limit can be taken from the start, and no actual regularisation is necessary. A closely related method to adiabatic subtraction is Pauli-Villars regularisation.

The range applicability of adiabatic expansion is mainly in the UV regime, which can be seen from that the expansion in (3.49) corresponds to an expansion in powers of inverse momentum.[6] This is similar to the proper-time expansion in (3.42), and the two expansion schemes are in fact related. The Schwinger-DeWitt expansion corresponds to an adiabatic expansion of the propagator [44], while the adiabatic expansion is made at the level of the mode functions.

While adiabatic subtraction is a more straightforward route to obtaining a finite expression for the energy-momentum tensor than via the renormalised effective action, it is not a renormalisation scheme. The absence of an explicit dependence on a renormalisation scale poses a challenge for establishing physical interpretations. In the case of a free scalar field, it was shown in [94] that adiabatic subtraction corresponds to a reparametrisation of the original constants of the theory. The same does not apply to interacting theories since in this case the finite expression contains terms that are not polynomials in the field, see e.g. [67]. A proposal to circumvent this was made in [95] in which (3.47) was chosen as renormalisation conditions and computed using a modified Schwinger-DeWitt expansion of the propagator. This however undermines the computational simplicity of the adiabatic scheme.

In [67] a renormalisation scheme was suggested with renormalisation conditions reminiscent to (3.45) but for the energy-momentum tensor. The procedure is based on that the quantity of interest is expanded in mode

---

[6]This can be seen e.g. at leading WKB order, $\Omega_k^0 = \omega_k$, for which (3.49) gives

$$(a\Omega_k^0)^2 = (a\omega_k)^2 \left[1 - \frac{a''/a}{(a\omega_k)^2}\left(1 + \frac{1}{2}\left(\frac{aM}{a\omega_k}\right)^2\right) - \frac{\mathcal{H}^2}{(a\omega_k)^2}\left(\frac{1}{2}\left(\frac{aM}{a\omega_k}\right)^2 - \frac{5}{4}\left(\frac{aM}{a\omega_k}\right)^4\right)\right].$$

solutions around an appropriate vacuum and the divergences are absorbed by counterterms from both the matter- and extended gravitational sectors. Schematically the renormalised energy-momentum tensor is given by

$$\langle \hat{T}_{\mu\nu} \rangle_{\text{ren}} := \langle \hat{T}_{\mu\nu} \rangle_{\text{bare}} + \delta T^{\text{m}}_{\mu\nu} - \delta T^{\text{g}}_{\mu\nu}, \qquad (3.50)$$

where $\delta T^{\text{m}}_{\mu\nu}$ is the counterterm from the matter sector and the corresponding one from the gravitational sector reads

$$\delta T^{\text{g}}_{\mu\nu} = -g_{\mu\nu}\delta\Lambda_{\text{cc}} + 2\delta c_1 G_{\mu\nu} + 2\delta c_2 H^{(1)}_{\mu\nu} + 2c_3 H^{(2)}_{\mu\nu} + 2\delta c_4 H_{\mu\nu}, \quad (3.51)$$

where the above gravitational tensors are defined in Appendix 3.A. The renormalisation conditions amount to fixing the parameters of the effective energy-momentum tensor to the ones of the classical energy-momentum tensor. For example, on an FRW background, the parameters can be fixed using the temporal component of the energy-momentum tensor,

$$\langle \hat{T}_{00} \rangle|_{X_\mu} = \bar{T}_{00}|_{X_\mu}, \quad \left.\frac{\partial\langle \hat{T}_{00} \rangle}{\partial X}\right|_{X_\mu} = \left.\frac{\partial\bar{T}_{00}}{\partial X}\right|_{X_\mu}, \qquad (3.52)$$

with

$$X = \{\dot{\phi}^2,\ \phi^2,\ \phi^4,\ \phi\dot{\phi}(\dot{a}/a),\ (\dot{a}/a)^2,\ (\dot{a}/a)^2(\ddot{a}/a),\ (\ddot{a}/a)^2,\ (\dot{a}/a)^4\}.$$
$$(3.53)$$

Note that the renormalisation conditions can equally well be formulated in terms of any other component of $T_{\mu\nu}$.

The above renormalisation procedure shares the advantages of adiabatic subtraction, but with the important difference that the mode expansion is not restricted to be adiabatic, i.e. around Minkowski space. Instead one may use for instance the (semi-)de Sitter solution (2.46), as was done in [69]. On a (semi-)de Sitter background, the asymptotic UV behaviour of the modes is the same as in Minkowski, given that they are chosen to annihilate the Bunch-Davies vacuum (2.51). However, unlike in the Schwinger-DeWitt procedure, the renormalisation conditions (3.52) do not imply the parameters to be fixed in flat space.

In chapter 5 we compute the effective equations of motion in a semi-de Sitter spacetime including metric scalar- and tensor degrees of freedom.

While we chose an MS-like renormalisation prescription, we expect that the method proposed in [67] would be an appropriate alternative.

The Schwinger-DeWitt procedure and adiabatic regularisation scheme provide good descriptions of physics at small length scales. While these methods can successfully regulate and remove UV divergences, they do not address potential IR divergences that may arise in certain situations. It is therefore necessary to supplement the renormalisation procedure with an appropriate IR treatment for a complete description of a given quantum field theory on curved spacetime.

3.3.3 Renormalisation on black hole spacetimes

The renormalisation procedures of the quantised energy-momentum tensor discussed in the previous section can be applied to backgrounds other than the FRW metric. We will in this section briefly remark on the interesting case that is the spherically symmetric black hole spacetime. Hawking discovered black hole evaporation by utilising the Bogoliubov coefficients in a Schwarzschild metric [96]. The notion of particle number in terms of Bologubov coefficients is a global concept, as it concerns only the field modes defined on a given large-scale background. However, since a physical detector is at least semi-local in space, it is often more useful to compute locally defined quantities to obtain information concerning the number of particles that are present. The energy-momentum tensor is often the most relevant locally defined quantity of interest, and it is the more appropriate quantity for analysing the semi-classical evolution of an evaporating black hole.

The renormalised energy-momentum tensor was first computed for a Schwarzschild background in [97, 98] and for static spherically symmetric spacetimes in [99, 100], using methods based on the point-splitting procedure of [101]. While point-splitting is the preferred regularisation scheme on black hole backgrounds,[7] the fact that the mode functions have to be solved for numerically presents its own set of challenges.

---

[7]On black hole spacetimes the divergences in metric coefficients that arise close to the event horizon complicates the use of dimensional regularisation. Dimensional regularisation involves manipulating the metric in a global way, which can introduce new divergences. In contrast, point-splitting is in general coordinate-independent and for this reason often the regularisation method of choice in the context of black holes.

Namely, in [97] a method was developed for numerical implementations of point-splitting based on a WKB expansion of the modes set in Euclidean time. However, this procedure can not be applied to evolving backgrounds, and computing the renormalised energy-momentum tensor in a four-dimensional, spherically symmetric and time-dependent background remains a challenging task and is an active area of research. See e.g. [102–105].

Numerical simulations of black hole formation following gravitational collapse has been subject to intensive study in the case of classical scalar fields, see e.g. [106–113]. However, to date only a limited number of studies have investigated the quantum field dynamics around black holes formed by gravitational collapse of the quantum fields themselves. See however [114–116]. The quest for numerical evidence of black hole evaporation following the collapse of a quantum field will be commented on in the last chapter of this thesis.

3.A   Geometric tensors

In this appendix we gather some identities for the functional variation of some gravitational quantities with respect to the metric $g^{\mu\nu}$. The Einstein tensor is given by

$$G_{\mu\nu} := \frac{1}{\sqrt{-g}} \frac{\delta}{\delta g^{\mu\nu}} \int \mathrm{d}^d x \sqrt{-g} R = -\frac{1}{2} g_{\mu\nu} R + R_{\mu\nu}, \qquad (3.54)$$

and for an action with some arbitrary scalar function $f(x)$ multiplied with the curvature, a metric variation gives

$$\frac{1}{\sqrt{-g}} \frac{\delta}{\delta g^{\mu\nu}} \int \mathrm{d}^d x \sqrt{-g} R f(x) = \left[-\frac{1}{2} g_{\mu\nu} R + R_{\mu\nu} - \partial_\mu \partial_\nu + g_{\mu\nu} \Box \right] f(x).$$
$$(3.55)$$

The variation of the higher-order gravitational tensors in (3.44) are given by [95]

$$
\begin{aligned}
H_{\mu\nu}^{(1)}(x) &:= \frac{1}{\sqrt{-g}} \frac{\delta}{\delta g^{\mu\nu}} \int \mathrm{d}^d x \sqrt{-g}\, R^2 \\
&= -\tfrac{1}{2} g_{\mu\nu} R^2 + 2 R_{\mu\nu} R - 2 \partial_\mu \partial_\nu R + 2 g_{\mu\nu} \Box R, \quad\quad (3.56)
\end{aligned}
$$

$$
\begin{aligned}
H_{\mu\nu}^{(2)}(x) &:= \frac{1}{\sqrt{-g}} \frac{\delta}{\delta g^{\mu\nu}} \int \mathrm{d}^d x \sqrt{-g}\, R_{\mu\nu} R^{\mu\nu} \\
&= -\tfrac{1}{2} g_{\mu\nu} R_{\rho\sigma} R^{\rho\sigma} + 2 R_{\rho\nu\sigma\mu} R^{\rho\sigma} - \nabla_\mu \nabla_\nu R + \tfrac{1}{2} g_{\mu\nu} \Box R + \Box R_{\mu\nu},
\end{aligned}
$$
$$(3.57)$$

$$
\begin{aligned}
H_{\mu\nu}(x) &:= \frac{1}{\sqrt{-g}} \frac{\delta}{\delta g^{\mu\nu}} \int \mathrm{d}^d x \sqrt{-g}\, R_{\mu\nu\rho\sigma} R^{\mu\nu\rho\sigma} \\
&= -\tfrac{1}{2} g_{\mu\nu} R_{\rho\sigma\kappa\lambda} R^{\rho\sigma\kappa\lambda} + 2 R_\mu{}^{\rho\sigma\kappa} R_{\nu\sigma\kappa} - 4 R_{\mu\rho} R^\rho{}_\nu + 4 \Box R_{\mu\nu} \\
&\quad - 2 \nabla_\mu \nabla_\nu R. \quad\quad (3.58)
\end{aligned}
$$

In four dimensions the higher-order tensors are related by the Gauss-Bonnet theorem,

$$
\frac{1}{\sqrt{-g}} \frac{\delta}{\delta g^{\mu\nu}} \int \mathrm{d}^d x \sqrt{-g} \left[R^2 - 4 R_{\mu\nu} R^{\mu\nu} + R_{\mu\nu\rho\sigma} R^{\mu\nu\rho\sigma} \right] = 0, \quad (3.59)
$$

such that

$$
H_{\mu\nu} = -H_{\mu\nu}^{(1)} + 4 H_{\mu\nu}^{(2)}. \quad\quad (3.60)
$$

4 The two-particle-irreducible formalism

By operating with dressed quantities, resummation schemes provide an improvement of perturbation theory by summing certain classes of diagrams to all orders. The 2PI formalism extends the concept of the 1PI effective action by treating the propagators of the theory, in addition to the mean fields, as fundamental degrees of freedom. The field and propagator equations of motion are self-consistent and involve infinite loop resummations. Approximations to the exact theory are obtained by truncating the diagrammatic expansion at some order in a small expansion parameter, and provides a systematic resummation prescription. All truncations of the 2PI effective action satisfy the global symmetries of the Lagrangian. In particular, this means that all truncations are energy conserving, which makes them appropriate to study field dynamics in closed systems.

The 2PI resummation scheme was first developed for condensed matter applications in [32–34] and extended to relativistic theories in [35]. In this chapter we present the 2PI formalism for non-equilibrium quantum field dynamics, its connection to classical-statistical descriptions and the main features of its renormalisation procedure. In the last parts of this chapter we introduce the main subtleties and issues regarding the 2PI description for gauge fields, which sets the stage for the investigation in chapter 7. We refer the reader to [29, 86] for a detailed introduction to the 2PI framework, its properties and applications.

4.1 The 2PI effective action

The two-particle irreducible action extends the non-equilibrium generating functional (3.8) by incorporating an additional bi-local source term $R(x, y)$, such that

$$
\begin{aligned}
Z[\rho, J] = \text{Tr} \Bigg\{ & \rho(t_i) T_C \exp \Bigg[i \int_{x,C} [\mathcal{L}[\varphi] + J(x)\varphi(x)] \\
& + \frac{i}{2} \int_{xy,C} \varphi(x) R(x, y) \varphi(y)] \Bigg] \Bigg\}.
\end{aligned}
\tag{4.1}
$$

Here the macroscopic field $\phi(x) := \langle \varphi(x) \rangle$ and connected two-point function $G(x, y)$ are obtained by functional variation of the effective action $W[J, R] := -i \ln Z[J, R]$ as

$$\phi(x) := \frac{\delta W[J, R]}{\delta J(x)}, \quad G(x, y) := 2 \frac{\delta W[J, R]}{\delta R(x, y)} - \phi(x)\phi(y). \quad (4.2)$$

The 2PI effective action is obtained by a Legendre transform with respect to the one-point and two-point source terms,

$$\Gamma[\phi, G] = W[J, R] - \int_x \phi(x)J(x)$$
$$- \frac{1}{2} \int_{xy} R(x, y)\phi(x)\phi(y) - \frac{1}{2} \int_{xy} R(x, y)G(y, x), \quad (4.3)$$

where the source terms can be expressed as

$$\frac{\delta \Gamma[\phi, G]}{\delta \phi(x)} = -J(x) - \int_y R(x, y)\phi(y), \quad (4.4)$$

$$\frac{\delta \Gamma[\phi, G]}{\delta G(x)} = -\frac{1}{2} R(x, y). \quad (4.5)$$

In the 2PI formalism, the mean field ϕ and dressed propagator G constitute the fundamental degrees of freedom. The effective action (4.3) can be parametrised as

$$\Gamma[\phi, G] = S_0[\phi] + ic\text{Tr}[\ln G^{-1} + G_0^{-1}G] + \Gamma_2[\phi, G] + \text{const.,} \quad (4.6)$$

where $c = 1/2$ for bosons, $c = -1$ for fermions and

$$S_0[\phi] = \frac{1}{2} \int_{xy} \phi(x)G_0^{-1}(x, y)\phi(y), \quad (4.7)$$

is the free action. The functional Γ_2 contains all closed 2PI skeleton diagrams of the theory, i.e. the diagrams that are void of self-energy insertions, consisting only of dressed propagators and tree-level vertices. Since each internal line in the diagrammatic expansion corresponds to a dressed propagator, the expansion is resummed. The 2PI effective action (4.6) is an exact representation of the generating functional Z of the theory, and a truncation of the series of diagrams in Γ_2 defines a systematic

approximation to it. For a given truncation, the approximate mean field and propagators can be defined by means of functional variation.

The equations of motion for the mean field and propagator are given by the stationarity conditions, i.e. (4.5) with vanishing source terms,

$$\frac{\delta\Gamma[\phi, G]}{\delta\phi(x)} = \int_y G_0^{-1}(x, y)\phi(y) + \frac{\delta\Gamma_2[\phi, G]}{\delta\phi(x)} = 0, \tag{4.8}$$

$$\frac{\delta\Gamma[\phi, G]}{\delta G(x, y)} = ic\left[-G^{-1}(x, y) + G_0^{-1}(x, y)\right] + \frac{\delta\Gamma_2[\phi, G]}{\delta G(x, y)} = 0. \tag{4.9}$$

By defining the self-energy

$$\Sigma(x, y; \phi, G) := \frac{i}{c}\frac{\delta\Gamma_2[\phi, G]}{\delta G(x, y)}, \tag{4.10}$$

the propagator equation of motion (4.9) reads

$$G^{-1}(x, y) = G_0^{-1}(x, y) - \Sigma(x, y). \tag{4.11}$$

The equations of motion for the mean field (4.8) and propagator (4.9) are self-consistent and provide a resummation scheme for each quantity.

In a similar way the nPI effective action can be defined as the generating functional of n-point functions with $n > 2$, by including higher-point external source terms $K(x, y, z)$, $L(x, y, z, w)$, ... in the generating functional $W[J, R, K, L, \dots]$ and performing Legendre transformations. The nPI effective action resums all 1-, ..., n-point functions of the theory. In the absence of sources, the nPI effective action is reduced to the $(n-1)$PI effective action when the n-point functions are evaluated at their stationary point, i.e. when they fulfil their stationarity condition. For example, the 1PI effective action is equivalent to the 2PI effective action when the propagator is the solution to (4.9), i.e. $\Gamma_{1\text{PI}}[\phi] \equiv \Gamma_{2\text{PI}}[\phi, \bar{G}]$ with $\bar{G}$ being the stationary point solution for the propagator. This property is known as the equivalence hierarchy for nPI effective actions. Note that this hierarchy is only valid for the exact theory, it is not conserved in truncations of the nPI effective action in general.

4.1.1 Statistical and spectral propagators

It is useful to make the time-ordering of the Keldysh contour C explicit in the above relations. With the two-point functions given by (3.13), the

time-ordered part of the propagator (3.14) can be rewritten as a sum of time-ordered expectation values of an anti-commutator and commutator of the field operators. Explicitly,

$$\begin{aligned}
\langle T_C \varphi(x)\varphi(y) \rangle &= \langle \varphi(x)\varphi(y) \rangle \Theta_C(x^0 - y^0) - \langle \varphi(y)\varphi(x) \rangle \Theta_C(y^0 - x^0) \\
&= \tfrac{1}{2} \langle \{\varphi(x), \varphi(y)\} \rangle [\Theta_C(x^0 - y^0) + \Theta_C(y^0 - x^0)] \\
&\quad + \tfrac{1}{2} \langle [\varphi(x), \varphi(y)] \rangle [\Theta_C(x^0 - y^0) - \Theta_C(y^0 - x^0)].
\end{aligned}$$
$$(4.12)$$

The propagator can then be expressed as

$$G(x, y) = G_{(F)}(x, y) - \frac{i}{2} G_{(\rho)}(x, y) \mathrm{sign}_C(x^0 - y^0), \qquad (4.13)$$

where the expectation values of the anti-commutator and commutator in (4.12) define the statistical and spectral two-point functions,

$$G_{(F)}(x, y) := \tfrac{1}{2} \langle \{\varphi(x), \varphi(y)\} \rangle - \phi(x)\phi(y), \qquad (4.14)$$

$$G_{(\rho)}(x, y) := i \langle [\varphi(x), \varphi(y)] \rangle. \qquad (4.15)$$

Here we have used that $\Theta_C(x^0 - y^0) - \Theta_C(y^0 - x^0) = \mathrm{sign}_C(x^0 - y^0)$. The statistical propagator $G_{(F)}$ contains information about the occupation of states, whereas the spectral propagator $G_{(\rho)}$ carries information about the allowed states. Both propagators are real and have the symmetry properties $G_{(F)}(x, y) = G_{(F)}(y, x)$ and $G_{(\rho)}(x, y) = -G_{(\rho)}(y, x)$. The spectral function reflects the canonical commutation relations via

$$\partial_{x^0} G_{(\rho)}(x, y)\big|_{x^0 = y^0} = -\partial_{y^0} G_{(\rho)}(x, y)\big|_{x^0 = y^0} = \delta^{(3)}(\mathbf{x} - \mathbf{y}). \qquad (4.16)$$

In the above sense, $G_{(F)}$ and $G_{(\rho)}$ correspond to the classical and quantum parts of the total propagator G, respectively. The decomposition (4.13) can also be made analogously for the self-energy Σ defined in (4.10).

Out of equilibrium, the statistical and spectral propagators are independent from each other, whereas in thermal equilibrium they are related via the fluctuation-dissipation theorem, $G(x, y)|_{x^0=0} = G(x, y)|_{x^0=-i\beta}$. In terms of $G_{(F)}$ and $G_{(\rho)}$ this condition reads

$$G_{(F)}^{\mathrm{eq}}(p^0, \mathbf{p}) + \frac{i}{2} G_{(\rho)}^{\mathrm{eq}}(p^0, \mathbf{p}) = e^{-\beta p^0} \left[G_{(F)}^{\mathrm{eq}}(p^0, \mathbf{p}) - \frac{i}{2} G_{(\rho)}^{\mathrm{eq}}(p^0, \mathbf{p}) \right],$$
$$(4.17)$$

where the propagators are expressed in four-dimensional Fourier space,

$$G(x, y) = \int \frac{dp^0 d^3\mathbf{p}}{(2\pi)^4} G(p^0, \mathbf{p}) \exp\{-ip^0(x^0 - y^0) + i\mathbf{p} \cdot (\mathbf{x} - \mathbf{y})\}.$$
(4.18)

In a free bosonic theory, the relation (4.17) becomes

$$G^{\mathrm{eq}}_{(F)}(p^0, \mathbf{p}) = -i\left[\tfrac{1}{2} + n_{\mathrm{BE}}(p^0)\right] G^{\mathrm{eq}}_{(\rho)}(p^0, \mathbf{p}),$$
(4.19)

where $n_{\mathrm{BE}} = (\exp \beta p^0 - 1)^{-1}$ is the Bose-Einstein distribution.

4.1.2 Evolution equations

The gap equation (4.11) can be rewritten as partial integro-differential equations that are well-suited for solving initial value problems. This can be done by convoluting (4.11) with the dressed propagator, such that

$$\int_z G_0^{-1}(x, z)G(z, y) - \int_z \Sigma(x, z)G(z, y) = \delta(x - y),$$
(4.20)

where $\int_z G^{-1}(y, z)G(z, y) = \delta(x - y)$. In terms of the statistical and spectral components, the real and imaginary parts of (4.20) are given by two coupled equations for the statistical and spectral correlators. For a scalar theory, they read

$$[\Box_x + M^2(x)]G_{(F)}(x, y) = -\int_{t_i}^{x^0} dz \Sigma_\rho(x, z)G_{(F)}(z, y)$$

$$+ \int_{t_i}^{y^0} dz \Sigma_F(x, z)G_{(\rho)}(z, y), \qquad (4.21)$$

$$[\Box_x + M^2(x)]G_{(\rho)}(x, y) = -\int_{y^0}^{x^0} dz \Sigma_\rho(x, z)G_{(\rho)}(z, y), \qquad (4.22)$$

where we have used the identity

$$\int_C dy^0 \mathrm{sign}_C(x^0 - y^0) = \int_{t_i}^{x^0} dy^0 + \int_{x^0}^{t_i} dy^0(-1) = 2\int_{t_i}^{x^0} dy^0. \quad (4.23)$$

The diagrammatic expansion of the 2PI effective action can be arranged in terms of e.g. the number of loops or inverse number of field components N of the theory. The 2PI loop expansion is analogue to the

perturbative coupling expansion, the difference being that the internal lines are resummed and only 2PI diagrams are kept. For this reason the convergence of the 2PI loop expansion requires a small coupling. In the $1/N$-expansion the diagrams are arranged according to their powers of N as $N, N^0, N^{-1}, \ldots$, and for sufficiently large N the $1/N$-expansion is not restricted to small couplings.

For a given diagrammatic expansion of Γ_2, the self-energies originating from local diagrams effectively contribute as a time-dependent mass shift to the propagator equation of motion. For this reason, it is useful to define the effective mass and self-energy according to

$$M^2(x) := m^2 + \Sigma_{\text{loc}}(x, x), \quad \Sigma(x, y) := -i\Sigma_{\text{loc}}(x, x) + \Sigma_{\text{nl}}(x, y). \quad (4.24)$$

Note that only the statistical propagator contributes to the effective mass. The non-local self-energies $\Sigma_{\text{nl}}(x, y)$ reflect off-shell and scattering effects that leads to damping, which is necessary for thermalisation of the system [24, 26].

4.1.3 Initial conditions

In order to solve for the equations of motion (4.21) and (4.22), it is necessary to specify the initial conditions. With the parametrisation of the initial density matrix as an exponentiated polynomial of n-point functions in (3.9), the polynomial terms can be thought of as source terms that exist only at initial time. By truncating the polynomial (3.10) at quadratic order, these initial source terms can then be absorbed into the local and bi-local source terms in the generating functional (4.1). This choice of initial density matrix corresponds to Gaussian initial conditions, for which the generating functional takes the form

$$Z[J, R] = \int \mathcal{D}\varphi \exp\left[i\left(S[\varphi] + \int_x J(x)\varphi(x) + \frac{1}{2}\int_{xy} \varphi(x)R(x, y)\varphi(y)\right)\right],$$
$$(4.25)$$

with an implicit closed time-path ordering.

There are several instances where the choice of a Gaussian initial density matrix is well-motivated. One example of this, mentioned in the previous chapter, is the initial conditions for post-inflationary field

dynamics. For instance, field dynamics during reheating have been studied in e.g. [117, 118] using the 2PI formalism with Gaussian initial conditions. In the case of a non-Gaussian initial density matrix, it is necessary to account for the additional initial-time sources. For this reason it is more efficient to describe them in terms of nPI effective actions. However, while technically more involved, it is nevertheless possible to implement non-Gaussian initial conditions in the 2PI framework. See e.g. [119] for an implementation of a thermal initial density matrix.

To solve the second-order differential evolution equations in (4.21) and (4.22), it is necessary to specify the values of the propagators and their first time derivatives at initial time. The spectral function is constrained to satisfy the canonical commutation relation (4.16) at all times. The statistical propagator is not subjected to any constraints at initial time and the solution to (4.21) must therefore be supplemented with initial conditions on $G_{(F)}(x, y)$ and its first derivative. Since Gaussian initial conditions correspond to a free theory, we may write for the statistical propagator[1]

$$
\begin{aligned}
G_{(F)}(t, t'; \mathbf{p})\big|_{t,t'=0} &= \frac{1}{2}\langle\{\varphi_{\mathbf{p}}(t)\varphi_{\mathbf{p}}^*(t')\}\rangle = \frac{1}{\omega_{\mathbf{p}}}\left(n_{\mathbf{p}} + \tfrac{1}{2}\right), \\
\partial_t G_{(F)}(t, t'; \mathbf{p})\big|_{t=t'=0} &= \frac{1}{2}\langle\{\pi_{\mathbf{p}}(t)\varphi_{\mathbf{p}}^*(t')\}\rangle = 0, \qquad\qquad (4.26) \\
\partial_t \partial_{t'} G_{(F)}(t, t'; \mathbf{p})\big|_{t=t'=0} &= \frac{1}{2}\langle\{\pi_{\mathbf{p}}(t)\pi_{\mathbf{p}}^*(t')\}\rangle = \omega_{\mathbf{p}}\left(n_{\mathbf{p}} + \tfrac{1}{2}\right),
\end{aligned}
$$

where $\pi_{\mathbf{p}}(t)$ is the conjugate momentum of $\phi_{\mathbf{p}}(t)$, the frequency is $\omega_{\mathbf{p}} = \sqrt{\mathbf{p}^2 + m^2}$ with m the renormalised mass and $n_{\mathbf{p}}$ is some particle number distribution. For example, a vacuum initial state corresponds to $n_{\mathbf{p}} = 0$. For a (free) bosonic system that is initially in thermal equilibrium, one may set $n_{\mathbf{p}}$ to the Bose-Einstein distribution, $n_{\mathbf{p}} = (\exp\beta\omega_{\mathbf{p}} - 1)^{-1}$. Note that all ingoing quantities in (4.26) should be understood to be evaluated at initial time.

---

[1]Assuming spatial isotropy, we define the spatial Fourier transform of a propagator $G(x, y)$ as

$$
G(x, y) = G(t, t'; \mathbf{x} - \mathbf{y}) = \int \frac{\mathrm{d}^3\mathbf{p}}{(2\pi)^3} e^{i\mathbf{p}\cdot(\mathbf{x}-\mathbf{y})} G(t, t'; \mathbf{p}),
$$

where $t := x^0$ and $t' := y^0$.

4.1.4 The classical limit

When a non-equilibrium quantum system becomes highly occupied, its evolution can be approximated by its classical equations of motion. The non-perturbative dynamics of the system can then be captured by classical-statistical lattice simulations. The classical-statistical approximation amounts to replacing the quantum evolution of n-point correlators with the classical evolution of an ensemble consisting of random field realisations drawn from a specific initial field distribution. That is, the ensemble reproduces the initial conditions of the quantum system, e.g. (4.26), and each field realisation is evolved according to the classical equations of motion. Observables are then obtained by averaging over the ensemble.

Quantum dynamics can be compared to classical dynamics when the statistical and spectral correlators satisfy the classicality condition

$$G^2_{(F)}(x, y) \gg G^2_\rho(x, y), \quad \forall x, y, \tag{4.27}$$

which can be understood in the sense of the (anti-)commutation relations (4.14) and (4.15). It may also be inferred by comparing quantum with classical diagrammatics [120, 121]. The classicality requirement (4.27) for all spacetime points is fulfilled only for limited time- and momentum ranges. An alternative and more intuitive representation of the constraint (4.27) can be expressed in terms of (particle) occupation numbers, which may be inferred from the free field solution of the statistical and spectral propagators. Namely, in the case of free fields, solving the evolution equations (4.21) and (4.22) with the Gaussian initial conditions of (4.26) results in the plane wave solutions

$$G_{(F)}(t, t'; \mathbf{p}) = \frac{1}{\omega_{\mathbf{p}}} \left(n_{\mathbf{p}} + \tfrac{1}{2} \right) \cos\big(\omega_{\mathbf{p}}(t - t')\big),$$
$$G_{(\rho)}(t, t'; \mathbf{p}) = \frac{1}{\omega_{\mathbf{p}}} \sin\big(\omega_{\mathbf{p}}(t - t')\big). \tag{4.28}$$

In terms of these quantities, the condition (4.27) takes the form

$$n_{\mathbf{p}} \gg \frac{1}{2}. \tag{4.29}$$

Hence, we expect that the classical-statistical description captures the dynamics of modes with much larger occupancies than the quantum half.

Classical-statistical simulations therefore provide a means to perform precision tests of approximated quantum dynamics in the regime of large occupation numbers. Comparisons between the classical and quantum time evolution was carried out in [122–124] for NLO truncations of scalar 2PI effective actions, and the results displayed a remarkable agreement at early to intermediate times. At late times the quantum and classical evolution deviate due to their distinct characteristics of thermal equilibrium.

4.2 Renormalisation

It was first shown in [125, 126] that all 2PI truncations can be renormalised with temperature-independent counterterms. The scheme is based on the Bogolubov-Parasiuk-Hepp-Zimmermann (BPHZ) procedure [127, 128] and was first applied to scalar theories in real-time formalism in [129, 130] and imaginary-time formalism in [131, 132]. See also [133] for a detailed treatment for scalar n-point functions with non-vanishing mean field. The renormalisation procedure was later extended to fermions in [134] and QED in [135–137]. A renormalisation procedure for the non-Abelian case has so far not been developed. In this section we start by briefly summarising the general renormalisation procedure, where in Appendix 4.A we complement with a minimal demonstrative example in φ^4-theory truncated at leading (Hartree) order. We then proceed to discuss the generalisation to gauge theories with a special emphasis on the 2PI versions of the standard (1PI) Ward (or Slanov-Taylor) identities.

4.2.1 General procedure

The 2PI renormalisation scheme uses the same power counting arguments as perturbative renormalisation to identify the superficial degree of divergence of a given diagram. In general the self-energies and four-point kernels, obtained by differentiation of a given self-energy with respect to a propagator, are divergent. Once the divergence structure of these quantities have been identified, the next step is to expand the self-energy diagrams around the vacuum propagator, which carries the

leading UV-divergent behaviour. The corresponding vacuum four-point kernels satisfy Bethe-Salpeter equations, and by imposing appropriate renormalisation conditions, the counterterms can be fixed to absorb the divergences in the self-energy and four-point kernel *simultaneously*. This is exemplified in Appendix 4.A. In scalar and fermionic theories, the counterterms and renormalisation conditions are similar to those encountered in perturbation theory.

The 2PI renormalisation procedure is implicit in the sense that the counterterms cancel both sub- and overall divergences simultaneously. This corresponds to an iterative procedure in which the absorption of an overall divergence of a diagram regularises the sub-divergences of the next diagram in the resummation hierarchy, and so on. In this way, the BPHZ prescription is a natural choice for a renormalisation procedure in the context of self-consistent resummation schemes.

We remark that an alternative renormalisation procedure for scalar theories was proposed in [138] and notably applied to a leading-order (Hartree) scalar 2PI approximation in FRW spacetime in [139].

4.2.2 2PI Ward identities

While the global symmetries of the classical action are preserved exactly in all truncations, it was found in [129] (see also [140, 141]) that, for a given truncation, the physical propagator defined by the stationarity condition (4.9) do not fulfil the standard (1PI) Ward identities. This is not surprising, since the 1PI effective action (and the vertices derived from it) is only equal to the 2PI effective action as $\Gamma[\phi] \equiv \Gamma[\phi, \bar{G}]$ in the exact theory.

It was shown in [135, 136, 142] that while the standard Ward identities are not satisfied in 2PI truncations in general, the n-point functions defined as functional field derivatives of the truncated 2PI effective action do obey generalised (2PI) Ward identities. Importantly, the 2PI Ward identities only constrain the field derivatives of $\bar{G}$, but put no constraints on $\bar{G}$ itself. This is due to the fact that in the 2PI framework, the propagator is defined by the stationarity condition (4.9) rather than as two functional field derivatives of the effective action. It is a general feature of nPI

effective actions that the n-point functions with $n \geq 2$ can be obtained in different ways. While the various definitions are equal in the exact theory, this is not the case in truncations. For example, in a truncated theory, the two n-point functions

$$\Lambda^{(n)}_{1...n} := \left.\frac{\delta^n \Gamma[\phi]}{\phi_n \ldots \phi_1}\right|_{\bar{\phi}}, \quad \Gamma[\phi] \equiv \Gamma[\phi, \bar{G}], \tag{4.30}$$

and

$$V^{(p+2)}_{\alpha\beta;1...p} := \left.\frac{\delta^p \Sigma_{\alpha\beta}[\phi]}{\delta\phi_p \ldots \delta\phi_1}\right|_{\bar{\phi}}, \tag{4.31}$$

are different in general. However, for systematic truncations, e.g. loop- or $1/N$-expansions, the non-equivalence of these vertex definitions appears at a higher order than the order of truncation. This is a consequence of the definition of the self-energy Σ in (4.10). In (4.31) and in the following we employ a compact notation with indices α, β denoting both discrete group and Lorentz indices, e.g. $\varphi_\alpha = A^a_\mu(x)$ with $\phi_\alpha = \langle \varphi_\alpha \rangle$, in order to keep the discussion at a more general level.

To see what symmetry properties the classical action imposes on the different n-point functions in the 2PI formalism, it is useful to first separate the classical action into a gauge-symmetric and gauge-fixing parts,

$$S[\phi] = S_{\text{gs}}[\phi] + S_{\text{gf}}[\phi]. \tag{4.32}$$

The gauge-symmetric part of the action $S_{\text{gs}}[\phi]$ in (4.32) is invariant under the field transformations

$$\phi_\alpha \to \delta^\chi \phi_\alpha, \quad \delta^\chi \phi_\alpha = A_{\alpha\beta}\phi_\beta + B_\alpha, \tag{4.33}$$

for linear gauge symmetries, where $A_{\alpha\beta}$ and B_α are some field-independent two- and one-point functions. Under this variation the propagator transforms as

$$G \to \delta^\chi G = AGA^T, \tag{4.34}$$

where T denotes transposition. The field variation (4.33) corresponds at the level of the effective action $W[J, R]$ to a change of integration variables. The fact that a variable change has no effect on $W[J, R]$ can then be expressed as

$$\left\langle \delta^\chi \left(S_{\text{gf}}[\phi] + \phi_\alpha J_\alpha + \phi_\alpha \phi_\beta R_{\alpha\beta} \right) \right\rangle = 0, \tag{4.35}$$

at linear order in the gauge transformation. Using the expressions for the source terms (4.5) this may be rewritten in terms of the 2PI effective action as

$$\left[\delta^\chi \phi_\alpha \frac{\delta}{\delta\phi_\alpha} + \delta^\chi G_{\alpha\beta} \frac{\delta}{\delta G_{\alpha\beta}} \right] (\Gamma[\phi, G] - S_{\text{gf}}[\phi]) = 0, \qquad (4.36)$$

where in component form,

$$\delta^\chi G_{\alpha\beta} = \langle (\delta^\chi \phi_\alpha)\phi_\beta + \phi_\alpha \delta^\chi \phi_\beta \rangle_{\text{conn}} = A_{\alpha\beta} G_{\beta\alpha} + G_{\alpha\beta} A_{\beta\alpha}. \qquad (4.37)$$

The variation (4.36) generalises the 1PI Ward identities

$$\delta^\chi \phi_\alpha \frac{\delta}{\delta\phi_\alpha} (\Gamma[\phi] - S_{\text{gf}}[\phi]) = 0, \qquad (4.38)$$

specified by (4.8), and defines the gauge-symmetric 2PI effective action

$$\Gamma_{\text{gs}}[\phi, G] := \Gamma[\phi, G] - S_{\text{gf}}[\phi]. \qquad (4.39)$$

The 2PI Ward identity (4.36) can be rewritten in a way more familiar to the standard Ward identities as conditions on the various *n*-point vertices. By first taking a derivative of (4.36) with respect to G, we have

$$\delta^\chi \phi_\alpha \frac{\delta^2 \Gamma_{\text{gs}}[\phi, G]}{\delta\phi_\alpha \delta G_{\gamma\sigma}} + \delta^\chi G_{\alpha\beta} \frac{\delta^2 \Gamma_{\text{gs}}[\phi, G]}{\delta G_{\alpha\beta} \delta G_{\gamma\sigma}} + \frac{\delta(\delta^\chi G_{\alpha\beta})}{\delta G_{\gamma\sigma}} \frac{\delta\Gamma_{\text{gs}}[\phi, G]}{\delta G_{\alpha\beta}} = 0. \qquad (4.40)$$

The stationarity condition (4.9) can be expressed in terms of $\Gamma_{\text{gs}}[\phi, G]$ as

$$\left. \frac{\delta\Gamma_{\text{gs}}[\phi, G]}{\delta G_{\alpha\beta}} \right|_{\bar{G}} = 0, \qquad (4.41)$$

and taking a derivative of (4.41) with respect to the field and reinserting the result into (4.40), one finds that

$$\left[\delta^\chi \phi_\alpha \frac{\delta\bar{G}_{\alpha\beta}}{\delta\phi_\alpha} - \delta^\chi \bar{G}_{\alpha\beta} \right] \left. \frac{\delta^2 \Gamma_{\text{gs}}[\phi, G]}{\delta G_{\alpha\beta} \delta G_{\gamma\sigma}} \right|_{\bar{G}} = 0. \qquad (4.42)$$

Assuming $\delta^2 \Gamma_{\text{gs}}/\delta G \delta G|_{\bar{G}}$ can be inverted, (4.42) reduces to

$$\delta^\chi \phi_\alpha \frac{\delta\bar{G}_{\alpha\beta}}{\delta\phi_\alpha} = \delta^\chi \bar{G}_{\alpha\beta} \quad \Leftrightarrow \quad \delta^\chi \phi_\alpha \frac{\delta\bar{\Sigma}_{\alpha\beta}[\phi]}{\delta\phi_\alpha} = -\delta^\chi \bar{G}_{\alpha\beta}^{-1}[\phi], \quad (4.43)$$

where in the second equality we have used (4.10). The variation of the inverse propagator is given analogously to (4.37), i.e. $\delta^{\chi}\bar{G}^{-1} = -[A^{T}\bar{G}^{-1} + \bar{G}^{-1}A]$. Ward identities for higher-order n-point functions are then obtained from functional field derivatives of the second identity in (4.43).[2]

An important finding of [143] is that it is possible to construct gauge-invariant classes of diagrams that respect the symmetry identity (4.36). This can be achieved by considering the effect of the symmetry transformations (4.33) and (4.34) on the 2PI effective action (4.6).

Considering each part of the action (4.6) individually, we see that the first classical part of the action is gauge-invariant by definition. A gauge transformation of the second term, which is a Gaussian integral, can be absorbed by a change of integration variable. It is gauge-invariant up to a constant. As for the third term in (4.6), it is useful to separate the classical inverse propagator into a gauge-invariant and gauge-fixing part as $G_{0}^{-1} := G_{\text{gs}}^{-1} + G_{\text{gf}}^{-1}$, where the inverse propagators are defined by two functional field derivatives of their corresponding classical action terms in (4.32). From (4.34) we then have that

$$G_{\text{gs}}^{-1}[\phi] = A^{T}G_{\text{gs}}^{-1}[\delta^{\chi}\phi]A, \qquad (4.46)$$

and using cyclicity of trace,

$$\text{Tr}\big[G_{\text{gs}}^{-1}[\delta^{\chi}\phi]\delta^{\chi}G\big] = \text{Tr}\big[G_{\text{gs}}^{-1}[\phi]G\big], \qquad (4.47)$$

---

[2]For comparison, the n-point vertices defined by the 1PI effective action are given by (4.30) and satisfies the standard Ward identities. In particular, the two-point function

$$\Lambda_{\alpha\beta}^{(2)}[\phi] := \frac{\delta^{2}\Gamma[\phi]}{\delta\phi_{\alpha}\delta\phi_{\beta}}, \qquad (4.44)$$

is the object from which these (resummed) n-point functions are obtained by functional derivatives evaluated at the stationary point. The Ward identities can be obtained by taking two field derivatives of (4.38), and assuming that the gauge-fixing action is quadratic in the gauge field, to find

$$\delta^{\chi}\phi_{\gamma}\frac{\delta\Lambda_{\alpha\beta}^{(2)}[\phi]}{\delta\phi_{\gamma}} = \delta^{\chi}\Lambda_{\alpha\beta}^{(2)}, \qquad (4.45)$$

where $\delta^{\chi}\Lambda^{(2)} \equiv -[A^{T}\Lambda^{(2)} + \Lambda^{(2)}A]$. The standard Ward identities for n-point functions with $n \geq 3$ are given by functional derivatives of (4.45). Note that this identity has the same form as (4.43). While the identities (4.43) and (4.45) are different in truncated theories, the authors of [143] showed that if a given truncation satisfies the symmetry requirement (4.36), then the vertex functions (4.30) and (4.31) satisfy the 1PI Ward identities independently.

it is clear that the G_{gs}^{-1} part of the third term in (4.6) is gauge-invariant. For the remaining gauge-fixing dependent term, we note that, for a quadratic gauge-fixing action, the inverse propagator G_{gf}^{-1} does not depend on the field ϕ. As a consequence, a gauge transformation enter $\text{Tr}\, G_{\text{gf}}^{-1} G$ only via G, which is gauge-invariant by (4.34).

As will be discussed in section 4.3, the functional Γ_2 is in general not invariant under the gauge transformation (4.33), but it is possible to isolate gauge-invariant classes of diagrams. A gauge-invariant set of diagrams can be identified by expressing the functional Γ_2 in terms of classical vertices [143],

$$\Lambda_{1\ldots n}^{\text{cl}(n)}[\phi] := \frac{\delta^n S[\phi]}{\delta\phi_n \ldots \delta\phi_1}. \tag{4.48}$$

Since the gauge-fixing action, which accounts for all B-dependent terms from the variation (4.33), is quadratic, the gauge transformation of the vertex (4.48) must satisfy

$$\Lambda_{m_1\ldots m_n}^{\text{cl}(n)}[\delta^\chi\phi] = \Lambda_{m_1\ldots m_n}^{\text{cl}(n)}[\phi] A_{m_1 p_1}^{-1} \ldots A_{m_n p_n}^{-1}. \tag{4.49}$$

Diagrams built from the vertex (4.48) will then be of the form

$$\Lambda_{m_1\ldots m_n}^{\text{cl}(n)}[\phi] G_{m_1 p_1} \ldots G_{m_n p_n}, \tag{4.50}$$

where the endpoints $m_1, \ldots, m_n$ can attach to other classical vertices, and so on. A gauge transformation of such a diagram can then be expressed using (4.34) as

$$\begin{aligned}
\Lambda_{m_1\ldots m_n}^{\text{cl}(n)}&[\delta^\chi\phi]\delta^\chi G_{m_1 p_1} \ldots \delta^\chi G_{m_n p_n} \\
&= \Lambda_{m_1\ldots m_n}^{\text{cl}(n)}[\delta^\chi\phi] A_{m_1 q_1} \ldots A_{m_n q_n} G_{q_1 p_1} \ldots G_{q_n p_n} A_{p_1 q_1}^T \ldots A_{p_n q_n}^T \\
&= \Lambda_{m_1\ldots m_n}^{\text{cl}(n)}[\phi] G_{q_n p_n} A_{p_1 q_1}^T \ldots A_{p_n q_n}^T,
\end{aligned} \tag{4.51}$$

where in the second equality the gauge transformation in (4.49) was inserted. This shows that the diagrams (4.50) constructed with the classical vertex (4.48) are gauge-invariant. However, it is worth emphasising that while these approximation schemes satisfy the correct gauge transformation properties, they do not imply that observable quantities are gauge-invariant.

4.2.3 Renormalisation prescription for Abelian gauge theories

While the fact that 2PI Ward identities do not impose any constraints on the two-point functions might seem unsettling, this property also allows for a consistent renormalisation of (Abelian) gauge theories, as was shown in [135, 137]. In particular, the additional degrees of freedom provided by the gauge symmetry in (4.36), i.e.

$$\Gamma_2[G] = \Gamma_2[\delta^\chi G], \tag{4.52}$$

allow for new counterterms respecting (4.52) to be introduced to the effective action compared to the ones of usual perturbation theory. These additional counterterms without any perturbative analogue can be fixed to absorb e.g. the non-transverse divergences in the photon propagator and four-point function [135, 137]. The renormalisation procedure using these counterterms can then be made analogously to the scalar case (see Appendix 4.A) by renormalising self-energies and the Bethe-Salpeter equation for the (resummed) vertices of the theory simultaneously. Note that in theories involving more than one field, the Bethe-Salpeter equations are typically nested.

When fixing the coupling counterterms it is important to ensure that the renormalised expansion scheme still converges to the exact theory, which is absent of the additional counterterms allowed by the 2PI Ward identities (4.52). This can be guaranteed by imposing renormalisation conditions that are trivially satisfied in the exact theory, as shown in [135].

Although rigorous 2PI renormalisation schemes have been developed, their practical implementation is relatively limited and has not been extensively studied. See however [126, 138, 144]. The main reason for this is that, except for the simplest cases, the evolution equations (4.21) and (4.22) must be solved numerically. The bare divergent quantities are then regulated by the lattice and it is common to simply subtract the dominant divergences. This can be done given that the momentum scales relevant to the situation at hand are significantly smaller than the lattice cutoff and that the results converge in the large-volume limit. In addition, some renormalised quantities can be inferred from the evolution of the unrenormalised propagator. For instance the renormalised mass can be

inferred from the oscillation frequency of $G(t, t'; \mathbf{p})$.

4.3 Gauge-fixing dependence in 2PI truncations

It was first shown in [36] that 2PI approximations for gauge theories breaks gauge invariance, which is indicated by an explicit gauge-fixing dependence. This is due to the fact that the 2PI truncation resums specific topologies, which do not need to satisfy the Ward or Slanov-Taylor identities. The gauge-fixing dependence appears parametrically at a higher order in the expansion parameter than the order of truncation. In this section we review the appearance of this gauge dependency by means of the Nielsen identity [145] generalised to 2PI theories in [37].

We start by considering the 1PI effective action,

$$\Gamma[\phi] = W[J] - J_\alpha \phi^\alpha, \tag{4.53}$$

in terms of the generating functional $W[J]$ for connected 1PI diagrams and one-point source term J_α. Since $\phi^\alpha = \langle \varphi^\alpha \rangle = \delta W / \delta J_\alpha$, the equations of motion are given by

$$\frac{\delta \Gamma[\phi]}{\delta \phi^\alpha} = -J_\alpha. \tag{4.54}$$

The 1PI Nielsen identity states the effect of a gauge transformation on the 1PI effective action. For a gauge transformation $\varphi \rightarrow \varphi + \delta^\chi \varphi$, the Nielsen identity for the 1PI effective action (4.53) reads [145]

$$\delta^\chi \Gamma \Big|_{J=\text{const.}} = -i \frac{\delta \Gamma[\phi]}{\delta \phi^\alpha} \frac{\delta \Gamma[\phi]}{\delta \phi^\beta} \langle (\varphi^\alpha - \phi^\alpha) \delta^\chi \varphi^\beta \rangle, \tag{4.55}$$

where the source term is assumed constant. It follows from (4.54) that for the physical field $\bar{\phi}_\alpha$, obtained from the stationarity condition $J_\alpha = 0$, the gauge variation (4.55) vanishes, and the 1PI effective action is gauge-invariant.

As for the 2PI effective action, the equations of motion are given by

$$\frac{\delta \Gamma[\phi, G]}{\delta \phi^\alpha} = J_\alpha - R_{\alpha\beta} \phi^\beta, \quad \frac{\delta \Gamma[\phi, G]}{\delta G^{\alpha\beta}} = -\frac{1}{2} R_{\alpha\beta}, \tag{4.56}$$

66

and the corresponding Nielsen identity was derived in [37] and reads

$$\delta^\chi \Gamma = -i \Bigg\langle \left[\frac{\delta\Gamma}{\delta\phi^\alpha} \delta^\chi \varphi^\alpha + \frac{\delta\Gamma}{\delta G^{\alpha\beta}} \left(\delta^\chi \varphi^\alpha (\varphi^\beta - \phi^\beta) + \delta^\chi \varphi^\beta (\varphi^\alpha - \phi^\alpha) \right) \right]$$
$$\times \left[\frac{\delta\Gamma}{\delta\phi^\alpha} (\varphi^\alpha - \phi^\alpha) + \frac{\delta\Gamma}{\delta G^{\alpha\beta}} \left((\varphi^\alpha - \phi^\alpha)(\varphi^\beta - \phi^\beta) - G^{\alpha\beta} \right) \right] \Bigg\rangle, \tag{4.57}$$

where the source J in Γ is again assumed to be constant. Also in this case it is clear from (4.57) that the 2PI effective action is gauge-invariant at its stationary point. Let us now proceed to consider a truncated 2PI effective action. For a given truncation of the effective action at L loops, the exact action can be expressed simply as

$$\Gamma = \Gamma_L + \Gamma_{\text{rest}}, \tag{4.58}$$

where $\Gamma_L \sim g^{2L-2}$ is the approximated action with g being the gauge coupling constant and $\Gamma_{\text{rest}} \sim O(g^{2L})$ is the remaining parts of the exact theory. The approximate stationarity conditions are given by

$$\left.\frac{\delta\Gamma_L}{\delta\phi^\alpha}\right|_{\bar\phi,\bar G} = 0, \quad \left.\frac{\delta\Gamma_L}{\delta G^{\alpha\beta}}\right|_{\bar\phi,\bar G} = 0. \tag{4.59}$$

In terms of the exact effective action, the approximate stationarity condition (4.59) implies that

$$\left.\frac{\delta\Gamma}{\delta\phi^\alpha}\right|_{\bar\phi,\bar G} = \left.\frac{\delta\Gamma_{\text{rest}}}{\delta\phi^\alpha}\right|_{\bar\phi,\bar G} \sim \Gamma_{\text{rest}} \sim g^{2L}, \tag{4.60}$$

where the last equality follows from the fact that the derivative with respect to ϕ^α does not change the dependence of the effective action on the coupling g. The same argument can be made for variation with respect to the propagator $G^{\alpha\beta}$. With the coupling power counting of (4.60) in mind, the 2PI Nielsen identity (4.57) implies that

$$\delta^\chi \Gamma \sim \Gamma_{\text{rest}}^2 = \delta\Gamma_L + \delta\Gamma_{\text{rest}}, \tag{4.61}$$

which suggest that

$$\delta^\chi \Gamma_L \sim \delta^\chi \Gamma_{\text{rest}} + O(g^{4L}). \tag{4.62}$$

As in the case of a functional differentiation with respect to a field, we do not expect a gauge variation to change the coupling in the effective action. For this reason, the gauge transformation should leave the the coupling-dependence in the "rest" action unchanged, i.e. $\delta^\chi \Gamma_{\text{rest}} \sim g^{2L}$, which implies for (4.62) that

$$\delta^\chi \Gamma_L \sim g^{2L} \equiv g^2 \Gamma_L. \tag{4.63}$$

The truncated effective action is therefore gauge-dependent, and the dependence appears at a higher order than the order of truncation. This is a consequence of the approximate stationarity condition (4.59), and the argument follows analogously for other expansion schemes.

The residual gauge-dependence in 2PI truncations is the topic of chapter 7, where we investigate the degree of gauge-dependence in the two-loop truncated SU(2)-Higgs model by performing comparisons with classical-statistical simulations.

4.A A minimal example of renormalisation: Hartree loop

Outlining the procedure of [130], we consider a massive, self-interacting scalar theory,

$$\mathcal{L} = \tfrac{1}{2}\partial_\mu \varphi_{\text{b}} \partial^\mu \varphi_{\text{b}} - \tfrac{1}{2}m_{\text{b}}^2 \varphi - \tfrac{1}{4!}\lambda_{\text{b}}^2 \varphi_{\text{b}}^2, \tag{4.64}$$

and introduce counterterms related to the bare quantities in the usual manner as

$$\begin{aligned} \delta Z &= Z - 1, \quad Z m_{\text{b}}^2 = m^2 + \delta m^2, \\ \varphi_{\text{b}} &= \sqrt{Z}\varphi, \quad Z^2 \lambda_{\text{b}}^2 = \lambda^2 + \delta\lambda^2. \end{aligned} \tag{4.65}$$

The 2PI effective action is given by (4.6) and we consider only the leading order (Hartree) contribution to Γ_2. The physical propagator and self-energy is here defined as

$$\frac{\delta\Gamma_2}{\delta G} = \frac{1}{2}\Sigma, \quad G^{-1} = G_0^{-1} + \Sigma[G]. \tag{4.66}$$

As a consequence of Weinbergs theorem, interactions do not modify the asymptotic large-momentum behaviour of the n-point functions in a

given theory. This means that the power counting employed in perturbation theory remains valid for 2PI approximations. In four dimensions, we therefore expect divergent two- and four-point functions.

A second differentiation of Γ_2 with respect to the propagator yields the 2PI kernel

$$\Lambda(p, q) = 2 \frac{\delta \Sigma(p)}{\delta G(q)} = \Lambda(q, p), \qquad (4.67)$$

where p, q denotes four-momenta. The kernel in (4.67) enters into the equation of motion for the resummed four-point function $V(p, q)$, given by the Bethe-Salpeter equation

$$V(p, q) = \Lambda(p, q) - \frac{1}{2} \int_k \Lambda(p, k) G^2(k) \Lambda(k, q). \qquad (4.68)$$

Note that the four-point function $V(p, q)$ is the four-point analogue of $G(p)$.

The renormalisation procedure for 2PI truncations is based on that the resummed propagator and four-point function can be renormalised simultaneously. In particular, the Bethe-Salpeter equation (4.68) is required to determine the coupling constant counterterms that regularise the sub-divergences in the self-energy.

The renormalised Hartree loop can be expressed as

$$\Sigma = \frac{\lambda^2}{2} \int_p G(p) - \delta m^2. \qquad (4.69)$$

The UV divergence can be renormalised by the mass counterterm, but would in the finite-temperature case be temperature-dependent. Instead we note that the resummation in the gap equation (4.66) implies that overall divergences contribute to sub-divergences at the next iterative order in resummation. For this reason it is necessary to remove the sub-divergences by coupling constant renormalisation before δm^2 is set to absorb the overall divergence at each order. This implies that the renormalised coupling in (4.69) should be replaced by $\lambda^2 \rightarrow \lambda_0^2 :=$ $\lambda^2 + \delta \lambda^2$. With this definition, the kernel in (4.67) becomes $\Lambda = \lambda_0^2$, and the renormalised four-point vertex takes the form

$$V = \lambda_0^2 - \frac{\lambda_0^2}{2} V \int_p G^2(p). \qquad (4.70)$$

where $\delta\lambda^2$ can be tuned to absorb the divergence of the integral. The divergence in (4.70) does not depend on the self-energy (or mass), and $\delta\lambda^2$ can therefore equally well be determined from the free propagator G_0. To this end we can introduce the auxiliary vertex V_0 as

$$V_0 := \lambda_0^2 - \frac{\lambda_0^2}{2} V_0 \int_p G_0^2(p), \tag{4.71}$$

where the difference $V - V_0$ is finite.

The next step is to show that the renormalised vertex (4.71) simultaneously renormalises the self-energy. For this to be realised, the counterterm δm^2 should be independent of Σ, and in the following we will see that this can be guaranteed if Σ is a solution to the gap equation.

To this end it is useful to expand the propagator in Σ,

$$G = G_0 + G_1, \quad G_1 := -G_0 \Sigma G_0 + G_2, \tag{4.72}$$

where $G_2 = O(\Sigma^2)$ so that $\int_p G_2(p)$ is finite. The Hartree contribution (4.69) can then be split accordingly,

$$\Sigma_2 := \frac{\lambda_0^2}{2} \int_p G_0(p) - \delta m^2, \quad \Sigma_0 := \frac{\lambda_0^2}{2} \int_p G_1(p), \tag{4.73}$$

where the subscripts $2, 0$ in the self-energies indicate the superficial degrees of divergence. Importantly, in (4.73) only Σ_0 depends on Σ, and the gap equation (4.66) now reads $\Sigma = \Sigma_2 + \Sigma_0$.

By expressing g_0^2 in favour of V_0 via (4.71), the self-energy in (4.73) becomes

$$\Sigma_0 = \frac{V_0}{2} \int_p G_1(p) + \frac{V_0}{2} \Sigma_0 \int_p G_0^2(p), \tag{4.74}$$

where both integrals are divergent. However, by using (4.72) in the first term and inserting $\Sigma_0^{\mathrm{H}} = \Sigma - \Sigma_2$ in the last term, the divergences proportional to Σ cancel identically. The gap equation then reduces to

$$\Sigma = \frac{V_0}{2} \int_p G_2(p) + \Sigma_2 \left(1 - \frac{V_0}{2} \int_p G_0^2(p) \right). \tag{4.75}$$

Finally, using (4.71) and (4.73) again, the self-energy reduces to

$$\Sigma = \frac{V_0}{2} \left[\int_p [G_0(p) + G_2(p)] + 2\frac{\delta m^2}{\lambda_0^2} \right]. \tag{4.76}$$

Hence, the divergence in the integral over $G_0(p)$ can be absorbed in the counterterm δm^2.

The separate treatment of the part of the propagator that carries the leading divergence in the self-energy is the key to making the counterterms temperature-independent. In the case of finite temperature, the self-energy (4.69) can be expressed as

$$\Sigma = \frac{\lambda_0^2}{2} \int_p \left[G(p) + \frac{n_\mathbf{p}}{\omega_\mathbf{p}} \right] + \delta m^2, \qquad (4.77)$$

after summation over Matsubara frequencies, where $\mathbf{p}$ denotes three-dimensional Euclidean momentum. The particle number density is $n_\mathbf{p} = (\exp \beta \omega_\mathbf{p} - 1)^{-1}$ with $\omega_\mathbf{p}^2 = \mathbf{p}^2 + m^2 + \Sigma$. Since the divergences in the $n_\mathbf{p}/\omega_\mathbf{p}$-term above is sub-leading, this term can be absorbed into the definition of Σ_0 in (4.73), and the corresponding divergences can be eliminated as before. The above procedure generalises for higher-order truncations of Γ_2.

5 Quantum corrections to slow-roll inflation: scalar and tensor modes

Inflation is often described through the dynamics of a scalar field, slow-rolling in a suitable potential. Ultimately, this inflaton must be identified with the expectation value of a quantum field, evolving in a quantum effective potential. The shape of this potential is determined by the underlying tree-level potential, dressed by quantum corrections from the scalar field itself and the metric perturbations. Following [76], we compute the effective scalar field equations and the corrected Friedmann equations to quadratic order in both scalar field, scalar metric and tensor perturbations. We identify the quantum corrections from different sources at leading order in slow-roll, and estimate their magnitude in benchmark models of inflation. We comment on the implications of non-minimal coupling to gravity in this context.

5.1 Introduction

Cosmological observations show that the very early Universe underwent a stage of accelerated expansion [47]. This is possible when the matter in the Universe exhibits some specific thermodynamical properties, often phrased in terms of the equation of state. An inflationary equation of state emerges naturally, if during this inflationary epoch, the thermodynamics was dominated by a scalar field degree of freedom (fundamental or composite), evolving in an appropriate potential. Fairly generically, if the field is initially displaced far from its equilibrium value, it will slow-roll back to the potential minimum in such a way that inflation is achieved. In this well-known and elegant formalism, the homogeneous scalar field is treated as a single classical degree of freedom ϕ, and the combined system of field equation and Einstein (Friedmann) equations for the cosmological expansion may be readily solved (see e.g. [146]).

In a homogeneous FRW background, field and metric perturbations are introduced, and their spectra can be computed in a straightforward way. Through a well-established procedure, these primordial quantum fluctuations can be shown to seed the temperature fluctuations of the CMB, and hence the formation of structure in the Universe. Direct comparison with observations allows us to constrain the parameters and form of the scalar field potential [147].

Ultimately, the scalar field must be treated quantum mechanically, and then an adjustment of the terminology is required. The object ϕ may be identified as the time-dependent expectation value of the scalar field.[1] This degree of freedom now evolves in the quantum effective potential, and the minimum of this potential corresponds to the thermodynamic equilibrium state.

An important distinction is that this is not an effective potential in the sense of a low-energy effective theory, where degrees of freedom above a certain cutoff have been integrated out. Such effective potentials are often invoked in inflationary model-building to motivate a wide range of functional forms of classical potentials. The quantum effective potential is the free energy of the system, once all quantum and thermal fluctuations have been included at all scales (see for instance [78]), and for cosmological applications it includes gravitational corrections as well. From the quantum effective action, equations of motion for both the scalar mean field and the metric may be derived, and these then include all quantum corrections and hence all the thermodynamical information for the system.[2]

In practice, computing this quantum effective potential in an expanding cosmological background is possible, but less straightforward than in Minkowski space (see e.g. [44, 148]). As in Minkowski space, an expansion in terms of Feynman diagrams is introduced and truncated. The issue of renormalisation arises, and just as for Minkowski space, consistency limits the set of viable tree-level potentials.

An alternative, but equivalent approach to the quantum dynamics of

---

[1] Or, according to taste, as the mean field, order parameter, one-point function or condensate.

[2] The quantum effective action reduces to the quantum effective potential if the mean fields are constant, in which case it is given by the classical potential plus the quantum corrections to it.

inflation is to introduce quantum corrections at the level of the operator equations of motion. Starting from the classical Friedmann and scalar field equations, we may expand in powers of the perturbations around the FRW solution, and by taking quantum averages generate a Schwinger-Dyson-like set of evolution equations for the correlators. These may then in principle be solved (see for instance [66, 149]).

As a consequence of gravity's highly non-linear properties, including metric perturbations in this scheme is technically challenging, and wholesale resummations have not been performed. The most common avenue is to include the effect of the homogeneous time-dependent metric in the computation of scalar field correlators and quantum effective actions, leading to higher order curvature contributions to the system. One recurring result from this procedure is that the "potential" appearing in the energy, the pressure and the force of the Friedmann and scalar field equations receive different corrections. This means that the ubiquitous slow-roll formalism must be adjusted, and a number of standard identities correct to some order in a slow-roll expansion, are in addition also correct only at tree-level (or some order in perturbations) [69, 150].

In [76], scalar metric perturbations were introduced in a computation of quantum-corrected Friedmann and scalar field equations, to leading order in slow-roll and leading order in fluctuations. The constrained quantisation of the field and metric degrees of freedom were given particular emphasis, and the result was a manageable set of evolution equations. The scalar fluctuations came out slow-roll suppressed, and the numerical effect of including them turned out to be negligible, except near the end of inflation, and then only for small-field inflation.

In the present work, we revisit this picture and include the tensor perturbations, for which we compute the corresponding leading order corrections to both scalar field evolution and Friedmann equations. We will find that these new corrections enter differently in the evolution than the scalar metric perturbations, and that they are larger than the scalar corrections.

We also consider non-minimal coupling between the scalar field and the curvature, and although we will not carry this complication along

throughout the calculation, we will be able to illustrate how a non-minimal coupling may affect the results.

Quantum effects during and after inflation have received significant attention in many different contexts and in many different guises. Prominent examples are non-Gaussian effects in cosmological observables due to self-interactions of metric perturbations (see e.g. [56, 57]); logarithmic infrared divergences of correlators in de Sitter and slow-roll backgrounds and methods to handle them (see [70, 151] for a review), including the stochastic approximation [39, 152]; and effective actions for the inflaton field itself (without metric perturbations), in various resummation schemes, both in an adiabatic expansion (around Minkowski space $H = 0$) [75, 148] and a slow-roll expansion (around de Sitter space $\dot{H} = 0$) [19, 69, 71, 72], as well as in strict de Sitter space (see e.g. [74, 153, 154]).

What we are concerned with here is yet another context; quantum corrections to evolution equations of the inflaton and metric between horizon exit and the end of inflation, taking into account both field and metric fluctuations. These fluctuations influence the relation between the slow-roll parameters at the end of inflation and at horizon crossing, which in turn enter in observables in the sky.

The chapter is organised as follows. In section 5.2 we set up our action, the standard Friedmann and scalar equations at tree-level. We then introduce metric fluctuations in Newtonian gauge and compute the field equations for them. These are then quantised in sections 5.2.3 and 5.2.4. We proceed to derive the corrected Friedmann and scalar field equation to second order in perturbations in section 5.3 and discuss renormalisation. In section 5.4, we briefly consider the magnitude of corrections and estimate the effect of quantum corrections on the inflationary dynamics. We conclude in section 5.5. Details of the calculations are listed in Appendices 5.A–5.D for completeness.

5.2 Background and field equations in Newtonian gauge

We consider a single inflaton field ϕ non-minimally coupled to gravity with action of the form (following the sign convention (+++) of [155])

$$S = \int d^4x \sqrt{-g} \left[\tfrac{1}{2} M_{\text{Pl}}^2 F(\phi) R - \tfrac{1}{2} g^{\mu\nu} \phi_{,\mu} \phi_{,\nu} - V(\phi) \right], \qquad (5.1)$$

where $M_{\text{Pl}}^2 := (8\pi G)^{-1}$ is the reduced Planck mass and where for the moment $F(\phi)$ and the tree-level potential $V(\phi)$ are kept general.[3] The scalar field ϕ lives in a spacetime defined by the metric $\hat{g}_{\mu\nu}$, and we will assume that field and metric may be written as

$$\begin{aligned} \phi(x) &= \phi(t) + \delta\phi(t, x^i), \\ \hat{g}_{\mu\nu}(x) &= g_{\mu\nu}(t) + \delta g_{\mu\nu}(t, x^i), \end{aligned} \qquad (5.2)$$

where $g_{\mu\nu}$ is the spatially flat FRW metric; $g_{\mu\nu} = \text{diag}[-1, a^2(t)\delta_{ij}]$, with $a(t)$ being the scale factor and where t denotes cosmic time. Latin indices run from one to three and Greek indices from zero to three.

The metric perturbations may be decomposed into scalar, vector, and tensor modes. It is common to immediately discard the vector perturbations, as they decay away in an expanding Universe. We will do so here as well. Choosing to work in Newtonian gauge, we may write for the line element

$$ds^2 = -(1 + 2\Phi)dt^2 + a^2[1 + 2(-\Psi\delta_{ij} + E_{ij})]dx^i dx^j, \qquad (5.3)$$

where Φ and Ψ are scalar potentials and E_{ij} is a traceless, transverse matrix containing the tensor perturbations, i.e. E_{ij} satisfies $\partial^i E_{ij} = 0$ and $E^i{}_i = 0$.

The Einstein field equations are obtained by variation of the action in (5.1) with respect to the metric, which yields

$$G_{\mu\nu} := R_{\mu\nu} - \tfrac{1}{2} R g_{\mu\nu} = \frac{1}{M_{\text{Pl}}^2} \frac{1}{F(\phi)} \tilde{T}_{\mu\nu} := \frac{1}{M_{\text{Pl}}^2} T_{\mu\nu}, \qquad (5.4)$$

---

[3] In some cases, it can be convenient by a conformal transformation to perform the calculation in the Einstein frame and then transform the results back again. In the Einstein frame the non-minimal coupling is absent but the field potential and normalisation are different. We have chosen to stay in the Jordan frame throughout.

where

$$\tilde{T}_{\mu\nu} := \phi_{,\mu}\phi_{,\nu} - g_{\mu\nu}[\tfrac{1}{2}g^{\rho\kappa}\phi_{,\rho}\phi_{,\kappa} + V(\phi)] + F(\phi)_{;\mu,\nu} - g_{\mu\nu}\square F(\phi). \quad (5.5)$$

Here and in the following a comma subscript denotes a partial derivative, a semi-colon denotes a covariant derivative and the "box" operator is the d'Alembertian in curved spacetime

$$\square = \frac{1}{\sqrt{-g}}\partial_\mu\sqrt{-g}\partial^\mu. \quad (5.6)$$

The effective energy-momentum tensor $T_{\mu\nu}$ is covariantly conserved, and we will assume that $F(\phi) \neq 0$. Variation of the action with respect to ϕ yields the scalar field equation

$$\square\phi + \tfrac{1}{2}M_{\text{Pl}}^2 F_{,\phi}R - V_{,\phi} = 0. \quad (5.7)$$

Next, we insert the perturbed fields of (5.2) and (5.3) into (5.4)–(5.7) and extract equations to zeroth order in perturbations (the "classical" Friedmann and inflaton equations); to first order in perturbations (the mode equations for the field and metric scalar and tensor perturbations in the background FRW metric); and to quadratic order in perturbations (the "quantum-corrected" Friedmann and inflaton equations).

The zeroth-order equations will provide a slow-roll background in which to solve the first-order (linear) mode equations. These will in turn be quantised and inserted into the quadratic-order equations, in order to explicitly compute the quantum corrections to the cosmological evolution.

5.2.1 Zeroth order in perturbations: the classical equations

To zeroth order the Friedmann equation (5.4) and the scalar field equation (5.7) reduce to the familiar expressions

$$3H^2 = \frac{1}{M_{\text{Pl}}^2}\frac{1}{F}\left(\tfrac{1}{2}\dot{\phi}^2 + V\right) - 3H\frac{\dot{F}}{F}, \quad (5.8)$$

$$2\dot{H} + 3H^2 = -\frac{1}{M_{\text{Pl}}^2}\frac{1}{F}\left(\tfrac{1}{2}\dot{\phi}^2 - V\right) - 2H\frac{\dot{F}}{F} - \frac{\ddot{F}}{F}, \quad (5.9)$$

$$0 = \ddot{\phi} + 3H\dot{\phi} + V_{,\phi} - 3M_{\text{Pl}}^2 F_{,\phi}(\dot{H} + 2H^2), \quad (5.10)$$

where $H = \dot{a}/a$ and the right-hand side of (5.8) and (5.9) represents energy density and pressure, respectively. Here the dots are derivatives with respect to cosmic time t and we have inserted $R = 6(\dot{H} + 2H^2)$, the FRW Ricci scalar. We note that in the limit of Einstein gravity, $F(\phi) = 1$, we recover the standard Friedmann equations. Also, since we assume that $F := F(\phi)$, we have $\dot{F} \propto \dot{\phi}$, $\ddot{F} \propto \ddot{\phi}, \dot{\phi}^2$. We also note that the same object V (or $V_{,\phi}$) appears in all three equations, which then allows for the direct application of the slow-roll formalism.

It will therefore be convenient to introduce the dimensionless slow-roll parameters

$$\epsilon_H = -\frac{\dot{H}}{H^2} = 1 - \frac{\mathcal{H}'}{\mathcal{H}^2} \,,$$

$$\delta_H = -\frac{\ddot{\phi}}{H\dot{\phi}} = 1 - \frac{\phi''}{\mathcal{H}\phi'} \,, \tag{5.11}$$

$$\epsilon_F = \frac{1}{2}\frac{\dot{F}}{HF} = \frac{1}{2}\frac{F'}{\mathcal{H}F}.$$

The primes refer to derivatives with respect to conformal time η, where

$$a(\eta)\mathrm{d}\eta = \mathrm{d}t, \quad \eta = \int \frac{\mathrm{d}t}{a}, \quad \mathcal{H} = \frac{a'}{a} \,. \tag{5.12}$$

Inflation is equivalent to the slow-roll parameters being small, i.e. less than unity, and evolving slowly in time.

One may apply the slow-roll formalism to solve (5.8)–(5.10) to any order in slow-roll parameters one chooses. However, as was emphasised in [69, 150], at the quantum level, corrections manifest themselves differently in different relations, and the effective potential V is no longer the same. Hence, when including quantum corrections, some of the elegance of the slow-roll formalism is lost. We will see this explicitly below.

5.2.2 First order in perturbations: equations of motion for the fluctuations

The perturbations of the scalar field and the metric (5.2) give rise to linear perturbations in F, $G_{\mu\nu}$ and $\tilde{T}_{\mu\nu}$, which we denote by δF, $\delta G_{\mu\nu}$ and $\delta\tilde{T}_{\mu\nu}$,

respectively. The Einstein equation can then be written as

$$(F + \delta F)(G_{\mu\nu} + \delta G_{\mu\nu}) = \frac{1}{M_{\text{Pl}}^2}(\tilde{T}_{\mu\nu} + \delta\tilde{T}_{\mu\nu}), \qquad (5.13)$$

Using the zeroth-order equations, one immediately finds (now in mixed index notation)

$$\delta G^\mu{}_\nu = \frac{1}{M_{\text{Pl}}^2}\frac{1}{F}\left(\delta\tilde{T}^\mu{}_\nu - \frac{\delta F}{F}\tilde{T}^\mu{}_\nu\right), \qquad (5.14)$$

with the understanding, that since F is a function of ϕ only, $\delta F := F_{,\phi}\delta\phi$. The 00- and 0$i$-components of (5.14) are

$$
\begin{aligned}
3H(\dot{\Psi} + H\Phi) - \frac{1}{a^2}\nabla^2\Psi = {} & \frac{1}{2M_{\text{Pl}}^2 F}\left(-\dot{\phi}\dot{\delta\phi} + \dot{\phi}^2\Phi - V_{,\phi}\delta\phi\right) \\
& - \frac{3\dot{F}}{2F}(\dot{\Psi} + 2H\Phi) \\
& + \frac{3H}{2}\frac{\dot{\delta F}}{F} - \frac{1}{2a^2}\nabla^2\frac{\delta F}{F} \\
& + \frac{1}{2}\frac{\delta F}{F}\left(\frac{\frac{1}{2}\dot{\phi}^2 + V}{M_{\text{Pl}}^2 F} - 3H\frac{\dot{F}}{F}\right), \qquad (5.15)
\end{aligned}
$$

$$
\begin{aligned}
\dot{\Psi} + H\Phi = {} & \frac{1}{2M_{\text{Pl}}^2 F}\dot{\phi}\delta\phi - \frac{1}{2}\frac{\dot{F}}{F}\Phi \\
& + \frac{1}{2}\frac{\dot{\delta F}}{F} - \frac{H}{2}\frac{\delta F}{F}. \qquad (5.16)
\end{aligned}
$$

We note that in the minimal coupling case $F(\phi) = 1$, the relations simplify substantially. The *ii*-component gives us

$$\ddot{\Psi} + 3H\dot{\Psi} + H\dot{\Phi} + (2\dot{H} + 3H^2)\Phi \tag{5.17}$$

$$= \frac{1}{2M_{\text{Pl}}^2 F}\left(\dot{\phi}\dot{\delta\phi} - \dot{\phi}^2\Phi - V_{,\phi}\delta\phi\right)$$

$$- \frac{\ddot{F}}{F}\Phi + H\frac{\dot{\delta F}}{F} - \frac{1}{2}\frac{\dot{F}}{F}(4H\Phi + \dot{\Phi} + 2\dot{\Psi})$$

$$+ \frac{1}{2}\frac{\ddot{\delta F}}{F} - \frac{1}{2a^2}\nabla^2\left(\frac{\delta F}{F}\right)$$

$$- \frac{1}{2}\frac{\delta F}{F}\left(\frac{\frac{1}{2}\dot{\phi}^2 - V}{M_{\text{Pl}}^2 F} + 2H\frac{\dot{F}}{F} + \frac{\ddot{F}}{F}\right), \tag{5.18}$$

Again, the non-minimal coupling is responsible for substantial complexity. For the off-diagonal components $i \neq j$ of the perturbed Einstein equation (5.14), we may treat the longitudinal and transverse components separately, to find

$$\frac{1}{a^2}\partial^i\partial_j(\Psi - \Phi) = \partial^i\partial_j\left(\frac{1}{a^2}\frac{\delta F}{F}\right), \tag{5.19}$$

$$\ddot{E}^i_{\ j} + 3H\dot{E}^i_{\ j} - \frac{1}{a^2}\nabla^2 E^i_{\ j} = -\frac{\dot{F}}{F}\dot{E}^i_{\ j}. \tag{5.20}$$

We make a few important observations. The right-hand side of (5.19) is an anisotropic stress, and in the presence of a space-dependent non-minimal coupling, it is nonzero. The equality $\Psi = \Phi$ is often used to simplify the system of equations, but since $\delta F \propto \delta\phi$ is in general space-dependent, this is no longer possible. In the absence of non-minimal coupling ($F(\phi) = 1$), this relation is recovered. For Einstein gravity, (5.20) is a free wave equation with cosmological redshift. However, once F becomes time-dependent, an additional damping/amplification is introduced, with explicit dependence on $\dot{\phi}$. The new damping is proportional to the slow-roll parameter ϵ_F.

By combining (5.15) and (5.18), we arrive at the scalar mode equation

$$\ddot{\Psi} + 6H\dot{\Psi} + H\dot{\Phi} + 2(\dot{H} + 3H^2)\Phi - \frac{1}{a^2}\nabla^2\Psi$$

$$= -\frac{V_{,\phi}\delta\phi}{M_{\mathrm{Pl}}^2 F} - \frac{\ddot{F}}{F}\Phi - \frac{\dot{F}}{2F}\left[5(2H\Phi + \dot{\Psi}) + \dot{\Phi}\right]$$

$$+ \frac{1}{2}\frac{\ddot{\delta F}}{F} + \frac{5H}{2}\frac{\dot{\delta F}}{F} - \frac{1}{a^2}\nabla^2\left(\frac{\delta F}{F}\right)$$

$$+ \frac{1}{2}\frac{\delta F}{F}\left(\frac{2V}{M_{\mathrm{Pl}}^2 F} - \frac{\ddot{F}}{F} - 5H\frac{\dot{F}}{F}\right), \qquad (5.21)$$

and inserting (5.19) into (5.16), we obtain

$$\dot{\Psi} + \left(H + \frac{\dot{F}}{2F}\right)\Psi = \frac{1}{2}\left(\frac{1}{M_{\mathrm{Pl}}^2 F}\dot{\phi}\delta\phi + \frac{\dot{\delta F}}{F} + H\frac{\delta F}{F} + \frac{\dot{F}\delta F}{F^2}\right). \qquad (5.22)$$

At this stage, one procedure could be to solve (5.22) for $\delta\phi$ and substitute the result into (5.21). An elegant field redefinition allows us to absorb the anisotropic stress in (5.19) into new variables $\check{\Psi}$ and $\check{\Phi}$,

$$\check{\Psi} := -\Psi + \frac{\delta F}{2F}, \quad \check{\Phi} := \Phi + \frac{\delta F}{2F}, \quad \check{\Psi} + \check{\Phi} = 0, \qquad (5.23)$$

so that (5.21) becomes homogeneous [156, 157]. This is what we need to carry out the quantisation of the modes. However, eventually, we will be interested in the Friedmann and inflaton equations to quadratic order, and these turn out not to be easily written in terms of these new variables (see Appendix 5.B). In effect, the procedure is ruined in the general case by the appearance of $\dot{\delta\phi}$ in (5.22).

The equation of motion for the scalar field perturbations is found to be

$$\ddot{\delta\phi} + 3H\dot{\delta\phi} - \frac{1}{a^2}\nabla^2\delta\phi + V_{,\phi\phi}\delta\phi - \frac{1}{2}M_{\mathrm{Pl}}^2 R F_{,\phi\phi}\delta\phi$$
$$= -2V_{,\phi}\Phi + \dot{\phi}(\dot{\Phi} + 3\dot{\Psi}) + M_{\mathrm{Pl}}^2 F_{,\phi}(R\Phi + \frac{1}{2}\delta R), \qquad (5.24)$$

where the perturbation of the Ricci scalar is given by

$$\delta R = -12(\dot{H} + 2H^2)\Phi - 6H(\dot{\Phi} + 4\dot{\Psi}) - 6\ddot{\Psi} + \frac{2}{a^2}\nabla^2(2\Psi - \Phi). \qquad (5.25)$$

The above equations capture the dynamics of the fluctuating fields, and we will proceed by quantising them in the next two sections.

5.2.3 Quantisation of the tensor modes

The field equations for the inflaton fluctuations and the metric scalar perturbations are too complicated to quantise in the case of a general F. The tensor fluctuation equation has a simpler form, and we will consider that first, before we specialise to $F(\phi) = 1$. We have from (5.20) that in conformal time

$$E_{ij}'' + 2\mathcal{H}\left(1 + \epsilon_F\right) E_{ij}' - \nabla^2 E_{ij} = 0. \tag{5.26}$$

Introducing $z_g = \sqrt{F}a$ and $v\delta_{ij} = z_g E_{ij}$ (for each pair of i, j), this reduces in momentum space $v(q)$ to

$$v'' + \left(q^2 - \frac{z_g''}{z_g}\right)v = 0. \tag{5.27}$$

Using the slow-roll expression for conformal time

$$\eta = -\frac{1}{aH}\frac{1}{1 - \epsilon_H} = -\frac{1}{\mathcal{H}}\frac{1}{1 - \epsilon_H}, \tag{5.28}$$

we find

$$\frac{z_g''}{z_g} = \frac{1}{\eta^2}\frac{(1 + \epsilon_F)(2 - \epsilon_H + \epsilon_F)}{(1 - \epsilon_H)^2} := \frac{n}{\eta^2}. \tag{5.29}$$

Treating n as a constant, the solution to (5.27) is

$$v(\eta, q) = \sqrt{|\eta|}\left[c_1(\mathbf{q})H_\nu^{(1)}(q|\eta|) + c_2(\mathbf{q})H_\nu^{(2)}(q|\eta|)\right], \quad \nu = \sqrt{n + \frac{1}{4}}, \tag{5.30}$$

where $H_\nu^{(1)}(x)$ and $H_\nu^{(2)}(x)$ are Hankel functions of the first and second kind, respectively. Choosing the Bunch-Davies vacuum, the coefficients are set to $c_1(\mathbf{q}) = 0$ and $c_2(\mathbf{q}) = 1$ [44]. We still need the overall normalisation of the mode and so we write the quantised tensor field as

$$E_{ij}(\eta, \mathbf{x}) = \int \frac{\mathrm{d}^3 q}{(2\pi)^{3/2}} \sum_{\lambda=+,\times} \left[\hat{a}_{\lambda\mathbf{q}}\tilde{h}_{\lambda\mathbf{q}}(\eta)e_{ij}^{(\lambda)}(\mathbf{q})e^{i\mathbf{q}\cdot\mathbf{x}} + \text{h.c.}\right], \tag{5.31}$$

where $a_{\lambda\mathbf{q}}$ and $a^\dagger_{\lambda\mathbf{q}}$ are annihilation and creation operators and $\tilde{h}_{\lambda\mathbf{q}}$ are scalar functions. The subscripts $+, \times$ refer to the two polarisation states of the polarisation tensors $e^{(\lambda)}_{ij}$, that satisfy

$$e^{(\lambda)}_{ij}(\mathbf{q})e^{(\lambda')}_{ij}(\mathbf{q}) = 2\delta_{\lambda\lambda'}, \quad e^{(\lambda)}_{ij} = e^{(\lambda)}_{ji}, \quad e^{(\lambda)i}{}_i = 0, \quad \partial^i e^{(\lambda)}_{ij} = 0. \tag{5.32}$$

The creation and annihilation operators satisfy the commutation relation

$$[\hat{a}_{\lambda\mathbf{q}}, \hat{a}^\dagger_{\lambda'\mathbf{q}'}] = \delta_{\lambda\lambda'}\delta^3(\mathbf{q} - \mathbf{q}'), \tag{5.33}$$

with all other commutators vanishing. Inserting the ansatz of (5.31) into the action, one finds that the quadratic contributions S_t from the tensor may be written

$$S_\text{t} = M_{\text{Pl}}^2 \int \mathrm{d}\eta \mathrm{d}^3x a^2 F \sum_\lambda [\hat{h}'^2 - \hat{h}_\lambda{}^{,i}\hat{h}_{\lambda,i}], \tag{5.34}$$

where

$$\hat{h}_\lambda(\eta, \mathbf{x}) = \int \frac{\mathrm{d}^3q}{(2\pi)^{3/2}} \left[\hat{a}_{\lambda\mathbf{q}}\tilde{h}_{\lambda\mathbf{q}}(\eta)e^{i\mathbf{q}\cdot\mathbf{x}} + \text{h.c.} \right]. \tag{5.35}$$

The canonical quantisation condition is

$$[\hat{h}_\lambda(\eta, \mathbf{x}), \hat{\pi}_\lambda(\eta, \mathbf{x}')] = i\delta^3(\mathbf{x} - \mathbf{x}'), \tag{5.36}$$

and defining the conjugate momentum

$$\hat{\pi}_\lambda(\eta, \mathbf{x}) = \frac{\partial \mathcal{L}}{\partial \hat{h}'_\lambda} = 2a^2 M_{\text{Pl}}^2 F\hat{h}'_\lambda, \tag{5.37}$$

together with (5.33), we may write down the Wronskian for the mode functions themselves as

$$\tilde{h}_{\lambda\mathbf{q}}(\eta)\tilde{h}'^*_{\lambda\mathbf{q}}(\eta) - \tilde{h}^*_{\lambda\mathbf{q}}(\eta)\tilde{h}'_{\lambda\mathbf{q}}(\eta) = \frac{i}{2a^2 M_{\text{Pl}}^2 F}. \tag{5.38}$$

This gives us the final normalisation

$$\tilde{h}_{\lambda\mathbf{q}}(\eta) = \sqrt{\frac{\pi|\eta|}{8a^2 M_{\text{Pl}}^2 F}} H^{(2)}_\nu(q|\eta|), \tag{5.39}$$

where ν is approximated as

$$\nu \approx \tfrac{3}{2} + \epsilon_F + \epsilon_H + O(\epsilon^2), \qquad (5.40)$$

to first order in slow-roll parameters. We see that the effect of non-minimal coupling on the evolution of the tensor modes enters through ϵ_F and the overall normalisation.

5.2.4 Quantisation of the scalar modes

Since it is not possible to express all scalar-perturbation dependence in the quadratic-order quantum corrections solely in terms of the new variable $\hat{\Psi}$ of (5.23), we now consider the Einstein gravity limit where $F(\phi) = 1$. In this case, (5.21) reduces to

$$\ddot{\Psi} + H(1 + 2\delta_H)\dot{\Psi} + 2H^2(\delta_H - \epsilon_H)\Psi - \frac{1}{a^2}\nabla^2\Psi = 0, \qquad (5.41)$$

using (5.10) and (5.22) and the slow-roll parameters in (5.11). The scalar field equations (5.15)–(5.19) in combination with the equation of motion for $\delta\phi$ in (5.24) is an overdetermined system, and hence requires a constrained quantisation procedure [158]. To this end we introduce the canonical momenta

$$\pi_\Phi := \frac{\partial \mathcal{L}}{\partial \Phi'} = 0, \qquad (5.42)$$

$$\pi_\Psi := \frac{\partial \mathcal{L}}{\partial \Psi'} = -6a^2 M_{\text{Pl}}^2 [\Psi' + \mathcal{H}(\Phi + \Psi)], \qquad (5.43)$$

$$\pi_{\delta\phi} := \frac{\partial \mathcal{L}}{\partial \delta\phi'} = a^2 [\delta\phi' - \phi'(\Phi + 3\Psi)], \qquad (5.44)$$

and encode the constraints of the field equations by introducing the conjugate momenta

$$\chi_1 := \pi_\Phi, \qquad (5.45)$$

$$\chi_2 := \nabla^2\Psi + 3\mathcal{H}'\Psi - \frac{1}{2M_{\text{Pl}}^2}\left(a^2 V_{,\phi}\delta\phi + \frac{\phi'}{a^2}\pi_{\delta\phi} - \frac{\mathcal{H}}{a^2}\pi_\Psi\right), \qquad (5.46)$$

$$\chi_3 := \mathcal{H}\Psi + \frac{1}{2M_{\text{Pl}}^2}\left(\phi'\delta\phi + \frac{1}{3a^2}\pi_\Psi\right), \qquad (5.47)$$

$$\chi_4 := \Phi - \Psi, \qquad (5.48)$$

where then

$$\chi_\alpha = 0, \quad \alpha = 1, 2, 3, 4. \tag{5.49}$$

The constrained quantisation is realised by way of the Dirac bracket defined as

$$[A, B]_D := [A, B]_P - [A, \chi_m]_P (C^{-1})_{mn} [\chi_n, B]_P, \quad m, n = 2, 3, \tag{5.50}$$

where the Poisson bracket is defined as

$$[A, B]_P := \sum_{\varphi = \Psi, \delta\phi} \left(\frac{\partial A}{\partial \varphi} \frac{\partial B}{\partial \Pi_\varphi} - \frac{\partial B}{\partial \varphi} \frac{\partial A}{\partial \Pi_\varphi} \right), \tag{5.51}$$

and C_{mn} is a non-singular constraint matrix

$$C_{mn} := [\chi_m, \chi_n]_P. \tag{5.52}$$

The quantised variables will then have equal-time commutation relations given by

$$[A, B] = i[A, B]_D, \tag{5.53}$$

for which we obtain

$$[\Psi(\mathbf{x}), \Psi(\mathbf{x'})] = [\delta\phi(\mathbf{x}), \delta\phi(\mathbf{x'})] = 0,$$
$$[\Psi(\mathbf{x}), \Psi'(\mathbf{x'})] = i \frac{\phi'^2}{4M_{\text{Pl}}^4 a^2 \nabla^2} \delta^3(\mathbf{x} - \mathbf{x'}), \tag{5.54}$$

and where the resulting commutation relations for Ψ, $\delta\phi$ combined with the conjugate momenta π_Ψ, $\pi_{\delta\phi}$ are listed in Appendix 5.A.

The field Ψ can be promoted to an operator and decomposed in terms of mode functions $\tilde{f}_{\mathbf{k}}(\eta)$ as

$$\hat{\Psi}(\eta, \mathbf{x}) = \int \frac{\mathrm{d}^3 k}{(2\pi)^{3/2}} \left(\hat{b}_{\mathbf{k}} \tilde{f}_{\mathbf{k}}(\eta) e^{i\mathbf{k}\cdot\mathbf{x}} + \text{h.c.} \right), \tag{5.55}$$

where the creation and annihilation operators $\hat{b}_{\mathbf{k}}, \hat{b}_{\mathbf{k}}^\dagger$ fulfil the standard commutation relations

$$[\hat{b}_{\mathbf{k}}, \hat{b}_{\mathbf{k'}}] = [\hat{b}_{\mathbf{k}}^\dagger, \hat{b}_{\mathbf{k'}}^\dagger] = 0, \quad [\hat{b}_{\mathbf{k}}, \hat{b}_{\mathbf{k'}}^\dagger] = \delta^3(\mathbf{k} - \mathbf{k'}), \tag{5.56}$$

so that the equation of motion for the mode functions becomes

$$\tilde{f}_{\mathbf{k}}'' - \frac{2\delta_H}{\eta}\tilde{f}_{\mathbf{k}}' + \left(\frac{2(\delta_H - \epsilon_H)}{\eta^2} + k^2\right)\tilde{f}_{\mathbf{k}} = 0. \tag{5.57}$$

Here we have approximated the Hubble parameter $\mathcal{H} \simeq -1/\eta$ to zeroth order in slow-roll. From the equal-time commutation relation in (5.56), the Wronskian is calculated to be

$$\tilde{f}_{\mathbf{k}}(\eta)\tilde{f}_{\mathbf{k}}'^*(\eta) - \tilde{f}_{\mathbf{k}}^*(\eta)\tilde{f}_{\mathbf{k}}'(\eta) = i\left(\frac{\phi'}{2M_{\text{Pl}}^2 a|\mathbf{k}|}\right)^2. \tag{5.58}$$

The solution to the mode equation (5.57) is then given by

$$\begin{aligned}
\tilde{f}_{\mathbf{q}}(\eta) &= \frac{\sqrt{\pi|\eta|}}{2}\frac{\phi'}{2M_{\text{Pl}}^2 a|\mathbf{k}|}H_\upsilon^{(2)}(k|\eta|) \\
&= \sqrt{\frac{\pi\epsilon_H}{8}}\frac{\mathcal{H}}{M_{\text{Pl}}^2 a|\mathbf{k}|}(-\eta)^{1/2}H_\upsilon^{(2)}(-k\eta),
\end{aligned} \tag{5.59}$$

where the index υ is approximated as

$$\upsilon = \tfrac{1}{2}\sqrt{1 + 8\epsilon_H - 4\delta_H} \approx \tfrac{1}{2} + 2\epsilon_H - \delta_H. \tag{5.60}$$

5.3 Quantum-corrected equations of motion in the Einstein-gravity limit

Taking the vacuum expectation value of the perturbed equations of motion, we calculate the quantum corrections in the Einstein gravity limit $F(\phi) = 1$. The second-order terms of the Friedmann and mean-field equations are listed in Appendix 5.B (with F general), where the number of terms reduces significantly after taking the vacuum expectation value. In the end, the equations may be expressed in terms of just a few two-point correlators, which we will therefore consider first.

5.3.1 Correlation functions and renormalisation

The quantum-corrected Friedmann and mean-field equations can be expressed in terms of the two-point correlation functions

$$\left\langle\varphi^2\big|\varphi^2\right\rangle, \quad \left\langle\varphi\nabla^2\varphi\big|\varphi\nabla^2\varphi\right\rangle, \quad \left\langle\varphi\nabla^4\varphi\big|\varphi\nabla^4\varphi\right\rangle, \tag{5.61}$$

with $\varphi = E_{ij}, \Psi$, by using the relations in Appendix 5.C. Having obtained the mode solutions for the tensors in (5.39) and scalars in (5.59), these correlators can now be calculated explicitly. By use of the field decompositions in (5.31) and (5.33), we obtain for the tensor correlators:

$$C_0 := \langle E_{ij} E_{ij} | E_{ij} E_{ij} \rangle$$

$$= \frac{1}{2\pi^2} \frac{H^2}{M_{\mathrm{Pl}}^2 F} \left[\left(\frac{1}{2(\epsilon_H + \epsilon_F)} + \log 2 + \psi(\tfrac{3}{2}) \right) \left(-1 + \Lambda_{\mathrm{IR}}^{-2(\epsilon_H + \epsilon_F)} \right) \right.$$

$$\left. + \tfrac{1}{2} \Lambda_{\mathrm{UV}}^2 + \log \Lambda_{\mathrm{UV}} \right] + O(\epsilon), \tag{5.62}$$

$$C_2 := \langle E_{ij} \nabla^2 E_{ij} | E_{ij} \nabla^2 E_{ij} \rangle$$

$$= -\frac{1}{4\pi^2} \frac{a^2 H^4}{M_{\mathrm{Pl}}^2 F} \left[\tfrac{1}{2} \Lambda_{\mathrm{UV}}^4 + \Lambda_{\mathrm{UV}}^2 - \tfrac{1}{2} \Lambda_{\mathrm{IR}}^4 - \Lambda_{\mathrm{IR}}^2 \right], \tag{5.63}$$

where $\psi(x)$ denotes the digamma function and $\Lambda_{\mathrm{IR,UV}}$ are infrared and ultraviolet cutoffs respectively, see the details in Appendix 5.D. For the tensor modes, we have for illustration retained the non-minimal coupling through ϵ_F and the overall normalisation $1/F$.

For the scalars we obtain

$$D_0 := \langle \Psi^2 | \Psi^2 \rangle$$

$$= \frac{\epsilon_H H^2}{8\pi^2 M_{\mathrm{Pl}}^2} \left[\left(\frac{1}{2(2\epsilon_H - \delta_H)} + \log 2 + \psi(\tfrac{1}{2}) \right) \left(-1 + \Lambda_{\mathrm{IR}}^{-2(2\epsilon_H - \delta_H)} \right) \right.$$

$$\left. + \log \Lambda_{\mathrm{UV}} \right] + O(\epsilon), \tag{5.64}$$

$$D_2 := \langle \Psi \nabla^2 \Psi | \Psi \nabla^2 \Psi \rangle = -\frac{\epsilon_H a^2 H^4}{16\pi^2 M_{\mathrm{Pl}}^2} \left(\Lambda_{\mathrm{UV}}^2 - \Lambda_{\mathrm{IR}}^2 \right) + O(\epsilon), \tag{5.65}$$

$$D_4 := \langle \Psi \nabla^4 \Psi | \Psi \nabla^4 \Psi \rangle = \frac{\epsilon_H a^4 H^6}{32\pi^2 M_{\mathrm{Pl}}^2} \left(\Lambda_{\mathrm{UV}}^4 - \Lambda_{\mathrm{IR}}^4 \right) + O(\epsilon). \tag{5.66}$$

We notice that the scalar correlators each have an overall factor of ϵ_H, which is absent in the tensor correlators. This is a direct consequence of the mode function normalisation, where the constrained quantisation procedure of the scalars gives an additional factor of ϕ'^2 in the commutation relations in (5.54). However, we will see that once the correlators

88

are reinstated in the equations of motion, they appear at the same order in slow-roll.

The correlators have both IR and UV divergences. A careful treatment of the UV involves applying dimensional regularisation, which automatically removes all power law divergences, and where logarithmic divergences are absorbed into counterterms for higher-order invariant operators R^2, $R^{\mu\nu}R_{\mu\nu}$, etc. [67]. The computations in Appendix 5.D employ a simpler cutoff regularisation to identify where UV and IR divergences appear, after which we assume that the UV can be dealt with, so that only the physical IR effects remain. Based on this discussion, the tensor correlators will hereafter be taken to be

$$
\begin{aligned}
C_0 &= -\frac{H^2}{4\pi^2 M_{\text{Pl}}^2 F(\epsilon_H + \epsilon_F)} \left(1 - \Lambda_{\text{IR}}^{-2(\epsilon_H+\epsilon_F)}\right), \\
C_2 &= \frac{a^2 H^4}{4\pi^2 M_{\text{Pl}}^2 F} (\tfrac{1}{2}\Lambda_{\text{IR}}^4 + \Lambda_{\text{IR}}^2),
\end{aligned}
\tag{5.67}
$$

and the scalar correlators by

$$
\begin{aligned}
D_0 &= -\frac{\epsilon_H H^2}{16\pi^2 M_{\text{Pl}}^2 (2\epsilon_H - \delta_H)} \left(1 - \Lambda_{\text{IR}}^{-2(2\epsilon_H-\delta_H)}\right), \\
D_2 &= \frac{\epsilon_H a^2 H^4}{16\pi^2 M_{\text{Pl}}^2} \Lambda_{\text{IR}}^2, \\
D_4 &= -\frac{\epsilon_H a^4 H^6}{32\pi^2 M_{\text{Pl}}^2} \Lambda_{\text{IR}}^4.
\end{aligned}
\tag{5.68}
$$

Furthermore, we should only keep terms of leading order in slow-roll, since the mode functions are only valid to that order. The correlators C_2, D_2 and D_4 are proportional to the infrared cutoff, and as we imagine $\Lambda_{\text{IR}} \ll 1$, they give negligible contributions (and are set to zero). This leaves the IR-divergent C_0, D_0, for which we may write

$$
\begin{aligned}
1 - \Lambda_{\text{IR}}^{-2(\epsilon_H+\epsilon_F)} &= 2(\epsilon_H + \epsilon_F)|\log \Lambda_{\text{IR}}| + O(\epsilon^2), \\
1 - \Lambda_{\text{IR}}^{-2(2\epsilon_H-\delta_H)} &= 2(2\epsilon_H - \delta_H)|\log \Lambda_{\text{IR}}| + O(\epsilon^2).
\end{aligned}
\tag{5.69}
$$

This yields

$$C_0 = -\frac{1}{2\pi^2}\frac{H^2}{M_{\text{Pl}}^2 F}|\log \Lambda_{\text{IR}}| + O(\epsilon),$$

$$D_0 = -\frac{\epsilon_H}{8\pi^2}\frac{H^2}{M_{\text{Pl}}^2}|\log \Lambda_{\text{IR}}| + O(\epsilon^2).$$

(5.70)

We will in the following count C_0 as $O(1)$ and D_0 as $O(\epsilon)$. Below we will have a further analysis of the magnitude of the IR-cutoff.

5.3.2 Friedmann equations

Perturbing the Einstein equations to quadratic order in fluctuations, the quantum-corrected equation will take the form

$$G^\mu{}_\nu = \frac{1}{M_{\text{Pl}}^2}(\tilde{T}^\mu{}_\nu + \langle \delta_2\tilde{T}^\mu{}_\nu|\delta_2\tilde{T}^\mu{}_\nu\rangle) - \langle \delta_2 G^\mu{}_\nu|\delta_2 G^\mu{}_\nu\rangle,$$ (5.71)

where the quadratic-order contributions $\delta_2\tilde{T}_{\mu\nu}$ and $\delta_2 G_{\mu\nu}$ are given in Appendix 5.B. For the 00-component of (5.71), we obtain

$$
\begin{aligned}
3H^2 &= \frac{1}{M_{\text{Pl}}^2}\left[\tfrac{1}{2}\dot{\sigma}^2 + V - \langle\delta_2\tilde{T}^0{}_0|\delta_2\tilde{T}^0{}_0\rangle\right] + \langle\delta_2 G^0{}_0|\delta_2 G^0{}_0\rangle \\
&= \frac{1}{M_{\text{Pl}}^2}\left[\tfrac{1}{2}\dot{\sigma}^2 + V + \tfrac{1}{2}\left\langle\dot{\delta\phi}^2\big|\dot{\delta\phi}^2\right\rangle + \frac{1}{2a^2}\left\langle(\nabla\delta\phi)^2\big|(\nabla\delta\phi)^2\right\rangle\right. \\
&\quad \left. - 2\dot{\phi}\left\langle\Phi\dot{\delta\phi}\big|\Phi\dot{\delta\phi}\right\rangle + 2\dot{\phi}^2\left\langle\Phi^2\big|\Phi^2\right\rangle + \tfrac{1}{2}V_{,\phi\phi}\left\langle\delta\phi^2\big|\delta\phi^2\right\rangle\right] \\
&\quad + \tfrac{1}{2}\left\langle\dot{E}^{ij}\dot{E}_{ij}\big|\dot{E}^{ij}\dot{E}_{ij}\right\rangle + 4H\left\langle E^{ij}\dot{E}_{ij}\big|E^{ij}\dot{E}_{ij}\right\rangle - 12H^2 D_0 \\
&\quad - 3\left\langle\dot{\Psi}^2\big|\dot{\Psi}^2\right\rangle - \frac{1}{a^2}\left[5D_2 + \tfrac{3}{2}C_2\right] \\
&= \frac{1}{M_{\text{Pl}}^2}\left(\tfrac{1}{2}\dot{\sigma}^2 + V\right) + \frac{H^2}{\epsilon_H}\left[\tfrac{1}{4}\epsilon_H\frac{\partial_t^2 C_0}{H^2} + \tfrac{19}{8}\epsilon_H\frac{\partial_t C_0}{H} - \tfrac{7}{4}\epsilon_H\frac{1}{a^2}\frac{C_2}{H^2}\right. \\
&\quad + (-\tfrac{3}{2}\epsilon_H + \tfrac{1}{2}\delta_M)\frac{\partial_t^2 D_0}{H^2} + (-6\delta_H + \tfrac{9}{2}\epsilon_H + \tfrac{3}{2}\delta_M)\frac{\partial_t D_0}{H} \\
&\quad + (-12\epsilon_H + \delta_M)D_0 - \frac{1}{a^2}\frac{\partial_t^2 D_2}{H^4} - (2 + \delta_H)\frac{1}{a^2}\frac{\partial_t D_2}{H^3} \\
&\quad \left. - (1 + 2\delta_H + 4\epsilon_H + \delta_M)\frac{1}{a^2}\frac{D_2}{H^2} + \frac{1}{a^4}D_4\right],
\end{aligned}
$$

(5.72)

where we used the constraint relations in (5.16) and (5.19) to express Φ and $\delta\phi$ in terms of Ψ. Furthermore, we have introduced a new slow-roll parameter

$$\delta_M := \frac{V_{,\phi\phi}}{H^2} \simeq 3(\delta_H + \epsilon_H),\tag{5.73}$$

where the last relation follows from (5.10) and (5.11), and is correct at leading order in slow-roll. We have also used that

$$\epsilon_H H^2 = \frac{\dot{\phi}^2}{2M_{\mathrm{Pl}}^2},\tag{5.74}$$

which can be obtained by combining (5.8) and (5.9) with (5.11). For the spatial component of the Friedmann equations with $i = j$, we get

$$
\begin{aligned}
2\dot{H} + 3H^2 &= \frac{1}{M_{\mathrm{Pl}}^2}\Bigg[-\tfrac{1}{2}\dot{\phi}^2 + V - \tfrac{1}{2}\left\langle \dot{\delta\phi}^2 \big| \dot{\delta\phi}^2 \right\rangle - \frac{1}{2a^2}\left\langle (\nabla\delta\phi)^2 \big| (\nabla\delta\phi)^2 \right\rangle \\
&\quad + 2\dot{\phi}\left\langle \Phi\dot{\delta\phi} \big| \Phi\dot{\delta\phi} \right\rangle - 2\dot{\phi}^2\left\langle \Phi^2 \big| \Phi^2 \right\rangle + \tfrac{1}{2}V_{,\phi\phi}\left\langle \delta\phi^2 \big| \delta\phi^2 \right\rangle \Bigg] \\
&\quad - \tfrac{1}{2}\left\langle \dot{E}^{ij}\dot{E}_{ij} \big| \dot{E}^{ij}\dot{E}_{ij} \right\rangle - \frac{5}{2a^2}\left\langle E^{ij}\nabla^2 E_{ij} \big| E^{ij}\nabla^2 E_{ij} \right\rangle \\
&\quad - 4(2\dot{H} + 3H^2)\left\langle \Psi | \Psi \right\rangle^2 - 8H\left\langle \Psi\dot{\Psi} \big| \Psi\dot{\Psi} \right\rangle - \left\langle \dot{\Psi}^2 \big| \dot{\Psi}^2 \right\rangle \\
&\quad + \frac{1}{a^2}\left\langle \Psi\nabla^2\Psi \big| \Psi\nabla^2\Psi \right\rangle \\
&= \frac{1}{M_{\mathrm{Pl}}^2}\left(-\tfrac{1}{2}\dot{\phi}^2 + V \right) + \frac{H^2}{\epsilon_H}\Bigg[-\tfrac{1}{4}\epsilon_H\frac{\partial_t^2 C_0}{H^2} - \tfrac{3}{8}\epsilon_H\frac{\partial_t C_0}{H} \\
&\quad - \tfrac{9}{4}\epsilon_H\frac{1}{a^2}\frac{C_2}{H^2} + \left(-\tfrac{1}{2}\epsilon_H + \delta_M \right)\frac{\partial_t^2 D_0}{H^2} \\
&\quad + \left(6\delta_H - \tfrac{21}{2}\epsilon_H + \tfrac{3}{2}\delta_M \right)\frac{\partial_t D_0}{H} + \left(-12\epsilon_H + \delta_M \right)D_0 \\
&\quad + \frac{1}{a^2}\frac{\partial_t^2 D_2}{H^4} + \left(2 + \delta_H \right)\frac{1}{a^2}\frac{\partial_t D_2}{H^3} \\
&\quad + \left(1 + 2\delta_H + 4\epsilon_H - \delta_M \right)\frac{1}{a^2}\frac{D_2}{H^2} - \frac{1}{a^4}\frac{D_4}{H^4} \Bigg].
\end{aligned}
\tag{5.75}
$$

For illustration, we have included contributions to leading order in slow-roll and quantum corrections, but also (parts of) the higher order con-

tributions in slow-roll. However, for consistency, we must again truncate the whole expression at leading order. Remembering also that $D_2 \simeq D_4 \simeq C_2 \simeq 0$, we then find:

$$3H^2 = \frac{1}{M_{\text{Pl}}^2}\left(\tfrac{1}{2}\dot{\phi}^2 + V\right) + H^2\left(-12 + \frac{\delta_M}{\epsilon_H}\right)D_0 + \tfrac{19}{8}H\partial_t C_0, \quad (5.76)$$

$$2\dot{H} + 3H^2 = \frac{1}{M_{\text{Pl}}^2}\left(-\tfrac{1}{2}\dot{\phi}^2 + V\right) + H^2\left(-12 + \frac{\delta_M}{\epsilon_H}\right)D_0 - \tfrac{3}{8}H\partial_t C_0. \quad (5.77)$$

We recall that $C_0 \sim O(1)$, while $D_0 \sim O(\epsilon) \sim \partial_t C_0$. Hence, we see that scalar and tensor contributions to the effective potential appear at the same order $O(\epsilon)$, even though the correlators themselves are of different order.

The corrections to the classical relations involve terms that could equally be grouped with the left-hand side ($\propto H^2$) and the right-hand side (ϕ-dependent). Interpreting the quantum corrections as corrections to the potential, we see that the resulting effective potential is different in the two Friedmann equations. At this level in slow-roll, this difference originates from the tensor contributions only, while the scalar contributions are the same.

5.3.3 Mean-field equation

The perturbed mean-field equation (5.7) is displayed in (5.114), which in the Einstein gravity limit reduces to

$$\begin{aligned}
0 = {} & \ddot{\phi} + 3H\dot{\phi} + V_{,\phi} + \ddot{\phi}(6\Psi^2 + E^i{}_j E^j{}_i) \\
& + \dot{\phi}\left[3H(6\Psi^2 + E^i{}_j E^j{}_i) + 12\Psi\dot{\Psi} + 2\dot{E}^i{}_j E^j{}_i\right] \\
& - 4\ddot{\delta\phi}\Psi - 4\dot{\delta\phi}[3H\Psi + \dot{\Psi}] + \frac{2}{a^2}\partial_i[E^{ij}\partial_j\delta\phi] \\
& - V_{,\phi}(2\Psi^2 + E^i{}_j E^j{}_i) - 2V_{,\phi\phi}\Psi\delta\phi + \tfrac{1}{2}V_{,\phi\phi\phi}\delta\phi^2.
\end{aligned}$$

Taking the vacuum expectation value of this, we arrive at the quantum-corrected equation

$$
\begin{aligned}
0 = \ddot{\phi} &\left[1 + \frac{1}{\epsilon_H}\left(\epsilon_H C_0 + (14\epsilon_H - 8\delta_H)D_0 - 4(1+\delta_H)\frac{\partial_t D_0}{H} \right.\right. \\
&\left.\left. - 2\frac{\partial_t^2 D_0}{H^2} + \frac{4}{a^2}\frac{D_2}{H^2} \right) \right] + 3H\dot{\phi}\left[1 + \frac{1}{3\epsilon_H}\left(3\epsilon_H C_0 + \epsilon_H \partial_t C_0 \right.\right. \\
&\left.\left. + (18\epsilon_H + 2\delta_M)D_0 - (4\epsilon_H - \delta_M)\frac{\partial_t D_0}{H} - \frac{4}{a^2}\frac{D_2}{H^2} - \frac{4}{a^2}\frac{\partial_t D_2}{H^3} \right) \right] \\
&+ V_{,\phi}(1 + 6D_0 - C_0) + \frac{M_{\text{Pl}}^2}{\epsilon_H}V_{,\phi\phi\phi}\left[(1 + 2\delta_H - 2\epsilon_H)D_0 \right. \\
&\left. + (\tfrac{3}{2} + \delta_H)\frac{\partial_t D_0}{H} + \frac{1}{2}\frac{\partial_t^2 D_0}{H^2} - \frac{1}{a^2}\frac{D_2}{H^2} \right].
\end{aligned}
\tag{5.78}
$$

This equation can be derived via two routes. Either using the field equation (5.16) to re-express $\ddot{\delta\phi}$ in terms of Ψ, or by using (5.24). Here we have chosen the latter way, as it is more straightforward, although both methods must yield the same result at leading order in slow-roll parameters. We may further truncate in slow-roll, and again set $D_2 \simeq D_4 \simeq C_2 \simeq 0$, to obtain

$$
\begin{aligned}
0 = \ddot{\phi} &\left[1 + C_0 + \left(14 - 8\frac{\delta_H}{\epsilon_H} \right)D_0 \right] \\
&+ 3H\dot{\phi}\left[1 + C_0 + \tfrac{1}{3}\partial_t C_0 + \left(6\epsilon_H + \frac{2}{3}\frac{\delta_M}{\epsilon_H} \right)D_0 \right] \\
&+ V_{,\phi}(1 - C_0 + 6D_0) + M_{\text{Pl}}^2 V_{,\phi\phi\phi}\frac{1 + 2\delta_H - 2\epsilon_H}{\epsilon_H}D_0.
\end{aligned}
\tag{5.79}
$$

Here we notice that the quantum corrections already appear at $O(1)$, and treating $\ddot{\phi}$ as higher order, we may further truncate to get

$$
0 = 3H\dot{\phi}\,(1 + C_0) + V_{,\phi}(1 - C_0) + M_{\text{Pl}}^2 V_{,\phi\phi\phi}\frac{D_0}{\epsilon_H}.
\tag{5.80}
$$

As for the Friedmann equation, corrections from scalars and tensor enter at the same order, but the tensor contributions now enter as a multiplicative correction to the potential and the damping (Hubble) rate.

Comparing to the classical field equation (where $C_0 = D_0 = 0$), it is not possible to identify the corrections as simply modifying the potential. On the other hand, we note that for $C_0 = 0$ (ignoring tensors), when comparing to (5.76), the term $V_{,\phi\phi\phi}D_0/\epsilon$ may be related to (the derivative of) $\delta_M D_0/\epsilon$, provided D_0/ϵ is assumed not to depend on ϕ. Once $C_0 \neq 0$ this correspondence is lost, showing that tensor modes make a qualitative difference.

5.4 Magnitude of corrections: examples

In this section, we estimate the magnitude of the quantum corrections to the mean-field and Friedmann equations for large-field monomial inflation and quartic hilltop inflation. We wish to compute their values during inflation, and we choose the time of horizon crossing, which we take to be $N = 50 - 60$ e-foldings before the end of inflation.

First, we need a prescription to evaluate the IR-divergent correlators. As noted in section 5.3.1, with a small IR cutoff $\Lambda_{\mathrm{IR}} \to 0$, all correlators become negligible except C_0 and D_0, which diverge logarithmically. The IR logarithm can be related to the number of e-foldings during inflation. If we assume that the IR cutoff is set to exclude superhorizon modes from the loop integrals, i.e. so that the comoving momenta is cut off by the initial Hubble radius as $k \geq a_{\mathrm{in}}H_{\mathrm{in}}$, then for $x := -k\eta \geq \Lambda_{\mathrm{IR}}$ the cutoff is

$$\Lambda_{\mathrm{IR}} = \frac{a_{\mathrm{in}}H_{\mathrm{in}}}{aH(1 - \epsilon_H)}. \tag{5.81}$$

With approximately constant ϵ_H, the scale factor and Hubble parameter are solved by

$$a = a_{\mathrm{in}}e^N, \quad H = H_{\mathrm{in}}e^{-\epsilon_H N}, \quad N := \int_{t_{\mathrm{in}}}^{t} \mathrm{d}t' H(t'), \tag{5.82}$$

where N is the number of e-foldings from horizon exit to the end of inflation. The assumption $\epsilon_H \simeq$ const. signifies that we are working at leading order in slow-roll. Inserting the solutions of (5.82) into (5.81), the IR limit can be written

$$\Lambda_{\mathrm{IR}} = \frac{1}{1 - \epsilon_H} e^{-(1-\epsilon_H)N}, \tag{5.83}$$

so that for $\Lambda_{\text{IR}} \ll 1$ its logarithm can be approximated to

$$|\log \Lambda_{\text{IR}}| \simeq (1 - \epsilon_H)N. \tag{5.84}$$

The role of IR-divergences and ways to deal with them are discussed for instance in [70, 152].

Now, when comparing the magnitude of the tensor and scalar corrections, we must consider the minimal-coupling limit in which the tensor correlator of (5.67) is given by

$$C_0 = \frac{1}{2\pi^2} \frac{H^2}{M_{\text{Pl}}^2} N_t, \tag{5.85}$$

where we have introduced a number N_t related to N as

$$N_t := -\frac{1}{2\epsilon_H} \left(1 - e^{2\epsilon_H |\log \Lambda_{\text{IR}}|} \right) \simeq -\frac{1}{2\epsilon_H} \left(1 - e^{2\epsilon_H N} \right). \tag{5.86}$$

Similarly for the scalars, we write

$$D_0 = \frac{\epsilon_H}{8\pi^2} \frac{H^2}{M_{\text{Pl}}^2} N_s, \tag{5.87}$$

introducing the quantity N_s according to

$$
\begin{aligned}
N_s &:= -\frac{1}{2(2\epsilon_H - \delta_H)} \left(1 - e^{2(2\epsilon_H - \delta_H)|\log \Lambda_{\text{IR}}|} \right) \\
&\simeq -\frac{1}{2(2\epsilon_H - \delta_H)} \left(1 - e^{2(2\epsilon_H - \delta_H)N} \right).
\end{aligned}
\tag{5.88}
$$

We can relate the combination of slow-roll parameters to the measured spectral index (see below for the definition of the "potential" slow-roll parameters ϵ_V, δ_V) according to

$$-0.035 = n_s - 1 := \tfrac{2}{3}\delta_M - 6\epsilon_H = 2\delta_H - 4\epsilon_H \simeq 2\delta_V - 6\epsilon_V. \tag{5.89}$$

Using this in (5.88), we find for the range $N = 50-60$ that $N_s \simeq 136-205$. It is less straightforward to infer ϵ_H from n_s. If $\delta_H \simeq 2\epsilon_H \simeq (n_s - 1)/2$, then $N_t = 33-37$ or $80-108$ depending on the sign of ϵ_H. There are also models where $\epsilon_H \ll \delta_H$ during inflation, in which case we may expand N_t so that $N_t \simeq N$. We conclude that $N_{s,t} \simeq 100$, within a factor of a few. This will be sufficient for our estimates.

5.4.1 Monomial models

The simplicity of monomial potentials makes them a natural first choice to apply our calculations to. Hence, we consider a general power-law inflaton potential of the form

$$V(\phi) = \frac{\lambda_p}{p!} \frac{\phi^p}{M_{\text{Pl}}^{p-4}}, \tag{5.90}$$

where λ_p is a dimensionless scalar self-coupling. The corresponding slow-roll parameters are

$$\epsilon_V = \frac{1}{2} \left(\frac{p M_{\text{Pl}}}{\phi} \right)^2, \quad \delta_V = p(p-1) \left(\frac{M_{\text{Pl}}}{\phi} \right)^2, \tag{5.91}$$

The requirement for slow-roll inflation is $\epsilon_H \simeq \epsilon_V < 1$, which determines the end of inflation to be $\phi/M_{\text{Pl}} = p/\sqrt{2}$. We estimate the magnitude of the correlators at horizon exit for which

$$\left(\frac{\phi_*}{M_{\text{p}}} \right)^2 = 2pN \left(1 + \frac{p}{4N} \right). \tag{5.92}$$

The number of e-foldings between horizon crossing and the end of inflation is given by the scale of inflation and the thermal history of the Universe after inflation. As indicated, we will simply assume that N is in the interval $50 - 60$.

The spectral index is given by

$$n_{\text{s}} - 1 = 2\delta_H - 4\epsilon_H \simeq 2\delta_V - 6\epsilon_V = -\frac{p+2}{2N \left(1 + \frac{p}{4N} \right)}. \tag{5.93}$$

For $p = 2$ and $N = 57$ we get the observed value of $n_{\text{s}} \simeq 0.965$ [147]. This determines $\epsilon_H \simeq 0.00875$ and $N_{\text{t}} \simeq 96$, $N_{\text{s}} \simeq 175$. The tensor correlator in (5.85) is then of the order

$$C_0 \simeq 4.8 \frac{H^2}{M_{\text{Pl}}^2}. \tag{5.94}$$

Similarly for the scalars, we use the relation of (5.89) in (5.87), to obtain

$$D_0 \simeq 2.2 \frac{\epsilon_H H^2}{M_{\text{Pl}}^2}. \tag{5.95}$$

For $p = 4$, we need $N = 85$ to get the correct spectral index. This is ruled out by observations, but for illustration, this then gives $\epsilon_H \simeq 0.012$, $N_t \simeq 259$, $N_s \simeq 507$ and

$$C_0 \simeq 13.1 \frac{H^2}{M_{\text{Pl}}^2}, \quad D_0 \simeq 6.4 \frac{\epsilon_H H^2}{M_{\text{Pl}}^2}. \tag{5.96}$$

In the mean-field equation (5.80), we have

$$0 = 3H\dot{\phi}\,(1 + C_0) + V_{,\phi}(1 - C_0) + M_{\text{Pl}}^2 V_{,\phi\phi\phi} \frac{D_0}{\epsilon_H}. \tag{5.97}$$

With $p = 2$ then $V_{,\phi\phi\phi} = 0$, and so scalar fluctuations give no corrections at leading order. The tensor modes do, although they are numerically very small. For $p = 4$ then $V_{,\phi\phi\phi} = \Lambda_4 \phi$, so both scalars and tensors contribute, and we may write

$$\frac{V_{,\phi} C_0}{M_{\text{Pl}}^2 V_{,\phi\phi\phi} \frac{D_0}{\epsilon_H}} = \frac{2}{3} \frac{\phi_*^2}{M_{\text{Pl}}^2} \frac{N_t}{N_s}, \tag{5.98}$$

which in this case is $\sim O(10^2)$. Hence, the tensor contributions dominate.

But of course, the overall magnitude of the corrections is controlled by the quantity H^2/M_{Pl}^2, which is related to the overall amplitude of the CMB (scalar) spectrum and constrained to be strictly smaller than $(2.5 \times 10^{-5})^2$ [147]. Since N_s is fixed by $n_s - 1$ and N, large corrections can only arise if N_t would become large in a small-ϵ_H regime. In order for C_0 to be comparable to unity, then $N_t \simeq N$ must be of order 10^{10}.

The corrections to the Friedmann equations become (taking $N_{t,s}$ to be constant)

$$\begin{aligned}
\Delta\rho &:= H^2 \left[(-9\epsilon_H + 3\delta_H) \frac{N_s}{8\pi^2} - \frac{19}{8} \epsilon_H \frac{N_t}{\pi^2} \right] \frac{H^2}{M_{\text{Pl}}^2}, \\
\Delta p &:= H^2 \left[(-9\epsilon_H + 3\delta_H) \frac{N_s}{8\pi^2} + \frac{3}{8} \epsilon_H \frac{N_t}{\pi^2} \right] \frac{H^2}{M_{\text{Pl}}^2},
\end{aligned} \tag{5.99}$$

for (5.76) and (5.77) respectively. Estimates of these corrections are summarised in Table 5.1 for the potentials considered in this section. For both of the monomial potentials the corrections are of order $\Delta\rho \sim O(10^{-1} H^2/M_{\text{Pl}}^2)$ and $\Delta p \sim O(10^{-2} H^2/M_{\text{Pl}}^2)$, which are again completely negligible.

	ϕ^2	ϕ^4	$V_0(1-\lambda_4\phi^4)\vert_{N=50}$	$V_0(1-\lambda_4\phi^4)\vert_{N=60}$
C_0 $[H^2/M_{\mathrm{Pl}}^2]$	4.8	13.1	2.8	3.1
D_0 $[H^2/M_{\mathrm{Pl}}^2]$	$2.2\epsilon_H$	$6.4\epsilon_H$	$1.7\epsilon_H$	$2.6\epsilon_H$
$\Delta\rho$ $[H^4/M_{\mathrm{Pl}}^2]$	-0.26	-0.86	-0.12	-0.15
Δp $[H^4/M_{\mathrm{Pl}}^2]$	-0.025	-0.016	-0.10	-0.14

Table 5.1: Estimates of the tensor and scalar correlators (C_0 resp. D_0) as well as the Friedmann corrections in (5.99) for two monomial potentials and the quartic hilltop potential of (5.100). For the quartic hilltop potential the parameter λ_4 is estimated given a selected value of the number of *e*-foldings N.

5.4.2 Quartic hilltop

A general hilltop model [159] of the inflaton potential can be written

$$V(\phi) = V_0 \left[1 - \lambda_p \left(\frac{\phi}{M_{\mathrm{Pl}}} \right)^p + \dots \right], \quad p \geq 2, \qquad (5.100)$$

where V_0 is a constant energy density scale, λ_p is some parameter, p is often an integer, and the dots indicate that some higher power-law terms must kick in at larger values of ϕ, for the potential to be bounded from below. We will take $p = 4$.

The quantum contributions for this model can be estimated in much the same way as before. In fact, because N_s is a function of the slow-roll parameters in the combination $2\delta_H - 4\epsilon_H = n_s - 1$, if we insist that the spectral index is the observed one, then N_s is independent of the inflation model.

Since the potential in (5.100) is a constant plus a monomial, the expressions in (5.98) and (5.99) are left unchanged, and to find N_t we only need to compute $\epsilon_H \simeq \epsilon_V$ at horizon crossing (since δ_H follows from $n_s - 1$ and ϵ_H).

With $p = 4$, the potential slow-roll parameters are

$$\epsilon_V(\phi) = \frac{8\lambda_4^2 \left(\frac{\phi}{M_{\mathrm{Pl}}} \right)^6}{\left(1 - \lambda_4 \left(\frac{\phi}{M_{\mathrm{Pl}}} \right)^4 \right)^2}, \quad \delta_V(\phi) = -\frac{12\lambda_4 \left(\frac{\phi}{M_{\mathrm{Pl}}} \right)^2}{1 - \lambda_4 \left(\frac{\phi}{M_{\mathrm{Pl}}} \right)^4}, \qquad (5.101)$$

and we define the end of inflation by $\epsilon_V(\phi_e) := 1$. From the definition of N we find

$$\left(\frac{\phi_*}{M_{\text{Pl}}}\right)^2 + \frac{1}{\lambda_4}\left(\frac{\phi_*}{M_{\text{Pl}}}\right)^{-2} = 8N + \left(\frac{\phi_e}{M_{\text{Pl}}}\right)^2 + \frac{1}{\lambda_4}\left(\frac{\phi_e}{M_{\text{Pl}}}\right)^{-2}, \qquad (5.102)$$

from which we compute $\epsilon_V(\phi_*)$ and $\delta_V(\phi_*)$. For $N = 50$ we find the values $\lambda_4 = 4.3 \times 10^{-6}$, $(\phi_*)^2 = 200 M_{\text{Pl}}^2$, $N_t = 55$ and $N_s = 136$. With $N = 60$ then we find $\lambda_4 = 3.2 \times 10^{-5}$, $(\phi_*)^2 = 40 M_{\text{Pl}}^2$, $N_t = 62$ and $N_s = 205$. The fraction of (5.98) then becomes about 50 for $N = 50$ and 8 for $N = 60$. The Friedmann corrections of are of order $\Delta\rho, \Delta p \sim O(10^{-1}H^2/M_{\text{Pl}}^2)$ as listed in Table 5.1.

5.5 Conclusions

We have computed the leading-order (in slow-roll and quantum fluctuations) corrections to the inflaton equation of motion and the Friedmann equations during inflation. We have included the fluctuations in the inflaton field, and both scalar and tensor fluctuations in the metric. Starting out including a non-minimal coupling to gravity $F(\phi)$, we solved the mode equation for the tensor modes, and were able to derive expressions for the scalar mode equations and the corrected Friedmann and field equations. We then proceeded in the limit $F(\phi) = 1$ to explicitly compute the leading-order corrections to the evolution equations.

We found that both the tensor and scalar correlators enter at leading order for a self-interacting inflaton, the scalars as an additive contribution, the tensors as multiplicative contributions. The tensors contribute also for a quadratic inflaton potential, where the scalar contribution decouples. While the tensor contribution is larger by one or two orders of magnitude, the overall size of the corrections is very small.

The correlators are logarithmically IR-divergent, and we introduced an ad hoc IR-cutoff in order to estimate their magnitude. Infrared divergences in Minkowski space are well-known from finite-temperature and finite-density calculations. They are more severe in the former case due to phase-space effects (dimensional reduction), but in both cases they are unphysical in the sense that the real physical medium effects are screening

them. This is resolved by resummation of classes of certain diagrams to all orders in perturbation theory, for example by using the resummation program of [160] or the 2PI effective action formalism [35]. A mass can also be generated non-perturbatively in curved spacetime [69, 74] that screens infrared divergences.[4] For example, in de Sitter space, the generated mass for a classical massless scalar field is of order H. In Minkowski space, there are quantum fluctuations at all scales, however, in de Sitter space, the scale is set by H and this is the scale of the important quantum fluctuations.

Since quantum corrections during inflation seems to anyway be suppressed by H^2/M_{Pl}^2, computing them with high accuracy may seem futile. However, quantum and thermal corrections are known to be important for a number of phenomena in cosmology, with examples including infrared effects in de Sitter space [74, 153, 154], corrections to the effective potential of the Standard Model [68, 161] and thermalisation [75].

Although significantly more challenging than field theory in a classical FRW background, exploring metric corrections to the field equations is part of that story.

Much work remains to be done on resummation of IR-divergences, including metric fluctuations and away from de Sitter space, as well as the further inclusion of non-minimal coupling to gravity and other more general theories of gravity. Also, although in this chapter we have insisted that ϕ is the inflaton, quantum corrections arise for spectator fields as well (curvaton, other matter fields), due the background metric and its fluctuations. Although the Friedmann equations remain dominated by the inflaton, each subdominant spectator field acquires its own effective equation of motion. This opens up a number of new model-building opportunities to explore.

---

[4]The mass is non-perturbative in the sense that it is not seen at any finite order in perturbation theory, but shows up after summing classes of diagrams to all orders.

5.A Scalar commutation relations

For completeness, we list a number of commutation relations in addition to those given in (5.54). They are

$$[\pi_\Psi(\mathbf{x}), \pi_{\delta\phi}(\mathbf{x}')] = i3a^2 \left(\phi' + \frac{2(3\mathcal{H}'\phi' + a^2\mathcal{H}V_{,\phi})}{\nabla^2} \right) \delta^3(\mathbf{x} - \mathbf{x}'),$$

$$[\Psi(\mathbf{x}), \pi_{\delta\phi}(\mathbf{x}')] = -i\frac{3\mathcal{H}\phi' + a^2 V_{,\phi}}{2M_{\text{Pl}}^2 \nabla^2} \delta^3(\mathbf{x} - \mathbf{x}'),$$

$$[\delta\phi(\mathbf{x}), \pi_{\delta\phi}(\mathbf{x}')] = i \left(1 + \frac{3\phi'^2}{M_{\text{Pl}}^2 \nabla^2} \right) \delta^3(\mathbf{x} - \mathbf{x}'),$$

$$[\delta\phi(\mathbf{x}), \pi_\Psi(\mathbf{x}')] = i\frac{6\mathcal{H}\phi'}{\nabla^2} \delta^3(\mathbf{x} - \mathbf{x}'),$$

$$[\Psi(\mathbf{x}), \pi_\Psi(\mathbf{x}')] = -i\frac{3\phi'^2}{2M_{\text{Pl}}^2 \nabla^2} \delta^3(\mathbf{x} - \mathbf{x}'),$$

$$[\Psi(\mathbf{x}), \delta\phi(\mathbf{x}')] = i\frac{\phi'}{2M_{\text{Pl}}^2 a^2 \nabla^2} \delta^3(\mathbf{x} - \mathbf{x}'),$$

$$[\delta\phi(\mathbf{x}), \delta\phi'(\mathbf{x}')] = \frac{i}{a^2} \left(1 + \frac{3\phi'^2}{2M_{\text{Pl}}^2 \nabla^2} \right) \delta^3(\mathbf{x} - \mathbf{x}'),$$

$$(5.103)$$

where it is implicit that they apply at equal times.

5.B Second-order equations with general non-minimal coupling

We present the Friedmann and mean-field equations with a general non-minimal coupling to quadratic order in perturbations to illustrate the (rather non-trivial) dependence on F. A central ingredient to these equations is the perturbed inverse metric, which can be found from a Taylor expansion. To quadratic order in perturbations, we find

$$(g + \delta g)^{\mu\nu} = g^{\mu\nu} - \delta g^{\mu\nu} + \delta g^{\mu\lambda} \delta g_\lambda{}^\nu, \qquad (5.104)$$

with

$$(g + \delta g)^{00} = 1 + 2\Phi - 4\Phi^2,$$
$$(g + \delta g)^{0i} = (g + \delta g)^{i0} = 0,$$
$$(g + \delta g)^{ii} = \frac{1}{a^2}\left[\delta^{ij} + 2(\Psi\delta^{ij} - E^{ij}) + 4\Psi^2\delta^{ij} + 4E^{ik}E^j{}_k - 8\Psi E^{ij}\right],$$
(5.105)

and where indices on the perturbed metric are raised as $\delta g^{\mu\nu} = -g^{\alpha\mu}g^{\nu\beta}\delta g_{\mu\nu}$.

Similarly, using $\det g = \exp(\mathrm{Tr}(\ln g))$ and Taylor expanding, the perturbed metric determinant is given by

$$\begin{aligned}
\sqrt{-(g + \delta g)} &= \sqrt{-g}\left(1 + \tfrac{1}{2}\delta g^\mu{}_\mu + \tfrac{1}{8}\delta g^\mu{}_\mu\delta g^\nu{}_\nu - \tfrac{1}{4}\delta g^{\mu\nu}\delta g_{\nu\mu}\right) \\
&= a^3\big(1 + \Phi - 3\Psi + E^i{}_i - \tfrac{1}{2}\Phi^2 - 3\Phi\Psi + \Phi E^i{}_j \\
&\quad + \tfrac{3}{2}\Psi^2 - \Psi E^i{}_i + \tfrac{1}{2}E^i{}_i E^j{}_j - E^{ij}E_{ji}\big),
\end{aligned}$$
(5.106)

where $\delta g^\mu{}_\mu = g^{\mu\nu}\delta g_{\nu\mu}$. (5.104) and (5.106) are then inserted into the expressions for the energy-momentum tensor in (5.5) and mean-field equation (5.7), whose resulting expressions are truncated at quadratic order.

With a general F, the perturbed Einstein field equations to quadratic order read

$$(F + \delta F + \delta_2 F)(G_{\mu\nu} + \delta G_{\mu\nu} + \delta_2 G_{\mu\nu}) = \frac{1}{M_{\mathrm{Pl}}^2}(\tilde{T}_{\mu\nu} + \delta\tilde{T}_{\mu\nu} + \delta_2\tilde{T}_{\mu\nu}), \quad (5.107)$$

from which the quantum-corrected equations take the form

$$\begin{aligned}
G_{\mu\nu} &= \frac{1}{M_{\mathrm{Pl}}^2}\frac{1}{F}\left(\tilde{T}_{\mu\nu} + \left\langle\delta_2\tilde{T}_{\mu\nu}|\delta_2\tilde{T}_{\mu\nu}\right\rangle\right) - \left\langle\delta_2 G_{\mu\nu}|\delta_2 G_{\mu\nu}\right\rangle \\
&\quad - \left\langle\frac{\delta F}{F}\delta G_{\mu\nu}\right\rangle - \left\langle\frac{\delta_2 F}{F}\right\rangle G_{\mu\nu}.
\end{aligned}$$
(5.108)

Specialising to the FRW metric in Newtonian gauge, at linear order, the

perturbations to the Einstein tensor read

$$\delta G^0{}_0 = 6H^2\Phi + 6H\dot{\Psi} - \frac{2}{a^2}\nabla^2\Psi,$$

$$\delta G^i{}_j = \left[6H^2\Phi + 4\dot{H}\Phi + 2H\dot{\Phi} + 6H\dot{\Psi} + 2\ddot{\Psi} + \frac{1}{a^2}\nabla^2(\Phi - \Psi) \right]\delta^i{}_j$$
$$+ \frac{1}{a^2}\partial_j\partial^i(\Psi - \Phi) + \ddot{E}^i{}_j + 3H\dot{E}^i{}_j - \frac{1}{a^2}\nabla^2 E^i{}_j,$$

$$(5.109)$$

and the quadratic-order contributions are given by

$$\delta_2 G^0{}_0 = \tfrac{1}{2}\dot{E}_{ij}\dot{E}^{ij} + 4HE^{ij}\dot{E}_{ij} - 12H^2\Phi^2 - 12H\Phi\dot{\Psi} + 12H\Psi\dot{\Psi}$$
$$- 3\dot{\Psi}^2 + \frac{1}{a^2}\Big[-8\Psi\nabla^2\Psi - 3(\nabla\Psi)^2 + 2E^{ij}\partial_j\partial_i\Psi$$
$$- 2E^{ij}\nabla^2 E_{ij} + \partial_j E_{ik}\partial^k E^{ij} - \tfrac{3}{2}\partial_k E_{ij}\partial^k E^{ij} \Big],$$

$$(5.110)$$

respectively

$$
\begin{aligned}
\delta_2 G^i{}_j = {} & -2\dot{E}^{ik}\dot{E}_{jk} - 2E^{ik}\ddot{E}_{jk} + \tfrac{3}{2}\dot{E}_{kl}\dot{E}^{kl}\delta^i{}_j + 2E^{kl}\ddot{E}_{kl}\delta^i{}_j \\
& - 6HE^{ik}\dot{E}_{jk} + 6HE^{kl}\dot{E}_{kl}\delta^i{}_j - 2\ddot{E}^i{}_j\Phi - 6H\dot{E}^i{}_j\Phi \\
& - 12\delta^i{}_j H^2\Phi^2 - 8\delta^i{}_j\dot{H}\Phi^2 - \dot{E}^i{}_j\dot{\Phi} - 8\delta^i{}_j H\Phi\dot{\Phi} + 2\ddot{E}^i{}_j\Psi \\
& + 6H\dot{E}^i{}_j\Psi + \dot{E}^i{}_j\dot{\Psi} + 6HE^i{}_j\ddot{\Psi} - 12\delta^i{}_j H\Phi\dot{\Psi} - 2\delta^i{}_j\dot{\Phi}\dot{\Psi} \\
& + 12\delta^i{}_j H\Psi\dot{\Psi} + \delta^i{}_j\dot{\Psi}^2 + 2E^i{}_j\ddot{\Psi} - 4\delta^i{}_j\Phi\ddot{\Psi} + 4\delta^i{}_j\Psi\ddot{\Psi} \\
& + \frac{1}{a^2}\partial^i E^{kl}\partial_j E_{kl} + \frac{1}{a^2}\partial^i\Phi\partial_j\Phi - \frac{1}{a^2}\partial^i\Psi\partial_j\Phi - \frac{1}{a^2}\partial^i\Phi\partial_j\Psi \\
& + \frac{3}{a^2}\partial^i\Psi\partial_j\Psi + \frac{2}{a^2}E^{kl}\partial_j\partial^i E_{kl} + \frac{2}{a^2}\Phi\partial_j\partial^i\Phi - \frac{2}{a^2}\Psi\partial_j\partial^i\Phi \\
& + \frac{4}{a^2}\Psi\partial_j\partial^i\Psi + \frac{2}{a^2}E_j{}^k\partial_k\partial^i\Psi + \frac{2}{a^2}E^{ik}\partial_k\partial_j\Phi - \frac{4}{a^2}\Psi\nabla^2 E^i{}_j \\
& - \frac{2}{a^2}\delta^i{}_j\Phi\nabla^2\Phi + \frac{2}{a^2}\delta^i{}_j\Psi\nabla^2\Phi - \frac{2}{a^2}E^i{}_j\nabla^2\Psi - \frac{4}{a^2}\delta^i{}_j\Psi\nabla^2\Psi \\
& + \frac{1}{a^2}\partial^i E_{jk}\partial^k\Phi + \frac{1}{a^2}\partial_j E^i{}_k\partial^k\Phi - \frac{1}{a^2}\partial_k E^i{}_j\partial^k\Phi \\
& - \frac{1}{a^2}\delta^i{}_j\partial_k\Phi\partial^k\Phi + \frac{1}{a^2}\partial^i E_{jk}\partial^k\Psi + \frac{1}{a^2}\partial_j E^i{}_k\partial^k\Psi \\
& - \frac{3}{a^2}\partial_k E^i{}_j\partial^k\Psi - \frac{2}{a^2}\delta^i{}_j\partial_k\Psi\partial^k\Psi - \frac{2}{a^2}E^{kl}\partial_l\partial^i E_{jk} \\
& - \frac{2}{a^2}E^{kl}\partial_l\partial_j E^i{}_k + \frac{2}{a^2}E^{kl}\partial_l\partial_k E^i{}_j - \frac{2}{a^2}E^{kl}\delta^i{}_j\partial_l\partial_k\Phi \\
& + \frac{2}{a^2}E^{ik}\nabla^2 E_{jk} - \frac{2}{a^2}\partial_k E_{jl}\partial^l E^{ik} + \frac{2}{a^2}\partial_l E_{jk}\partial^l E^{ik} \\
& - \frac{2}{a^2}E^{kl}\delta^i{}_j\nabla^2 E_{kl} + \frac{1}{a^2}\delta^i{}_j\partial_l E_{km}\partial^m E^{kl} - \frac{3}{2a^2}\delta^i{}_j\partial_m E_{kl}\partial^m E^{kl}.
\end{aligned}
$$

$$(5.111)$$

We keep in mind that since the tensor and scalar degrees of freedom propagate separately, the two-point correlators that mix these, e.g. $\langle\delta\phi E_{ij}|\delta\phi E_{ij}\rangle$, vanish. Turning to the energy-momentum tensor, we determine the 00-

component to

$$
\begin{aligned}
\delta_2 \tilde{T}^0{}_0 = {} & -\tfrac{1}{2}\dot{\delta\phi}^2 - \tfrac{1}{2a^2}(\nabla\delta\phi)^2 + 2\dot{\phi}\Phi\dot{\delta\phi} - 2\dot{\phi}^2\Phi^2 - \tfrac{1}{2}V_{,\phi\phi}\delta\phi^2 \\
& + 3H\dot{\delta_2 F} - \frac{1}{a^2}\nabla^2\delta_2 F - 3\dot{\delta F}(2H\Phi + \dot{\Psi}) \\
& - \frac{1}{a^2}\left[\nabla(2\Phi - \Psi)\nabla\delta F + 2\Psi\nabla^2\delta F - 2\partial_i(E^{ij}\partial_j\delta F)\right] \\
& + 2\dot{F}\left[6H\Phi^2 + 3(\Phi - \Psi)\dot{\Psi} - \dot{E}^i{}_j E^j{}_i\right],
\end{aligned}
\tag{5.112}
$$

and for the ij-component, we get

$$
\begin{aligned}
\delta_2 \tilde{T}^i{}_j = {} & \frac{1}{a^2}\delta\phi^{,i}\delta\phi_{,j} + \Big[\tfrac{1}{2}\dot{\delta\phi}^2 - \tfrac{1}{2a^2}(\nabla\delta\phi)^2 - 2\dot{\phi}\Phi\dot{\delta\phi} + 2\dot{\phi}^2\Phi^2 \\
& - \tfrac{1}{2}V_{,\phi\phi}\delta\phi^2\Big]\delta^i{}_j + \frac{1}{a^2}\partial^i\partial_j\delta_2 F + \Big[\ddot{\delta_2 F} + 2H\dot{\delta_2 F} \\
& - \frac{1}{a^2}\nabla^2\delta_2 F\Big]\delta^i{}_j - 2\ddot{\delta F}\Phi - \dot{\delta F}[(4H\Phi + \dot{\Phi} + \dot{\Psi})\delta^i{}_j + 2\dot{E}^i{}_j] \\
& + \frac{1}{a^2}[\partial^i(-\Psi\delta^l{}_j + E^l{}_j) + \partial_j(-\Psi\delta^{li} + E^{li}) \\
& - \partial^l(-\Psi\delta_j{}^i + E_j{}^i)]\partial_l\delta F + \frac{2}{a^2}(\Psi\delta^{ik} - E^{ik})\partial_k\partial_j\delta F \\
& - \frac{1}{a^2}\left[\nabla(\Phi - \Psi)\nabla\delta F + 2\Psi\nabla^2\delta F - 2\partial_k(E^{kl}\partial_l\delta F)\right]\delta^i{}_j \\
& + 4\ddot{F}\Phi^2\delta^i{}_j + \dot{F}\big(8H\Phi^2 + 8\Phi\dot{\Psi} - 2\Psi\dot{\Psi} + 4\Phi\dot{\Phi} - 2\dot{E}^k{}_l E^l{}_k\big)\delta^i{}_j \\
& + 2\dot{F}\left[(\Phi - 2\Psi)\dot{E}^i{}_j - 2\dot{\Psi}E^i{}_j + 2E^{ik}\dot{E}_{jk}\right].
\end{aligned}
\tag{5.113}
$$

Finally, for the mean-field equation, we obtain

$$
\begin{aligned}
0 = {} & \ddot{\phi} + 3H\dot{\phi} + V_{,\phi} \\
& + \ddot{\phi}\big[\tfrac{3}{2}(\Phi + \Psi)^2 + E^i{}_j E^j{}_i\big] \\
& + \dot{\phi}\big[3H\big(\tfrac{3}{2}(\Phi + \Psi)^2 + E^i{}_j E^j{}_i\big) + 3(\Phi + \Psi)(\dot{\Phi} + \dot{\Psi}) + 2\dot{E}^i{}_j E^j{}_i\big] \\
& - \ddot{\delta\phi}(\Phi + 3\Psi) - \dot{\delta\phi}[3H(\Phi + 3\Psi) + \dot{\Phi} + 3\dot{\Psi}] \\
& - \frac{1}{a^2}\big(\nabla[(\Phi - \Psi)\nabla\delta\phi] - 2\partial_i[E^{ij}\partial_j\delta\phi]\big) \\
& + \big(-\tfrac{1}{2}\Phi^2 - 3\Phi\Psi + \tfrac{3}{2}\Psi^2 - E^i{}_j E^j{}_i\big)V_{,\phi} \\
& + (\Phi - 3\Psi)V_{,\phi\phi}\delta\phi + \tfrac{1}{2}V_{,\phi\phi\phi}\delta\phi^2 \\
& - \tfrac{1}{2}\big[\big(-\tfrac{1}{2}\Phi^2 - 3\Phi\Psi + \tfrac{3}{2}\Psi^2 - E^i{}_j E^j{}_i\big)F_{,\phi} \\
& + (\Phi - 3\Psi)\delta F_{,\phi} + \delta_2 F_{,\phi}\big]R \\
& - \tfrac{1}{2}\big[(\Phi - 3\Psi)F_{,\phi} + \delta F_{,\phi}\big]\delta R - \tfrac{1}{2}F_{,\phi}\delta_2 R,
\end{aligned}
\tag{5.114}
$$

where δR is given in (5.25) and the second-order perturbation to the Ricci scalar is given by

$$
\begin{aligned}
\delta_2 R = {} & -3\dot{E}_{ij}\dot{E}^{ij} - 4E_{ij}\ddot{E}^{ij} - 16HE_{ij}\dot{E}^{ij} + 24(\dot{H} + 2H^2)\Phi^2 \\
& + 24H\Phi\dot{\Phi} + 48H(\Phi - \Psi)\dot{\Psi} + 6\dot{\Phi}\dot{\Psi} + 12(\Phi - \Psi)\ddot{\Psi} \\
& + \frac{1}{a^2}\left(4E_{ij}\nabla^2 E^{ij} - 2\partial_j E_{ik}\partial^k E^{ij} + 3\partial_k E_{ij}\partial^k E^{ij}\right) \\
& + \frac{2}{a^2}\left[2(\Phi - \Psi)\nabla^2\Phi + 8\Psi\nabla^2\Psi + (\nabla\Phi)^2 + 3(\nabla\Psi)^2 + \partial_i\Psi\partial^i\Phi\right].
\end{aligned}
\tag{5.115}
$$

5.C Correlator relations

The various quadratic-order terms in the Friedmann equations can be related to the two-point functions of the quantised fields via correlator relations. These relations can be obtained by differentiation and by use of the fields' equations of motion. The expectation values at quadratic

order are defined to be symmetric. For the tensors we have that

$$\left\langle \dot{E}_{ij} E^{ij} \middle| \dot{E}_{ij} E^{ij} \right\rangle := \tfrac{1}{2} \left\langle \dot{E}_{ij} E^{ij} + E_{ij} \dot{E}^{ij} \middle| \dot{E}_{ij} E^{ij} + E_{ij} \dot{E}^{ij} \right\rangle$$
$$= \tfrac{1}{2} \partial_t \left\langle E_{ij} E^{ij} \middle| E_{ij} E^{ij} \right\rangle, \tag{5.116}$$

$$\left\langle \dot{E}_{ij} \dot{E}^{ij} \middle| \dot{E}_{ij} \dot{E}^{ij} \right\rangle = \tfrac{1}{2} \partial_t^2 \left\langle E_{ij} E^{ij} \middle| E_{ij} E^{ij} \right\rangle$$
$$- \tfrac{1}{2} \left\langle \ddot{E}_{ij} E^{ij} + E_{ij} \ddot{E}^{ij} \middle| \ddot{E}_{ij} E^{ij} + E_{ij} \ddot{E}^{ij} \right\rangle, \tag{5.117}$$

$$\left\langle \ddot{E}_{ij} E^{ij} \middle| \ddot{E}_{ij} E^{ij} \right\rangle = -H(\tfrac{3}{2} + \epsilon_F) \partial_t \left\langle E_{ij} E^{ij} \middle| E_{ij} E^{ij} \right\rangle$$
$$+ \frac{1}{a^2} \left\langle E_{ij} \nabla^2 E^{ij} \middle| E_{ij} \nabla^2 E^{ij} \right\rangle, \tag{5.118}$$

where the last relation is obtained from the tensors equation of motion (5.26). The scalar degrees of freedom are constrained via the field equations (5.16) and (5.19), that in the Einstein limit can be expressed in terms of the single field Ψ. The correlator relations of Ψ are then obtained as

$$\left\langle \dot{\Psi}\Psi \middle| \dot{\Psi}\Psi \right\rangle = \tfrac{1}{2} \partial_t D_0,$$

$$\left\langle \ddot{\Psi}\Psi \middle| \ddot{\Psi}\Psi \right\rangle = -\tfrac{1}{2} H(1 + 2\delta_H) \partial_t D_0 - 2H^2(\delta_H - \epsilon_H) D_0 + \frac{1}{a^2} D_2,$$

$$\left\langle \dot{\Psi}^2 \middle| \dot{\Psi}^2 \right\rangle = \tfrac{1}{2} \partial_t^2 D_0 - \left\langle \ddot{\Psi}\Psi \middle| \ddot{\Psi}\Psi \right\rangle,$$

$$\left\langle \ddot{\Psi}\dot{\Psi} \middle| \ddot{\Psi}\dot{\Psi} \right\rangle = -H(1 + 2\delta_H) \left\langle \dot{\Psi}^2 \middle| \dot{\Psi}^2 \right\rangle - H^2(\delta_H - \epsilon_H) \partial_t D_0 + \frac{1}{2a^2} \partial_t D_2,$$

$$\left\langle \ddot{\Psi}\Psi \middle| \ddot{\Psi}\Psi \right\rangle = -\tfrac{1}{2} \left[\partial_t [H(1 + 2\delta_H)] + 2H^2(\delta_H - \epsilon_H) - H^2(1 + 2\delta_H)^2 \right] \partial_t D_0$$
$$+ \left[2H^3(1 + 2\delta_H)(\delta_H - \epsilon_H) - 2\partial_t [H^2(\delta_H - \epsilon_H)] \right] D_0$$
$$+ \frac{1}{2a^2} \partial_t D_2 - H(3 + 2\delta_H) \frac{1}{a^2} D_2,$$

$$\left\langle \ddot{\Psi}^2 \middle| \ddot{\Psi}^2 \right\rangle = H^2(1 + 2\delta_H)^2 \left\langle \dot{\Psi}^2 \middle| \dot{\Psi}^2 \right\rangle + 2H^3(1 + 2\delta_H)(\delta_H - \epsilon_H) \partial_t D_0$$
$$+ 4H^4(\delta_H - \epsilon_H)^2 D_0 - H(1 + 2\delta_H) \frac{1}{a^2} \partial_t D_2$$
$$- 4H^2(\delta_H - \epsilon_H) \frac{1}{a^2} D_2 + \frac{1}{a^4} D_4, \tag{5.119}$$

using the equation of motion for the scalar metric perturbation in (5.41). Again, all of the correlators should be understood to have equal time and space arguments.

5.D   Calculation of two-point correlators

From its mode decomposition in (5.31), the tensor correlator is given by

$$
\begin{aligned}
C_0 &:= \left\langle E_{ij} E^{ij} \middle| E_{ij} E^{ij} \right\rangle \\
&= \int \frac{\mathrm{d}^3 q}{(2\pi)^{3/2}} \int \frac{\mathrm{d}^3 p}{(2\pi)^{3/2}} \sum_\lambda \sum_{\lambda'} e_{ij}^{(\lambda)} e^{(\lambda')*ij} \langle \hat{a}_{\lambda \mathbf{q}} \hat{a}_{\lambda' \mathbf{p}}^\dagger \rangle \tilde{h}_{\lambda \mathbf{q}} \tilde{h}_{\lambda' \mathbf{p}},
\end{aligned}
\tag{5.120}
$$

where $\tilde{h}_{\lambda \mathbf{q}}$ is given in (5.39). We have already assumed that we are in the vacuum state, where the expectation value of the number operators $\hat{a}_{\lambda \mathbf{q}}^\dagger \hat{a}_{\lambda \mathbf{q}}$ vanish. Then inserting

$$
[\hat{a}_{\lambda \mathbf{q}}, \hat{a}_{\lambda \mathbf{q}}^\dagger] = \delta_{\lambda \lambda'} \delta^3(\mathbf{q} - \mathbf{q}'),
\tag{5.121}
$$

we arrive at

$$
\begin{aligned}
C_0 &:= \left\langle E_{ij} E^{ij} \middle| E_{ij} E^{ij} \right\rangle \\
&= \int \frac{\mathrm{d}^3 q}{(2\pi)^3} \sum_\lambda e_{ij}^{(\lambda)} e^{(\lambda)*ij} |\tilde{h}_{\lambda \mathbf{q}}| \\
&= \frac{4}{2\pi^2} \int \mathrm{d}q \, q^2 |\tilde{h}_{\lambda \mathbf{q}}|^2,
\end{aligned}
$$

In the last line, we have summed over i, j and λ (giving a factor of 4) and used that the mode functions $\tilde{h}_{\lambda \mathbf{q}}$ only depend on the length of $\mathbf{q}$, and not on λ.

By introducing the new variable $x := -q\eta$, as $\eta < 0$ inside the horizon, (5.120) can be written as

$$
C_0(\eta) = \frac{1}{4\pi} \frac{1}{M_{\mathrm{Pl}}^2 a^2 F} (-\eta)^{-2} \int_{\Lambda_{\mathrm{IR}}}^{\Lambda_{\mathrm{UV}}} \mathrm{d}x \, x^2 |H_\nu^{(2)}(-x)|^2,
\tag{5.122}
$$

where we have chosen a branch such that $|H_\nu^{(1)}(x)|^2 = |H_\nu^{(2)}(-x)|^2$ for $x > 0$. We split the remaining radial integration interval into three according to

$$
\int_{\Lambda_{\mathrm{IR}}}^{\Lambda_{\mathrm{UV}}} \mathrm{d}x = \int_{\Lambda_{\mathrm{IR}}}^{\kappa_{\mathrm{IR}}} \mathrm{d}x + \int_{\kappa_{\mathrm{IR}}}^{\kappa_{\mathrm{UV}}} \mathrm{d}x + \int_{\kappa_{\mathrm{UV}}}^{\Lambda_{\mathrm{UV}}} \mathrm{d}x,
\tag{5.123}
$$

with $\Lambda_{\mathrm{IR}} \ll \kappa_{\mathrm{IR}} \ll 1 \ll \kappa_{\mathrm{UV}} \ll \Lambda_{\mathrm{UV}}$ so that we can use different approximations of the Hankel functions $H_\nu^{(1)}(x)$ appropriate for each interval.

In the low-momentum (IR) region, we use the asymptotic expansion

$$H^{(1)}_{\nu,\text{IR}}(x) := -\frac{i}{\pi}\left(\frac{2}{x}\right)^{\nu}\Gamma(\nu) + \dots,$$

(5.124)

and in the intermediate-momentum region, we may let $\epsilon_{H,F} \to 0$, so that the relevant Hankel function for the tensors reduces to

$$H^{(1)}_{\frac{3}{2}}(x) = -\sqrt{\frac{2}{\pi x^3}}(i+x)e^{ix}.$$

(5.125)

In the large-momentum (UV) region we use the large-$|x|$ expansion of the Hankel function:

$$H^{(1)}_{\nu,\text{UV}}(x) := \frac{2}{\pi}\left[\frac{1}{x} - \frac{1-4\nu^2}{8x^3}\right] + O(x^{-7/2}).$$

(5.126)

Calculating the contributions from each momentum interval, the correlator in (5.120) becomes

$$
\begin{aligned}
C_0 &:= \left\langle E_{ij}E^{ij}\middle|E_{ij}E^{ij}\right\rangle \\
&= \frac{1}{2\pi^2}\frac{H^2}{M_{\text{Pl}}^2 F}\left[\left(\frac{1}{2(\epsilon_F+\epsilon_H)}+\log 2+\psi\!\left(\tfrac{3}{2}\right)\right)\left(-1+\Lambda_{\text{IR}}^{-2(\epsilon_H+\epsilon_F)}\right)\right. \\
&\quad \left.+ \tfrac{1}{2}\Lambda_{\text{UV}}^2 + \log\Lambda_{\text{UV}}\right] + O(\epsilon),
\end{aligned}
$$

(5.127)

where we have switched back to cosmic time and $\psi(x)$ denotes the digamma function. For the correlator involving two gradients, we have that

$$
\begin{aligned}
C_2 &:= \left\langle E_{ij}\nabla^2 E^{ij}\middle|E_{ij}\nabla^2 E^{ij}\right\rangle \\
&= -4\int\frac{\mathrm{d}^3 q}{(2\pi)^3}q^2|\tilde{h}_{\lambda\mathbf{q}}|^2 \\
&= -\frac{1}{4\pi^2}\frac{a^2 H^4}{M_{\text{Pl}}^2 F}\left[\tfrac{1}{2}\Lambda_{\text{UV}}^4 + \Lambda_{\text{UV}}^2 - \tfrac{1}{2}\Lambda_{\text{IR}}^4 - \Lambda_{\text{IR}}^2\right],
\end{aligned}
$$

(5.128)

having performed the same procedure as for C_0. Note that keeping the non-minimal slow-roll parameter ϵ_F is straightforward for the tensors contributions.

For the scalars we work in the limit $F(\phi) = 1$, so that the first correlator is given by

$$
\begin{aligned}
D_0(\eta) &:= \left\langle \Psi^2 \middle| \Psi^2 \right\rangle \\
&= \int \frac{\mathrm{d}^3 k}{(2\pi)^3} |f_{\mathbf{k}}|^2 = \frac{1}{16\pi} \frac{\epsilon_H \mathcal{H}^2}{M_{\mathrm{Pl}}^2 a^2} \int_{\Lambda_{\mathrm{IR}}}^{\Lambda_{\mathrm{UV}}} \mathrm{d}x |H_\nu^{(2)}(-x)|^2,
\end{aligned} \tag{5.129}
$$

and with the mode function given by (5.59). We then perform the same evaluation as for the tensors, with the difference being that the approximation to the Hankel function in the intermediate-momentum region reads

$$
H_{\frac{1}{2}}^{(1)}(x) = -\sqrt{\frac{2}{\pi x}} e^{ix}, \tag{5.130}
$$

when $\epsilon_H, \delta_H \to 0$. For the various loop integrals we then obtain

$$
D_0 = \frac{\epsilon_H H^2}{8\pi^2 M_{\mathrm{Pl}}^2} \left[\left(\frac{1}{2(2\epsilon_H - \delta_H)} + \log 2 + \psi(\tfrac{1}{2}) \right) \right. \tag{5.131}
$$

$$
\left. \times \left(-1 + \Lambda_{\mathrm{IR}}^{-2(2\epsilon_H - \delta_H)} \right) + \log \Lambda_{\mathrm{UV}} \right] + O(\epsilon), \tag{5.132}
$$

$$
D_2 = -\frac{\epsilon_H a^2 H^4}{16\pi^2 M_{\mathrm{Pl}}^2} \left(\Lambda_{\mathrm{UV}}^2 - \Lambda_{\mathrm{IR}}^2 \right) + O(\epsilon), \tag{5.133}
$$

$$
D_4 = \frac{\epsilon_H a^4 H^6}{32\pi^2 M_{\mathrm{Pl}}^2} \left(\Lambda_{\mathrm{UV}}^4 - \Lambda_{\mathrm{IR}}^4 \right) + O(\epsilon). \tag{5.134}
$$

The correlators in (5.127), (5.128) and (5.131)–(5.134) all contain powers and logarithms of the UV and IR cutoffs. Had we chosen to carry out the computation in dimensional regularisation, all powers would have immediately disappeared, leaving us only with the logarithmic divergences both in the UV and IR. The logarithmic UV divergences should be cancelled by counterterms, as in e.g. [67]. The IR divergences, on the other hand, are physical in the sense that they indicate that a higher order effect (such as an infinite resummation) will generate a regulator (such as a gap) [71, 74]. With this in mind, we find it illuminating through the use of a simple cutoff regularisation to identify where divergence show up, but allow ourselves to assume that UV-divergences may be removed through a proper choice of counterterms. Simply discarding the UV-divergent terms amounts to a MS-like renormalisation condition.

6 Stochastic inflation from quantum field theory and the parametric dependence of the effective noise amplitude

The non-linear dynamics of long-wavelength cosmological fluctuations may be phrased in terms of an effective classical, but stochastic evolution equation. The stochastic noise represents short-wavelength modes that continually redshift into the long-wavelength domain. The effective evolution may be derived from first principles quantum field theory in an expanding background, through a sequence of approximations calling for additional scrutiny. We perform such an analysis, putting particular emphasis on the amplitude of the stochastic noise, which ultimately determines the cosmological correlations and provides a non-perturbative IR regulator to the dynamics.

6.1 Introduction

The primordial density perturbations in the Universe are expected to have originated as vacuum fluctuations of a light, weakly-interacting scalar field ϕ, amplified during a period of accelerating cosmological expansion known as inflation (see for instance [43, 146]. However, it has long been known that when computing cosmological correlations in perturbative quantum field theory (QFT), the (near-)massless propagator leads to unphysical divergent and secular IR behaviour, which call for regularisation [152, 162].

One way to achieve this is through resumming infinite sets of perturbative diagrams, using resummation techniques well-known from Minkowski space computations, adapted to de Sitter space (dS). These include the large-N expansion [74, 163], truncations of the two-particle-irreducible (2PI) effective action formalism [164, 165], the non-perturbative renor-

malisation group (RG) [166], and dressing of the Euclidean zero mode by summing an infinite class of diagrams [73, 167, 168]. These all reveal that a dynamical mass is generated by non-linear interactions, regularising the correlation functions, even in the case of minimally coupled massless scalar fields.

An alternative to the diagrammatic QFT analysis is stochastic inflation [38, 39], where a separation of scales is introduced between the (far) super-horizon (IR) modes and the near- and sub-horizon (UV) modes. By integrating out the UV modes, an effective classical, but stochastic, IR theory arises, which retains much of the nonlinear, nonperturbative dynamics of the exact theory. The IR dynamics again generate a dynamical mass. This is reminiscent of similar approaches to quantum thermal field theories of gauge and fermion fields [169], where UV degrees of freedom source classical IR dynamics in the form of a stochastic noise. One important difference is that in stochastic inflation, the noise is the result of a sliding scale separation turning UV modes into IR modes. It therefore appears even in the non-interacting theory, and is hence unsuppressed by powers of the couplings. It also follows that the stochastic approach is specific to near-de Sitter geometries in that the Hubble horizon is used as a separation scale between the long and short wavelength modes, with modes leaving the horizon only for an accelerating expansion.

In the simplest overdamped (slow-roll) limit, $\ddot{\phi} \ll 3H\dot{\phi}$, and in addition neglecting spatial gradients, the effective IR dynamics can be described by a Langevin equation, and field correlations be obtained via the corresponding Fokker-Planck equation. This is the framework most often applied to models of inflation, although the problem is still numerically tractable even when relaxing some of these assumptions [170].

The stochastic approach has been shown to reproduce the correct IR behaviour of the full QFT statistical propagator to leading order in the coupling [152, 171–174] and was recently favourably compared at two-loop order in perturbation theory [175]. Other authors have studied the evolution of the density matrix for the IR modes to recover a Fokker-Planck equation [176, 177], and Ref. [178] argued the emergence of the stochastic formalism from a leading-log diagrammatic analysis at

coincident points. The conceptual and computational tractability offered by the stochastic approach has made it a popular method (see e.g. [179, 180] for example applications), and in recent years there has been an upsurge in activity aiming to extend it e.g. to beyond leading order in the coupling [177, 181, 182], the slow-roll approximation [170, 183], or to include derivative interactions [184]. However, compared to its extensive use, studies of the embedding and range of validity of the stochastic approach in QFT remain scarce (see however [185, 186]), which has motivated the present work.

In this chapter we will revisit the first-principles derivation at the level of the path integral, paying attention to the sequence of approximations required to reach the standard form of the effective dynamics. These include the coarse graining procedure, the scale separation specified by a so-called window function and the parametrisation of the free UV vacuum sourcing the horizon-crossing modes. In particular, the stochastic noise is often taken to have a particular, universal amplitude, which we will see only arises in some very specific parametric limits.

The article is organised as follows. In the following subsection 6.1.1, we present the effective stochastic theory, and how it is applied to compute IR field correlators given an inflation model. Having described the objective of our discussion, we in section 6.2 introduce the real-time QFT formalism for the problem at hand, and show how an effective IR theory arises (sections 6.2.2 and 6.2.4) and how to interpret it as a stochastic theory (section 6.2.5). We reconnect to the standard form of the stochastic noise resulting from the choice of a sharp window function applied to the field variables in momentum space [39] (section 6.2.6). This allows us to identify the set of assumptions and approximations going into the derivation, and their validity. We investigate an alternative mode separation procedure at the level of the path integral in section 6.2.7, and proceed to again derive the target theory, in the process identifying the approximations required. The procedure is illustrated and approximations checked through an example (Gaussian) window function in section 6.3. In section 6.4 we compute and compare the amplitude of the stochastic noise for a selection of window functions, considering both massless and

massive UV modes, dS and slow-roll spacetimes, and test the validity of
the central assumptions. Conclusions are gathered in section 6.5.

6.1.1 Application of stochastic dynamics to inflationary perturbations

We first briefly review the stochastic inflationary formalism, and how a
dynamical mass is generated. The dynamics of the coarse-grained IR
field ϕ_{IR} on super-Hubble scales is described by a Langevin equation

$$\dot{\phi}_{\text{IR}}(t) + \frac{V'(\phi_{\text{IR}})}{3H} = \xi_\phi(t), \tag{6.1}$$

where $H := \dot{a}(t)/a(t)$ is the Hubble rate,

$$V(\phi) = \tfrac{1}{2}m^2\phi^2 + V_{\text{I}}(\phi), \tag{6.2}$$

is the potential and ξ_ϕ is a Gaussian stochastic noise with the correlation

$$\langle \xi_\phi(t)\xi_\phi(t') \rangle = \frac{H^3}{4\pi^2}f(\epsilon_H, \epsilon_M, \dots)\delta(t - t'), \tag{6.3}$$

corresponding to white, Markovian, noise statistics. Most commonly, the
function f is taken to be trivial, $f = 1$, but we will allow for the noise
amplitude to a priori depend on several variables, including the slow-roll
and mass parameters ϵ_H and ϵ_M defined as

$$\epsilon_H := -\frac{\dot{H}}{H^2}, \qquad \epsilon_M := \frac{m^2}{3H^2}. \tag{6.4}$$

The Langevin equation gives rise to a Fokker-Planck equation for the
one-point probability distribution of the IR field

$$\partial_t P(t, \phi_{\text{IR}}) = \left(\frac{V''(\phi_{\text{IR}})}{3H} + \frac{V'(\phi_{\text{IR}})}{3H}\partial_{\phi_{\text{IR}}} + \frac{H^3 f}{8\pi^2}\partial^2_{\phi_{\text{IR}}} \right) P(t, \phi_{\text{IR}}). \tag{6.5}$$

Given an initial distribution at the beginning of inflation, the distribution
at any later time then follows, and observables may be computed as

$$\langle O(\phi_{\text{IR}}(t)) \rangle = \int \mathrm{d}\phi_{\text{IR}} P(t, \phi_{\text{IR}}) O(\phi_{\text{IR}}). \tag{6.6}$$

Often, the late-time equilibrium solution is assumed to have been reached[1]

$$P_{\text{eq}}(\phi_{\text{IR}}) \sim \exp\left\{-\frac{8\pi^2 V(\phi_{\text{IR}})}{3fH^4}\right\}, \tag{6.7}$$

and for instance for a free, massive theory, $V(\phi) = \frac{1}{2}m^2\phi^2$, the variance is given by

$$\langle\phi_{\text{IR}}^2\rangle = \frac{3fH^4}{8\pi^2 m^2}. \tag{6.8}$$

For $f = 1$, this is indeed the finite part of the field correlator in the Bunch-Davies vacuum at leading order in the limit $m^2 \ll H^2$. This can be seen directly from expanding the free semi-dS propagator in the same limit [189, 190],

$$G_F(y) = \frac{H^2}{4\pi^2}\left(\frac{1}{y} - \frac{1}{2}\ln y + \frac{1}{2(\epsilon_M - \epsilon_H)} - 1 + \ln 2 + O(\epsilon_M, \epsilon_H)\right), \tag{6.9}$$

where y is the dS invariant length scale,

$$y(x, x') = 4\sin^2\left(\frac{1}{2}l(x, x')H\right), \tag{6.10}$$

with $l(x, x')$ denoting the geodesic distance. Setting $\epsilon_H = 0$ and inserting (6.4) into the leading finite term, we recover (6.8).

However, when applying the stochastic formalism to a massless self-interacting field with $V_{\text{I}}(\phi) = \frac{\lambda}{4}\phi^4$, the late-time Fokker-Planck distribution straightforwardly leads to [39]

$$\lim_{t\to\infty}\langle\phi_{\text{IR}}^2(t)\rangle = \sqrt{\frac{3f}{2\pi^2}\frac{\Gamma\left[\frac{3}{4}\right]}{\Gamma\left[\frac{1}{4}\right]}}\frac{H^2}{\sqrt{\lambda}}. \tag{6.11}$$

One may then infer that a mass has been generated dynamically by comparing the massive dS result (6.8) with (6.11), i.e.,

$$m_{\text{dyn}}^2 = \frac{\sqrt{6}}{\sqrt{f}8\pi}\frac{\Gamma\left[\frac{1}{4}\right]}{\Gamma\left[\frac{3}{4}\right]}\sqrt{\lambda}H^2 \simeq 0.288\frac{\sqrt{\lambda}}{\sqrt{f}}H^2. \tag{6.12}$$

The effective mass squared is proportional to H^2 and importantly to $\sqrt{\lambda}$, rather than an integer power of the coupling. This non-analytic dependence suggests that the stochastic prescription amounts to a resummation

---

[1]Although this may not always be the case [187, 188].

of Feynman diagrams from all orders of perturbation theory, providing an IR regulator in an expanding background ($H \neq 0$). We see that the amplitude of the noise, including the function $f(\ldots)$, sets the scale for correlators and the dynamical mass.

The original stochastic formalism was restricted to the slow-roll limit where $\ddot{\phi}_{\text{IR}}$ is neglected, and where also $V''/H^2 \ll 1$. However, one may generalise to include second-order derivatives in time by introducing a "momentum noise" ξ_π to accompany the new degree of freedom. The Langevin dynamics can then be written as two coupled equations for the IR field and its time derivative:

$$\dot{\phi}_{\text{IR}} = \pi_{\text{IR}} + \xi_\phi, \qquad \dot{\pi}_{\text{IR}} + 3H\pi_{\text{IR}} + V'(\phi_{\text{IR}}) = \xi_\pi, \qquad (6.13)$$

alternatively,

$$\ddot{\phi}_{\text{IR}} + 3H\dot{\phi}_{\text{IR}} + V'(\phi_{\text{IR}}) = 3H\xi_\phi + \dot{\xi}_\phi + \xi_\pi := \xi. \qquad (6.14)$$

For later reference, we note that in the particular case, when $3H\xi_\phi \gg \dot{\xi}_\phi, \xi_\pi$ (in a sense to be discussed below), the normalisation (6.3) implies

$$\langle \xi(t)\xi(t') \rangle \to 9H^2 \langle \xi_\phi(t)\xi_\phi(t') \rangle = \frac{9H^5}{4\pi^2} f(\epsilon_H, \epsilon_M, \ldots)\delta(t - t'). \quad (6.15)$$

In the following we will see that these results emerge also (in certain limits) in QFT. Starting from the closed-time-path (CTP) action, we will derive the Langevin equation using a suitable set of approximations. In particular we keep track of the normalisation of the noise, parametrised by a function $f(\ldots)$, which as we have seen appears prominently in the late-time Fokker-Planck distribution and hence the computed observables. The variance for the non-interacting dS vacuum corresponds to $f = 1$ to leading order in the mass, and provides a natural benchmark for comparison.

6.2 Stochastic dynamics from quantum field theory

We first revisit the derivation of the Langevin evolution from a field theoretical perspective, paying special attention to the scale separation between the long- and short-wavelength degrees of freedom [39, 185, 191].

6.2.1 The closed-time-path formalism for inflation

We consider the real-time evolution of an interacting scalar field in an FRLW spacetime, whose line element is given by

$$\mathrm{d}s^2 = -\mathrm{d}t^2 + a^2(t)\mathrm{d}\mathbf{x}^2, \tag{6.16}$$

where $a(t)$ is the scale factor and the slow-roll parameter ϵ_H parameterises the deviation from a constant expansion rate, corresponding to dS space where $a(t) \propto e^{Ht}$. Expectation values for operators are computed using the CTP formalism[2] of QFT [192, 193]. In the CTP formalism, the time coordinate runs on a closed time path from t_{in} to t (the '+' branch) and back again (the '−' branch). The field ϕ and source J are split up into path-ordered constituents $\phi^\pm$ and $J^\pm$, where for equal time $\phi^+(t) = \phi^-(t)$. The quantum correlators evaluated at time t can be obtained by functional differentiation of the generating functional

$$Z[\mathbb{J}] = \int \mathcal{D}\Phi \exp\left\{\frac{i}{2}\int_x \left(\Phi^T \mathbb{G}^{-1}\Phi - 2V_{\mathrm{I}}(\Phi) + \mathbb{J}^T\Phi\right)\right\}, \tag{6.17}$$

where $\int_x := \int \mathrm{d}^4x \sqrt{-g(x)}$ for brevity, $V_{\mathrm{I}}(\Phi) = V_{\mathrm{I}}(\phi^+) - V_{\mathrm{I}}(\phi^-)$ is the interacting potential and we define

$$\Phi(x) := \begin{bmatrix} \phi^+(x) \\ \phi^-(x) \end{bmatrix}, \quad \mathbb{J}(x) := \begin{bmatrix} J^+(x) \\ -J^-(x) \end{bmatrix}, \tag{6.18}$$

and

$$\mathbb{G}^{-1}(x, x') := \begin{bmatrix} G^{-1}(x) & 0 \\ 0 & -G^{-1}(x) \end{bmatrix} \delta(x, x'). \tag{6.19}$$

The free inverse propagator is $G^{-1}(x) = \Box_x - m^2$. The matrix $\mathbb{G}(x, x')$ consists of the CTP propagators with all four possible time orderings:

$$\begin{aligned} \mathbb{G}(x, x') &= \begin{bmatrix} G^{++}(x, x') & G^{+-}(x, x') \\ G^{-+}(x, x') & G^{--}(x, x') \end{bmatrix} \\ &= -i \begin{bmatrix} \langle T\phi^+(x)\phi^+(x')\rangle & \langle \phi(x)^+\phi^-(x')\rangle \\ \langle \phi^-(x')\phi^+(x)\rangle & \langle \bar{T}\phi^-(x)\phi^-(x')\rangle \end{bmatrix}, \end{aligned} \tag{6.20}$$

---

[2]Also known as the in-in or Schwinger-Keldysh formalism.

where T ($\bar{T}$) denote (anti-)time ordering, satisfying

$$\langle T\phi(x)\phi(x')\rangle = \Theta(t - t')\langle\phi(x)\phi(x')\rangle + \Theta(t' - t)\langle\phi(x')\phi(x)\rangle, \quad (6.21)$$

$$\langle \bar{T}\phi(x)\phi(x')\rangle = \Theta(t - t')\langle\phi(x')\phi(x)\rangle + \Theta(t' - t)\langle\phi(x)\phi(x')\rangle. \quad (6.22)$$

The two-point functions are related via

$$G^{++}(x, x') + G^{--}(x, x') = G^{+-}(x, x') + G^{-+}(x, x'). \quad (6.23)$$

For classical considerations it is useful to work in the Keldysh basis, in which the Schwinger basis fields $\phi^\pm$ are transformed into "classical" and "quantum" fields ϕ^c, ϕ^q via a transformation matrix U as

$$\Phi(x) \rightarrow U\Phi(x) = \begin{bmatrix} \frac{1}{2}[\phi^+(x) + \phi^-(x)] \\ \phi^+(x) - \phi^-(x) \end{bmatrix} := \begin{bmatrix} \phi^c(x) \\ \phi^q(x) \end{bmatrix}, \quad U = \begin{bmatrix} \frac{1}{2} & \frac{1}{2} \\ 1 & -1 \end{bmatrix}. \quad (6.24)$$

This notation can be understood heuristically in the sense that ϕ^q expresses the amplitude of the quantum fluctuations around the mean field value ϕ^c. The kinetic operator in the Keldysh basis is

$$\mathbb{G}^{-1}(x, x') \rightarrow U\mathbb{G}^{-1}(x, x')U^T = \begin{bmatrix} 0 & G^{-1}(x) \\ G^{-1}(x) & 0 \end{bmatrix}\delta(x, x'), \quad (6.25)$$

and the propagators are

$$\mathbb{G}(x, x') = \begin{bmatrix} -iG_F(x, x') & G_R(x, x') \\ G_A(x, x') & 0 \end{bmatrix}, \quad (6.26)$$

with

$$-iG_F(x, x') = \tfrac{1}{2}\left[G^{+-}(x, x') + G^{-+}(x, x')\right] = -\tfrac{i}{2}\langle\{\phi(x), \phi(x')\}\rangle,$$
$$G_R(x, x') = G^{++}(x, x') - G^{+-}(x, x') = -i\Theta(t - t')\langle[\phi(x), \phi(x')]\rangle,$$
$$G_A(x, x') = G^{++}(x, x') - G^{-+}(x, x') = -i\Theta(t' - t)\langle[\phi(x'), \phi(x)]\rangle. \quad (6.27)$$

We recognise the statistical Feynman propagator G_F and spectral retarded/advanced propagators $G_R(x, x') = G_A(x', x)$. The free propagators satisfy the equations of motion

$$G^{-1}(x)G_F(x, x') = 0, \qquad G^{-1}(x)G_{R,A}(x, x') = \frac{\delta(x - x')}{\sqrt{-g(x)}}. \quad (6.28)$$

6.2.2 Coarse graining and window functions

In order to derive the effective IR dynamics of the inflaton field ϕ, one may proceed to split it into UV and IR parts as $\phi = \phi_{\text{UV}} + \phi_{\text{IR}}$. The field split has been addressed at the level of the effective action in earlier work [185] (see also [186, 194]), where an effective IR equation of motion is obtained by integrating out the UV modes.

The IR/UV field split is a coarse-graining procedure, in the sense that it amounts to averaging in position space using a smoothing window function $\overline{W}$ dependent on a characteristic smoothing scale L as [195]

$$\phi_{\text{IR}}(x) = \int \mathrm{d}^3\mathbf{x}'\phi(x')\overline{W}(\mathbf{x} - \mathbf{x}', L). \tag{6.29}$$

The IR field value at a given point in space is then given by the value of the full field ϕ averaged over a region of size L. The convolution of the window function in position space then corresponds to multiplication in momentum space. Implicit in (6.29) is that $\overline{W}$ is taken to be local in time, through a form

$$\overline{W}(x, x') = \delta(t - t') \int \frac{\mathrm{d}^3\mathbf{k}}{(2\pi)^3} \overline{W}(k, t) e^{i\mathbf{k}\cdot(\mathbf{x} - \mathbf{x}')}. \tag{6.30}$$

Note that k is the co-moving momentum, with $k/a(t)$ being the physical momentum. We will use this form in the following as well. From the field split $\phi = \phi_{\text{UV}} + \phi_{\text{IR}}$ with ϕ_{IR} defined as in (6.29), it follows that we can define the UV part of the field in terms of a completing function W,

$$W(x, x') + \overline{W}(x, x') = \delta(x - x'), \tag{6.31}$$

such that

$$\phi_{\text{UV}}(x) = \int_{x'} W(x, x')\phi(x'), \qquad \phi_{\text{IR}}(x) = \int_{x'} \overline{W}(x, x')\phi(x'). \tag{6.32}$$

In order for the window function to truly split the field into an IR and UV part, we require them to satisfy $W(k, t) = 1$ for field modes with $k \gg aH$ and $W(k, t) = 0$ for $k \ll aH$, and vice versa for $\overline{W}(k, t)$. In particular, if $W(k, t)$ has precisely the value 1 or 0 for a given mode, that entire mode belongs to either the UV or IR field. For a smooth window function

interpolating between 1 and 0, modes of all k will contribute to both the IR and the UV field. In that case, the field split is into a "mostly-UV" and "mostly-IR" part.

We will perform the split in terms of physical momentum $k/a(t)$, rather than the co-moving momentum defining the mode functions. In practice, this introduces a time-dependence of the window function, as the UV modes are continuously red-shifted and join the coarse-grained classical IR modes. For the IR modes the effect of these quantum fluctuations crossing the Hubble horizon is what amounts to a continuous noise source.

6.2.3 The UV vacuum mode functions

Expanding the propagator in terms of quantised field momentum modes

$$\phi(x) = \int \frac{d^3\mathbf{k}}{(2\pi)^3} \left[a_{\mathbf{k}} \phi(k,t) e^{i\mathbf{k}\cdot\mathbf{x}} + \text{h.c.} \right], \qquad (6.33)$$

with $[a_{\mathbf{k}}, a_{\mathbf{k}'}^{\dagger}] = (2\pi)^3 \delta^3(\mathbf{k} + \mathbf{k}')$ and $a_{\mathbf{k}}$ annihilating the Bunch-Davies vacuum, the free equation of motion (6.28) has the standard solution

$$\phi(k,t) = \frac{\sqrt{\pi}}{2\sqrt{a^3 H(1-\epsilon_H)}} H_\nu^{(1)}\left(\frac{k}{aH(1-\epsilon_H)} \right), \qquad (6.34)$$

where $\nu^2 = \frac{9}{4} - 3\epsilon_M + 3\epsilon_H$ and $H_\nu^{(1)}(x)$ are the Hankel functions of the first kind [196]. In the massless dS case, $\nu = \frac{3}{2}$ and the mode solution reduces to

$$\phi(k,t) = -\frac{H}{\sqrt{2k^3}}\left(i + \frac{k}{aH} \right) e^{ik/aH}, \quad \epsilon_M = 0,\ \epsilon_H = 0. \qquad (6.35)$$

In the long-wavelength limit, the Hankel function can be approximated[3] such that the leading term in k/aH of the mode function (6.34) is given by

$$\phi(k,t) \simeq -i\frac{H(1-\epsilon_H)}{\sqrt{2k^3}}\left(\frac{k}{aH(1-\epsilon_H)} \right)^{\epsilon_M - \epsilon_H}, \quad \epsilon_M \ll 1,\ k/aH \ll 1. \qquad (6.36)$$

---

[3]For small x and $\nu > 0$ the leading terms are $H_\nu^{(1)}(x) \simeq -i\frac{\Gamma[\nu]}{\pi}\left(\frac{x}{2}\right)^{-\nu}\left[1 + \frac{1}{\nu-1}\left(\frac{x}{2}\right)^2 + \dots\right]$.

In the following, whenever the quantum UV modes enter through their correlators, these will be represented by the free vacuum state through the above mode functions (6.34)–(6.36). The long-wavelength approximate solution (6.36) applies to our UV modes, since as we will see below, the modes responsible for the stochastic noise are in fact super-horizon, in the sense required by (6.36). They are modes transitioning from the UV to the IR.

Interacting UV mode functions. In order to solve explicitly for the UV mode functions, it is usually assumed that interactions may be neglected. It is however worth noting, that since the mass only enters through ϵ_M, the expressions generalise trivially to Gaussian interacting UV modes including an effective mass $M^2 = m^2 + \dots$. In the complete theory, where also the UV modes experience an effective mass $\propto \sqrt{\lambda}H^2$, modes are never truly massless, and for $m^2 = 0$, the small-mass criterion $\epsilon_M \ll 1$ becomes a constraint on the coupling, $\sqrt{\lambda} \ll 1$.

6.2.4 IR effective theory

In the language of open quantum systems, the quantum UV modes can be viewed as a bath affecting the system of classical IR modes. The generating functional (6.17) can then be written in terms of an influence functional $\mathcal{F}$ as

$$Z[\mathbb{J}] = \int \mathcal{D}\Phi_{\mathrm{IR}} e^{i(S[\Phi_{\mathrm{IR}}] - \mathbb{J}^T \Phi_{\mathrm{IR}})} \mathcal{F}[\Phi_{\mathrm{IR}}, \mathbb{J}], \qquad (6.37)$$

where

$$\mathcal{F}[\Phi_{\mathrm{IR}}, \mathbb{J}] = \int \mathcal{D}\Phi_{\mathrm{UV}} \exp\left[i \int_x \left(\tfrac{1}{2}\Phi_{\mathrm{UV}}^T \mathbb{G}^{-1}\Phi_{\mathrm{UV}} + \Phi_{\mathrm{IR}}^T \mathbb{G}^{-1}\Phi_{\mathrm{UV}} \right. \right.$$
$$\left. \left. - V_{\mathrm{I}}(\Phi_{\mathrm{IR}}, \Phi_{\mathrm{UV}}) + \mathbb{J}^T \Phi_{\mathrm{UV}} \right) \right], \qquad (6.38)$$

contains all the instances of Φ_{UV} and is to become an effective contribution the IR dynamics upon integrating out the UV part of the field. Here we have defined $V_{\mathrm{I}}(\Phi_{\mathrm{IR}}, \Phi_{\mathrm{UV}}) := V_{\mathrm{I}}(\Phi_{\mathrm{IR}} + \Phi_{\mathrm{UV}}) - V_{\mathrm{I}}(\Phi_{\mathrm{IR}})$, which typically includes non-linear self-interactions among the UV modes, and between

the UV and IR modes. We are interested in the stochastic noise that arises solely from the time-dependent field split of the free theory, and we will therefore simply neglect this non-linear interaction in our calculation, and as in the preceding section consider only free UV fields.[4] The self-interaction of the IR field is retained in (6.37) Setting also $\mathbb{J} = 0$ in (6.38), we may complete the square and perform the path integral over Φ_{UV}, to obtain

$$\mathcal{F}_0[\Phi_{\text{IR}}] = N \exp\left[-\frac{i}{2}\int_x\int_{x'}\Phi_{\text{IR}}^T(x)\,\mathbb{G}^{-1}(x)\,\mathbb{G}_{\text{UV}}(x,x')\,\mathbb{G}^{-1}(x')\Phi_{\text{IR}}(x')\right],$$
(6.39)

where $N \propto (\det \mathbb{G}_{\text{UV}}^{-1})^{-1/2}$ is a normalisation factor and UV propagator is defined by (6.26) with (6.32) as

$$\mathbb{G}_{\text{UV}}(x,x') = W(x)\,\mathbb{G}(x,x')\,W(x'),$$
(6.40)

Here $G^{-1}(x')$ can be integrated by parts to act on $G_{\text{UV}}(x,x')$ rather than the field $\Phi_{\text{IR}}(x')$. Later we will also consider departures from strict dS space ($\epsilon_H \neq 0$), but for the moment we continue with simply

$$G^{-1}(x) = -\partial_t^2 - 3H\partial_t + \frac{\nabla_{\mathbf{x}}^2}{a^2(t)} - m^2.$$
(6.41)

Writing out the kernel in (6.39) in the Keldysh c-q matrix form, we explicitly have

$$\mathcal{F}_0[\Phi_{\text{IR}}] = N \exp\left[-\frac{i}{2}\int_x\int_{x'}\left(-i[\phi_{\text{IR}}^c(x),\phi_{\text{IR}}^q(x)]\int\frac{d^3\mathbf{k}}{(2\pi)^3}e^{i\mathbf{k}\cdot(\mathbf{x}-\mathbf{x}')}\right.\right.$$

$$\left.\left.\times\begin{bmatrix} 0 & [Q_t+W_tG_t^{-1}][Q_{t'}+W_{t'}G_{t'}^{-1}]G_A(t,t') \\ [Q_t+W_tG_t^{-1}][Q_{t'}+W_{t'}G_{t'}^{-1}]G_R(t,t') & -iQ_tQ_{t'}G_F(t,t') \end{bmatrix}\begin{bmatrix} \phi_{\text{IR}}^c(x') \\ \phi_{\text{IR}}^q(x') \end{bmatrix}\right)\right],$$
(6.42)

where the UV propagator components G_F, $G_{R/A}$, G^{-1} and the window function W enter through their momentum space counterparts, and we have defined the operator

$$Q_t(k) := -\ddot{W}(k,t) - 3H\dot{W}(k,t) - 2\dot{W}(k,t)\partial_t,$$
(6.43)

---

[4]Stochastic contributions from the non-linear IR-UV interactions involve powers of a coupling which for inflation tend to be small.

where

$$Q_x = \int \frac{\mathrm{d}^3\mathbf{k}}{(2\pi)^3} Q_t(k) e^{i\mathbf{k}\cdot(\mathbf{x}-\mathbf{x}')}. \tag{6.44}$$

As we will argue below, the off-diagonal c-q terms in (6.42) may under some circumstances be neglected compared to the diagonal q-q component. Since the UV fields are taken to be non-interacting, we can make use of (6.28), and after partially integrating with respect to time, one may write for the off-diagonal components

$$\int_x \int_{x'} \phi_{\mathrm{IR}}^{\mathrm{q}}(x)\phi_{\mathrm{IR}}^{\mathrm{c}}(x')[Q_x + W_x G_x^{-1}][Q_{x'} + W_{x'} G_{x'}^{-1}]G_R(x,x')$$

$$= \int_x \int_{x'} \phi_{\mathrm{IR}}^{\mathrm{q}}(x)\Bigg[\Upsilon(x,x') \tag{6.45}$$

$$+ \frac{\delta(t-t')}{a^3(t)}\left(W_{x'}G_{x'}^{-1} + 2Q_{x'}W_{x'} + 2W_{x'}\dot{W}_{x'}\partial_{t'}\right)\Bigg]\phi_{\mathrm{IR}}^{\mathrm{c}}(x'),$$

where we have defined the quantity

$$\Upsilon(x,x') := \int \frac{\mathrm{d}^3\mathbf{k}}{(2\pi)^3} Q_t Q_{t'} G_R(k,t,t') e^{i\mathbf{k}\cdot(\mathbf{x}-\mathbf{x}')}. \tag{6.46}$$

The last three terms in (6.45) include a window function W acting on an IR-field. As pointed out in [185], if $W(k,t)$ is a projection operator (so that $W^2\phi = W\phi$, $\overline{W}W\phi = 0$), terms for which the IR field $\phi_{\mathrm{IR}} = \overline{W}\phi$ is directly convoluted with W vanish.

Requiring window functions to be projections is a rather strict constraint, since it requires W to take on only the values 0 and 1, and hence be a (sequence of) discontinuous step functions. A smooth window function is not a projection, but one may still expect that terms of the form $W\phi_{\mathrm{IR}}$ are suppressed also for e.g. a smoothed-out step function. Discarding the last three terms of (6.45) then implies that the window function is assumed to be "sufficiently step-like". In the following we will neglect these terms, but keep in mind this requirement on the window function. The final off-diagonal term Υ does not contain any W that gets directly convoluted with the $\phi_{\mathrm{IR}}^{\mathrm{c}}, \phi_{\mathrm{IR}}^{\mathrm{q}}$ fields. In section 6.3.2 we will show by an explicit computation that Υ is subleading compared to the q-q component in (6.42), but until then it is kept in the remainder of this section.

When the simplifications discussed above can be made, the influence functional can be written as

$$
\mathcal{F}_0[\Phi_{\text{IR}}] = N \exp\left[i \int_x \int_{x'} \left(\frac{i}{2} \phi_{\text{IR}}^{\text{q}}(x) \operatorname{Re} \Pi(x, x') \phi_{\text{IR}}^{\text{q}}(x') \right. \right.
$$
$$
\left. \left. - 2\Theta(t - t') \phi_{\text{IR}}^{\text{q}}(x) \operatorname{Im} \Pi(x, x') \phi_{\text{IR}}^{\text{c}}(x') \right) \right], \tag{6.47}
$$

with

$$
\Pi(x, x') = \int \frac{\mathrm{d}^3 \mathbf{k}}{(2\pi)^3} Q_t Q_{t'} \phi(k, t) \phi^*(k, t') e^{i\mathbf{k} \cdot (\mathbf{x} - \mathbf{x}')}, \tag{6.48}
$$

having used that (for $t > t'$)

$$
G_F(k, t, t') = \operatorname{Re} \phi(k, t) \phi^*(k, t'), \tag{6.49}
$$
$$
G_R(k, t, t') = 2\Theta(t - t') \operatorname{Im} \phi(k, t) \phi^*(k, t'). \tag{6.50}
$$

In order to compute these quantities explicitly, one is required to choose a concrete representation for the UV field mode functions $\phi(k, t)$ as well as a window function $W(k, t)$. To this end we will be using the mode solutions defined in section 6.2.3, at different levels of approximation.

6.2.5   Stochastic IR theory

Following a well-known procedure for turning our effective theory into a stochastic one [197, 198], the q-q component of (6.47) is represented by a real-valued quantity by introducing an auxiliary field $\xi(x)$ via a Hubbard-Stratonovich transformation,

$$
e^{-\frac{1}{2} \int_x M \phi_{\text{IR}}^2} = \int \mathcal{D}\xi e^{-\frac{1}{2} \int_x M^{-1} \xi^2 + i \int_x \xi \phi_{\text{IR}}}, \tag{6.51}
$$

for which we obtain

$$
\mathcal{F}_0[\Phi_{\text{IR}}] = N \int \mathcal{D}\xi \exp\left[\int_x \int_{x'} \left(-\tfrac{1}{2} \xi(x) \operatorname{Re} \Pi(x, x')^{-1} \xi(x') \right. \right.
$$
$$
\left. \left. + i\xi(x) \phi_{\text{IR}}^{\text{q}}(x') - i2\Theta(t - t') \phi_{\text{IR}}^{\text{q}}(x) \operatorname{Im} \Pi(x, x') \phi_{\text{IR}}^{\text{c}}(x') \right) \right]. \tag{6.52}
$$

124

Here the variables ξ are defined to be Gaussian, with

$$\langle \xi(x)\xi(x') \rangle = \int \mathcal{D}\xi \mathcal{P}[\xi]\xi(x)\xi(x') = \operatorname{Re} \Pi(x, x'). \qquad (6.53)$$

In this relation $\langle \cdot \rangle$ denotes the ensemble average and the right-hand-side is evaluated as a quantum expectation value.

An equivalent, but perhaps more familiar form of the stochastic noise correlator (6.53) can be obtained by rewriting (6.48) into[5]

$$\operatorname{Re} \int_x \int_{x'} \phi_{\text{IR}}^{\text{q}}(x)\Pi(x, x')\phi_{\text{IR}}^{\text{q}}(x')$$

$$= \operatorname{Re} \int_x \int_{x'} \int \frac{d^3\mathbf{k}}{(2\pi)^3} \left(-\dot{\phi}_{\text{IR}}^{\text{q}}(t)\phi(t) + \phi_{\text{IR}}^{\text{q}}(t)\dot{\phi}(t) \right) \dot{W}_t \qquad (6.54)$$

$$\times \dot{W}_{t'} \left(-\dot{\phi}_{\text{IR}}^{\text{q}}(t')\phi^*(t') + \phi_{\text{IR}}^{\text{q}}(t')\dot{\phi}^*(t') \right) e^{i\mathbf{k}\cdot(\mathbf{x}-\mathbf{x}')},$$

and introducing instead two auxiliary fields ξ_ϕ and ξ_π. Writing $\pi = \dot{\phi}$, the generating functional becomes

$$\mathcal{F}_0[\Phi_{\text{IR}}] = N \int \mathcal{D}\xi_\phi \mathcal{D}\xi_\pi$$

$$\times \exp\left[\int_x \int_{x'} \left(-\tfrac{1}{2} \left[\xi_\phi(x), \xi_\pi(x) \right] \mathcal{M}^{-1}(x, x') \begin{bmatrix} \xi_\phi(x') \\ \xi_\pi(x') \end{bmatrix} \right. \right.$$

$$+ i \left[-\pi_{\text{IR}}^{\text{q}}(x), \phi_{\text{IR}}^{\text{q}}(x) \right] \begin{bmatrix} \xi_\phi(x') \\ \xi_\pi(x') \end{bmatrix}$$

$$\left. \left. - i2\Theta(t - t')\phi_{\text{IR}}^{\text{q}}(x) \operatorname{Im} \Pi(x, x')\phi_{\text{IR}}^{\text{c}}(x') \right) \right],$$

$$(6.55)$$

where

$$\mathcal{M}(x, x') = \operatorname{Re} \int \frac{d^3\mathbf{k}}{(2\pi)^3} e^{i\mathbf{k}\cdot(\mathbf{x}-\mathbf{x}')}$$

$$\times \dot{W}_t \begin{bmatrix} \phi(k, t)\phi^*(k, t') & \phi(k, t)\pi^*(k, t') \\ \pi(k, t)\phi^*(k, t') & \pi(k, t)\pi^*(k, t') \end{bmatrix} \dot{W}_{t'}. \qquad (6.56)$$

---

[5]Using the metric determinant to write $-a^3(t)Q_t\phi(k, t) = \partial_t[a^3(t)\dot{W}(k, t)\phi(k, t)] + a^3(t)\dot{W}(k, t)\dot{\phi}(k, t)$ and partial integrating the first term in the action.

Schematically, we may then write for the stochastic noise

$$
\xi_\phi(x) = \int \frac{\mathrm{d}^3 \mathbf{k}}{(2\pi)^{\frac{3}{2}}} \dot{W}_t \big[a_\mathbf{k} \phi(k,t) e^{i\mathbf{k}\cdot\mathbf{x}} + \mathrm{h.c.} \big],
$$
$$
\xi_\pi(x) = \int \frac{\mathrm{d}^3 \mathbf{k}}{(2\pi)^{\frac{3}{2}}} \dot{W}_t \big[a_\mathbf{k} \pi(k,t) e^{i\mathbf{k}\cdot\mathbf{x}} + \mathrm{h.c.} \big],
\tag{6.57}
$$

keeping in mind that $\xi(x)$ is a number and the right-hand side is an operator, and the correspondence is at the level of expectation values.

The stochastic equation. Combining the expressions (6.38) and (6.52), the influence functional (6.37) now reads

$$
Z[0] = \int \mathcal{D}\Phi_{\mathrm{IR}}\, e^{iS[\Phi_{\mathrm{IR}}]} \mathcal{F}_0[\Phi_{\mathrm{IR}}] = \int \mathcal{D}\Phi_{\mathrm{IR}} \mathcal{D}\xi\, e^{iS_{\mathrm{eff}}}[\Phi_{\mathrm{IR}}, \xi],
\tag{6.58}
$$

with

$$
S[\Phi_{\mathrm{IR}}] = \int_x \left(\tfrac{1}{2} \phi_{\mathrm{IR}}^{\mathrm{c}} G^{-1} \phi_{\mathrm{IR}}^{\mathrm{q}} - V_{\mathrm{I}}[\phi_{\mathrm{IR}}^{\mathrm{c}}, \phi_{\mathrm{IR}}^{\mathrm{q}}] \right).
\tag{6.59}
$$

By variation of the effective action, we finally arrive at the stochastic equation of motion for the IR field, which becomes[6]

$$
0 = \left. \frac{\delta S_{\mathrm{eff}}}{\delta \phi_{\mathrm{IR}}^{\mathrm{q}}(x)} \right|_{\phi_{\mathrm{IR}}^{\mathrm{q}}=0} = \ddot{\phi}_{\mathrm{IR}}^{\mathrm{c}}(x) + 3H\dot{\phi}_{\mathrm{IR}}^{\mathrm{c}}(x) - \frac{\nabla_\mathbf{x}^2}{a^2(t)} \phi_{\mathrm{IR}}^{\mathrm{c}}(x) + V'(\phi_{\mathrm{IR}}^{\mathrm{c}}(x))
$$
$$
- \xi(x) + \int_{x'} 2\Theta(t-t')\, \mathrm{Im}\, \Pi(x,x') \phi_{\mathrm{IR}}^{\mathrm{c}}(x').
\tag{6.60}
$$

One may note that if the IR field is sufficiently super-horizon, the gradient term is negligible, since by construction

$$
\frac{k^2}{a^2(t)H^2} \phi_{\mathrm{IR}}^{\mathrm{c}} \ll \phi_{\mathrm{IR}}^{\mathrm{c}}.
\tag{6.61}
$$

This must then be compared to the remaining terms. To the extent that $\Upsilon(x,x') = 2\Theta(t-t')\, \mathrm{Im}\, \Pi(x,x')$ may be neglected, we recover the stochastic equation advertised in (6.14);

$$
\ddot{\phi}_{\mathrm{IR}} + 3H\dot{\phi}_{\mathrm{IR}} + V'(\phi_{\mathrm{IR}}) = \xi.
\tag{6.62}
$$

---

[6]We note that the potential term $V_{\mathrm{I}}[\Phi] = V_{\mathrm{I}}[\phi^+] - V_{\mathrm{I}}[\phi^-]$ in the Keldysh basis has the property that $\mathrm{d}V_{\mathrm{I}}[\Phi]/\mathrm{d}\phi^{\mathrm{q}}|_{\phi^{\mathrm{q}}=0} = V_{\mathrm{I}}'[\phi^{\mathrm{c}}]$.

One may equivalently vary instead (6.55), to obtain the identification

$$3H\xi_\phi(x) + \dot{\xi}_\phi(x) + \xi_\pi(x) := \xi(x), \tag{6.63}$$

as discussed in section 6.1.1. In the following sections we will show explicitly that in certain limits, $3H\xi_\phi$ is indeed the dominant contribution to the noise. For the moment, we will simply note that for $k \ll aH$ the mode derivative is $\dot{\phi}(k,t) \simeq \epsilon_M H \phi(k,t)$, as can be seen from e.g. (6.57) and (6.84). It follows that for small ϵ_M, the remaining correlators in (6.56) are $O(\epsilon_M)$.

Under the above assumptions, and additionally in the slow-roll regime where $\ddot{\phi} \ll 3H\dot{\phi}$, the original stochastic inflation form (6.1) is recovered,

$$\dot{\phi}_{\text{IR}}(t) + \frac{V'(\phi_{\text{IR}}(t))}{3H} = \xi_\phi(t). \tag{6.64}$$

Let us summarise the procedure so far. Before applying standard slow-roll and large wavelength assumptions common to inflationary dynamics, we have ignored UV-UV and UV-IR self-interactions, made use of W being close to a projection onto UV modes, neglected Υ and neglected noise contributions other than ξ_ϕ. The IR fields have also implicitly been assumed classical, so that the variation of the path integral with respect to $\phi_{\text{IR}}^{\text{q}}$ gives the complete dynamics. Only then do we recover the standard form of the stochastic equation. A number of these assumptions will be checked explicitly below.

Before we proceed, we emphasise that expressing the path integral in terms of a stochastic process does not imply any physical reality to each individual stochastic trajectory. Only the ensemble average over initial conditions and realisations of the noise have meaning, and so conceptually, the corresponding Fokker-Planck equation and distribution is perhaps the preferred object to work with.

6.2.6 An example: the step window function

The simplest example of a window function is the step function

$$W(k,t) = \Theta(k/aH - \mu), \tag{6.65}$$

which projects out modes with $k < \mu a H$, and was the original choice made in [38, 39]. It is a true projection, and so some of the simplifications discussed above go through straightforwardly. The dimensionless parameter $\mu < 1$ is taken to be small but non-vanishing, and the coarse-graining scale is then $(\mu a H)^{-1}$.

The noise correlations can be computed from (6.56), where from (6.36) we obtain to first order in mass and slow-roll parameters,

$$
\begin{bmatrix} \langle \xi_\phi(x)\xi_\phi(x')\rangle \\ \langle \xi_\phi(x)\xi_\pi(x')\rangle \\ \langle \xi_\pi(x)\xi_\pi(x')\rangle \end{bmatrix} = \frac{H^3}{4\pi^2}(1-\epsilon_H)^3 \frac{\sin \mu a H r}{\mu a H r}\delta(t-t')\left(\frac{\mu}{1-\epsilon_H}\right)^{2\epsilon_M - 2\epsilon_H}
$$
$$
\times \begin{bmatrix} 1 + \mu^2(1+2\epsilon_M) \\ \left(-\epsilon_M + \mu^2(1+\frac{3}{2}\epsilon_M - \epsilon_H)\right)H \\ \left(\epsilon_M^2 + 2\mu^2\epsilon_M\right)H^2 \end{bmatrix} + O(\mu^4).
$$

$$(6.66)$$

In the limit $\epsilon_M, \epsilon_H \to 0$ the first noise correlator in (6.66) reduces to the original result [39] to leading order in μ. It remains to take the limits $\mu \ll 1$ and $r < aH$ to recover the correlation,

$$
\langle \xi_\phi(x)\xi_\phi(x')\rangle = \frac{H^3}{4\pi^2}\delta(t-t'). \tag{6.67}
$$

This result is elegant in its simplicity, but as we have seen, it relies on a number of approximations and assumptions. An early discussion of noise resulting from non-linear interactions between the IR-UV fields with a cutoff scale separation includes [199].

The expression (6.66) is our first encounter of the correction function $f(\epsilon_M, \epsilon_H, \mu, ...)$ advertised in section 6.1.1. We see that the limits $\epsilon_M, \epsilon_H \to 0$ do not commute with $\mu \to 0$. Indeed, as soon at μ is taken to be small, the standard noise normalisation (6.67) only follows in the strict massless and dS limit. From (6.66) it is also apparent that the contribution of ξ_ϕ dominates for small μ.

It was pointed out in [195] that some window functions fail to reproduce the correct long-distance behaviour of the full (non-coarse grained) correlators, and that some result in coloured noise [195, 200].[7] The step

---

[7]For instance, the resulting correlations $\langle \dot{\phi}_{\text{IR}}(x)\dot{\phi}_{\text{IR}}(x')\rangle$ from the Langevin equation should at least

function is one such example, and in the following, we will consider smooth window functions.

6.2.7 Momentum decomposition of the propagator

An alternative method for the scale separation between IR and UV modes was applied in [191], where the propagator rather than the field itself is subject to a window function in momentum space. The propagator is decomposed into two constituents that are dominant in the IR and UV respectively:

$$\mathbb{G}(x, x') = \mathbb{G}_{\text{IR}}(x, x') + \mathbb{G}_{\text{UV}}(x, x'), \qquad (6.69)$$

where the IR propagator is weighted according to

$$\mathbb{G}_{\text{IR}}(x, x') := \int_y \int_{y'} \overline{W}(x, y)\mathbb{G}(y, y')\overline{W}(y', x'), \qquad (6.70)$$

and $\overline{W}$ is as earlier used to project the field onto long wavelengths. The UV propagator is constructed from (6.69) as (c.f. (6.40))

$$\mathbb{G}_{\text{UV}}(x, x') = \int_{y'} \int_y \Big[\mathbb{G}(x, y)W(y, x') + W(x, y)\mathbb{G}(y, x') \\ - W(x, y)\mathbb{G}(y, y')W(y', x') \Big]. \qquad (6.71)$$

An additional step is to make the formal rewriting of the field into two constituents,

$$\Phi(x) = \Phi_1(x) + \Phi_2(x). \qquad (6.72)$$

Unlike when decomposing at the level of the fields, these field constituents are not under any constraints: they are simply two new field variables defined over all of momentum space. The decomposition (6.72) is used as a tool together with the propagator constituents (6.69) to make use of a

---

match the behaviour of $\langle \dot{\phi}(x)\dot{\phi}(x')\rangle \sim r^{-4}$ at large distances. This can be achieved by demanding sufficient smoothness of the window function, such that the noise correlation

$$\langle \xi_\phi(x)\xi_\phi(x')\rangle \sim \int \mathrm{d}k h(k)\sin kr = \frac{h(0)}{r} - \frac{h''(0)}{r^3} + \frac{h'''(0)}{r^5} - \dots, \qquad (6.68)$$

has at least $h'''(0)$ finite. The authors of [195] provided a sufficient (but not necessary or exhaustive) condition for a window function to satisfy this.

Gaussian identity[8] in order to rewrite the generating functional (6.17) as

$$
Z[\mathbb{J}] = \int \mathcal{D}\Phi_1 \mathcal{D}\Phi_2 \exp\left[\frac{i}{2} \int_x \left(\Phi_1^T \mathbb{G}_{\text{IR}}^{-1} \Phi_1 + \Phi_2^T \mathbb{G}_{\text{UV}}^{-1} \Phi_2 \right. \right.
$$
$$
\left. \left. - 2V_{\text{I}}(\Phi_1 + \Phi_2) + \mathbb{J}^T(\Phi_1 + \Phi_2) \right) \right]. \tag{6.74}
$$

We have in mind a smooth window function $W(\overline{W})$ that suppresses the IR(UV). From the construction of the propagators, the UV components of the Φ_1 field will have suppressed contributions to the path integral, and analogously the IR components of the Φ_2 field. Note that when decomposing at the level of the propagator, we no longer have bilinear kinetic terms mixing the UV and IR physics in the generating functional. To obtain an expression for the IR kinetic operator in (6.74), we write (formally, suppressing integration labels)

$$
\mathbb{G}_{\text{IR}}^{-1} = \frac{1}{1 - \mathbb{G}^{-1}\mathbb{G}_{\text{UV}}} \mathbb{G}^{-1}. \tag{6.75}
$$

For the large-wavelength dynamics governed by $\mathbb{G}_{\text{IR}}^{-1}$, the propagator $\mathbb{G}_{\text{UV}}$ is by construction acting on a subspace of the field configuration in which it is suppressed, hence allowing the expansion

$$
\mathbb{G}_{\text{IR}}^{-1} = \mathbb{G}^{-1} + \mathbb{G}^{-1}\mathbb{G}_{\text{UV}}\mathbb{G}^{-1} + \mathbb{G}^{-1}\mathbb{G}_{\text{UV}}\mathbb{G}^{-1}\mathbb{G}_{\text{UV}}\mathbb{G}^{-1} + \dots . \tag{6.76}
$$

To clarify, the "small quantity" in the expansion is the degree to which the "mostly-UV" propagator $\mathbb{G}_{\text{UV}}$ is small when acting on the "mostly-IR" field Φ_1.[9] For a given window function, it may be prudent to confirm convergence a posteriori, and we will do this below.

The first term in (6.76) replaces G_{IR}^{-1} by G^{-1} in the quadratic part of

---

[8]For some function $f(x)$ depending only on the combination $x = y + z$ the relation

$$
\sqrt{\frac{|a+b|}{2\pi ab}} \int \mathrm{d}y \int \mathrm{d}z \exp\left\{ -\left(\frac{y^2}{2a} + \frac{z^2}{2b} + f(y+z) \right) \right\} = \int \mathrm{d}x \exp\left\{ -\left(\frac{x^2}{2(a+b)} + f(x) \right) \right\}, \tag{6.73}
$$

can be verified e.g. by a change of variables $x = y + z$ and integration over $u = by - az$.

[9]For a strict step function such as (6.65), this procedure is ill-defined, since the denominator of (6.75) vanishes for UV modes.

the action (6.74), such that

$$Z[0] = \int \mathcal{D}\Phi_1 \exp\left[\frac{i}{2}\int_x \left(\Phi_1^T \mathbb{G}^{-1}\Phi_1 - 2V_I(\Phi_1)\right)\right]$$

$$\times \exp\left[\frac{i}{2}\int_x \Phi_1^T \mathbb{G}^{-1}\mathbb{G}_{\text{UV}}\mathbb{G}^{-1}\Phi_1 + \Phi_1^T \mathbb{G}^{-1}\mathbb{G}_{\text{UV}}\mathbb{G}^{-1}\mathbb{G}_{\text{UV}}\mathbb{G}^{-1}\Phi_1 + \ldots\right]$$

$$\times \int \mathcal{D}\Phi_2 \exp\left[\frac{i}{2}\int_x \left(\Phi_2^T \mathbb{G}_{\text{UV}}^{-1}\Phi_2 - 2V_I(\Phi_1, \Phi_2)\right)\right].$$

$$(6.77)$$

where similarly to (6.38), we have defined $V_I(\Phi_1, \Phi_2) := V_I(\Phi_1 + \Phi_2) - V_I(\Phi_1)$.

By the same logic as when the UV-IR and UV-UV self-interactions were neglected in the previous section, we will treat the Φ_2 field as non-interacting, in which case the integral over Φ_2 is Gaussian and only provides a multiplicative constant. The second line will now play the role of the influence functional, while the first line is the free action $S[\Phi_1]$.

Our new influence functional has as its leading term (corresponding to the next-to-leading order (NLO) in the inverse propagator expansion (6.76))

$$\mathbb{G}^{-1}\mathbb{G}_{\text{UV}}\mathbb{G}^{-1} = W\mathbb{G}^{-1} + \mathbb{G}^{-1}W - \mathbb{G}^{-1}W\mathbb{G}W\mathbb{G}^{-1}, \qquad (6.78)$$

which includes the integrand in (6.39). The derivation of the Langevin equation then goes through in the same manner as previously described. The additional terms $\mathbb{G}^{-1}W$ and $W\mathbb{G}^{-1}$ become directly convoluted with Φ_1. By construction, Φ_1 has a suppressed short-wavelength component, and similarly to the discussion above, we expect the contribution of these terms to be negligible only for a sharp enough window function.

Unlike in section 6.2.4, the inverse propagator expansion in (6.76) gives further contributions at higher order. At next-to-next-to-leading

order (NNLO) one finds

$$
\begin{aligned}
\mathbb{G}^{-1}\mathbb{G}_{\mathrm{UV}}\mathbb{G}^{-1}\mathbb{G}_{\mathrm{UV}}\mathbb{G}^{-1} = {}& \mathbb{G}^{-1}W^2 + W^2\mathbb{G}^{-1} + W\mathbb{G}^{-1}W \\
& - \mathbb{G}^{-1}W^2\mathbb{G}W\mathbb{D}^{-1} - \mathbb{G}^{-1}W\mathbb{G}W^2\mathbb{G}^{-1} \\
& - W\mathbb{G}^{-1}W\mathbb{G}W\mathbb{G}^{-1} \\
& - \mathbb{G}^{-1}W\mathbb{G}W\mathbb{G}^{-1}W \\
& + \mathbb{G}^{-1}W\mathbb{G}W\mathbb{G}^{-1} \\
& + \mathbb{G}^{-1}W\mathbb{G}W\mathbb{G}^{-1}W\mathbb{G}W\mathbb{G}^{-1},
\end{aligned}
\tag{6.79}
$$

where we note the reappearance of the NLO term on the last line with the opposite sign. It is not manifest that (6.79) is subleading compared to (6.78), and we shall return to this point in the next section when considering a concrete example.

6.3 Testing approximations

In order to make explicit the central approximations needed to recover the Langevin equation in its standard form (6.1) a smooth window function that separates the IR and UV scales is used as an example. As discussed in the previous section, checking these approximations entails a comparison of the stochastic noise of (6.53) with the white noise case (6.66) and the justification to neglect the off-diagonal (c-q) components in (6.45). In addition, we examine the expansion of the inverse IR propagator (6.76) from the alternative derivation presented in section 6.2.7. Lastly, we study the impact of the choice of UV mode function on the noise correlations. We take the common example of a Gaussian as a smooth window function,

$$
W(k,t) = 1 - e^{-\frac{1}{2}\left(\frac{k}{\sigma a_t H}\right)^2}.
\tag{6.80}
$$

The Gaussian window function fulfills the criteria set out in Ref. [195], and is parameterised by a dimensionless parameter σ, controlling both the location and steepness of the transition from IR to UV. This is in contrast to a smoothed step function (which will also be considered in section 6.4), where the location is fixed by a parameter μ (as in (6.65)) and σ controls the steepness of the transition. In other words, the Gaussian

does not become a step function in the limit $\sigma \to 0$, since the cutoff besides from steepening then also moves $k \to 0$. The Gaussian window function has been considered in a number of works, including [186, 201].

6.3.1 Noise correlations

The noise correlation (6.53) can be simplified slightly using that the time derivative of the full mode solution can be factorised as

$$\dot{\phi}(k, t) = q_\nu(k, t) H \phi(k, t), \tag{6.81}$$

such that

$$\langle \xi(x)\xi(x')\rangle = \text{Re} \int \frac{k\,\mathrm{d}k}{2\pi^2 r} \sin kr \tilde{Q}(k, t)\tilde{Q}^*(k, t')\phi(k, t)\phi^*(k, t'). \tag{6.82}$$

Here we have defined

$$\tilde{Q}(k, t) := -\ddot{W}(k, t) - [3 + 2q_\nu(k, t)]H\dot{W}(k, t). \tag{6.83}$$

where q_ν may be expressed as

$$q_\nu(k, t) = -\epsilon_M - \frac{k}{a(t)H} \frac{H^{(1)}_{\nu-1}\left(\frac{k}{a(t)H(1-\epsilon_H)}\right)}{H^{(1)}_\nu\left(\frac{k}{a(t)H(1-\epsilon_H)}\right)} \, . \tag{6.84}$$

to first order in ϵ_M, ϵ_H. We will proceed with $\epsilon_H = 0$ and generalise to $\epsilon_H \neq 0$ later.

To begin with, using the approximate mode solution (6.36) for which $q_\nu(k, t) \simeq -\epsilon_M$, the noise correlator is found to be

$$\langle \xi(x)\xi(x')\rangle = \frac{H^6}{8\pi^2}\sigma^{2\epsilon_M}(\text{sech}\,H\tau)^{2+\epsilon_M}$$
$$\times \left[\text{sech}^2\,H\tau\Gamma[4 + \epsilon_M]\,_1F_1\left(4 + \epsilon_M; \frac{3}{2}; -\frac{r^2}{4\alpha}\right) \right.$$
$$+ 2(1 - 2\epsilon_M)\Gamma[3 + \epsilon_M]\,_1F_1\left(3 + \epsilon_M; \frac{3}{2}; -\frac{r^2}{4\alpha}\right)$$
$$\left. + (1 - 2\epsilon_M)^2\Gamma[2 + \epsilon_M]\,_1F_1\left(2 + \epsilon_M; \frac{3}{2}; -\frac{r^2}{4\alpha}\right) \right], \tag{6.85}$$
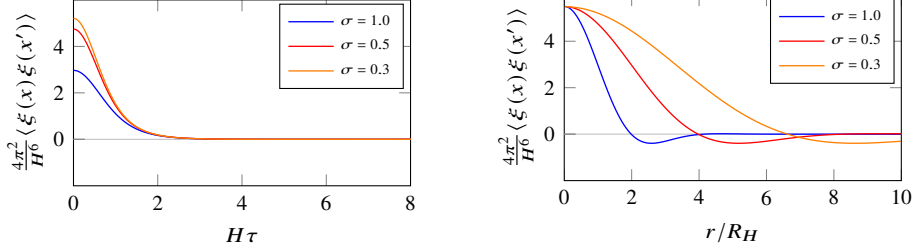
Figure 6.1: Noise correlation (6.85) with $\epsilon_M = 0.001$ as a function of spatial separation r/R_H with Hubble scale $R_H := R(t = t')$ (left panel) and as a function of time separation $\tau := t - t'$ for fixed spatial separation $r/R = 1$ (right panel).

where $\tau := t - t'$ denotes the time separation, $r := |\mathbf{x} - \mathbf{x}'|$ the spatial separation, ${}_1F_1(a, b, z)$ is a confluent hypergeometric function [196], and

$$\alpha := \frac{1}{2\sigma^2 H^2} \left[\frac{1}{a^2(t)} + \frac{1}{a^2(t')} \right] = \frac{R^2}{\sigma^2 \operatorname{sech} H\tau}, \qquad (6.86)$$

with

$$R^2 := \frac{1}{a(t)a(t')H^2} . \qquad (6.87)$$

Because a number of similar expressions will appear later, it is worth pausing at this point. For equal time $t = t'$, we see that R is the Hubble scale in time, and the spatial separation r then enters the correlation in units of the Gaussian width $(R/\sigma)^2$. Away from the equal-time limit, $r^2/4\alpha$ grows exponentially with τ, resulting in the whole expression decaying exponentially (see left panel of Fig. 6.1). For large spatial separations $r \gg R$, the noise correlation decays exponentially (see right panel of Fig. 6.1), signifying that the noise evolution can be considered local for patches of length scales $r < R/\sigma$. It becomes apparent that for smaller σ, the decay is slower. On the other hand, since R decreases very fast in time, the localisation in space is not very sensitive to the choice of σ.

In addition, due to the overall factor of $\sigma^{2\epsilon_M}$, the limit $\sigma \to 0$ does not commute with the massless limit. This factor can be replaced by 1 if we choose σ in such a way that $\ln \sigma \ll \epsilon_M^{-1}/2$. If ϕ is the inflaton, in which case $\epsilon_M \simeq 10^{-5} - 10^{-6}$, then this requirement is easily satisfied, however in principle one may tune σ and ϵ_M to give any noise amplitude.

To get a better understanding of the contributions to the noise correlation (6.85), one may consider the decomposed noise terms ξ_ϕ and ξ_π of (6.63), where schematically

$$\dot{\xi}_\phi(x) = \int \frac{d^3\mathbf{k}}{(2\pi)^{\frac{3}{2}}} \left(\ddot{W}_t + q_\nu(k,t)\dot{W}_t\right)\left[a_\mathbf{k}\phi(k,t)e^{i\mathbf{k}\cdot\mathbf{x}} + \text{h.c.}\right]. \quad (6.88)$$

In particular, we obtain

$$\langle\xi_\phi(x)\xi_\phi(x')\rangle = \frac{H^4}{8\pi^2}\sigma^{2\epsilon_M}\Gamma[2+\epsilon_M](\text{sech}\,H\tau)^{2+\epsilon_M}\,_1F_1\left(2+\epsilon_M, \frac{3}{2}, -\frac{r^2}{4\alpha}\right)$$

$$\simeq \frac{H^4}{8\pi^2}\,\text{sech}^2\,H\tau + O(\epsilon_M),$$

$$(6.89)$$

where the last equality applies for $r = 0$. The long-wavelength approximate result (6.89) reproduces the result at leading order in σ obtained using the exact massless mode solution (6.35) in earlier works [186, 195].

For the correlation of (6.88) one finds

$$\langle\dot{\xi}_\phi(x)\dot{\xi}_\phi(x')\rangle = \frac{H^6}{8\pi^2}\sigma^{2\epsilon_M}(\text{sech}\,H\tau)^{2+\epsilon_M}$$

$$\times \left[\Gamma[4+\epsilon_M]\,\text{sech}^2\,H\tau\,_1F_1\left(4+\epsilon_M, \frac{3}{2}, -\frac{r^2}{4\alpha}\right)\right.$$

$$-4\Gamma[3+\epsilon]\,_1F_1\left(3+\epsilon_M, \frac{3}{2}, -\frac{r^2}{4\alpha}\right) \quad (6.90)$$

$$\left.+4\Gamma[2+\epsilon]\,_1F_1\left(2+\epsilon_M, \frac{3}{2}, -\frac{r^2}{4\alpha}\right)\right]$$

$$\simeq \frac{H^6}{8\pi^2}\,\text{sech}^2\,H\tau(6\,\text{sech}^2\,H\tau - 4) + O(\epsilon_M).$$

with the last equality again in the limit $r \to 0$. For the cross terms, we find

$$\langle\dot{\xi}_\phi(x)\xi_\phi(x')\rangle + \langle\xi_\phi(x)\dot{\xi}_\phi(x')\rangle$$

$$= \frac{H^5}{4\pi^2}\sigma^{2\epsilon_M}(\text{sech}\,H\tau)^{2+\epsilon_M}\left[\Gamma[3+\epsilon_M]\,_1F_1\left(3+\epsilon_M, \frac{3}{2}, -\frac{r^2}{4\alpha}\right)\right.$$

$$\left.-2\Gamma[2+\epsilon]\,_1F_1\left(2+\epsilon_M, \frac{3}{2}, -\frac{r^2}{4\alpha}\right)\right]$$

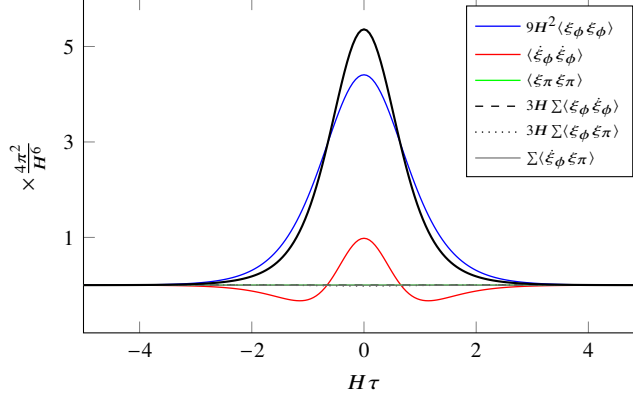$$\simeq 0 + O(\epsilon_M).$$

$$(6.91)$$

Figure 6.2: Decomposed noise correlations at coincident spatial points for the Gaussian window with $\sigma = 0.1$ and $\epsilon_M = 0.005$. Here we denote $\sum \langle \xi_\phi \dot{\xi}_\phi \rangle :=$ $\langle \xi_\phi(x) \dot{\xi}_\phi(x') \rangle + \langle \dot{\xi}_\phi(x) \xi_\phi(x') \rangle$, etc. The combined noise $\langle \xi(x) \xi(x') \rangle$ of (6.85) is displayed in black for comparison.

Correlations involving $\xi_\pi \propto q_\nu \simeq -\epsilon_M$ are similarly suppressed. In Fig. 6.2, we show all the contributions to the noise correlators at $r = 0$ as a function of time separation $H\tau$. We see that ξ_ϕ indeed dominates, while $\dot{\xi}_\phi$ has both positive and negative contributions.

The noise correlator is localised around $H\tau = 0$, but has more features than simply a delta-function. Nevertheless, a final connection to the white noise delta function can be made, even for finite σ, through the replacement (for this example, in the massless limit $\epsilon_M = 0$)

$$\mathrm{sech}^2 H\tau \to 2\delta(H\tau) = \frac{2}{H}\delta(t - t'), \qquad (6.92)$$

where the factor of 2 is chosen so that

$$\int \mathrm{d}(H\tau)\, \mathrm{sech}^2 H\tau = \frac{2}{H} \int \mathrm{d}\tau \delta(t - t'). \qquad (6.93)$$

In other words, we replace a moderately localised noise distribution by a fully localised one with the same integrated power, i.e., such that

$$\langle \xi_\phi(x) \xi_\phi(x') \rangle \simeq \frac{H^4}{8\pi^2} \mathrm{sech}^2 H\tau \simeq \frac{H^3}{4\pi^2}\delta(t - t'). \qquad (6.94)$$

With this procedure, it can be seen that the integral of the $\langle \dot{\xi}_\phi \dot{\xi}_\phi \rangle$ correlator vanishes identically to leading order, and so non-local time correlations

(positive and negative) are ignored in this procedure. Only the $\langle \xi_\phi \xi_\phi \rangle$ contribution remains.

In section 6.4, we will further investigate how the noise distribution depends on the choice of window function and its parameters, as well as the choice of approximation for the UV mode functions (6.34)–(6.36). The dependence on the mass parameter ϵ_M and the generalisation beyond leading order in slow-roll, $\epsilon_H \neq 0$, will also be considered. Ultimately, we will compute the amplitude of the localised noise, making use of the prescription (6.92). The prefactor of the delta-function will be referred to as the noise amplitude.

Before doing so, however, we will use the Gaussian window function to explicitly check some of the assumptions made with the derivations in the previous section. The conclusions will hold also for the other window functions considered below.

6.3.2 Off-diagonal (q-c) contributions to the IR field evolution

In our derivation of the stochastic evolution equation for the IR modes (6.60), we made the claim that the off-diagonal c-q contributions, including the term Υ, can be neglected. In the following we will check this explicitly for the terms that do not contain any operators acting directly on the IR field ϕ_{IR}.

With the approximate solution (6.36) for the dS UV mode functions, we first find for the retarded propagator

$$
G_R(k, t, t') \simeq -\frac{H^2}{3} \Theta(t - t') \big[(a_t H)^{-3+\epsilon_M} (a_{t'} H)^{-\epsilon_M} \\
- (a_{t'} H)^{-3+\epsilon_M} (a_t H)^{-\epsilon_M} \big],
\tag{6.95}
$$

which for $\epsilon_M \to 0$ goes as $a^{-3}(t)$. We can then straightforwardly compute

$$
\begin{aligned}
\Upsilon(x,x') = {} & \frac{H^7}{4\pi^2}\sigma^3(a_t a_{t'})^{\frac{3}{2}} \operatorname{sech}^{\frac{7}{2}} H\tau \Big[\Gamma\left[\tfrac{11}{2}\right] \operatorname{sech}^2 H\tau \, {}_1F_1\Big(\frac{11}{2},\frac{3}{2},-\frac{r^2}{4\alpha}\Big) \\
& + 2\Gamma\left[\tfrac{9}{2}\right] {}_1F_1\Big(\frac{9}{2},\frac{3}{2},-\frac{r^2}{4\alpha}\Big)\Big(1 + \operatorname{sech} H\tau \Big(\frac{a_{t'}}{a_t}\frac{\partial_{t'}}{H} + \frac{a_t}{a_{t'}}\frac{\partial_t}{H}\Big)\Big) \\
& + (-5 + 12\epsilon_M)\Gamma\left[\tfrac{7}{2}\right] {}_1F_1\Big(\frac{7}{2},\frac{3}{2},-\frac{r^2}{4\alpha}\Big)\Big] G_R(x,x') \\
& - \frac{H^6}{3\pi^2}(3 - 2\epsilon_M)\sigma^3 \Gamma\left[\tfrac{7}{2}\right] {}_1F_1\Big(\frac{7}{2},\frac{3}{2},-\frac{1}{4}(r\sigma a_t H)^2\Big)\delta(H\tau),
\end{aligned}
$$
$$(6.96)$$

where we have used

$$
(\partial_t + \partial_{t'})G_R = -3HG_R, \tag{6.97}
$$

$$
\partial_t \partial_{t'} G_R = (3 - \epsilon_M)\epsilon_M H^2 G_R + \frac{\delta(t - t')}{\Theta(t - t')}\partial_{t'}G_R. \tag{6.98}
$$

As an example, in the $r = 0$, $\epsilon_M = 0$ limit this reduces to

$$
\begin{aligned}
\Upsilon(x,x') = {} & \frac{H^6}{\pi^2}\sigma^3 \Gamma\left[\tfrac{7}{2}\right] \Big[\operatorname{sech}^{\frac{7}{2}} H\tau \Big(\tfrac{21}{8}\sinh\tfrac{3}{2}H\tau \operatorname{sech}^2 H\tau \\
& - \tfrac{7}{2}\sinh\tfrac{1}{2}H\tau \operatorname{sech} H\tau + \tfrac{1}{3}\sinh\tfrac{3}{2}H\tau\Big)\Theta(\tau) - \delta(H\tau)\Big].
\end{aligned}
$$
$$(6.99)$$

The important result is a suppression by an overall factor of σ^3, but not by e.g. powers of the scale factor. This is still much faster than for the diagonal correlator (6.85), which has a leading $\sigma^{2\epsilon_M}$.

Similarly, in (6.45), one of the terms may by partial integration be

made not to act explicitly on the ϕ_{IR}. We find for this term,

$$
\frac{2}{a_{t'}^3}\delta(t - t') \int \frac{\mathrm{d}^3\mathbf{k}}{(2\pi)^3} e^{i\mathbf{k}\cdot(\mathbf{x}-\mathbf{x}')} \tilde{Q}_{t'} W_{t'}
$$

$$
= \delta(H\tau) \frac{H^6 \sigma^3}{2\pi^2}
$$

$$
\times \left[3\Gamma[\tfrac{7}{2}] \left({}_1F_1(\tfrac{7}{2}, \tfrac{3}{2}, -\tfrac{1}{4}(r\sigma a H)^2) - 2^{\frac{7}{2}}{}_1F_1(\tfrac{7}{2}, \tfrac{3}{2}, -\tfrac{1}{2}(r\sigma a H)^2) \right) \right.
$$

$$
\left. + \Gamma\left[\tfrac{5}{2}\right] \left({}_1F_1(\tfrac{5}{2}, \tfrac{3}{2}, -\tfrac{1}{4}(r\sigma a H)^2) - 2^{\frac{5}{2}}{}_1F_1(\tfrac{5}{2}, \tfrac{3}{2}, -\tfrac{1}{2}(r\sigma a H)^2) \right) \right]
$$

$$
\simeq \frac{H^6}{\pi^2}\sigma^3 \Gamma\left[\tfrac{7}{2}\right] \left(\frac{17 - 128\sqrt{2}}{10} \right) \delta(H\tau),
$$

$$(6.100)$$

where again the limits $r = 0$, $\epsilon_M = 0$ are taken in the last line. It is clear that also this quantity is suppressed by σ^3.

In Ref. [185], Υ was also reported to decay as μ^3 for a step window function (6.65). This is consistent, since for the Gaussian window function, σ also parametrises the cutoff μ. We conclude that neglecting the off-diagonal contributions in the influence functional is consistent in the small-σ (or μ) regime, for $\sigma^3 \ll \sigma^{2\epsilon_M}$.

6.3.3 Inverse IR propagator expansion

The expansion of the IR propagator (6.76) relies on the smallness of the overlap between the IR field and the UV propagator. To at least get an idea of the convergence, we proceed to consider the stochastic noise at NNLO in (6.79), given by the q-q component

$$
i(\mathbb{G}^{-1}\mathbb{G}_{\text{UV}}\mathbb{G}^{-1}\mathbb{G}_{\text{UV}}\mathbb{G}^{-1})_{qq} = G^{-1}WG_FWG^{-1}
$$

$$
- WG^{-1}WG_FWG^{-1}
$$

$$
- G^{-1}WG_FWG^{-1}W
$$

$$
- G^{-1}W^2G_FWG^{-1}
$$

$$
- G^{-1}WG_FW^2G^{-1} \qquad (6.101)
$$

$$
+ G^{-1}WG_FWG^{-1}WG_AWG^{-1}
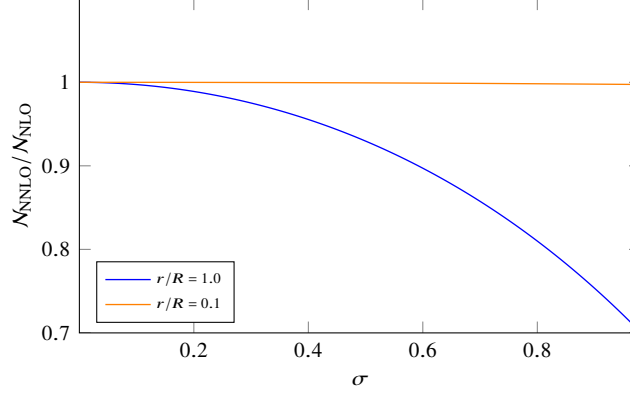$$

$$
+ G^{-1}WG_RWG^{-1}WG_FWG^{-1}.
$$

Figure 6.3: The ratio of the noise amplitude from the NNLO contributions (6.102) to the NLO noise (6.85) (with the Gaussian window function) as a function of σ with $\epsilon_M, \epsilon_H = 0$.

Assuming that it is valid to discard terms where the window function W is directly convoluted with the IR field constituents, and in addition that the contribution involving retarded/advanced propagators is negligible, (6.101) reduces to

$$
\begin{aligned}
i(\mathbb{G}^{-1}\mathbb{G}_{\text{UV}}\mathbb{G}^{-1}\mathbb{G}_{\text{UV}}\mathbb{G}^{-1})_{qq} \simeq\ & G^{-1}WG_F WG^{-1} \\
& - G^{-1}W^2 G_F WG^{-1} \\
& - G^{-1}WG_F W^2 G^{-1}.
\end{aligned}
\tag{6.102}
$$

Here we note that if the window function is a projection so that $W^2 = W$, all the terms add up to become equal to the NLO contribution considered above (6.78). Clearly, the step function is a pathological case, for which this expansion fails.

For a general window function, one can compute the three contributions in (6.102) explicitly. Using again the Gaussian window function as

a test case, we obtain

$$G^{-1}W^2G_FWG^{-1} = 2G^{-1}WG_FWG^{-1} - \frac{H^6}{4\pi^2}\sigma^{2\epsilon_M}\left(\frac{2}{2e^{-H\tau} + e^{H\tau}}\right)^{2+\epsilon_M}$$

$$\times \left[2\Gamma[4 + \epsilon_M]\left(\frac{2}{2e^{-H\tau} + e^{H\tau}}\right)^2 {}_1F_1\left(4 + \epsilon_M, \frac{3}{2}, -\frac{r^2}{4\tilde{\alpha}_t}\right)\right.$$

$$+ 2(1 - 2\epsilon_M)\Gamma[3 + \epsilon_M]{}_1F_1\left(3 + \epsilon_M, \frac{3}{2}, -\frac{r^2}{4\tilde{\alpha}_t}\right)$$

$$+ \left. (1 - 2\epsilon_M)^2\Gamma[2 + \epsilon_M]{}_1F_1\left(2 + \epsilon_M, \frac{3}{2}, -\frac{r^2}{4\tilde{\alpha}_t}\right)\right],$$

$$(6.103)$$

with

$$\tilde{\alpha}_t := \frac{2e^{-H\tau} + e^{H\tau}}{2\sigma^2 a_t a_{t'} H^2}, \tag{6.104}$$

and similarly for $G^{-1}WGW^2G^{-1}$ with $2e^{-H\tau} + e^{H\tau} \leftrightarrow e^{-H\tau} + 2e^{H\tau}$. We notice the reappearance of the NLO noise kernel $G^{-1}WG_FWG^{-1}$ as the first term on the right-hand-side of (6.103).

To quantify the relation between the two orders of the expansion, we perform the localisation procedure of (6.93), i.e., replacing the noise by a delta function and matching the normalisation. The ratio of the noise amplitude for the NNLO noise terms (6.102) and the NLO result (6.85) is plotted in Fig. 6.3. Judging only by the subset of terms computed, there is no suppression of the NNLO contributions compared to that of NLO. Hence, we cannot confirm that truncating the inverse propagator expansion at NLO is a controlled approximation.

6.3.4 Exact or long-wavelength UV mode functions

Another approximation worthy of examination is the use of the IR-approximate mode solutions (6.36) instead of the exact mode solutions (6.34). The latter are complicated to treat analytically and so we compare the two numerically. As a first example, we continue our analysis of the Gaussian window function by computing the noise amplitude $\mathcal{N}$ with both the approximate and the exact mode functions, shown in Fig. 6.4. For very small σ, the two can be seen to agree asymptotically, but diverge
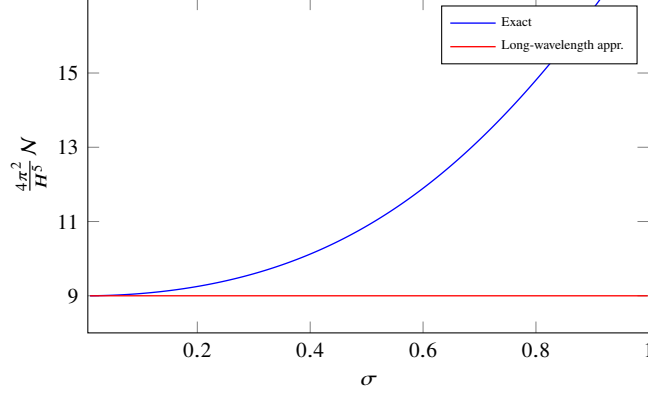
Figure 6.4: Noise amplitude using the Gaussian window function in massless dS using the exact (6.35) and long-wavelength approximate propagator (6.36) as a function of σ with sub-horizon spatial separation $r/R = 0.01$.

for larger values. Apparently, the $\sigma \to 0$ is a crucial ingredient of the standard result for the noise amplitude.

6.4 The noise amplitude and its parameter dependence

As we illustrated for the Gaussian window function, for spatial separations much smaller than the horizon, the noise correlations are localised near $t = t'$. For many smooth window functions, this is a general property, although the noise is not white in a strict sense. Making the interpretation of the distribution being a smoothed delta function, we can attempt to extract a characteristic noise amplitude as described in (6.93), suitable for the stochastic inflationary dynamics. Ultimately, this normalisation is what enters into observables, as described in section 6.1.1. To this end we consider the noise on patches larger than the cutoff scale and define the amplitude $\mathcal{N}$ as

$$\langle \xi(x)\xi(x') \rangle \to \mathcal{N}\delta(t - t')\Theta(1 - \mu r a H), \qquad (6.105)$$

where $\mathcal{N}$ is defined as described in section 6.3.1 through the matching

$$\mathcal{N} := \int \mathrm{d}\tau \langle \xi\xi \rangle(\tau). \qquad (6.106)$$

142
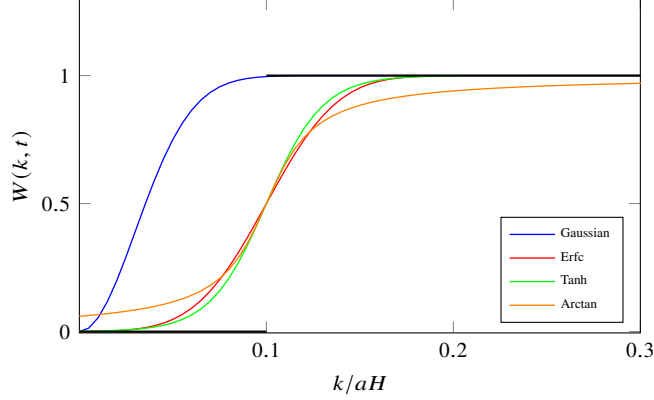
Figure 6.5: Window functions with $\mu = 0.1$ and $\sigma = 0.03$ compared to a step function (black line). For the Gaussian, σ parameterises both the cutoff scale and the sharpness of the transition.

As mentioned in section 6.2.5, when the noise component ξ_ϕ dominates, we may write

$$\langle \xi(x)\xi(x') \rangle \to 9H^2\delta(t - t')\Theta(1 - \mu r a H) \int \mathrm{d}\tau \langle \xi_\phi \xi_\phi \rangle(\tau). \quad (6.107)$$

In addition to the Gaussian window function, we will consider three smoothed step functions, all with the property than in certain limits, they become a strict step function (in contrast to the Gaussian). In particular we consider an error (Erfc) function, which turns out to be particularly tractable analytically. In section 6.4.2 we consider two other sigmoid functions for comparison, namely the Tanh and Arctan functions.

For the smoothed step functions, the parameter μ controls the position of the cutoff, just as for the strict step function (6.65). Small μ means that the cutoff is far in the super-horizon IR region. The parameter σ controls the width of the smoothed step function, and in the limit $\sigma \to 0$, we recover the sharp step function. This is illustrated in Fig. 6.5.

6.4.1 Erfc window function

A smooth approximate step function can be constructed from the (complementary) error function as

$$W(k,t) = \frac{1}{2}\text{erfc}\left[\frac{1}{\sqrt{2}\sigma}\left(\mu - \frac{k}{a_t H}\right)\right]. \qquad (6.108)$$

Inserting first the long-wavelength approximate mode solution (6.36) into (6.82), the noise correlation is found [196] to be

$$\langle \xi(x)\xi(x')\rangle = -\frac{iH^6 e^{M_1 - \frac{\mu^2}{\sigma^2}}}{16\pi^3}\frac{R}{r}\left[\frac{4(1-\epsilon_M)^2}{\sigma^2}\mathcal{T}_{-(1+2\epsilon_M)}\right.$$

$$+\frac{4(1-\epsilon_M)}{\sigma^4}\left(\frac{1}{\text{sech}\,H\tau}\mathcal{T}_{-(3+2\epsilon_M)} - \frac{\mu}{\text{sech}\,\frac{H\tau}{2}}\mathcal{T}_{-(2+2\epsilon_M)}\right)$$

$$\left.+\frac{1}{\sigma^6}\left(\mathcal{T}_{-(5+2\epsilon_M)} - \frac{2\mu}{\text{sech}\,\frac{H\tau}{2}}\mathcal{T}_{-(4+2\epsilon_M)} + \mu^2\mathcal{T}_{-(3+2\epsilon_M)}\right)\right]. \qquad (6.109)$$

Here we have defined

$$\mathcal{T}_{-n} := \Gamma[n]\left(\frac{\sigma^2\,\text{sech}\,H\tau}{2}\right)^{\frac{n}{2}} \qquad (6.110)$$

$$\times \left[\exp\{M_2\}D_{-n}(M_3) - \exp\{M_2^*\}D_{-n}(M_3^*)\right],$$

where $D_{-n}(x)$ is the parabolic cylinder function. The arguments are

$$M_1 := \frac{\beta^2 - r^2}{8\alpha}, \quad M_2 := -\frac{ir\beta}{4\alpha}, \quad M_3 := \frac{\beta - ir}{\sqrt{2\alpha}}, \qquad (6.111)$$

with α as in (6.86) and β defined as

$$R^2 := \frac{1}{a(t)a(t')H^2}, \quad \alpha := \frac{R^2}{\sigma^2\,\text{sech}\,H\tau}, \quad \beta := -\frac{2\mu R}{\sigma^2\,\text{sech}\,\frac{H\tau}{2}}. \qquad (6.112)$$

The cutoff scale μ is intended to be finite, in order to retain some modes in the IR. The sharpness parameter σ can however be arbitrarily small. We are interested in the noise amplitude in the limit of a steep step momentum transition $\sigma \ll 1$. To study this limit, we proceed by eliminating the

spatial dependence by expanding the noise (6.109) to leading order in spatial separation $\mu r/R \ll 1$,

$$
\begin{aligned}
\langle \xi(x)\xi(x') \rangle \simeq \frac{H^6}{8\pi^3} e^{\frac{\mu^2}{\sigma^2}\left(\frac{1}{2}\frac{\operatorname{sech} H\tau}{\operatorname{sech}^2 \frac{H\tau}{2}}-1\right)} \Bigg[& \frac{4(1-\epsilon_M)^2}{\sigma^2}\tilde{\mathcal{T}}_{-(1+2\epsilon_M)} \\
+ \frac{4(1-\epsilon_M)}{\sigma^4}&\left(\frac{1}{\operatorname{sech} H\tau}\tilde{\mathcal{T}}_{-(3+2\epsilon_M)} - \frac{\mu}{\operatorname{sech}\frac{H\tau}{2}}\tilde{\mathcal{T}}_{-(2+2\epsilon_M)}\right) \\
+ \frac{1}{\sigma^6}&\left(\tilde{\mathcal{T}}_{-(5+2\epsilon_M)} - \frac{2\mu}{\operatorname{sech}\frac{H\tau}{2}}\tilde{\mathcal{T}}_{-(4+2\epsilon_M)} + \mu^2\mathcal{T}_{-(3+2\epsilon_M)}\right)\Bigg],
\end{aligned}
$$

(6.113)

where[10]

$$
\tilde{\mathcal{T}}_{-n} := \Gamma[n+1]\left(\frac{\sigma^2 \operatorname{sech} H\tau}{2}\right)^{\frac{n+1}{2}} D_{-n-1}\left(-\sqrt{2}\frac{\mu}{\sigma}\frac{\sqrt{\operatorname{sech} H\tau}}{\operatorname{sech}\frac{H\tau}{2}}\right).
$$

(6.114)

For large negative arguments, this may be further approximated as[11]

$$
\begin{aligned}
\tilde{\mathcal{T}}_{-n} \simeq \sqrt{\pi}e^{\frac{1}{2}\frac{\mu^2}{\sigma^2}\frac{\operatorname{sech} H\tau}{\operatorname{sech}^2 \frac{H\tau}{2}}}\left(\mu\frac{\operatorname{sech} H\tau}{\operatorname{sech}\frac{H\tau}{2}}\right)^n \sigma\sqrt{\operatorname{sech} H\tau} \\
\times\Bigg[1 + \left(\frac{\sigma}{\mu}\right)^2\frac{n(n-1)}{4}\frac{\operatorname{sech}^2 \frac{H\tau}{2}}{\operatorname{sech} H\tau} \\
+ \left(\frac{\sigma}{\mu}\right)^4\frac{n(n-1)(n-2)(n-3)}{32}\frac{\operatorname{sech}^4 \frac{H\tau}{2}}{\operatorname{sech}^2 H\tau} + \dots\Bigg],
\end{aligned}
$$

(6.115)

---

[10]We use the recurrence relation $D_{-n}(x) - \frac{1}{x}D_{-n+1}(x) = -\frac{n}{x}D_{-n-1}(x)$.

[11]The parabolic cylinder functions have the asymptotic behaviour

$$
D_{-n-1}(-|x|)\big|_{x\to\infty} \simeq \frac{\sqrt{2\pi}}{\Gamma[n+1]}e^{x^2/4}|x|^n\left[1 + \frac{n(n-1)}{2x^2} + \frac{n(n-1)(n-2)(n-3)}{8x^4} + \dots\right].
$$

which is then valid for large values of μ/σ. In the limit $\epsilon_M \to 0$, the noise correlator becomes

$$
\begin{aligned}
\langle \xi(x)\xi(x') \rangle \simeq \; & \frac{H^6}{4\pi^2} \frac{1}{2\sqrt{\pi}} \exp\left[\frac{\mu^2}{\sigma^2} \left(\frac{\operatorname{sech} H\tau}{\operatorname{sech} \frac{H\tau}{2}} - 1 \right) \right] \\
& \times \left[-\left(\frac{\mu}{\sigma}\right)^5 \cosh^3 \tfrac{H\tau}{2} \operatorname{sech}^{\frac{11}{2}} H\tau \sinh^2 \tfrac{H\tau}{2} \right. \\
& \left. + \frac{1}{4}\left(\frac{\mu}{\sigma}\right)^3 \cosh \tfrac{H\tau}{2} (7 - 2\cosh H\tau - 3\cosh 2H\tau) \operatorname{sech}^{\frac{9}{2}} H\tau \right. \\
& \left. + \frac{1}{4}\frac{\mu}{\sigma} (31 - 6\cosh H\tau + 16\cosh 2H\tau) \cosh \tfrac{H\tau}{2} \operatorname{sech}^{\frac{7}{2}} H\tau \right].
\end{aligned}
$$
(6.116)

Noise localisation and amplitude. The noise distribution (6.116) is centered around $t = t'$, and becomes more localised for increasing values of the ratio μ/σ, as illustrated in Fig. 6.6. Therefore we may expand in $H\tau$, to find

$$
\begin{aligned}
\langle \xi(x)\xi(x') \rangle \simeq \; & \frac{H^6}{4\pi^2} \frac{1}{2\sqrt{\pi}} e^{\left(\frac{\mu}{\sigma}\right)^2 \left(-\frac{1}{4}(H\tau)^2 + \frac{5}{48}(H\tau)^4 - \frac{61}{1440}(H\tau)^6 + \dots \right)} \\
& \times \left[\frac{\sigma}{\mu}\left(\frac{9}{4} + 8 \right) + \left(\frac{\sigma}{\mu}\right)^3 \left[\frac{1}{2} - \frac{45}{16}(H\tau)^2 \right] \right. \\
& \left. + \left(\frac{\sigma}{\mu}\right)^5 \left[-\frac{1}{4}(H\tau)^2 + \frac{55}{96}(H\tau)^4 \right] + \dots \right].
\end{aligned}
$$
(6.117)

The noise amplitude is then obtained by integrating (6.117) over time separation. It turns out that some contributions are recovered keeping only the first-order term in the exponential, i.e., following a Gaussian

distribution,

$$
\frac{H^6}{4\pi^2} \frac{1}{2\sqrt{\pi}} \int d(H\tau) \exp\left[-\frac{1}{4}\left(\frac{\mu}{\sigma}\right)^2 (H\tau)^2\right]
$$

$$
\times \left[\left(\frac{9}{4} + 8\right)\frac{\mu}{\sigma} - \frac{45}{16}\left(\frac{\sigma}{\mu}\right)^3 (H\tau)^2 + \frac{55}{96}\left(\frac{\sigma}{\mu}\right)^5 (H\tau)^4\right]
$$

$$
= \left(\frac{7}{2} + 8\right)\frac{H^6}{4\pi^2},
$$

(6.118)

while two terms receive corrections from the higher-order terms in the exponential,

$$
\frac{H^6}{4\pi^2} \frac{1}{2\sqrt{\pi}} \int d(H\tau) \left[-\frac{1}{4}\left(\frac{\sigma}{\mu}\right)^5 (H\tau)^4 + \frac{1}{2}\left(\frac{\sigma}{\mu}\right)^3\right]
$$

$$
\times \exp\left[\left(\frac{\mu}{\sigma}\right)^2 \left[-\frac{(H\tau)^2}{4} + \frac{5(H\tau)^4}{48} - \frac{61(H\tau)^6}{1440}\right]\right] \quad (6.119)
$$

$$
\simeq -\frac{5}{2}\frac{H^6}{4\pi^2}.
$$

The sum of contributions in this limit is the standard result $\mathcal{N} = 9H^5/4\pi^2$. This is confirmed using the exact mode solution (6.34) in (6.82), the noise amplitude of which is illustrated in Fig. 6.7. From this we see that the long-wavelength approximate mode solution (6.36) used in (6.109) is accurate for cutoff scales with $\mu \lesssim 0.1$ for small values of σ.

The dependence on σ is quite non-trivial. In particular, both positive and negative correlation regions arise as the ratio μ/σ increases, as can be seen in Fig. 6.6. For illustration we have also included the Gaussian window function result at the same value of σ. While a Gaussian distribution for small σ may be said to be well-approximated by a strict delta-function and a noise amplitude, a substantial amount of information is lost with such a replacement when the distribution is both negative and positive.

Splitting up the noise contributions. It is possible to identify the origin of both negative and positive correlations, and the dominant contribution
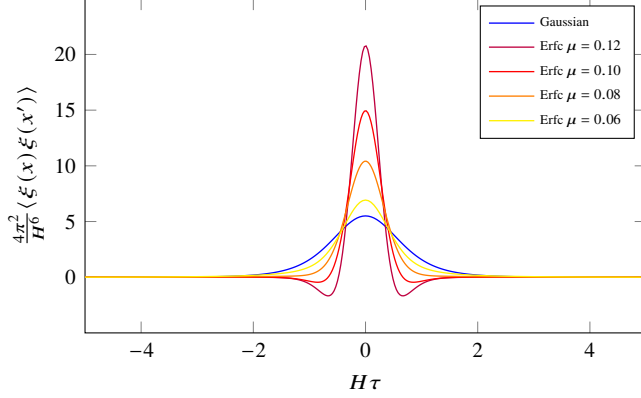
Figure 6.6: Noise correlation as a function of time separation $\tau := t - t'$ for the Erfc and Gaussian window functions with $\sigma = 0.03$, $\epsilon_M = 0$ and $r/R = 0.01$.

to the noise amplitude, by studying the decomposed noise correlations ξ_ϕ, ξ_π of (6.63). In particular, the visible negative correlation regions originate from the $\langle \dot{\xi}_\phi \dot{\xi}_\phi \rangle$ correlator with ξ_ϕ given by (6.57). In (6.88) only the first term contributes in the massless limit, and so

$$
\begin{aligned}
\langle \dot{\xi}_\phi(x)\dot{\xi}_\phi(x') \rangle \simeq{} & \frac{H^6}{8\pi^3} e^{\frac{\mu^2}{\sigma^2}\left(\frac{\operatorname{sech} H\tau}{\operatorname{sech}^2 \frac{H\tau}{2}} - 1 \right)} \left[\frac{\tilde{\mathcal{T}}_{-1}}{\sigma^2} \right. \\
& - \frac{2}{\sigma^4}\left(\frac{1}{\operatorname{sech} H\tau}\tilde{\mathcal{T}}_{-3} - \frac{\mu}{\operatorname{sech}\frac{H\tau}{2}}\tilde{\mathcal{T}}_{-2} \right) \\
& \left. + \frac{1}{\sigma^6}\left(\tilde{\mathcal{T}}_{-5} - \frac{2\mu}{\operatorname{sech}\frac{H\tau}{2}}\tilde{\mathcal{T}}_{-4} + \mu^2\mathcal{T}_{-3} \right) \right].
\end{aligned}
\tag{6.120}
$$

Given the parametric choices made above, the integral of this function over τ vanishes, and so does not contribute to the noise amplitude in our definition. Nevertheless, the function itself is both positive and negative. Similarly, for the cross terms,

$$
\begin{aligned}
& \langle \dot{\xi}_\phi(x)\xi_\phi(x') \rangle + \langle \xi_\phi(x)\dot{\xi}_\phi(x') \rangle \\
& \simeq \frac{H^5}{8\pi^3} e^{\frac{\mu^2}{\sigma^2}\left(\frac{\operatorname{sech} H\tau}{\operatorname{sech}^2 \frac{H\tau}{2}} - 1 \right)} \left[\frac{2}{\sigma^4}\left(\frac{1}{\operatorname{sech} H\tau}\tilde{\mathcal{T}}_{-3} - \frac{\mu}{\operatorname{sech}\frac{H\tau}{2}}\tilde{\mathcal{T}}_{-2} \right) - \frac{2}{\sigma^2}\tilde{\mathcal{T}}_{-1} \right],
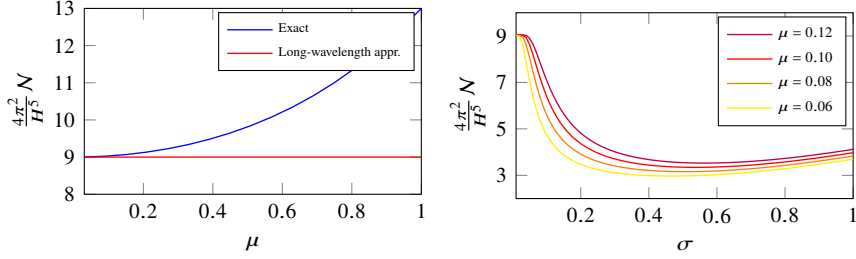\end{aligned}
\tag{6.121}
$$

148

Figure 6.7: Left panel: Noise amplitudes for the Erfc window function with exact (6.35) and long-wavelength approximate (6.36) massless dS propagators as a function of μ, with $\sigma = 0.005$ and spatial separation set to $r/R = 0.01$. Right panel: Noise amplitudes for different μ computed with the exact propagator (6.35) as a function of σ.

which vanish by (6.115). The decomposed noise correlators, including also ξ_π, are all illustrated in Fig. 6.8. From this we can conclude that although the resulting full noise correlator is rather complicated, the main contribution to the noise amplitude comes from the component

$$\langle \xi_\phi \xi_\phi \rangle = -\frac{iH^4}{16\pi^3} \frac{e^{M_1 - \left(\frac{\mu}{\sigma}\right)^2}}{\sigma^2} \frac{R}{r} \mathcal{T}_{-(1+2\epsilon_M)}, \tag{6.122}$$

whose behaviour when expanded near $\tau = 0$ is well-described by a Gaussian-like, positive function

$$\langle \xi_\phi \xi_\phi \rangle \simeq \frac{H^4}{4\pi^2} \frac{\mu^{2\epsilon_M}}{2\sqrt{\pi}} e^{-\frac{1}{4}\left(\frac{\mu}{\sigma}\right)^2 (H\tau)^2} \frac{\mu}{\sigma} \left[1 + \frac{\epsilon_M}{2} \left(\frac{\sigma}{\mu}\right)^2 \right.$$
$$\left. -\frac{1}{8}\left(5 + \frac{3}{2}\left(4 + \left(\frac{\sigma}{\mu}\right)^2\right)\epsilon_M\right)(H\tau)^2 + O\left(\left(\frac{\sigma}{\mu}\right)^4\right) \right]. \tag{6.123}$$

For small values of σ/μ, this is approximated rather well by a delta function. The noise amplitude in this case is then given by

$$\mathcal{N}_{\xi_\phi \xi_\phi} \simeq \frac{H^3}{4\pi^2} \mu^{2\epsilon_M} \left[1 - \left(\frac{\sigma}{\mu}\right)^2 \left(\frac{5}{4} + \epsilon_M\right) + O\left(\left(\frac{\sigma}{\mu}\right)^4\right) \right]$$
$$:= \frac{H^3}{4\pi^2} f(\epsilon_M, \mu, \sigma). \tag{6.124}$$

We now have an explicit example of the correction function f advertised in section 6.1. It involves the mass through ϵ_M as well as the parameters
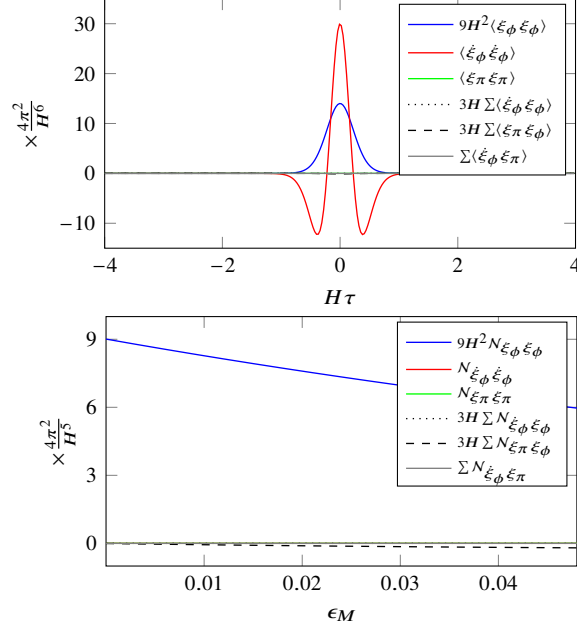
Figure 6.8: Top panel: Noise correlators for the Erfc window function using $\epsilon_M = 0.01$, $r/R = 0.01$ and values $\sigma = 0.005$, $\mu = 0.03$. As the ratio μ/σ increases the visible curves sharpen around $H\tau = 0$ and the visible peaks grow towards $\pm\infty$. Bottom panel: The corresponding noise amplitude contributions as a function of the mass parameter ϵ_M.

of the window function in the combination σ/μ with an overall factor of $\mu^{2\epsilon_M}$.

In the massless case, we get

$$f = 1 - \frac{5}{4}\left(\frac{\sigma}{\mu}\right)^2, \quad \epsilon_M = 0. \tag{6.125}$$

The standard result is then recovered upon taking the step-function limit $\sigma \to 0$. With a massive field, even in that limit we obtain

$$f = \mu^{2\epsilon_M}, \quad \sigma \to 0, \tag{6.126}$$

similar to the Gaussian window function, where the parameter σ also plays the role of μ. For small values of μ and σ, a nonzero mass $\epsilon_M \neq 0$ has the effect of decreasing the noise amplitude, as can be seen in Fig. 6.9. The dependence on mass occurs largely, but not entirely, through the
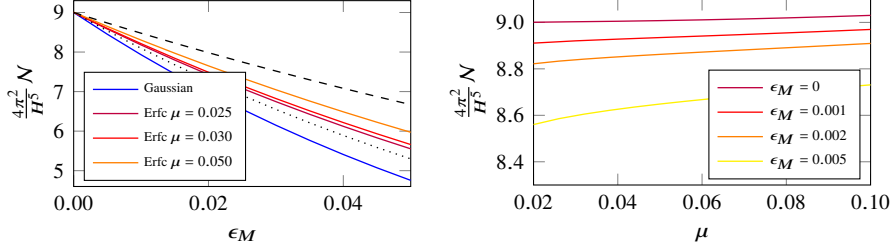
Figure 6.9: Left panel: Noise amplitude for the Gaussian and Erfc window functions using exact mode functions as a function of ϵ_M with $\sigma = 0.005$ and $r/R = 0.01$. Dashed line is $9\mu^{2\epsilon_M}$ with $\mu = 0.05$ and dotted line is $9\sigma^{2\epsilon_M}$. Right panel: Cutoff dependence of the noise amplitude with the Erfc window function for different choices of ϵ_M.

prefactor $\mu^{2\epsilon_M}$ (or $\sigma^{2\epsilon_M}$ in the Gaussian case). Any amplitude smaller than $9H^5/4\pi^2$ can be achieved by making a different choice of parameters.

6.4.2 Alternative smoothened step window functions

To illustrate that these results are fairly generic, we will also consider two other sigmoid functions,

$$W_{\text{tanh}}(k,t) = \frac{1}{2}\Big(1 + \tanh\Big[\frac{1}{\sigma}\Big(\frac{k}{a_t H} - \mu\Big)\Big]\Big), \tag{6.127}$$

$$W_{\text{arct}}(k,t) = \frac{1}{2}\Big(1 + \frac{2}{\pi}\arctan\Big[\frac{\pi}{2\sigma}\Big(\frac{k}{a_t H} - \mu\Big)\Big]\Big), \tag{6.128}$$

for which

$$\tilde{Q}_{\text{tanh}}(k,t) = -H^2 \frac{k}{\sigma a_t H}\operatorname{sech}^2\Big[\frac{1}{\sigma}\Big(\frac{k}{a_t H} - \mu\Big)\Big] \tag{6.129}$$

$$\times \Big(\frac{k}{\sigma a_t H}\tanh\Big[\frac{1}{\sigma}\Big(\frac{k}{a_t H} - \mu\Big)\Big] + 1 - \epsilon_M\Big), \tag{6.130}$$

and

$$\tilde{Q}_{\text{arct}}(k,t) = -H^2 \frac{\frac{k}{\sigma a_t H}}{1 + (\frac{\pi}{2\sigma})^2(\frac{k}{a_t H} - \mu)^2}\left[\frac{(\frac{\pi}{2\sigma})^2 \frac{k}{a_t H}(\frac{k}{a_t H} - \mu)}{1 + (\frac{\pi}{2\sigma})^2(\frac{k}{a_t H} - \mu)^2} + 1 - \epsilon_M\right]. \tag{6.131}$$
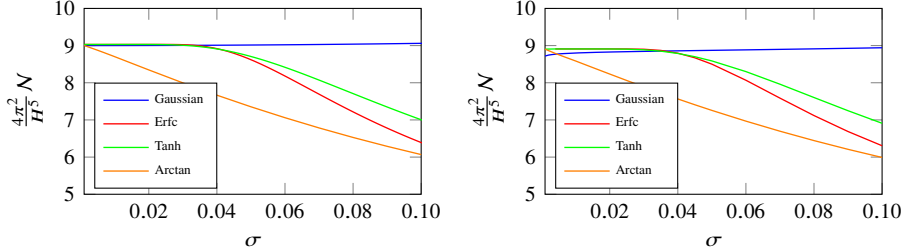
Figure 6.10: Noise amplitude for different window functions using the exact propagator (6.34) as a function of σ with masses $\epsilon_M = 0$ (left panel) and $\epsilon_M = 0.002$ (right panel) using $\mu = 0.1$ and $r/R = 0.01$.

Restricting ourselves to comparing numerical results, the noise amplitude $\mathcal{N}$ for all window functions is shown in Fig. 6.10. We see that in the limit $\sigma \to 0$, they all converge to the standard result, but for finite σ, they diverge from each other. The convergence for the Arctan window function to the value $9H^5/4\pi^2$ is particularly slow, and only agrees in the limit, whereas the other window functions start converging for finite values of $\sigma \simeq 0.04$. This qualitative behaviour persists for other values of μ and ϵ_M (see Fig. 6.11, right panel), and is likely a reflection of the fact that the Arctan window requires smaller values of σ to reach the step function shape compared to the other window functions. As for the Erfc window function, the noise correlations using the other sigmoid window functions also develop negative correlation regions for values $\mu/\sigma \gtrsim 3$, as illustrated in the left panel of Fig 6.11.

6.4.3 Away from dS: leading order in slow-roll

As a final generalisation, we consider the dependence of the slow-roll parameter ϵ_H. Using that the above window functions depend on k through the combination $W(t, k) := W(k/\sigma a(t)H(t))$, it is convenient to make the replacement,

$$\dot{W}_t = -Hz(1 - \epsilon_H)\partial_z W_t(z), \qquad z := \frac{k}{\sigma a(t)H(t)}, \tag{6.132}$$

$$\ddot{W}_t \simeq H^2(1 - \epsilon_H)z\partial_z W(z) + H^2(1 - 2\epsilon_H)z^2\partial_z^2 W(z), \tag{6.133}$$
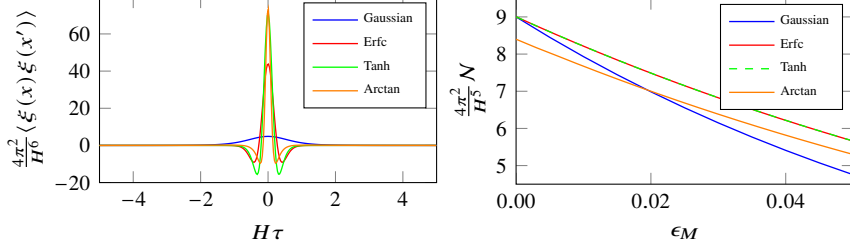
Figure 6.11: Left panel: The noise correlations for different window functions as a function of time separation with $\epsilon_M = 0.01$, $r/R = 0.01$, $\sigma = 0.005$ and in addition $\mu = 0.03$ for the sigmoids. Right panel: The corresponding noise amplitudes as a function of ϵ_M. For small σ the Erfc and Tanh windows integrate to very similar values. Smaller values of σ are required for the Arctan window function to recover the higher noise amplitudes of the other smooth step functions.
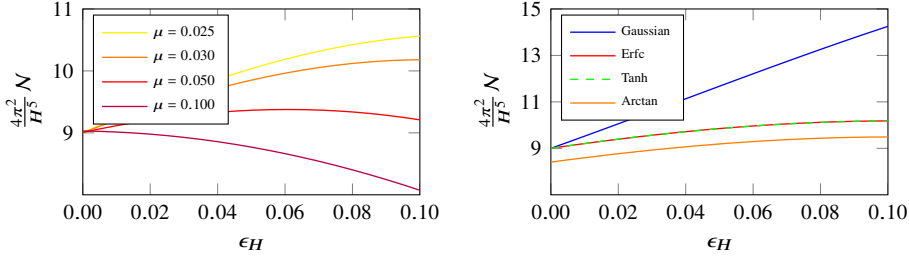

Figure 6.12: Left panel: Noise amplitude with the Erfc window function as a function of the slow-roll parameter ϵ_H for different values of μ. Right panel: For all window functions for a cutoff $\mu = 0.03$. Here $\epsilon_M = 0$, $\sigma = 0.005$ and $r/R = 0.01$. The Arctan window function requires even smaller values of σ to reach the asymptotic value $9H^5/4\pi^2$ in the $\epsilon_H \to 0$ limit.

where the last equality holds to first order in slow-roll. The function $\tilde{Q}_t$ in the correlator (6.82) is then

$$
\begin{aligned}
-\tilde{Q}_t &= \ddot{W}_t + (3 + 2q_\nu)H(1 - \epsilon_H)\dot{W}_t \\
&\simeq H^2(1 - 2\epsilon_H)\left[z^2\partial_z^2 - 2(1 + q_\nu)z\partial_z\right]W(z).
\end{aligned}
\tag{6.134}
$$

The slow-roll parameter ϵ_H appears both in the exact mode functions through the index ν, and through the derivative operators $\tilde{Q}_t$. The rest of the computation proceeds in the same way as before. For instance for the Erfc window with the long-wavelength approximate solution (6.36), the
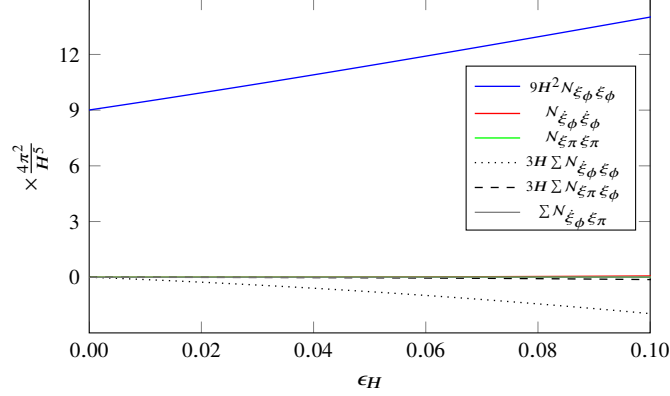
Figure 6.13: Slow-roll dependence of the noise amplitudes of the decomposed correlators (6.63) with the Erfc window function, in the massless case, for $r/R = 0.01$, $\sigma = 0.005$ and $\mu = 0.03$.

normalisation becomes

$$
\begin{aligned}
\mathcal{N}_{\xi_\phi \xi_\phi} &\simeq \frac{H^3}{4\pi^2} \frac{(1 - \epsilon_H)^4}{1 - \frac{1}{2}\epsilon_H} \left(\frac{\mu}{1 - \epsilon_H} \right)^{2\epsilon_M - 2\epsilon_H} \\
&\quad \times \left[1 - \left(\frac{\sigma}{\mu} \right)^2 \left(\frac{5}{4} + \epsilon_M - \epsilon_H \right) + O\left(\left(\frac{\sigma}{\mu} \right)^4 \right) \right] \qquad (6.135) \\
&:= \frac{H^3}{4\pi^2} f(\epsilon_M, \epsilon_H, \mu, \sigma).
\end{aligned}
$$

This is a further generalisation of (6.124), where now also different values of ϵ_H may alter the noise normalisation.

Inserting the exact mode solutions (6.34), we evaluate the noise numerically for the different window functions considered, and the resulting ϵ_H-dependence is shown in Fig. 6.12. We see that, as for ϵ_M, the dependence on the slow-roll parameter is also substantial, non-monotonic and dependent on the choice of both window function and the cutoff parameters. Away from dS, the contributions to the noise amplitude is spread to the other noise correlators in (6.63), as illustrated in Fig. 6.13 for the Erfc window function. With μ, σ small, the correlator $\langle \xi_\phi \xi_\phi \rangle$ remains the leading contributor to the noise amplitude.

6.5 Conclusions

In this chapter, we have revisited the derivation of stochastic inflation from first-principles quantum field theory. We have investigated the conditions under which the standard Langevin dynamics for the super-horizon component of a scalar field may be recovered. The agreement is subject to an appropriate choice of window function separating the UV and IR modes, and applies only in certain limits, which we have identified. We find that one must pay close attention to the magnitude of the off-diagonal components of the influence functional kernel (6.45), and compare these to the diagonal contribution that parametrise the stochastic noise. Only for a steep window function with a separation scale in the far super-horizon limit ($\sigma, \mu \ll 1$) is it consistent to neglect them.

The essential ingredient in achieving the conventional Langevin evolution is to note that noise correlations are exponentially suppressed both outside the spatial horizon $(aH)^{-1}$, and for large time separations ($H\tau > 1$). Inside the spatial horizon, one may then attempt to represent the correlations by a completely local noise amplitude, obtained through matching the integrated power. We showed that this may be a valid prescription in some cases (e.g. with a Gaussian window function), but that for others, important information may be lost (e.g. with the Erfc window function).

Our analysis confirms that in the limits $\epsilon_M, \epsilon_H \to 0$, and $\mu, \sigma \to 0$, the standard noise amplitude $9H^5/4\pi^2$ is recovered, at least asymptotically. This corresponds to an IR field which is essentially the $k \simeq 0$ homogeneous mode. However, as soon as these parameters take on finite values, the noise amplitude is modulated by a function f, which in principle can assume any value. We provided a number of examples of what such a function f could look like, for a selection of window functions. We also showed numerically, that the long-wavelength approximation to the UV mode functions only matches the exact mode-function results for very small μ and σ.

Because the stochastic formalism relies on a sequence of approximations and assumptions, it would be interesting to further map out its region of validity by comparing to other approaches. These include matching to

perturbative and resummed analytic results [74, 163, 172, 175], and numerical evaluation within (generalisations of) the target stochastic model [170]. One may also consider a full numerical implementation of the quantum dynamics, in a semi-dS background, similar to what was done in Ref. [75].

To summarise, stochastic inflation as a formalism remains a very elegant and powerful way of describing the dynamics of cosmological scalar fields at very long wavelengths. For it also to describe the dynamics of super-horizon modes in general ($k \neq 0$), the properties of the window function, the field mass and slow-roll parameters come into play. In particular, they enter in the explicit computation of the noise amplitude, which normalises observables, including the dynamical mass generated.

7 Probing the gauge dependence in a 2PI truncation of SU(2)-Higgs theory

Gauge symmetry in truncations of 2PI effective actions is guaranteed only up to the order of truncation. In this chapter we revisit the 2PI formulation for gauge theories in a two-loop truncation of SU(2)-Higgs theory. We study the convergence properties of real-time observables by comparing with classical-statistical evolution in the regime of high occupation numbers. This work is currently in progress, and we present some preliminary numerical results at leading order.

7.1 Introduction

The two-particle-irreducible (2PI) formalism [35] is an effective tool to study quantum field dynamics outside the regime of weak coupling or far from thermodynamic equilibrium. It has been used in numerous applications for scalar and fermionic theories, with topics ranging from early-Universe phenomena [75, 117, 118, 202, 203] to second-order phase transitions [204–207] to high-temperature physics [132, 208–213] and heavy-ion collisions [24, 25, 27, 28, 214] and condensed matter systems [215, 216]. See e.g. [29–31] for reviews.

The application of the 2PI framework to gauge theories has been delayed due to complications concerning gauge non-invariance in truncations and consistent renormalisation. However, significant progress in regards to renormalisation was made in [135–137], in which the authors shed light on the gauge symmetry properties of the 2PI formulation of QED. In particular, they showed that 2PI truncations satisfy identities that generalise the standard 1PI Ward identities. These 2PI Ward identities allow for additional counterterms to be added compared to perturbation theory and thereby enable consistent renormalisation of the truncated theory [135]. In [136] it was in addition shown how to construct 2PI truncations that systematically respect the corresponding Ward identities. However, even if the vertex functions of a given 2PI approximation can

be renormalised to exhibit the correct symmetry properties, this does not ensure that the related physical observables are gauge invariant. The gauge-dependency of (would-be) observable quantities is the topic of this work.

In [36, 37] it was shown that the gauge-dependent contributions enter at the earliest at the order following the order of truncation. For instance in an L-loop expansion, they are expected to arise at order g^{2L}, where g is the coupling constant, and are therefore parametrically suppressed. Since 2PI truncations have been observed to display good convergence properties in non-gauge theories [124, 217, 218], this suggest that (renormalised) 2PI truncations of gauge theories may also demonstrate proper convergence properties in the regime of weak coupling. Quantitative studies of this are however scarce, although see [143, 219, 220]. In [143] the thermodynamic pressure of a two-loop 2PI truncation of QED was studied and compared with perturbation theory. Their results showed that, in covariant gauge, the coefficients of the gauge-fixing parameter dependent terms do not spoil the convergence properties, and that the gauge dependence remain small ($\lesssim 1.5\%$) compared to perturbation theory for the choices of parameters considered. It was also observed that the dependence, comparable to that of the renormalisation scale, appears to decrease with the value of the gauge-fixing parameter and that Landau gauge minimised the dependence relative to the perturbative results. The authors of [219] studied the phase diagram of a three-loop 2PI SU(2)-Higgs theory in three-dimensional Euclidean space. Their results indicated similar qualitative features of a critical endpoint between the first order and cross-over regions compared to lattice data, although the quantitative discrepancy for the location of the critical endpoint, as well as the dependence on the gauge-fixing parameter, appeared to be quite significant.

Suggestions on how to deal with the breaking of gauge-invariance in truncated 2PI resummation schemes have been proposed in [141, 208, 220–222]. These proposals involve introducing additional approximations to the truncated diagram expansion [208, 221, 222] or exploit the freedom in the choice of field reparametrisations to make the truncated

action fulfil certain properties [141]. Unfortunately it is unclear how these approaches can be systematically generalised and so far no field reparametrisations which ensure that the propagator satisfies the corresponding BRST symmetries have been identified. Another strategy proposed in [220] is based on a perturbative re-expansion of the resummed propagators, for which gauge-independent terms in the thermodynamic pressure can be isolated at different perturbative orders. The procedure did not lead to an improvement in gauge-fixing parameter dependence, as it still appeared at next-after-truncation order, although the dependence appeared to be controlled.

In this work we probe the gauge dependence in the two-loop 2PI formulation of SU(2)-Higgs theory by comparison with classical-statistical simulations in the regime of high occupation numbers. We work in temporal gauge, and while the original proofs of the gauge non-invariance in [36, 37] used a Faddeev-Popov gauge-fixing procedure, we expect them to apply also for this choice of gauge. The choice of temporal gauge does not allow for variation of a gauge-fixing parameter, but it offers simplification in the 2PI lattice formulation by reducing the degrees of freedom of the system.

The chapter is organised as follows. In section 7.2 we describe the model at hand and present the continuum 2PI evolution equations in section 7.3. The numerical implementation and relevant observables are discussed in section 7.4. The initial conditions are described in section 7.4.2 and in section 7.5 we show some preliminary results at leading order. We conclude in section 7.6. Technical details are presented in the appendices.

7.2 The SU(2)-Higgs model at two-loop order

We study the SU(2)-Higgs model with classical action

$$S = -\int_x \left[\tfrac{1}{4} F^a_{\mu\nu} F^{\mu\nu}_a + (D_\mu \Phi)^\dagger (D^\mu \Phi) + m^2 \Phi^\dagger \Phi + \lambda (\Phi^\dagger \Phi)^2 \right], \quad (7.1)$$

where the covariant derivative is $D_\mu = \partial_\mu - igt^a A^a_\mu$ with gauge coupling g and generators $t^a = \sigma^a/2$ given in terms of the Pauli matrices σ^a. The

field strength tensor reads $F^a_{\mu\nu} = \partial_\mu A^a_\nu - \partial_\nu A^a_\mu + g\epsilon^{abc} A^b_\mu A^c_\nu$ where ϵ^{abc} is the Levi-Cevita tensor and our metric is $\eta_{\mu\nu} = \text{diag}(-1, 1, 1, 1)$. The Higgs doublet Φ is taken to have vanishing expectation value.

The 2PI effective action is given by

$$\Gamma[A, \Phi, D, G] = S[A, \Phi, D, G] + \frac{i}{2} \text{Tr} \log D^{-1} + \frac{i}{2} \text{Tr} D_0^{-1} D$$
$$+ \frac{i}{2} \text{Tr} \log G^{-1} + \frac{i}{2} \text{Tr} G_0^{-1} G + \Gamma_2[A, \Phi, D, G], \tag{7.2}$$

where the free inverse gauge and Higgs propagators are

$$iD^{ab}_{\mu\nu}(x, y)^{-1} = [g_{\mu\nu} \Box_x - \partial^x_\mu \partial^x_\nu] \delta^{ab} \delta^{(4)}_C(x - y),$$
$$iG(x, y)^{-1} = [\Box_x - m^2] \delta^{(4)}_C(x - y), \tag{7.3}$$

and the subscript C denote Keldysh time-ordering. At two-loop order, the 2PI generating functional is given by

$$\Gamma_2 = 2 \; \bigcirc\!\!\bigcirc \; + \; \text{\{diagram\}} \; + \; \frac{1}{8} \; \text{\{diagram\}} \; + \; \frac{1}{2} \; \text{\{diagram\}} \; + \; \frac{1}{12} \; \text{\{diagram\}}. \tag{7.4}$$

The equations of motion for the dressed propagators read

$$D^{ab-1}_{\mu\nu} = D^{ab-1}_{0\mu\nu} - \Pi^{ab}_{\mu\nu}, \quad \Pi^{ab}_{\mu\nu} := 2i \frac{\delta \Gamma_2}{\delta D^{\mu\nu}_{ab}}, \tag{7.5}$$

$$G^{-1} = G_0^{-1} - \Sigma, \quad \Sigma := 2i \frac{\delta \Gamma_2}{\delta G}, \tag{7.6}$$

where $\Pi^{ab}_{\mu\nu}$ and Σ are the gauge and scalar self-energies respectively. In temporal gauge, $A_0 = 0$, the temporal components of the gauge propagator vanish, $D^{ab}_{00} = D^{ab}_{0i} = 0$. Assuming colour and spatial isotropy, the gauge field propagator can be decomposed into transverse and longitudinal components in momentum space,

$$D^{ab}_{ij}(t, t'; \mathbf{p}) = \delta^{ab} \left[P^\perp_{ij}(\mathbf{p}) D^\perp(t, t'; |\mathbf{p}|) + P^\parallel_{ij}(\mathbf{p}) D^\parallel(t, t'; |\mathbf{p}|) \right], \tag{7.7}$$

using the projection operators

$$P^\perp_{ij}(\mathbf{p}) := \delta_{ij} - \frac{p_i p_j}{|\mathbf{p}|^2}, \quad P^\parallel_{ij}(\mathbf{p}) := \frac{p_i p_j}{|\mathbf{p}|^2}. \tag{7.8}$$

The transverse and longitudinal parts are then obtained by

$$D^\perp(|\mathbf{p}|) = \frac{1}{d-1}P_{ij}^\perp(\mathbf{p})D^{aaij}(\mathbf{p}), \quad D^\|(|\mathbf{p}|) = P_{ij}^\|(\mathbf{p})D^{aaij}(\mathbf{p}), \quad (7.9)$$

where $d = 3$ is the spatial dimension. The propagators can be further decomposed in terms of statistical and spectral components,

$$D^\alpha(t, t'; |\mathbf{p}|) = D_{(F)}^\alpha(t, t'; |\mathbf{p}|) - \frac{i}{2}D_{(\rho)}^\alpha(t, t'; |\mathbf{p}|)\text{sign}_C(t - t'), \quad (7.10)$$

$$G(t, t'; |\mathbf{p}|) = G_{(F)}(t, t'; |\mathbf{p}|) - \frac{i}{2}G_{(\rho)}(t, t'; |\mathbf{p}|)\text{sign}_C(t - t'), \quad (7.11)$$

where $\alpha = \perp, \|$ and $G(t, t'; \mathbf{p}) \equiv G(t, t'; |\mathbf{p}|)$.

7.3 Evolution equations

The equation of motions (7.5) and (7.6) can be written as partial integro-differential equations, and by projecting the statistical and spectral gauge propagators into their transverse and longitudinal components, we obtain six (effectively scalar) evolution equations. The local parts of the self-energies are absorbed into effective mass terms, i.e. by writing

$$\Pi_{ij}^{ab}(t, t'; \mathbf{p}) = -i\Pi_{ij\text{loc}}^{ab}(t, t; \mathbf{p}) + \Pi_{ij\text{nl}}^{ab}(t, t'; \mathbf{p}), \quad (7.12)$$

and similarly for the scalar self-energy, we define the effective masses as

$$M_D^{2ab}(t; \mathbf{p}) := \Pi_{ij\text{loc}}^{ab}(t, t; \mathbf{p}), \quad M_G^2(t; \mathbf{p}) := m^2 + \Sigma_{\text{loc}}(t, t; \mathbf{p}). \quad (7.13)$$

We obtain for the transverse propagators,

$$\left[\delta^{ab}(\partial_t^2 + |\mathbf{p}|^2) + M_D^{\perp 2ab}(t; \mathbf{p})\right]D_{(F)}^\perp(t, t'; |\mathbf{p}|)$$

$$= \int_0^{t'} dt''\Pi_{(F)}^{\perp ab}(t, t''; |\mathbf{p}|)D_{(\rho)}^\perp(t'', t'; |\mathbf{p}|)$$

$$- \int_0^t dt''\Pi_{(\rho)}^{\perp ab}(t, t''; |\mathbf{p}|)D_{(F)}^\perp(t'', t'; |\mathbf{p}|), \quad (7.14)$$

$$\left[\delta^{ab}(\partial_t^2 + |\mathbf{p}|^2) + M_D^{\perp 2ab}(t; \mathbf{p})\right]D_{(\rho)}^\perp(t, t'; |\mathbf{p}|)$$

$$= -\int_0^t dt''\Pi_{(\rho)}^{\perp ab}(t, t''; |\mathbf{p}|)D_{(\rho)}^\perp(t'', t'; |\mathbf{p}|), \quad (7.15)$$

and for the longitudinal,

$$\left[\delta^{ab}\partial_t^2 + M_D^{\|2ab}(t;\mathbf{p})\right] D_{(F)}^{\|}(t,t';|\mathbf{p}|)$$

$$= \int_0^{t'} \mathrm{d}t'' \Pi_{(F)}^{\|ab}(t,t'';|\mathbf{p}|) D_{(\rho)}^{\|}(t'',t';|\mathbf{p}|)$$

$$- \int_0^{t} \mathrm{d}t'' \Pi_{(\rho)}^{\|ab}(t,t'';|\mathbf{p}|) D_{(F)}^{\|}(t'',t';|\mathbf{p}|), \qquad (7.16)$$

$$\left[\delta^{ab}\partial_t^2 + M_D^{\|2ab}(t;\mathbf{p})\right] D_{(\rho)}^{\|}(t,t';|\mathbf{p}|)$$

$$= -\int_0^{t} \mathrm{d}t'' \Pi_{(\rho)}^{\|ab}(t,t'';|\mathbf{p}|) D_{(\rho)}^{\|}(t'',t';|\mathbf{p}|). \qquad (7.17)$$

The scalar equations of motion are given by

$$\left[\partial_t^2 + |\mathbf{p}|^2 + M_G^2(t;\mathbf{p})\right] G_{(F)}(t,t';|\mathbf{p}|)$$

$$= \int_0^{t'} \mathrm{d}t'' \Sigma_{(F)}(t,t'';|\mathbf{p}|) G_{(\rho)}(t'',t';|\mathbf{p}|)$$

$$- \int_0^{t} \mathrm{d}t'' \Sigma_{(\rho)}(t,t'';\mathbf{p}) G_{(F)}(t'',t';|\mathbf{p}|), \qquad (7.18)$$

$$\left[\partial_t^2 + |\mathbf{p}|^2 + M_G^2(t;\mathbf{p})\right] G_{(\rho)}(t,t';|\mathbf{p}|)$$

$$= -\int_0^{t} \mathrm{d}t'' \Sigma_{(\rho)}(t,t'';|\mathbf{p}|) G_{(\rho)}(t'',t';|\mathbf{p}|). \qquad (7.19)$$

The effective masses are obtained as

$$M_D^{\perp 2ab}(t;\mathbf{p}) = g^2 \delta^{ab} \int_\mathbf{q} \left\{ G_{(F)} + 2\left[(d-2)D_{(F)}^{\perp} + D_{(F)}^{\|}\right.\right.$$

$$\left.\left. + \frac{1}{d-1}\left(1 - \frac{(\mathbf{q}\cdot\mathbf{p})^2}{|\mathbf{q}|^2|\mathbf{p}|^2}\right)\left(D_{(F)}^{\perp} - D_{(F)}^{\|}\right)\right]\right\}, \qquad (7.20)$$

$$M_D^{\|2ab}(t;\mathbf{p}) = g^2 \delta^{ab} \int_\mathbf{q} \left\{ G_{(F)} + 2\left[(d-2)D_{(F)}^{\perp} + D_{(F)}^{\|}\right.\right.$$

$$\left.\left. + \frac{(\mathbf{q}\cdot\mathbf{p})^2}{|\mathbf{q}|^2|\mathbf{p}|^2}\left(D_{(F)}^{\perp} - D_{(F)}^{\|}\right)\right]\right\}, \qquad (7.21)$$

$$M_G^2(t;\mathbf{p}) = m^2 + \int_\mathbf{q} \left\{ g^2 \left[(d-1)D_{(F)}^{\perp} + D_{(F)}^{\|}\right] + 8\lambda G_{(F)}\right\}, \quad (7.22)$$

where we have suppressed the propagator arguments $(t, t; |\mathbf{q}|)$ and used the projection operator relations $g^i{}_k P_i^{\perp k}(\mathbf{p}) = d - 1$ and

$$
\begin{aligned}
P_k^{\perp i}(\mathbf{q}) P_i^{\perp k}(\mathbf{p}) &= d - 2 + \frac{(\mathbf{q} \cdot \mathbf{p})^2}{|\mathbf{q}|^2 |\mathbf{p}|^2}, \\
P_k^{\parallel i}(\mathbf{q}) P_i^{\perp k}(\mathbf{p}) &= 1 - \frac{(\mathbf{q} \cdot \mathbf{p})^2}{|\mathbf{q}|^2 |\mathbf{p}|^2}.
\end{aligned}
\tag{7.23}
$$

For the (non-local) self-energies, we obtain for the pure gauge sunset diagram contribution in (7.4),

$$
\begin{aligned}
\Pi_{(D^3)(\chi)}^{\perp ab}(t, t'; |\mathbf{p}|) = &-\frac{g^2}{d-1} \delta^{ab} \int_{\mathbf{q}} \sum_{\alpha\beta} N_{\mathrm{T}}^{\alpha\beta}(|\mathbf{p}|, |\mathbf{q}|) \\
&\times [D^\alpha(t, t'; |\mathbf{p} - \mathbf{q}|) D^\beta(t, t'; |\mathbf{q}|)]_{(\chi)},
\end{aligned}
\tag{7.24}
$$

$$
\begin{aligned}
\Pi_{(D^3)(\chi)}^{\parallel ab}(t, t'; |\mathbf{p}|) = &-g^2 \delta^{ab} \int_{\mathbf{q}} \sum_{\alpha\beta} N_{\mathrm{L}}^{\alpha\beta}(|\mathbf{p}|, |\mathbf{q}|) \\
&\times [D^\alpha(t, t'; |\mathbf{p} - \mathbf{q}|) D^\beta(t, t'; |\mathbf{q}|)]_{(\chi)},
\end{aligned}
\tag{7.25}
$$

where $\alpha, \beta = \perp, \parallel$ and the expressions for the coefficients N_{T} and N_{L} are gathered in Appendix 7.A.3. The bracket $[\cdot]_{(\chi)}$ is defined for a product of propagators $G(t, t'; |\mathbf{p}|) \equiv G(x)$ as

$$
\begin{aligned}
[G_1(x) G_2(x)]_{(F)} &:= G_{1(F)}(x) G_{2(F)}(x) - \tfrac{1}{4} G_{1(\rho)}(x) G_{2(\rho)}(x), \\
[G_1(x) G_2(x)]_{(\rho)} &:= G_{1(F)}(x) G_{2(\rho)}(x) + G_{1(\rho)}(x) G_{2(F)}(x).
\end{aligned}
\tag{7.26}
$$

Similarly for the mixed-field sunset diagram in (7.4), we obtain

$$
\begin{aligned}
\Pi_{(G^2D)}^{\perp ab(\chi)}(t, t'; |\mathbf{p}|) = &-\frac{g^2}{2(d-1)} \delta^{ab} \int_{\mathbf{q}} 4 \left(|\mathbf{q}|^2 - \frac{(\mathbf{p} \cdot \mathbf{q})^2}{|\mathbf{p}|^2} \right) \\
&\times [G(t, t'; |\mathbf{p} - \mathbf{q}|) G(t, t'; |\mathbf{q}|)]_{(\chi)},
\end{aligned}
\tag{7.27}
$$

$$
\begin{aligned}
\Pi_{(G^2D)}^{\parallel ab(\chi)}(t, t'; |\mathbf{p}|) = &-\frac{g^2}{2} \delta^{ab} \int_{\mathbf{q}} \left(|\mathbf{p}|^2 - 4\mathbf{p} \cdot \mathbf{q} + 4 \frac{(\mathbf{p} \cdot \mathbf{q})^2}{|\mathbf{p}|^2} \right) \\
&\times [G(t, t'; |\mathbf{p} - \mathbf{q}|) G(t, t'; |\mathbf{q}|)]_{(\chi)}.
\end{aligned}
\tag{7.28}
$$

The Higgs self-energy is given by

$$\Sigma_{(F)}(t, t'; |\mathbf{p}|) = -\frac{g^2}{2} \int_{\mathbf{q}} \left[\tilde{D}(t, t'; |\mathbf{p} - \mathbf{q}|) G(t, t'; |\mathbf{q}|) \right]_{(F)},$$

$$\Sigma_{(\rho)}(t, t'; |\mathbf{p}|) = -\frac{g^2}{2} \int_{\mathbf{q}} \left[\tilde{D}(t, t'; |\mathbf{p} - \mathbf{q}|) G(t, t'; |\mathbf{q}|) \right]_{(\rho)}.$$

(7.29)

where

$$\tilde{D}_{(\chi)}(t, t'; |\mathbf{p} - \mathbf{q}|) := c^{\perp}(\mathbf{p}, \mathbf{q}) D_{(\chi)}^{\perp}(t, t'; |\mathbf{p} - \mathbf{q}|)$$
$$+ c^{\parallel}(\mathbf{p}, \mathbf{q}) D_{(\chi)}^{\parallel}(t, t'; |\mathbf{p} - \mathbf{q}|),$$

(7.30)

with $\chi = F, \rho$ denoting the statistical or spectral propagator and the coefficients $c^{\perp}, c^{\parallel}$ are gathered in Appendix 7.A.3.

7.4 Numerical implementation

The starting point for comparisons between the 2PI evolution and the classical-statistical dynamics is the covariant lattice action formulation of the continuum action (7.1),

$$S_{\mathrm{L}} = \sum_{x,t} a_t a_s^3 \left[\frac{2}{(g a_t a_s)^2} \sum_i \mathrm{Tr}[2 - U_{0i}] - \frac{2}{(g a_s^2)^2} \sum_{i<j} \mathrm{Tr}[2 - U_{ij}] \right.$$
$$\left. + (D_0 \Phi_x)^{\dagger} D_0 \Phi_x - \sum_i (D_i \Phi_x)^{\dagger} D_i \Phi_x - V(|\Phi_x|) \right],$$

(7.31)

where the plaquette is defined as $U_{x,\mu\nu} := U_{x,\mu} U_{x+\mu,\nu} U_{x+\nu,\mu}^{\dagger} U_{x,\nu}^{\dagger}$, the potential is $V(|\Phi_x|) = m^2 \Phi_x^{\dagger} \Phi_x + \lambda (\Phi_x^{\dagger} \Phi_x)^2$ and we employ forward covariant derivatives defined in (7.45). The the link $U_{x,\mu}$ bonds neighbouring lattice sites and has the continuum form $U_{x,\mu} = \exp\left[-i g a_{\mu} A_{x,\mu}^a t^a\right]$.

In a two-loop expansion, the residual gauge dependence enter parametrically at the earliest at order g^4. If the gauge-dependence is controlled then the error it presents should also be suppressed as such. Naively discretising the continuum action (7.1) corresponds to expanding the link $U_{x,\mu}$ in the action (7.31) to $O(g)$. To compute observables in our two-loop truncation correctly up to order $O(g^3)$, it is necessary to expand the link

$U_{x,\mu}$ to $O(g^2)$. That is, the action (7.31) should be expanded to $O(a^2)$ in lattice spacing. The new vertices of the expanded action allows for new (lattice artefact) two-loop diagrams. However, as a first step, we find it instructive to consider the diagrams resulting from the $O(g)$ expansion of the link, which corresponds to the naively discretised continuum action (7.1). This allows us to confirm whether the gauge-dependence is controlled at this order.

Finally, we comment on renormalisation. While rigorous renormalisation schemes have been developed for Abelian theories in [135–137], their generalisation to non-Abelian theories have not yet been established. Since we are comparing classical dynamics, consistent renormalisation is not necessary for our purposes, and as a result we effectively bypass this issue.

7.4.1 Observables

Our goal is to study how observable quantities of the 2PI truncated action fares in comparisons with the gauge-invariant formulation of (7.31). Observables such as energy density, pressure, and number density are relevant, but a more direct quantity to consider is the Higgs equal-time propagator $G_{(F)}(t, t; |\mathbf{x} - \mathbf{y}|)$. Since it is both gauge invariant and enter into other observables, this quantity will be the main focus in this work.

In classical-statistical simulations, the anti-commutator of the Heisenberg operator fields Φ in (7.1) reduces to an average of product of classical fields,

$$G_{(F)}(x, y) = \tfrac{1}{2}\langle\{\Phi_x, \Phi_y\}\rangle \to \langle\Phi_x\Phi_y\rangle_{\mathrm{cl}}, \quad n_{\mathbf{p}} \gg 1, \tag{7.32}$$

where $\langle\cdot\rangle_{\mathrm{cl}}$ denotes the statistical average. The above relation applies analogously to the statistical gauge propagator $D^{ab}_{(F)ij}(x, y)$.

To extract the physical gauge field from the covariant lattice formulation (7.31), one may use that for small lattice spacings the gauge field can be defined as

$$A_i^a(x) := \frac{1}{2a_s g} \mathrm{Tr}\Big[i\sigma^a(U_{x,i} - U_{x,i}^\dagger)\Big]. \tag{7.33}$$

Since the physical gauge field is centred between lattice sites, i.e. at $x + \hat{\imath}/2$, we may define its Fourier transform as

$$A_i^a(\tilde{p}) = \sum_p e^{-i\mathbf{p}\cdot(\mathbf{x}+\hat{\imath}/2)} A_i^a(x) = e^{-i\mathbf{p}\cdot\hat{\imath}/2} \sum_p e^{-i\mathbf{p}\cdot\mathbf{x}} A_i^a(x), \qquad (7.34)$$

where $\mathbf{x} = a_s \mathbf{n}$ is the coordinate vector and $\mathbf{p} := 2\pi\tilde{\mathbf{n}}/(a_s N)$ is the lattice momentum where $\tilde{\mathbf{n}} = [\tilde{n}_1, \tilde{n}_2, \tilde{n}_3]$ denotes the reciprocal lattice, and $\tilde{\mathbf{n}} \cdot \mathbf{n} = \sum_i \tilde{n}_i n_i$ where $\tilde{n}_i = 0, \dots, \frac{N}{2} - 1, -\frac{N}{2}, \dots, -1$. The classical-statistical gauge field propagator is defined as

$$D_{ij}^{aa}(t, t; \tilde{p}) = \frac{1}{d_a V} \delta^{ab} \langle A_i^a(t, \tilde{p}) A_j^b(t, \tilde{p})^* \rangle_{\mathrm{cl}}, \qquad (7.35)$$

where we average over the spatial lattice volume V and dimension of the adjoint representation $d_a := N^2 - 1 = 3$. With the extra phase factor in (7.34), the physical momentum corresponds to

$$\tilde{p}_i = \frac{2}{a_s} \sin\left(\frac{\pi\tilde{n}_i}{N}\right). \qquad (7.36)$$

Note that the physical momentum for a field defined at x (rather than $x + \hat{\imath}/2$) using the forward derivative is $\tilde{p}_i = -i(\exp[2\pi\tilde{n}_i/N] - 1)/a_s$, which is the complex conjugate of the physical momentum obtained using the backward derivative. The transverse and longitudinal projection operators (7.8) are then defined in terms of (7.36) as

$$P^{\perp ij}(\tilde{p}) := \delta^{ij} - \frac{\tilde{p}^i \tilde{p}^j}{\tilde{p}^2}, \quad P^{\parallel ij}(\tilde{p}) := \frac{\tilde{p}^i \tilde{p}^j}{\tilde{p}^2}, \qquad (7.37)$$

where $\tilde{p}^2 = \sum_i [2 - 2\cos(2\pi\tilde{n}_i/N)]$. These operators are then used to project the gauge field propagator (7.35) into its transverse and longitudinal components,

$$D^{\perp}(t, t; \tilde{p}) := \frac{1}{d-1} P^{\perp ij} D_{ij}^{aa}(t, t; \tilde{p}), \qquad (7.38)$$

$$D^{\parallel}(t, t; \tilde{p}) := P^{\parallel ij} D_{ij}^{aa}(t, t; \tilde{p}). \qquad (7.39)$$

7.4.2 Initial conditions

We assume Gaussian initial conditions for the Higgs mode functions, although the Gauss constraint (see (7.49)) causes a small departure from

166

a strictly Gaussian distribution of the initial density matrix. In addition, we specialise to vacuum initial conditions $n_{\mathbf{p}} = 0$ at $t = 0$. The 2PI propagators are initialised using the initial averaged values of the classical-statistical propagators. For the scalar field, the initial conditions are

$$G_{(F)}(t, t'; |\mathbf{p}|)\big|_{t=t'=0} = \frac{1}{V}\langle \Phi_{\mathbf{p}}^{\dagger}(t)\Phi_{\mathbf{p}}(t')\rangle_{\mathrm{cl}}\big|_{t=t'=0},$$

$$\partial_t G_{(F)}(t, t'; |\mathbf{p}|)\big|_{t=t'=0} = \frac{1}{V}\langle \Pi_{\mathbf{p}}^{\dagger}(t)\Phi_{\mathbf{p}}(t')\rangle_{\mathrm{cl}}\big|_{t=t'=0}, \tag{7.40}$$

$$\partial_t \partial_{t'} G_{(F)}(t, t'; |\mathbf{p}|)\big|_{t=t'=0} = \frac{1}{V}\langle \Pi_{\mathbf{p}}^{\dagger}(t)\Pi_{\mathbf{p}}(t')\rangle_{\mathrm{cl}}\big|_{t=t'=0},$$

where $|\mathbf{p}| = |\tilde{p}|$. The initial Higgs field and conjugate momentum are initialised to satisfy the (global) Gauss constraint (7.61) assuming vanishing gauge fields at initial time, i.e. $A_{x,i}(t = 0) = 0$. The details of the initialisation for the classical-statistical simulation are collected in Appendix 7.A.2. The initial conditions for the spectral propagator are set by the canonical commutation relations

$$G_{(\rho)}(t, t', |\mathbf{p}|)\big|_{t=t'=0} = 0, \quad \partial_t G_{(\rho)}(t, t', |\mathbf{p}|)\big|_{t=t'=0} = 1. \tag{7.41}$$

The transverse and longitudinal propagators of the 2PI evolution are initialised at the first time step $t = a_t$ using

$$E_{x,i}^a(t = 0) = \partial_t A_{x,i}^a, \tag{7.42}$$

where the electric fields $E_{x,i}^a := U_{x+0,i}U_{x,i}^{\dagger}/a_t a_s g$ are initialised to satisfy the Gauss constraint (7.54). The gauge field propagator is then initialised as

$$D_{(F)ij}^{aa}(t, t'; |\mathbf{p}|)\bigg|_{t=t'=a_t} = \frac{a_t^2}{d_A V}\delta^{ab}\left\langle E_i^a(t, \tilde{p})E_j^b(t', \tilde{p})^*\right\rangle_{\mathrm{cl}}\bigg|_{t=t'=0}, \tag{7.43}$$

where its statistical transverse and longitudinal components $D_{(F)}^{\perp}(t, t'; |\mathbf{p}|)$ and $D_{(F)}^{\parallel}(t, t'; |\mathbf{p}|)$ are obtained by acting with the projection operators (7.38) and (7.39) on (7.43). The initial conditions for the spectral propagators $D_{(\rho)}^{\perp}(t, t'; |\mathbf{p}|)$ and $D_{(\rho)}^{\parallel}(t, t'; |\mathbf{p}|)$ are fixed by the same commutation relations as for the scalar statistical propagator in (7.41) at $t = t' = a_t$.
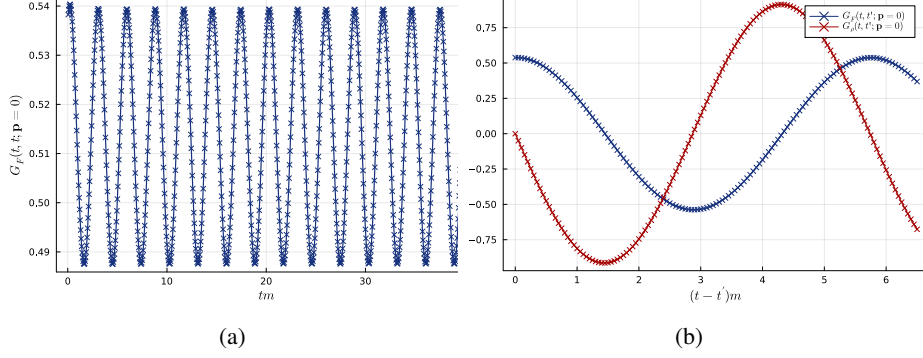
Figure 7.1: Evolution of the equal- (a) and unequal-time (b) Higgs propagators for vanishing external momentum $\mathbf{p} = 0$. Figure (b) shows the statistical (blue) and spectral (red) correlation functions (7.18) and (7.19).

7.5 Results (preliminary)

The 2PI evolution of the statistical and spectral Higgs field propagator obtained at leading order in truncation is displayed in figure 7.1 for equal and unequal time arguments. We fix the lattice spacing and coupling constants to $a_s m = 1$, $g = 0.667$ and $\lambda = 0.125$ throughout. The time evolution and spectrum of the Higgs propagator in the classical-statistical simulation is illustrated in figure 7.2 for (preliminary) comparison. The evolution of the Higgs effective mass is displayed in figure 7.3 and shows a quick damping in amplitude.
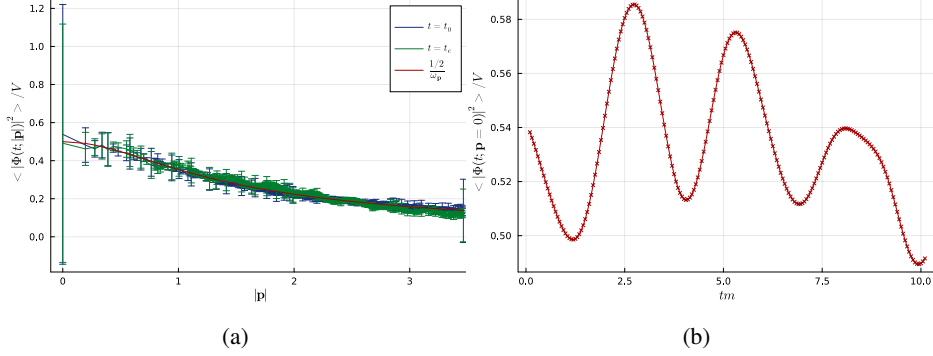
(a)   (b)

Figure 7.2: The spectrum (a) of the classical-statistical Higgs propagator (7.32) and time evolution (b) of its zero mode, averaged over 90 runs with $N_t = 200$ time steps. Figure (a) displays the spectrum at initial time (blue) and final time (green), as well as the Gaussian vacuum distribution $1/2\omega_{\mathbf{p}}$ (red).

With our choice of (vacuum) initial conditions, the amplitudes of the gauge fields are very small, and therefore has very little impact on the (short) simulated evolution of the Higgs field. In addition, with the time scales considered, the particle numbers of the Higgs field have not changed much since its initialisation, as indicated in figure 7.2a.

The energy density is ensured to be conserved throughout the simulations, see Appendix 7.B for details. The absolute violation of the Gauss constraint during the evolution in the classical-statistical evolution is at most $(G_x^a)^2/V \sim 10^{-14}$ and the relative error lies around $G_{x\mathrm{rel}}^a \sim 10^{-7}$. The quantities G_x^a and $G_{x\mathrm{rel}}^a$ are defined in (7.49) and (7.53) respectively.

7.6 Conclusions

In this chapter, we have begun to examine the evolution of the Higgs propagator within a two-loop truncation of the 2PI formulation of SU(2)-Higgs theory. With the aim of quantifying the effect of gauge non-invariance in a 2PI truncation of this model, we have initiated comparisons between the evolution of the statistical Higgs propagator obtained from the naively discretised continuum equations and the corresponding propagator obtained using the classical-statistical covariant lattice formulation. We presented some preliminary numerical results of the dynamics resulting from the
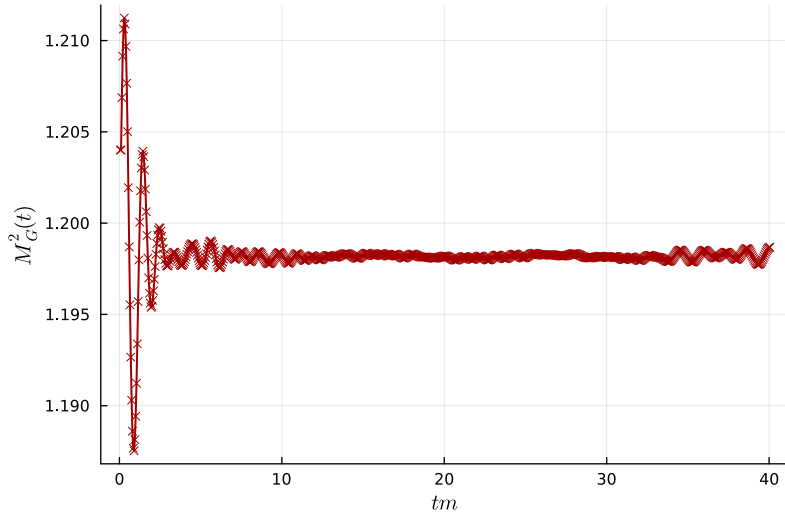
Figure 7.3: Time evolution of the Higgs effective mass (7.22).

leading-order truncation of the 2PI effective action, as the results from the NLO evolution are still pending. While the qualitative behaviour of the 2PI and classical-statistical results are similar, more statistics and checks are required before quantitative statements concerning the gauge-fixing dependence can be made. In addition, the 2PI evolution equations considered here are based on a naive discretisation of the continuum action. For the 2PI evolution to be accurate to $O(g^3)$, it would be necessary to include the $O(a^2)$ contribution of the link expansion to the action, which would result in new (lattice artefact) diagrams.

7.A Details of the lattice implementation

In this appendix we detail the numerical implementation of the 2PI evolution equations and classical-statistical simulations. We discretise the equations on a (3+1)-dimensional lattice of spatial volume $V = L^3 = (a_s N)^3$ with periodic spatial boundary conditions. The spatial lattice spacing is $a_s = a_1 = a_2 = a_3$ and the temporal spacing is taken to be $a_t := a_0$ where we take $dt := a_t/a_s = 0.05$ throughout. We consider $N = 32$ lattice sites.

7.A.1 Classical-statistical evolution

We adopt the lattice formulation of [223, 224]. The link $U_{x,\mu} := U_{\hat{\mu}}(x)$ is defined between two sites x and $x + a_\mu \hat{\mu}$, where a_μ is the lattice spacing in the spacetime direction $\hat{\mu}$. The action is given by (7.31) where the complex Higgs field can be written as an SU(2) matrix,

$$\Phi_x = \frac{1}{2} \begin{pmatrix} \phi_{3x} - i\phi_{4x} & \phi_{1x} + i\phi_{2x} \\ -\phi_{1x} + i\phi_{2x} & \phi_{3x} + i\phi_{4x} \end{pmatrix}, \tag{7.44}$$

where the ϕ_i are real components of the complex doublet $[\phi_1 + i\phi_2, \phi_3 + i\phi_4]^T / \sqrt{2}$. We employ the forward and backward derivatives

$$\begin{aligned} D_\mu \Phi_x &:= \frac{1}{a_\mu} [U_{x,\mu} \Phi_{x+\mu} - \Phi_x], \\ D'_\mu \Phi_x &:= \frac{1}{a_\mu} [\Phi_x - U^\dagger_{x-\mu,\mu} \Phi_{x-\mu}], \end{aligned} \tag{7.45}$$

where e.g. $(D_\mu \Phi_x)^\dagger = D'_\mu \Phi^\dagger_x$. The continuum form of the link is given by $U_{x,\mu} = \exp\left[-iga_\mu A^a_{x+\frac{\mu}{2},\mu} \sigma^a/2\right]$ and we define the electric field as

$$E_{x+\frac{0}{2},i} := \frac{1}{a_t a_s g} U_{x+0,i} U^\dagger_{x,i}, \tag{7.46}$$

which provides the link update rule. The equations of motion are obtained by variation of (7.31) with respect to $A_{x,\mu}$ and $\Phi^\dagger_x$. For the scalar field, we have

$$\Pi_{x+\frac{0}{2}} = \Pi_{x-\frac{0}{2}} + a_t \left\{ \frac{1}{a_s^2} \sum_i [U_{x,i} \Phi_{x+i} - 2\Phi_x + U^\dagger_{x-i,i} \Phi_{x-i}] - \frac{\partial V(\Phi)}{\partial \Phi^\dagger_x} \right\}, \tag{7.47}$$

where the conjugate momenta is defined by

$$\Pi_{x+\frac{0}{2}} := \frac{1}{a_t} (\Phi_{x+0} - \Phi_x). \tag{7.48}$$

In the following we will keep the half time step argument $\hat{0}/2$ in the definition of $E_{x+\frac{0}{2},i}$ and $\Pi_{x+\frac{0}{2}}$ implicit. Variation of (7.31) with respect to

$A_{x,0}$ gives the Gauss constraint

$$G_x^a := \sum_i \text{Tr}\Big[i\sigma^a(E_{x,i} - U_{x-i,i}^\dagger E_{x-i,i}U_{x-i,i})\Big] - g\,\text{Tr}\Big[i\Pi_x^\dagger \sigma^a \Phi_x\Big] = 0,$$

(7.49)

and the equation of motion for the spatial components is

$$E_{x,i}^a = E_{x-0,i}^a + a_t \Bigg\{ \frac{g}{a_s} \text{Tr}\Big[i\sigma^a \Phi_x \Phi_{x+i}^\dagger U_{x,i}^\dagger\Big]$$

$$- \frac{1}{ga_s^3} \sum_j \text{Tr}\Big[i\sigma^a(U_{x,ij} + U_{x,i(-j)})\Big] \Bigg\},$$

(7.50)

where $E_{x,i}^a := \text{Tr}\big[i\sigma^a E_{x,i}\big]$. In order to express $E_{x,i}$ in terms of $E_{x,i}^a$, as needed for the link update (7.46), we use that an SU(2) matrix u can be expanded in Pauli matrices,

$$u = u_0 \mathbb{1} + iu^a \sigma^a,$$

(7.51)

where $u_0^2 + (u^a)^2 = 1$. From (7.46), we then obtain

$$E_{x,i} = \frac{1}{ga_t a_s}\left[\sqrt{1 - \tfrac{1}{4}(ga_t a_s E_{x,i}^a)^2}\,\mathbb{1} - \tfrac{1}{2}iga_t a_s E_{x,i}^a \sigma^a \right].$$

(7.52)

To ensure that the Gauss constraint is fulfilled during the evolution it is useful to track the relative violation of the Gauss constraint (7.49), i.e.

$$G_{x\text{rel}}^a := \frac{1}{G_x^a}\Bigg\{ \sum_i \text{Tr}\Big[i\sigma^a(E_{x,i} - U_{x-i,i}^\dagger E_{x-i,i}U_{x-i,i})\Big] + g\,\text{Tr}\Big[i\Pi_x^\dagger \sigma^a \Phi_x\Big] \Bigg\},$$

(7.53)

in addition to the absolute violation given by $(G_x^a)^2/V$.

7.A.2 Initialisation

The gauge fields are taken to vanish at initial time, i.e. $A_\mu^a(t = 0) = 0$ such that $U_{x,i}(t = 0) = \mathbb{1}$. If the Gauss constraint is satisfied at initial time, it can be shown to hold during the entire subsequent evolution [225, 226]. At $t = 0$ the Gauss constraint reads

$$\sum_i \text{Tr}\Big[i\sigma^a(E_{x,i} - E_{x-i,i})\Big] + \rho_x^a = 0,$$

(7.54)

where we write $\rho_x^a := -g \, \text{Tr} \left[i \Pi_x^\dagger \sigma^a \Phi_x \right]$. Since the difference in electric fields in (7.54) corresponds to a backward derivative, i.e. $\partial_i' E_i^a = \sum_i \text{Tr} \left[i \sigma^a (E_{x,i} - E_{x-i,i}) \right]$, it is convenient to make the ansatz $E_{x,i}^a (t = 0) = -\partial_i \chi_x^a$ where χ_x^a is a scalar field, such that (7.54) becomes

$$-\partial_i' \partial_i \chi_x^a + \rho_x^a = 0. \tag{7.55}$$

By solving this equation in momentum space, the electric field can then be initialised by

$$E_{x,i}^a = -(\chi_{x+i}^a - \chi_x^a), \quad \chi_x^a = \int_{\mathbf{p}} \left(-\frac{\rho_p^a}{\mathbf{p}^2} \right) e^{i\mathbf{p}\cdot\mathbf{x}}, \quad \mathbf{p} \neq 0. \tag{7.56}$$

given a value of ρ_p^a, to which we turn to next.

We follow the procedure made in [227, 228] when initialising the Higgs field Φ_x. In particular, Φ_x can also be initialised from (7.54) by integrating (7.54) over the lattice, such that

$$\sum_x \rho_x^a = 0, \tag{7.57}$$

which can be thought of as a global Gauss constraint. The constraint (7.57) can then be imposed at the level of the mode functions,

$$\phi_{\gamma x} = \frac{1}{\sqrt{V}} \sum_p e^{i\mathbf{p}\cdot\mathbf{x}} \phi_{\gamma p}, \quad \pi_{\gamma x} = \frac{1}{\sqrt{V}} \sum_p e^{i\mathbf{p}\cdot\mathbf{x}} \pi_{\gamma p}, \tag{7.58}$$

where $\gamma = 1, 2, 3, 4$. The real fields $\pi_{\gamma x}$ are the matrix elements of Π_x, which is defined analogously to the field Φ_x in (7.44). Assuming Gaussian initial conditions, the mode functions $\phi_{\gamma p}$ and $\pi_{\gamma p}$ are given by

$$\phi_{\gamma p} = \phi_{\gamma(-p)}^* = \frac{1}{\sqrt{2\omega_p}} a_{\gamma p}, \quad \tilde{n} = 0, \tfrac{1}{2}N, \tfrac{\sqrt{2}}{2}N, \tfrac{\sqrt{3}}{2}N,$$

$$\pi_{\gamma p} = \pi_{\gamma(-p)}^* = \sqrt{\frac{\omega_p}{2}} c_{\gamma p}, \quad \tilde{n} = 0, \tfrac{1}{2}N, \tfrac{\sqrt{2}}{2}N, \tfrac{\sqrt{3}}{2}N, \tag{7.59}$$

and

$$\phi_{\gamma p} = \phi_{\gamma(-p)}^* = \frac{1}{\sqrt{2\omega_p}} \left(a_{\gamma p} + i b_{\gamma p} \right), \quad \tilde{n} \neq 0, \tfrac{1}{2}N, \tfrac{\sqrt{2}}{2}N, \tfrac{\sqrt{3}}{2}N,$$

$$\pi_{\gamma p} = \pi_{\gamma(-p)}^* = \sqrt{\frac{\omega_p}{2}} \left(c_{\gamma p} + i d_{\gamma p} \right), \quad \tilde{n} \neq 0, \tfrac{1}{2}N, \tfrac{\sqrt{2}}{2}N, \tfrac{\sqrt{3}}{2}N, \tag{7.60}$$

where the lattice momentum is $p = 2\pi\tilde{n}/N$ and the corner modes with $\tilde{n} = 0, \frac{1}{2}N, \frac{\sqrt{2}}{2}N, \frac{\sqrt{3}}{2}N$ in (7.59) are real. With four real fields for Φ_x and Π_x each, it is convenient to extend the Gauss constraint (7.57) to include a fourth constraint,

$$\sum_x \rho_x^\gamma = 0, \tag{7.61}$$

where the new constraint comes from $\sigma^4 = \frac{i}{2}\mathbb{1}$. Explicitly, in terms of the real field components $\phi_{\gamma x}$ and $\pi_{\gamma x}$, this constraint is solved by

$$
\begin{aligned}
-i\,\mathrm{Tr}\,\Pi_x^\dagger \sigma^1 \Phi_x &= \pi_{1x}^* \phi_{4x} - \pi_{4x}^* \phi_{1x} + \pi_{3x}^* \phi_{2x} - \pi_{2x}^* \phi_{3x} = 0, \\
-i\,\mathrm{Tr}\,\Pi_x^\dagger \sigma^2 \Phi &= \pi_{3x}^* \phi_{1x} - \pi_{1x}^* \phi_{3x} + \pi_{4x}^* \phi_{2x} - \pi_{2x}^* \phi_{4x} = 0, \\
-i\,\mathrm{Tr}\,\Pi_x^\dagger \sigma^3 \Phi_x &= \pi_{1x}^* \phi_{2x} - \pi_{2x}^* \phi_{1x} + \pi_{4x}^* \phi_{3x} - \pi_{3x}^* \phi_{4x} = 0, \\
-i\,\mathrm{Tr}\,\Pi_x^\dagger \sigma^4 \Phi_x &= \pi_{1x}^* \phi_{1x} + \pi_{2x}^* \phi_{2x} + \pi_{3x}^* \phi_{3x} + \pi_{4x}^* \phi_{4x} = 0,
\end{aligned}
\tag{7.62}
$$

where $\pi_{\gamma x}^* \equiv \pi_{\gamma x}$. At the level of the mode functions (7.58), the Gauss constraint can be written as a linear matrix equation,

$$\mathbf{Ac} + \mathbf{f} = \mathbf{0}, \tag{7.63}$$

to be solved by the zero modes $c_{\gamma(p=0)}$ of the π_p field, i.e.

$$
\mathbf{A} = \begin{pmatrix}
a_{4p} & -a_{3p} & a_{2p} & -a_{1p} \\
-a_{3p} & -a_{4p} & a_{1p} & a_{2p} \\
a_{2p} & -a_{1p} & -a_{4p} & a_{3p} \\
a_{1p} & a_{2p} & a_{3p} & a_{4p}
\end{pmatrix}_{p=0}, \quad
\mathbf{c} = \begin{pmatrix}
c_{1p} \\
c_{2p} \\
c_{3p} \\
c_{4p}
\end{pmatrix}_{p=0}, \quad
\mathbf{f} = \sum_{p\neq 0} \begin{pmatrix}
f_{1p} \\
f_{2p} \\
f_{3p} \\
f_{4p}
\end{pmatrix},
$$
$$\tag{7.64}$$

where

$$
\begin{aligned}
f_{1p} &= c_{1p}a_{4p} - c_{4p}a_{1p} + c_{3p}a_{2p} - c_{2p}a_{3p} \\
&\quad + d_{1p}b_{4p} - d_{4p}b_{1p} + d_{3p}b_{2p} - d_{2p}b_{3p}, \\
f_{2p} &= c_{3p}a_{1p} - c_{1p}a_{3p} + c_{4p}a_{2p} - c_{2p}a_{4p} \\
&\quad + d_{3p}b_{1p} - d_{1p}b_{3p} + d_{4p}b_{2p} - d_{2p}b_{4p}, \\
f_{3p} &= c_{1p}a_{2p} - c_{2p}a_{1p} + c_{4p}a_{3p} - c_{3p}a_{4p} \\
&\quad + d_{1p}b_{2p} - d_{2p}b_{1p} + d_{4p}b_{3p} - d_{3p}b_{4p}, \\
f_{4p} &= c_{1p}a_{1p} + c_{2p}a_{2p} + c_{3p}a_{3p} + c_{4p}a_{4p} \\
&\quad + d_{1p}b_{1p} + d_{2p}b_{2p} + d_{3p}b_{3p} + d_{4p}b_{4p},
\end{aligned}
\tag{7.65}
$$

174

using $\phi_{\gamma p} = \phi^*_{\gamma(-p)}$ or $a_{\gamma p} = a_{\gamma(-p)}$ and $b_{\gamma p} = -b_{\gamma(-p)}$. The modes then follow the modified Gaussian distribution

$$P'(\phi,\pi) = \prod_\gamma \int [\mathrm{d}\phi_{\gamma p}\mathrm{d}\pi_{\gamma p}] P(\phi_{\gamma p},\pi_{\gamma p})\delta(\mathbf{Ac}+\mathbf{f}), \qquad (7.66)$$

where P is the Gaussian distribution

$$
\begin{aligned}
P(\phi,\pi) &\propto \exp\left[-\frac{1}{2}\sum_{\gamma p}\frac{\phi^2_{\gamma p}}{\sigma^2_{\gamma p}} - \frac{1}{2}\sum_{\gamma p}\frac{\pi^2_{\gamma p}}{\tilde{\sigma}^2_{\gamma p}}\right] \\
&= \exp\Bigg[\sum_\gamma\bigg(-\frac{1}{2}\sum_{p_{\text{bulk}}}\frac{a^2_{\gamma p}+b^2_{\gamma p}+c^2_{\gamma p}+d^2_{\gamma p}}{n_p+1/2} \\
&\quad -\frac{1}{2}\sum_{p_{\text{corner}}}\frac{a^2_{\gamma p}+c^2_{\gamma p}}{2(n_p+1/2)} - \frac{1}{2}\frac{a^2_{\gamma(p=0)}+c^2_{\gamma(p=0)}}{2(n_{p=0}+1/2)}\bigg)\Bigg],
\end{aligned}
\qquad (7.67)
$$

with

$$
\begin{aligned}
\sigma^2_{\gamma p} &:= \langle\phi_{\gamma p}\phi^*_{\gamma p}\rangle = \frac{1}{\omega_p}(n_p+1/2), \\
\tilde{\sigma}^2_{\gamma p} &:= \langle\pi_{\gamma p}\pi^*_{\gamma p}\rangle = \omega_p(n_p+1/2),
\end{aligned}
\qquad (7.68)
$$

and

$$
\begin{aligned}
p_{\text{bulk}} &= 2\pi\tilde{n}/N, \quad \tilde{n} = 0, \tfrac{1}{2}N, \tfrac{\sqrt{2}}{2}N, \tfrac{\sqrt{3}}{2}N, \\
p_{\text{corner}} &= 2\pi\tilde{n}/N, \quad \tilde{n} \neq 0, \tfrac{1}{2}N, \tfrac{\sqrt{2}}{2}N, \tfrac{\sqrt{3}}{2}N.
\end{aligned}
\qquad (7.69)
$$

In (7.67) we have used that the Hermiticity of the mode functions result in that

$$\sum_p \phi_{\gamma p} = 2\sum_{p_{\text{bulk}}}(a_{\gamma p}+ib_{\gamma p}) + \sum_{p_{\text{corner}}} a_{\gamma p} + a_{\gamma 0}. \qquad (7.70)$$

By integrating out the zero modes $c_{\gamma(p=0)}$ in (7.67), we obtain

$$
\begin{aligned}
P'(\phi,\pi) &\propto \frac{1}{\det\mathbf{A}}\exp\Bigg[\sum_\gamma\bigg(-\frac{1}{2}\sum_{p_{\text{bulk}}}\frac{a^2_{\gamma p}+b^2_{\gamma p}+c^2_{\gamma p}+d^2_{\gamma p}}{n_p+1/2} \\
&\quad -\frac{1}{2}\sum_{p_{\text{corner}}}\frac{a^2_{\gamma p}+c^2_{\gamma p}}{2(n_p+1/2)} - \frac{1}{2}\frac{a^2_{\gamma(p=0)}}{2(n_{p=0}+1/2)}\bigg) - \frac{1}{2}\frac{(\mathbf{A}^{-1}\mathbf{f})^2}{2(n_{p=0}+1/2)}\Bigg],
\end{aligned}
\qquad (7.71)
$$

where $\det\mathbf{A} = \left[\sum_\gamma a^2_{\gamma(p=0)}\right]^2$. A sample of of modes is then obtained by first generating a set of random numbers following the distribution

(7.71). For a given such sampling, the corresponding zero modes $c_{\gamma(p=0)}$ are obtained as the solution to (7.63). The sampling of (7.71) can be made more efficient by noting that

$$(\mathbf{A}^{-1}\mathbf{f})^2 = \frac{\sum_\gamma f_\gamma^2}{\sqrt{\det \mathbf{A}}}.$$

(7.72)

Finally, the modes of $\phi_{\gamma x}$ are obtained via (7.59) and (7.60) which then enter into (7.44), and similarly for $\pi_{\gamma x}$.

7.A.3 2PI evolution equations

The 2PI equations of motion involve only absolute values of the (physical) lattice momentum $\tilde{p}^2 = \sum_i [2 - 2\cos(2\pi\tilde{n}_i/N)]$, e.g. such that $G(t, t'; \mathbf{p}) \equiv G(t, t'; |\mathbf{p}|) \equiv G(t, t'; |\tilde{p}|)$ for both statistical and spectral components. The evolution is set up to respect the symmetry and anti-symmetry properties $G_{(F)}(t, t'; |\mathbf{p}|) = G_{(F)}(t', t; |\mathbf{p}|)$ and $G_\rho(t, t'; |\mathbf{p}|) = -G_\rho(t', t; |\mathbf{p}|)$ and analogously for the gauge propagators. Derivatives are evaluated using the Euler method, i.e.,

$$\partial_t \partial_{t'} G(t, t'; \mathbf{p}) = \frac{1}{a_t^2} \big[G(t + a_t, t' + a_t; \mathbf{p}) - G(t + a_t, t'; \mathbf{p}) \\ - G(t, t' + a_t; \mathbf{p}) + G(t, t'; \mathbf{p}) \big].$$

(7.73)

Propagators are initialised by specifying $G(0, 0; \mathbf{p})$, $G(1, 0; \mathbf{p})$ and $G(1, 1; \mathbf{p})$ (and analogously for the gauge propagators) according to (7.73) using the initial conditions (7.40), (7.41) and (7.43). The initial values of the propagators are provided by the classical-statistical initialisation. The temporal (memory) integrals involving the self-energies in (7.15)–(7.19) are evaluated using the trapezoidal rule

$$\int_a^b \mathrm{d}t\, f(t) = a_t \left[\frac{1}{2} f(a) + \sum_{i=a+1}^{b-1} f(i) + \frac{1}{2} f(b) \right],$$

(7.74)

for some function $f(t)$. Propagators are then evolved by computing their values at unequal time arguments at each time step, e.g. $G_{(F)}(t, t'; \mathbf{p})$ for $1 < t' < t - 1$. The integrals involving the (non-local) self-energies in the evolution equations depend on all the past values of the propagators.

Note that at leading order it is not necessary to keep the entire memory of all past values. In this case evaluating the propagators at the next time step require only information about the propagator values involved in the last two time steps. The spectral components are updated in accordance to the commutation relations, e.g. for the scalar, $G_{(\rho)}(t + a_t, t'; \mathbf{p}) = \mathrm{d}t$ and $G_{(\rho)}(t, t'; \mathbf{p}) = 0$, at all times.

The coefficients for the transverse part of the gauge self-energy in (7.24) are

$$
\begin{aligned}
N_\mathrm{T}^{\parallel\perp} &= -\frac{p^4}{|\mathbf{p} - \mathbf{q}|^2} + (\mathbf{p} \cdot \mathbf{q})^2 \left[\frac{p^2}{q^2|\mathbf{p} - \mathbf{q}|^2} + \frac{1}{p^2} + \frac{4d - 5}{q^2} \right] \\
&\quad - \frac{2(\mathbf{p} \cdot \mathbf{q})^3}{p^2 q^2} + p^2 + (6 - 4d)\mathbf{p} \cdot \mathbf{q} + (d - 2)q^2, \\
N_\mathrm{T}^{\perp\parallel} &= \frac{(d - 2)p^4}{|\mathbf{p} - \mathbf{q}|^2} - \frac{2(d - 2)p^2 q^2}{|\mathbf{p} - \mathbf{q}|^2} + \frac{(d - 2)q^4}{|\mathbf{p} - \mathbf{q}|^2} \\
&\quad + (\mathbf{p} \cdot \mathbf{q})^2 \left[\frac{p^2}{q^2|\mathbf{p} - \mathbf{q}|^2} + \frac{q^2}{p^2|\mathbf{p} - \mathbf{q}|^2} - \frac{2}{|\mathbf{p} - \mathbf{q}|^2} \right], \\
N_\mathrm{T}^{\parallel\parallel} &= \frac{p^4}{|\mathbf{p} - \mathbf{q}|^2} - \frac{p^2(\mathbf{p} \cdot \mathbf{q})^2}{q^2|\mathbf{p} - \mathbf{q}|^2}, \qquad\qquad (7.75) \\
N_\mathrm{T}^{\perp\perp} &= -\frac{(d - 2)p^4}{|\mathbf{p} - \mathbf{q}|^2} + (5d - 6)p^2 + \frac{2(d - 2)p^2 q^2}{|\mathbf{p} - \mathbf{q}|^2} \\
&\quad + (\mathbf{p} \cdot \mathbf{q})^2 \left[\frac{5 - 4d}{p^2} - \frac{p^2}{q^2|\mathbf{p} - \mathbf{q}|^2} - \frac{q^2}{p^2|\mathbf{p} - \mathbf{q}|^2} \right. \\
&\quad \left. + \frac{2}{|\mathbf{p} - \mathbf{q}|^2} + \frac{5 - 4d}{q^2} \right] + \frac{2(\mathbf{p} \cdot \mathbf{q})^3}{p^2 q^2} \\
&\quad - \frac{(d - 2)q^4}{|\mathbf{p} - \mathbf{q}|^2} + (2d - 4)\mathbf{p} \cdot \mathbf{q} + (5d - 6)q^2,
\end{aligned}
$$

where we write $p := |\mathbf{p}|$, etc., and similarly the longitudinal counterparts

of (7.25) are given by

$$
\begin{aligned}
N_{\mathrm{L}}^{\parallel\perp} &= \frac{2(\mathbf{p}\cdot\mathbf{q})^3}{p^2 q^2} + (\mathbf{p}\cdot\mathbf{q})^2\left[-\frac{1}{p^2} - \frac{1}{q^2}\right] + p^2 - 2\mathbf{p}\cdot\mathbf{q} + q^2, \\
N_{\mathrm{L}}^{\perp\parallel} &= \frac{q^4}{|\mathbf{q}-\mathbf{p}|^2} - \frac{q^2(\mathbf{p}\cdot\mathbf{q})^2}{p^2|\mathbf{q}-\mathbf{p}|^2}, \\
N_{\mathrm{L}}^{\perp\perp} &= (d-2)p^2 + (\mathbf{p}\cdot\mathbf{q})^2\left[\frac{4d-5}{p^2} + \frac{q^2}{p^2|\mathbf{q}-\mathbf{p}|^2} + \frac{1}{q^2}\right] \\
&\quad - \frac{2(\mathbf{p}\cdot\mathbf{q})^3}{p^2 q^2} - \frac{q^4}{|\mathbf{q}-\mathbf{p}|^2} + (6-4d)\mathbf{p}\cdot\mathbf{q} + q^2, \\
N_{\mathrm{L}}^{\parallel\parallel} &= 0.
\end{aligned}
\tag{7.76}
$$

The coefficients entering the scalar self-energy of (7.29) read

$$
\begin{aligned}
c^{\perp} &= -\frac{4p^4}{|\mathbf{p}-\mathbf{q}|^2} - \frac{4p^2 q^2}{|\mathbf{p}-\mathbf{q}|^2} + \mathbf{p}\cdot\mathbf{q}\left[\frac{12p^2}{|\mathbf{p}-\mathbf{q}|^2} + \frac{6q^2}{|\mathbf{p}-\mathbf{q}|^2} - 4\right] \\
&\quad + 4p^2 - \frac{q^4}{|\mathbf{p}-\mathbf{q}|^2} - \frac{9(\mathbf{p}\cdot\mathbf{q})^2}{|\mathbf{p}-\mathbf{q}|^2} + q^2, \\
c^{\parallel} &= \frac{4p^4}{|\mathbf{p}-\mathbf{q}|^2} + \frac{4p^2 q^2}{|\mathbf{p}-\mathbf{q}|^2} - \mathbf{p}\cdot\mathbf{q}\left[\frac{12p^2}{|\mathbf{p}-\mathbf{q}|^2} + \frac{6q^2}{|\mathbf{p}-\mathbf{q}|^2}\right] \\
&\quad + \frac{q^4}{|\mathbf{p}-\mathbf{q}|^2} + \frac{9(\mathbf{p}\cdot\mathbf{q})^2}{|\mathbf{p}-\mathbf{q}|^2}.
\end{aligned}
\tag{7.77}
$$

When evaluating the equations of motion, all angle-dependent vector products are evaluated in terms of absolute values,

$$
\mathbf{p}\cdot\mathbf{q} = \tfrac{1}{2}\left[|\mathbf{p}|^2 + |\mathbf{q}|^2 - |\mathbf{p}-\mathbf{q}|^2\right].
\tag{7.78}
$$

For instance in the effective gauge masses in (7.20) and (7.21), we encounter terms of the form

$$
\int_{\mathbf{q}} \frac{(\mathbf{p}\cdot\mathbf{q})^2}{|\mathbf{p}|^2|\mathbf{q}|^2} f(|\mathbf{q}|),
\tag{7.79}
$$

where $f(|\mathbf{q}|)$ is a scalar function. Using (7.78), this can be evaluated by

introducing $\mathbf{k} := \mathbf{p} - \mathbf{q}$, such that

$$
\int_{\mathbf{q}} \frac{(\mathbf{p} \cdot \mathbf{q})^2}{|\mathbf{p}|^2 |\mathbf{q}|^2} f(|\mathbf{q}|) = \frac{1}{4} \int_{\mathbf{qk}} \frac{f(|\mathbf{q}|)}{|\mathbf{p}|^2 |\mathbf{q}|^2} \left(|\mathbf{p}|^2 + |\mathbf{q}|^2 - |\mathbf{k}|^2 \right)^2 \delta(\mathbf{k} + \mathbf{q} - \mathbf{p})
$$

$$
= \frac{1}{4} \int_{\mathbf{xqk}} f(|\mathbf{q}|) \left[\frac{|\mathbf{p}|^2}{|\mathbf{q}|^2} + \frac{|\mathbf{q}|^2}{|\mathbf{p}|^2} + \frac{|\mathbf{k}|^4}{|\mathbf{p}|^2 |\mathbf{q}|^2} + 2 \left(1 - \frac{|\mathbf{k}|^2}{|\mathbf{q}|^2} - \frac{|\mathbf{k}|^2}{|\mathbf{p}|^2} \right) \right] e^{-i\mathbf{x} \cdot (\mathbf{k} + \mathbf{q} - \mathbf{p})}
$$

$$
= \frac{1}{4} \int_{\mathbf{x}} \left[|\mathbf{p}|^2 \int_{\mathbf{q}} \frac{f(|\mathbf{q}|)}{|\mathbf{q}|^2} e^{-i\mathbf{x} \cdot \mathbf{q}} \int_{\mathbf{k}} e^{-i\mathbf{x} \cdot \mathbf{k}} + \frac{1}{|\mathbf{p}|^2} \int_{\mathbf{q}} |\mathbf{q}|^2 f(|\mathbf{q}|) e^{-i\mathbf{x} \cdot \mathbf{q}} \int_{\mathbf{k}} e^{-i\mathbf{x} \cdot \mathbf{k}} \right.
$$

$$
+ \frac{1}{|\mathbf{p}|^2} \int_{\mathbf{q}} \frac{f(|\mathbf{q}|)}{|\mathbf{q}|^2} e^{-i\mathbf{x} \cdot \mathbf{q}} \int_{\mathbf{k}} |\mathbf{k}|^4 e^{-i\mathbf{x} \cdot \mathbf{k}} + 2 \int_{\mathbf{q}} f(|\mathbf{q}|) e^{-i\mathbf{x} \cdot \mathbf{q}} \int_{\mathbf{k}} e^{-i\mathbf{x} \cdot \mathbf{k}}
$$

$$
\left. - 2 \int_{\mathbf{q}} \frac{f(|\mathbf{q}|)}{|\mathbf{q}|^2} e^{-i\mathbf{x} \cdot \mathbf{q}} \int_{\mathbf{k}} |\mathbf{k}|^2 e^{-i\mathbf{x} \cdot \mathbf{k}} - \frac{2}{|\mathbf{p}|^2} \int_{\mathbf{q}} f(|\mathbf{q}|) e^{-i\mathbf{x} \cdot \mathbf{q}} \int_{\mathbf{k}} |\mathbf{k}|^2 e^{-i\mathbf{x} \cdot \mathbf{k}} \right] e^{+i\mathbf{x} \cdot \mathbf{p}}.
$$

$$(7.80)$$

The dot product can therefore be evaluated as a Fourier transform of products of inverse Fourier transforms. For instance the self-energies in (7.27) and (7.28) can then be expressed as

$$
\Pi_{(G^2 D)}^{\perp ab(\chi)}(t, t'; p) = -\frac{g^2}{2(d-1)} \delta^{ab} \int_{\mathbf{xkq}} C^{\perp}(p, k, q) e^{i\mathbf{x} \cdot (\mathbf{p} - \mathbf{k} - \mathbf{q})}
$$

$$
\times \left[G(t, t'; k) G(t, t'; q) \right]_{(\chi)},
$$

$$
\Pi_{(G^2 D)}^{\| ab(\chi)}(t, t'; p) = -\frac{g^2}{2} \delta^{ab} \int_{\mathbf{xkq}} C^{\|}(p, k, q) e^{i\mathbf{x} \cdot (\mathbf{p} - \mathbf{k} - \mathbf{q})}
$$

$$
\times \left[G(t, t'; k) G(t, t'; q) \right]_{(\chi)},
$$

$$(7.81)$$

with

$$
C^{\perp}(p, k, q) = -p^2 + 2k^2 + 2q^2 - \frac{1}{p^2} \left(k^4 - 2k^2 q^2 + q^4 \right),
$$

$$
C^{\|}(p, k, q) = \frac{1}{p^2} \left(k^4 - 2k^2 q^2 + q^4 \right).
$$

$$(7.82)$$

In terms of k, the coefficients in (7.75) for the transverse self-energy

contribution from the D^3 diagram (7.24) take the form

$$
\begin{aligned}
N_{\mathrm{T}}^{\parallel\perp} &= \frac{p^6}{4k^2q^2} + p^4\left[(d-2)\frac{1}{q^2} - \frac{1}{2k^2}\right] + \frac{p^2}{2}\left[(7-4d)\frac{k^2}{q^2} + \frac{q^2}{2k^2} + 1\right] \\
&\quad + (d-2)\frac{k^4}{q^2} + \frac{1}{2}\left(k^2 - q^2\right) + \frac{1}{4p^2}\left[\frac{k^6}{q^2} - 2k^4 + k^2q^2\right], \\
N_{\mathrm{T}}^{\perp\parallel} &= \frac{p^6}{4k^2q^2} + p^4\left[(d-2)\frac{1}{k^2} - \frac{1}{2q^2}\right] + \frac{p^2}{2}\left[(7-4d)\frac{q^2}{k^2} + \frac{k^2}{2q^2} + 1\right] \\
&\quad + (d-2)\frac{q^4}{k^2} + \frac{1}{2}\left(q^2 - k^2\right) + \frac{1}{4p^2}\left[\frac{q^6}{k^2} - 2q^4 + k^2q^2\right], \\
N_{\mathrm{T}}^{\parallel\parallel} &= -\frac{p^6}{4k^2q^2} + \frac{p^4}{2}\left[\frac{1}{k^2} + \frac{1}{q^2}\right] + \frac{p^2}{4}\left[2 - \frac{k^2}{q^2} - \frac{q^2}{k^2}\right], \\
N_{\mathrm{T}}^{\perp\perp} &= -\frac{p^6}{4k^2q^2} - (d-2)p^4\left[\frac{1}{k^2} + \frac{1}{q^2}\right] \\
&\quad + p^2\left[3d - 4 - \frac{1}{2}(7-4d)\left(\frac{k^2}{q^2} + \frac{q^2}{k^2}\right)\right] \\
&\quad - (d-2)\left[\frac{k^4}{q^2} + \frac{q^4}{k^2}\right] + (3d-4)\left(k^2 + q^2\right) \\
&\quad - \frac{1}{p^2}\left[\frac{1}{4}\left(\frac{k^6}{q^2} + \frac{q^6}{k^2}\right) + \frac{1}{2}(7-4d)k^2q^2 + (d-2)(k^4 + q^4)\right],
\end{aligned}
\tag{7.83}
$$

and

$$
\begin{aligned}
N_{\mathrm{L}}^{\parallel\perp} &= -\frac{p^2}{4}\frac{k^2}{q^2} + \frac{1}{2}\left[\frac{k^4}{q^2} + k^2\right] - \frac{1}{4p^2}\left[\frac{k^6}{q^2} - 2k^4 + k^2q^2\right], \\
N_{\mathrm{L}}^{\perp\parallel} &= -\frac{p^2}{4}\frac{q^2}{k^2} + \frac{1}{2}\left[\frac{q^4}{k^2} + q^2\right] - \frac{1}{4p^2}\left[\frac{q^6}{k^2} - 2q^4 + k^2q^2\right], \\
N_{\mathrm{L}}^{\perp\perp} &= p^2\left[\frac{k^2}{4q^2} + \frac{q^2}{4k^2} - \frac{1}{2}\right] - \frac{1}{2}\left[\frac{k^4}{q^2} + \frac{q^4}{k^2}\right] + \frac{1}{2}(k^2 + q^2) \\
&\quad + \frac{1}{p^2}\left[\frac{1}{4}\left(\frac{k^6}{q^2} + \frac{q^6}{k^2}\right) + (d-2)(k^4 + q^4) + \frac{1}{2}(7-4d)k^2q^2\right], \\
N_{\mathrm{L}}^{\parallel\parallel} &= 0,
\end{aligned}
\tag{7.84}
$$

for the longitudinal part (7.76). Here we note the symmetries

$$N_{\mathrm{T}}^{\|\perp}(p, q, k) \equiv N_{\mathrm{T}}^{\perp\|}(p, k, q), \tag{7.85}$$

$$N_{\mathrm{L}}^{\|\perp}(p, q, k) \equiv N_{\mathrm{L}}^{\perp\|}(p, k, q). \tag{7.86}$$

For the coefficients of the scalar self-energy (7.77), we obtain

$$
\begin{aligned}
c^{\perp} &= -\frac{p^4}{4k^2} + \frac{p^2}{2}\left(\frac{q^2}{k^2} + 1\right) - \frac{1}{4}\left(\frac{q^4}{k^2} - 2q^2 + k^2\right), \\
c^{\|} &= \frac{p^4}{4k^2} + \frac{p^2}{2}\left(3 - \frac{q^2}{k^2}\right) + \frac{q^4}{4k^2} + \frac{3}{2}\left(\frac{3k^2}{2} - q^2\right).
\end{aligned}
\tag{7.87}
$$

Finally, we state the coefficients (7.82)–(7.84) and (7.87) in the cases of vanishing external or loop momentum. Namely, the dot products are $\mathbf{p} \cdot \mathbf{q} = 0$ for either $\mathbf{p}, \mathbf{q} = 0$ or $\mathbf{p} \cdot \mathbf{q} = p^2$ when $\mathbf{k} = 0$. In these cases the coefficients take the values

$$
\begin{aligned}
&N_{\mathrm{T}}^{\|\perp}\Big|_{p=0} = (d-2)q^2, &&N_{\mathrm{L}}^{\|\perp}\Big|_{p=0} = q^2, &&C^{\perp}\Big|_{p=0} = 4q^2, \\
&N_{\mathrm{T}}^{\perp\|}\Big|_{p=0} = (d-2)q^2, &&N_{\mathrm{L}}^{\perp\|}\Big|_{p=0} = q^2, &&C^{\|}\Big|_{p=0} = 4q^2, \\
&N_{\mathrm{T}}^{\|\|}\Big|_{p=0} = 0, &&N_{\mathrm{L}}^{\|\|}\Big|_{p=0} = 0, &&c^{\perp}\Big|_{p=0} = 0, \\
&N_{\mathrm{T}}^{\perp\perp}\Big|_{p=0} = 4(d-1)q^2, &&N_{\mathrm{L}}^{\perp\perp}\Big|_{p=0} = 0, &&c^{\|}\Big|_{p=0} = q^2,
\end{aligned}
\tag{7.88}
$$

for vanishing external momentum, and

$$
\begin{aligned}
&N_{\mathrm{T}}^{\|\perp}\Big|_{q=0} = 0, &&N_{\mathrm{L}}^{\|\perp}\Big|_{q=0} = p^2, &&C^{\perp}\Big|_{q=0} = 0, \\
&N_{\mathrm{T}}^{\perp\|}\Big|_{q=0} = (d-2)p^2, &&N_{\mathrm{L}}^{\perp\|}\Big|_{q=0} = 0, &&C^{\|}\Big|_{q=0} = p^2, \\
&N_{\mathrm{T}}^{\|\|}\Big|_{q=0} = p^2, &&N_{\mathrm{L}}^{\|\|}\Big|_{q=0} = 0, &&c^{\perp}\Big|_{q=0} = 0, \\
&N_{\mathrm{T}}^{\perp\perp}\Big|_{q=0} = 4(d-1)p^2, &&N_{\mathrm{L}}^{\perp\perp}\Big|_{q=0} = (d-2)p^2, &&c^{\|}\Big|_{q=0} = 4p^2,
\end{aligned}
\tag{7.89}
$$

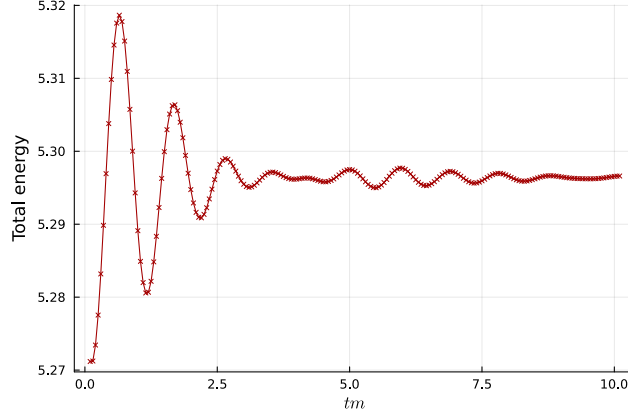for vanishing loop momentum, and finally for equal external and loop

Figure 7.4: Time evolution of the total classical-statistical energy (7.91).

momentum, $k = 0$,

$$
\begin{aligned}
N_{\mathrm{T}}^{\|\perp}\Big|_{k=0} &= (d-2)p^2, & N_{\mathrm{L}}^{\|\perp}\Big|_{k=0} &= 0, & C^{\perp}\Big|_{k=0} &= 0, \\
N_{\mathrm{T}}^{\perp\|}\Big|_{k=0} &= 0, & N_{\mathrm{L}}^{\perp\|}\Big|_{k=0} &= p^2, & C^{\|}\Big|_{k=0} &= p^2, \\
N_{\mathrm{T}}^{\|\|}\Big|_{k=0} &= p^2, & N_{\mathrm{L}}^{\|\|}\Big|_{k=0} &= 0, & c^{\perp}\Big|_{k=0} &= p^2, \\
N_{\mathrm{T}}^{\perp\perp}\Big|_{k=0} &= 4(d-1)p^2, & N_{\mathrm{L}}^{\perp\perp}\Big|_{k=0} &= (d-2)p^2, & c^{\|}\Big|_{k=0} &= 0.
\end{aligned} \tag{7.90}
$$

7.B Energy conservation

The energy for the classical lattice action is given by the Hamiltonian

$$
\begin{aligned}
H = \sum_{x,t} a_t a_s^3 \Bigg[&\frac{1}{2}(E_{x,i}^a)^2 + \frac{4}{(ga_s^2)^2} \sum_{i<j} \left[1 - \tfrac{1}{2}\operatorname{Tr} U_{x,ij} \right] \\
&+ \operatorname{Tr}\left[\pi_x^\dagger \pi_x \right] + \frac{2}{a_s^2} \sum_i \operatorname{Tr}\left[\Phi_x^\dagger \Phi_x - \Phi_x^\dagger U_{x,i}\Phi_{x-i} \right] + V(|\Phi_x|) \Bigg],
\end{aligned} \tag{7.91}
$$

which is conserved (within $\sim 1\%$) during the evolution, see figure 7.4. The fraction of each energy component relative to the total energy is illustrated in figure 7.5.
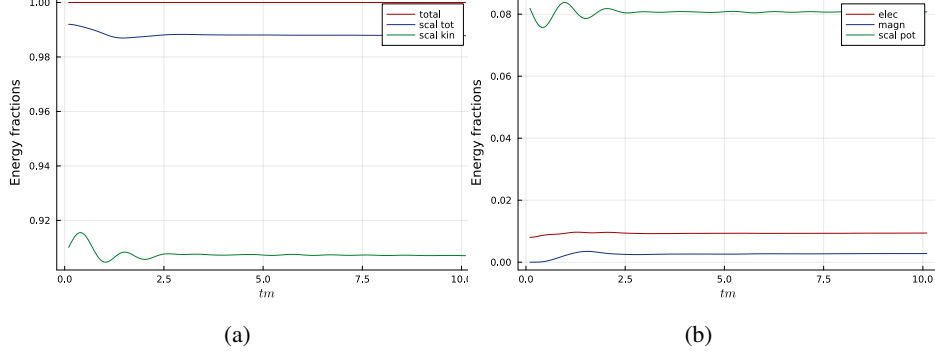
(a)

(b)

Figure 7.5: Ratio of the classical-statistical scalar kinetic and total scalar energies relative to the total energy of the system (a) and the corresponding ratios for the electric, magnetic and scalar potential energies (b).

For the 2PI effective action, the energy-momentum tensor is given by

$$T_{\mu\nu}(x) = -\frac{2}{\sqrt{-g(x)}}\frac{\delta\Gamma}{\delta g^{\mu\nu}(x)}. \tag{7.92}$$

where some useful variational identities include

$$\frac{\delta\sqrt{-g(z)}}{\delta g^{\mu\nu}(x)} = -\frac{1}{2}\sqrt{-g(z)}g_{\mu\nu}(z)\delta^{(4)}(z-x), \tag{7.93}$$

$$\frac{\delta g^{\rho\kappa}(z)}{\delta g^{\mu\nu}(x)} = \frac{1}{2}[\delta^\rho_\mu\delta^\kappa_\nu + \delta^\kappa_\mu\delta^\rho_\nu]\delta^{(4)}(z-x), \tag{7.94}$$

$$\frac{\delta g_{\rho\lambda}(z)}{\delta g^{\mu\nu}(x)} = -\frac{1}{2}[g_{\mu\rho}g_{\nu\lambda} + g_{\mu\lambda}g_{\nu\rho}](z)\delta^{(4)}(z-x). \tag{7.95}$$

With vanishing mean field, the contributions to the energy density are

$$\begin{aligned}T_{00}(x) = T_{00}^{1\text{loop}}(x) &+ T_{00}^{(G^2)}(x) + T_{00}^{(GD)}(x) \\ &+ T_{00}^{(D^2)}(x) + T_{00}^{(D^2G)}(x) + T_{00}^{(D^3)}(x),\end{aligned} \tag{7.96}$$

for each diagrammatic contribution to (7.4). In terms of isotropic com-

ponents, we obtain for the one-loop terms in (7.2),

$$
T_{00}^{\text{1loop}}(t) = \frac{1}{2} \int_{\mathbf{p}} \Big[(\partial_t \partial_{t'} + \mathbf{p} + m^2) G_{(F)}(t, t'; \mathbf{p})
$$
$$
+ (d-1)(\partial_t \partial_{t'} + \mathbf{p}) D_{(F)}^{\perp}(t, t'; \mathbf{p}) + \partial_t \partial_{t'} D_{(F)}^{\parallel}(t, t'; \mathbf{p}) \Big]_{t=t'}.
$$
(7.97)

The local two-loop diagrams contribute to the energy density with

$$
T_{00}^{(G^2)}(t) = 2\lambda \left(\int_{\mathbf{p}} G_{(F)}(t, t; \mathbf{p}) \right)^2 , \tag{7.98}
$$

$$
T_{00}^{(GD)}(t) = \frac{g^2}{2} \int_{\mathbf{p}} \Big[(d-1) D_{(F)}^{\perp}(t, t; \mathbf{p}) + D_{(F)}^{\parallel}(t, t; \mathbf{p}) \Big] \int_{\mathbf{q}} G_{(F)}(t, t; \mathbf{q}),
$$
(7.99)

$$
T_{00}^{(D^2)}(t) = \frac{1}{4} \int_{\mathbf{p}} \Big[(d-1) \Pi_{(F)}^{(D^2)\perp} D_{(F)}^{\perp} + \Pi_{(F)}^{(D^2)\parallel} D_{(F)}^{\parallel} \Big] (t, t; \mathbf{p}) \tag{7.100}
$$

and the non-local ones with

$$
T_{00}^{(D^2 G)}(t) = \int_0^t \mathrm{d}t' \int_{\mathbf{p}} \Big[(d-1) \left(\Pi_{(F)}^{(G^2 D)\perp} D_{(\rho)}^{\perp} + \Pi_{(\rho)}^{(G^2 D)\perp} D_{(F)}^{\perp} \right)
$$
$$
+ \Pi_{(F)}^{(G^2 D)\parallel} D_{(\rho)}^{\parallel} + \Pi_{(\rho)}^{(G^2 D)\parallel} D_{(F)}^{\parallel} \Big] (t, t'; |\mathbf{p}|), \tag{7.101}
$$

$$
T_{00}^{(D^3)}(t) = \frac{1}{3} \int_0^t \mathrm{d}t' \int_{\mathbf{p}} \Big[(d-1) \left(\Pi_{(F)}^{(D^3)\perp} D_{(\rho)}^{\perp} + \Pi_{(\rho)}^{(D^3)\perp} D_{(F)}^{\perp} \right)
$$
$$
+ \Pi_{(F)}^{(D^3)\parallel} D_{(\rho)}^{\parallel} + \Pi_{(\rho)}^{(D^3)\parallel} D_{(F)}^{\parallel} \Big] (t, t'; |\mathbf{p}|), \tag{7.102}
$$

where the above propagators all have the same time-momentum argument $(t, t'; |\mathbf{p}|)$.

8   Summary and outlook

In this thesis we have studied various aspects of non-equilibrium quantum field theory in early Universe applications. In this last section of the thesis we summarise our findings and discuss their implications for future research directions.

In chapter 5 we studied the effects of one-loop quantum corrections on the inflationary dynamics of a single scalar field with non-minimal coupling to gravity. We included fluctuations of the scalar inflaton field as well as scalar and tensor perturbations of the metric. By performing the field quantisation at the level of the classical action, or equivalently at the level of the classical equations of motion, we circumvented the issue of a lacking effective action description of gravity. We prescribed an MS-like renormalisation prescription and removed the logarithmic IR divergences of the correlation functions by imposing an IR cutoff to exclude the super-horizon modes. The value of the IR cutoff could then be related to the duration of inflation, as given by (5.84). The resulting quantum corrections were obtained at first order in slow-roll parameters and were found to enter the Friedmann equations differently, which implies that the standard slow-roll relations are not satisfied beyond tree level. It remains an interesting question whether a quantum generalisation of the slow-roll formalism could be established. The work considered in chapter 5 may be considered a first step in this direction.

Our results also showed one important difference between the one-loop scalar and metric tensor corrections. Namely, we found that the tensor corrections, as opposed to their scalar counterparts, are not slow-roll suppressed. All corrections are however suppressed by factors of $(H/M_{\mathrm{Pl}})^2$. We estimated the size of the quantum corrections for a sample of classical inflationary models belonging to the classes of monomial and quartic hilltop potentials. We found that the numerical coefficients of $(H/M_{\mathrm{Pl}})^2$ in the corrections for the models considered were equal or less than $\mathcal{O}(10)$, see table 5.1. Since Planck data constrain the inflationary Hubble rate to $H/M_{\mathrm{Pl}} \lesssim 2.5 \cdot 10^{-5}$ [47], this means that these corrections

are far from being observable, although it is not excluded that they could be larger for other choices of inflationary potentials. It also possible that they could be more significant in e.g. multi-field scenarios, as suggested in [229].

We computed the quantum corrected mean field and Friedmann equations using an MS-like renormalisation condition that amounted to simply discarding the UV-divergent terms, under the assumption that the UV divergences can be removed through a proper counterterm procedure. A well-defined set of counterterms could for instance be found using the method of [67] as discussed in chapter 5, by imposing renormalisation conditions on e.g. the effective potential or energy-momentum tensor. It should in principle be possible to extend this scheme to also include metric corrections, for example by imposing the renormalisation condition in (3.52) for the non-minimally coupled model considered in chapter 5.

A perhaps more pressing concern is the appropriate treatment of the IR divergences. The loop calculation for matter fields can be improved by e.g. a 2PI resummation truncated at leading order, which also can be renormalised by means of the method of [67], or using the 2PI renormalisation scheme developed in [125] or its alternative approach used in [139]. The renormalisation of an NLO-resummed theory on curved spacetimes has to our knowledge not yet been performed. As for the metric loop corrections, it remains unclear what a resummation procedure would look like, although see e.g. [72, 230] for attempts in this direction.

It was suggested in [38, 39] that the IR effective dynamics of scalar fields during inflation can be modelled by a stochastic evolution. In this picture, the IR modes experience a damping force proportional to the Hubble rate and an influence of the (free) UV modes in the form of a stochastic noise. In chapter 6 we revisited the quantum field theoretical foundations of this approach and emphasised the underlying assumptions and approximations needed to arrive at its standard formulation. In particular, we showed by partitioning the IR and UV modes by means of a general window function at the level of the path integral how effective stochastic evolution equations can be obtained. In the the standard formulation the mode separation is made in momentum space by means of

a step window function. This choice can be argued to be unphysical in configuration space, where it corresponds to a function that is not positive semi-definite and fails to reproduce the correct long-distance behaviour of the IR correlations. This was first pointed out in [195] where the authors also remarked that smooth window functions does not suffer from this problem.

The effective stochastic evolution equations include in general a dissipative term not present in the standard formulation, and we were able to demonstrate its (parametric and absolute) suppression compared to the noise term. In the analysis that followed we paid extra attention to the noise amplitude, which enter into observable n-point functions. As one might expect, when considering an alternative window function that differs from the conventional step function, the resulting noise is not white and the amplitude is in general different from the standard value $9H^5/4\pi^2$ (corresponding to $H^3/4\pi^2$ in the slow-roll approximated standard expression). A perhaps more surprising finding was that when the smooth window functions considered approached the asymptotic shape of the step function, that was also located far in the IR, the amplitude of the noise approached the value $9H^5/4\pi^2$. This occurred even though the noise correlations, while localised, did not correspond to white noise in a strict sense. The asymptotic standard noise amplitude $9H^5/4\pi^2$ was recovered for small values of all the ingoing parameters considered: the location and steepness of the window function, the mass and slow-roll parameters, but also in a specific order. Namely, we found the necessary hierarchy of small parameters to be $\epsilon_H, \epsilon_M \ll \sigma < \mu \ll 1$, with σ being the steepness and μ the location of the window function.

As a consequence, our results indicate that the stochastic inflation formalism can only confidently be said to be a valid approximation for the zero mode. It can therefore be used to derive the value of an IR regulator, but care should be exercised when applying this formalism to physical scenarios. Nevertheless, due to the computational and conceptual simplicity of the stochastic approach, it is of interest to find more precise quantitative estimates on its region of validity. This could be done by performing analytical comparisons with resummed quantum field theory

or numerical simulations. Progress in this direction has been made in e.g. [172], which involved a favourable two-loop diagrammatic comparison of the leading IR contributions to the variance found using the stochastic approach and resummed field theory. Another exciting route would be to attempt a simulation of 2PI dynamics and compare its late-time evolution with the stochastic dynamics. However, performing longer simulations that also include an evolving scale factor are likely to be computationally expensive, as was pointed out in [75]. A compromise could be to perform the evolution for a number of fixed values of the scale factor and interpolate the results. This issue is left for future research.

In chapter 7 we revisited the 2PI formulation for gauge theories in the case of a two-loop truncation of SU(2)-Higgs theory in the symmetric phase $\phi = 0$. The truncation of the 2PI effective action breaks gauge symmetry, for which a residual gauge-fixing dependence is expected to appear at the earliest at next-to-truncation order, as reviewed in chapter 4. We set out on a path to compare the real-time evolution of this system with a classical-statistical simulation set in temporal gauge. With this choice of gauge, only the spatial components of the gauge field propagators are non-zero which simplifies the analytical expressions considerably. A possible drawback of this choice of gauge is that the residual gauge-dependence becomes more implicit, as there is no gauge-fixing parameter to vary. Instead we must resort to comparing the parameter dependence of the two solutions. In addition, while gauge invariance is reflected by the Gauss constraint in the classical-statistical simulation, there is no corresponding constraint to impose on the propagators of the 2PI formalism. This is because the Ward (or Slanov-Taylor) identities in the 2PI framework does not impose any constraints on the propagator. The fields in the classical-statistical simulation are initialised as solutions of the Gauss constraint using Monte-Carlo sampling, and the average of these solutions are then used in the initialisation of the 2PI propagators.

We presented preliminary results for the (naively discretised) evolution of the statistical Higgs propagator obtained from the leading order truncation of the 2PI effective action, as the NLO results are still pending. While it is too early to make quantitative statements about residual

the gauge dependence, the 2PI and classical-statistical evolution of the Higgs propagator display a similar qualitative behaviour for the initial conditions and parameter choices considered. More statistics, consistency checks, and likely an inclusion of new lattice artefact diagrams for the 2PI evolution are required in order to make quantitative comparisons. We remain hopeful that these efforts will prove to be worthwhile. If the gauge-dependence turns out to be under control, this paves the way for numerous applications. Examples include electroweak symmetry breaking and thermalisation. The many available results from classical-statistical simulations would make good sources of comparison.

Finally, a few remarks on black hole evaporation. It is possible that numerical evidence for Hawking radiation following the collapse of a quantum field (in four dimensions) can be found also without proper regularisation of the correlator. For instance in [231] acoustic black holes in Bose-Einstein condensates was simulated and the results displayed (negative) correlations between Bogoliubov phonons located on opposite sides of the sonic horizon. Since the counterterms in a renormalisation scheme employing point-splitting regularisation are purely geometric quantities, as they are based on the expansion (3.35), then correlations $\langle \phi(x)\phi(y) \rangle$ for points x and y separated by the horizon could be detectable also away from the coincidence limit. This quest for detecting Hawking radiation following gravitational collapse of a quantum field is currently being pursued as a separate project.

In conclusion, the field of non-perturbative quantum field theory applied to early Universe scenarios offers exciting possibilities for future advancements. Non-equilibrium techniques offer robust means to carefully examine theories beyond the Standard Model and assess their potential effects on cosmological and astroparticle observables.

References

[1] Lev Kofman, Andrei D. Linde, and Alexei A. Starobinsky. Reheating after inflation. *Phys. Rev. Lett.*, 73:3195–3198, 1994.

[2] Lev Kofman, Andrei D. Linde, and Alexei A. Starobinsky. Towards the theory of reheating after inflation. *Phys. Rev. D*, 56:3258–3295, 1997.

[3] Tanguy Altherr and David Seibert. Problems of perturbation series in nonequilibrium quantum field theories. *Phys. Lett. B*, 333:149–152, 1994.

[4] Carsten Greiner and Stefan Leupold. Interpretation and resolution of pinch singularities in nonequilibrium quantum field theory. *Eur. Phys. J. C*, 8:517–522, 1999.

[5] Freeman J. Dyson. The S matrix in quantum electrodynamics. *Phys. Rev.*, 75:1736–1755, 1949.

[6] Julian S. Schwinger. On the Green's functions of quantized fields. 1. *Proc. Nat. Acad. Sci.*, 37:452–455, 1951.

[7] Julian S. Schwinger. On the Green's functions of quantized fields. 2. *Proc. Nat. Acad. Sci.*, 37:455–459, 1951.

[8] Reinhard Alkofer and Lorenz von Smekal. The Infrared behavior of QCD Green's functions: Confinement dynamical symmetry breaking, and hadrons as relativistic bound states. *Phys. Rept.*, 353:281, 2001.

[9] Craig D. Roberts and Anthony G. Williams. Dyson-Schwinger equations and their application to hadronic physics. *Prog. Part. Nucl. Phys.*, 33:477–575, 1994.

[10] Gerard 't Hooft. A Planar Diagram Theory for Strong Interactions. *Nucl. Phys. B*, 72:461, 1974.

[11] Christof Wetterich. Exact evolution equation for the effective potential. *Phys. Lett. B*, 301:90–94, 1993.

[12] Tim R. Morris. The Exact renormalization group and approximate solutions. *Int. J. Mod. Phys. A*, 9:2411–2450, 1994.

[13] C. Bagnuls and C. Bervillier. Exact renormalization group equations. An Introductory review. *Phys. Rept.*, 348:91, 2001.

[14] Jürgen Berges, Nikolaos Tetradis, and Christof Wetterich. Nonperturbative renormalization flow in quantum field theory and statistical physics. *Phys. Rept.*, 363:223–386, 2002.

[15] Jan M. Pawlowski. Aspects of the functional renormalisation group. *Annals Phys.*, 322:2831–2915, 2007.

[16] Holger Gies. Introduction to the functional RG and applications to gauge theories. *Lect. Notes Phys.*, 852:287–348, 2012.

[17] Nicolas Dupuis, Léonie Canet, Astrid Eichhorn, Walter Metzner, Jan M. Pawlowski, Matthieu Tissier, and Nicolás Wschebor. The nonperturbative functional renormalization group and its applications. *Phys. Rept.*, 910:1–114, 2021.

[18] Christof Gattringer and Kurt Langfeld. Approaches to the sign problem in lattice field theory. *Int. J. Mod. Phys. A*, 31(22):1643007, 2016.

[19] David Seery. One-loop corrections to a scalar field during inflation. *JCAP*, 11:025, 2007.

[20] Bei-Lok Hu. Infrared Behavior of Quantum Fields in Inflationary Cosmology – Issues and Approaches: an overview. 12 2018.

[21] Mustafa A. Amin, Mark P. Hertzberg, David I. Kaiser, and Johanna Karouby. Nonperturbative Dynamics Of Reheating After Inflation: A Review. *Int. J. Mod. Phys. D*, 24:1530003, 2014.

[22] Mark B. Hindmarsh, Marvin Lüben, Johannes Lumma, and Martin Pauly. Phase transitions in the early universe. *SciPost Phys. Lect. Notes*, 24:1, 2021.

[23] Pouya Asadi and et al. Early-Universe Model Building. 3 2022.

[24] Jürgen Berges and Jurgen Cox. Thermalization of quantum fields from time reversal invariant evolution equations. *Phys. Lett. B*, 517:369–374, 2001.

[25] Jürgen Berges, Szabolcs Borsanyi, and Julien Serreau. Thermalization of fermionic quantum fields. *Nucl. Phys. B*, 660:51–80, 2003.

[26] Sascha Juchem, Wolfgang Cassing, and Carsten Greiner. Quantum dynamics and thermalization for out-of-equilibrium phi**4 theory. *Phys. Rev. D*, 69:025006, 2004.

[27] Jürgen Berges, Szabolcs Borsanyi, and Christof Wetterich. Prethermalization. *Phys. Rev. Lett.*, 93:142002, 2004.

[28] Manfred Lindner and Markus Michael Muller. Comparison of Boltzmann equations with quantum dynamics for scalar fields. *Phys. Rev. D*, 73:125002, 2006.

[29] Jürgen Berges. Introduction to nonequilibrium quantum field theory. *AIP Conf. Proc.*, 739(1):3–62, 2004.

References

[30] Jürgen Berges, Michal P. Heller, Aleksas Mazeliauskas, and Raju Venugopalan. QCD thermalization: Ab initio approaches and interdisciplinary connections. *Rev. Mod. Phys.*, 93(3):035003, 2021.

[31] Alexander Branschadel and Thomas Gasenzer. 2PI nonequilibrium versus transport equations for an ultracold Bose gas. *J. Phys. B*, 41:135302, 2008.

[32] Joaquin M. Luttinger and John Clive Ward. Ground state energy of a many fermion system. 2. *Phys. Rev.*, 118:1417–1427, 1960.

[33] Gordon Baym. Self-consistent approximations in many-body systems. *Phys. Rev.*, 127:1391–1401, Aug 1962.

[34] Cyrano de Dominicis and Paul C. Martin. Stationary Entropy Principle and Renormalization in Normal and Superfluid Systems. I. Algebraic Formulation. *J. Math. Phys.*, 5:14–30, 1964.

[35] John M. Cornwall, R. Jackiw, and E. Tomboulis. Effective Action for Composite Operators. *Phys. Rev. D*, 10:2428–2445, 1974.

[36] Alejandro Arrizabalaga and Jan Smit. Gauge fixing dependence of Φ-derivable approximations. *Phys. Rev. D*, 66:065014, 2002.

[37] Margaret E. Carrington, Gabor Kunstatter, and Haitham Zaraket. 2PI effective action and gauge invariance problems. *Eur. Phys. J. C*, 42:253–259, 2005.

[38] Alexei A. Starobinsky. Stochastic de sitter (inflationary) stage in the early universe. *Lect. Notes Phys.*, 246:107–126, 1986.

[39] Alexei A. Starobinsky and Junichi Yokoyama. Equilibrium state of a selfinteracting scalar field in the De Sitter background. *Phys. Rev. D*, 50:6357–6368, 1994.

[40] Edward W. Kolb and Michael S. Turner. *The Early Universe*. Frontiers in physics. Addison-Wesley, 1990.

[41] Andrew R. Liddle and David H. Lyth. *Cosmological Inflation and Large-Scale Structure*. Cambridge University Press, paperback edition, 4 2000.

[42] Steven Weinberg. *Cosmology*. Oxford University Press, hardcover edition, 4 2008.

[43] Antonio Riotto. Inflation and the theory of cosmological perturbations. *ICTP Lect. Notes Ser.*, 14:317–413, 2003.

[44] Nicholas D. Birrell and Paul C. W. Davies. *Quantum Fields in Curved Space*. Cambridge Monographs on Mathematical Physics. Cambridge Univ. Press, Cambridge, UK, 2 1984.

References

[45] Viatcheslav Mukhanov and Sergei Winitzki. *Introduction to quantum effects in gravity*. Cambridge University Press, 6 2007.

[46] Daniel Baumann. *Cosmology*. Cambridge University Press, 6 2022.

[47] Nabila Aghanim et al. Planck 2018 results. VI. Cosmological parameters. *Astron. Astrophys.*, 641:A6, 2020. [Erratum: Astron.Astrophys. 652, C4 (2021)].

[48] Arjun Berera and Li-Zhi Fang. Thermally induced density perturbations in the inflation era. *Phys. Rev. Lett.*, 74:1912–1915, 1995.

[49] Arjun Berera. Interpolating the stage of exponential expansion in the early universe: A Possible alternative with no reheating. *Phys. Rev. D*, 55:3346–3357, 1997.

[50] Mar Bastero-Gil and Arjun Berera. Warm inflation model building. *Int. J. Mod. Phys. A*, 24:2207–2240, 2009.

[51] Hideo Kodama and Misao Sasaki. Cosmological Perturbation Theory. *Prog. Theor. Phys. Suppl.*, 78:1–166, 1984.

[52] Scott Dodelson. *Modern Cosmology*. Academic Press, Elsevier Science, 2003.

[53] Pavel D. Naselsky, Dmitry I. Novikov, and Igor D. Novikov. *The Physics of the Cosmic Microwave Background*. Cambridge Astrophysics. Cambridge University Press, 2006.

[54] Ruth Durrer. *The Cosmic Microwave Background*. Cambridge University Press, 2 edition, 2020.

[55] Yashar Akrami et al. Planck 2018 results. IX. Constraints on primordial non-Gaussianity. *Astron. Astrophys.*, 641:A9, 2020.

[56] Juan Martin Maldacena. Non-Gaussian features of primordial fluctuations in single field inflationary models. *JHEP*, 05:013, 2003.

[57] Nicola Bartolo, Eiichiro Komatsu, Sabino Matarrese, and Antonio Riotto. Non-Gaussianity from inflation: Theory and observations. *Phys. Rept.*, 402:103–266, 2004.

[58] G. I. Rigopoulos, E. P. S. Shellard, and B. J. W. van Tent. Large non-Gaussianity in multiple-field inflation. *Phys. Rev. D*, 73:083522, 2006.

[59] Thorsten Battefeld and Richard Easther. Non-Gaussianities in Multi-field Inflation. *JCAP*, 03:020, 2007.

[60] David J. Toms. The Effective Action and the Renormalization Group Equation in Curved Space-time. *Phys. Lett. B*, 126:37–40, 1983.

[61] Klaus Kirsten, Guido Cognola, and Luciano Vanzo. Effective Lagrangian for selfinteracting scalar field theories in curved space-time. *Phys. Rev. D*, 48:2813–2822, 1993.

[62] Emilio Elizalde and Sergei D. Odintsov. Renormalization group improved effective Lagrangian for interacting theories in curved space-time. *Phys. Lett. B*, 321:199–204, 1994.

[63] Eduard V. Gorbar and Ilya L. Shapiro. Renormalization group and decoupling in curved space. *JHEP*, 02:021, 2003.

[64] Eduard V. Gorbar and Ilya L. Shapiro. Renormalization group and decoupling in curved space. 2. The Standard model and beyond. *JHEP*, 06:004, 2003.

[65] Eduard V. Gorbar and Ilya L. Shapiro. Renormalization group and decoupling in curved space. 3. The Case of spontaneous symmetry breaking. *JHEP*, 02:060, 2004.

[66] Tommi Markkanen and Anders Tranberg. Quantum Corrections to Inflaton and Curvaton Dynamics. *JCAP*, 11:027, 2012.

[67] Tommi Markkanen and Anders Tranberg. A Simple Method for One-Loop Renormalization in Curved Space-Time. *JCAP*, 08:045, 2013.

[68] Matti Herranen, Tommi Markkanen, Sami Nurmi, and Arttu Rajantie. Spacetime curvature and the Higgs stability during inflation. *Phys. Rev. Lett.*, 113(21):211102, 2014.

[69] Matti Herranen, Tommi Markkanen, and Anders Tranberg. Quantum corrections to scalar field dynamics in a slow-roll space-time. *JHEP*, 05:026, 2014.

[70] David Seery. Infrared effects in inflationary correlation functions. *Class. Quant. Grav.*, 27:124005, 2010.

[71] Martin S. Sloth. On the one loop corrections to inflation and the CMB anisotropies. *Nucl. Phys. B*, 748:149–169, 2006.

[72] Antonio Riotto and Martin S. Sloth. On Resumming Inflationary Perturbations beyond One-loop. *JCAP*, 04:030, 2008.

[73] Arvind Rajaraman. On the proper treatment of massless fields in Euclidean de Sitter space. *Phys. Rev. D*, 82:123522, 2010.

[74] Julien Serreau. Effective potential for quantum scalar fields on a de Sitter geometry. *Phys. Rev. Lett.*, 107:191103, 2011.

[75] Anders Tranberg. Quantum field thermalization in expanding backgrounds. *JHEP*, 11:037, 2008.

[76] Matti Herranen, Asgeir Osland, and Anders Tranberg. Quantum corrections to inflaton dynamics: The semiclassical approach and the semiclassical limit. *Phys. Rev. D*, 92(8):083530, 2015.

[77] H. Lehmann, K. Symanzik, and W. Zimmermann. Zur Formulierung quantisierter Feldtheorien. *Nuovo Cimento*, 1:205–25, 1955.

[78] Michael E. Peskin and Daniel V. Schroeder. *An Introduction to quantum field theory*. Addison-Wesley, Reading, USA, 1995.

[79] Julian S. Schwinger. Brownian motion of a quantum oscillator. *J. Math. Phys.*, 2:407–432, 1961.

[80] Leonid V. Keldysh. Diagram technique for nonequilibrium processes. *Zh. Eksp. Teor. Fiz.*, 47:1515–1527, 1964.

[81] Takeo Matsubara. A New approach to quantum statistical mechanics. *Prog. Theor. Phys.*, 14:351–378, 1955.

[82] Jørgen Rammer. *Quantum Field Theory of Non-equilibrium States*. Cambridge University Press, 2007.

[83] Alex Kamenev. *Field Theory of Non-Equilibrium Systems*. Cambridge University Press, 2011.

[84] Joseph I. Kapusta and Charles Gale. *Finite-Temperature Field Theory: Principles and Applications*. Cambridge Monographs on Mathematical Physics. Cambridge University Press, 2 edition, 2006.

[85] Michel Le Bellac. *Thermal Field Theory*. Cambridge Monographs on Mathematical Physics. Cambridge University Press, 3 2011.

[86] Jürgen Berges. Nonequilibrium Quantum Fields: From Cold Atoms to Cosmology. 3 2015.

[87] Bryce S. DeWitt. Dynamical theory of groups and fields. *Conf. Proc. C*, 630701:585–820, 1964.

[88] Ian Jack and Leonard Parker. Proof of Summed Form of Proper Time Expansion for Propagator in Curved Space-time. *Phys. Rev. D*, 31:2439, 1985.

[89] Peter B. Gilkey. The Spectral geometry of a Riemannian manifold. *J. Diff. Geom.*, 10(4):601–618, 1975.

[90] Ivan G. Avramidi. The Covariant technique for the calculation of the heat kernel asymptotic expansion. *Phys. Lett. B*, 238:92–97, 1990.

[91] Leonard Parker and David J. Toms. New form for the coincidence limit of the feynman propagator, or heat kernel, in curved spacetime. *Phys. Rev. D*, 31:953–956, Feb 1985.

[92] Timothy S. Bunch and Paul C. W. Davies. Quantum Field Theory in de Sitter Space: Renormalization by Point Splitting. *Proc. Roy. Soc. Lond. A*, 360:117–134, 1978.

[93] Sidney R. Coleman and Erick J. Weinberg. Radiative Corrections as the Origin of Spontaneous Symmetry Breaking. *Phys. Rev. D*, 7:1888–1910, 1973.

[94] Timothy S. Bunch. Adiabatic regularisation for scalar fields with arbitrary coupling to the scalar curvature. *J. Phys. A*, 13:1297–1310, 1980.

[95] Juan Pablo Paz and Francisco D. Mazzitelli. Renormalized Evolution Equations for the Back Reaction Problem With a Selfinteracting Scalar Field. *Phys. Rev. D*, 37:2170–2181, 1988.

[96] Stephen W. Hawking. Particle Creation by Black Holes. *Commun. Math. Phys.*, 43:199–220, 1975. [Erratum: Commun.Math.Phys. 46, 206 (1976)].

[97] Philip Candelas and Kenneth W. Howard. Vacuum $\langle \varphi^2 \rangle$ in Schwarzschild spacetime. *Phys. Rev. D*, 29:1618–1625, 1984.

[98] Kenneth W. Howard. Vacuum $\langle T_\mu{}^\nu \rangle$ in schwarzschild spacetime. *Phys. Rev. D*, 30:2532–2547, Dec 1984.

[99] Paul R. Anderson. A method to compute $<\varphi^2>$ in asymptotically flat, static, spherically symmetric spacetimes. *Phys. Rev. D*, 41:1152–1162, Feb 1990.

[100] Paul R. Anderson, William A. Hiscock, and David A. Samuel. Stress-energy tensor of quantized scalar fields in static spherically symmetric spacetimes. *Phys. Rev. D*, 51:4337–4358, Apr 1995.

[101] Steven M. Christensen. Vacuum expectation value of the stress tensor in an arbitrary curved background: The covariant point-separation method. *Phys. Rev. D*, 14:2490–2501, Nov 1976.

[102] Adam Levi and Amos Ori. Pragmatic mode-sum regularization method for semiclassical black-hole spacetimes. *Phys. Rev. D*, 91:104028, 2015.

[103] Adam Levi and Amos Ori. Mode-sum regularization of $\langle \phi^2 \rangle$ in the angular-splitting method. *Phys. Rev. D*, 94(4):044054, 2016.

[104] Paul R. Anderson, Shohreh Gholizadeh Siahmazgi, Raymond D. Clark, and Alessandro Fabbri. Method to compute the stress-energy tensor for a quantized scalar field when a black hole forms from the collapse of a null shell. *Phys. Rev. D*, 102(12):125035, 2020.

[105] Shohreh Gholizadeh Siahmazgi, Paul R. Anderson, Raymond D. Clark, and Alessandro Fabbri. Stress-energy tensor for a quantized scalar field in a four-dimensional black hole that forms from the collapse of a null shell. In *16th Marcel Grossmann Meeting on Recent Developments in Theoretical and*

Experimental General Relativity, Astrophysics and Relativistic Field Theories, 11 2021.

[106] Demetrios Christodoulou. The Problem of a Selfgravitating Scalar Field. *Commun. Math. Phys.*, 105:337–361, 1986.

[107] Demetrios Christodoulou. A Mathematical Theory of Gravitational Collapse. *Commun. Math. Phys.*, 109:613–647, 1987.

[108] Dalia S. Goldwirth and Tsvi Piran. Gravitational collapse of massless scalar field and cosmic censorship. *Phys. Rev. D*, 36:3575–3581, Dec 1987.

[109] Matthew W. Choptuik. Universality and scaling in gravitational collapse of a massless scalar field. *Phys. Rev. Lett.*, 70:9–12, Jan 1993.

[110] Patrick R. Brady. Analytic example of critical behaviour in scalar field collapse. *Class. Quant. Grav.*, 11(5):1255–1260, 1994.

[111] Yoshimi Oshiro, Kouji Nakamura, and Akira Tomimatsu. Critical behavior of black hole formation in a scalar wave collapse. *Prog. Theor. Phys.*, 91:1265–1270, 1994.

[112] Michael Pürrer, Sascha Husa, and Peter C. Aichelburg. News from critical collapse: Bondi mass, tails, and quasinormal modes. *Phys. Rev. D*, 71:104005, May 2005.

[113] Carsten Gundlach and Jose M. Martin-Garcia. Critical phenomena in gravitational collapse. *Living Rev. Rel.*, 10:5, 2007.

[114] Benjamin Berczi, Paul M. Saffin, and Shuang-Yong Zhou. Gravitational collapse with quantum fields. *Phys. Rev. D*, 104(4):L041703, 2021.

[115] Benjamin Berczi, Paul M. Saffin, and Shuang-Yong Zhou. Gravitational collapse of quantum fields and Choptuik scaling. *JHEP*, 02:183, 2022.

[116] Jana N. Guenther, Christian Hoelbling, and Lukas Varnhorst. Semiclassical gravitational collapse of a radially symmetric massless scalar quantum field. *Phys. Rev. D*, 105(10):105010, 2022.

[117] Jürgen Berges and Julien Serreau. Parametric resonance in quantum field theory. *Phys. Rev. Lett.*, 91:111601, 2003.

[118] Alejandro Arrizabalaga, Jan Smit, and Anders Tranberg. Tachyonic preheating using 2PI-1/N dynamics and the classical approximation. *JHEP*, 10:017, 2004.

[119] Mathias Garny and Markus Michael Muller. Kadanoff-Baym Equations with Non-Gaussian Initial Conditions: The Equilibrium Limit. *Phys. Rev. D*, 80:085011, 2009.

[120] Gert Aarts and Jan Smit. Classical approximation for time dependent quantum field theory: Diagrammatic analysis for hot scalar fields. *Nucl. Phys. B*, 511:451–478, 1998.

[121] Fred Cooper, Avinash Khare, and Harvey Rose. Classical limit of time dependent quantum field theory: A Schwinger-Dyson approach. *Phys. Lett. B*, 515:463–469, 2001.

[122] Gert Aarts, Gian Franco Bonini, and Christof Wetterich. Exact and truncated dynamics in nonequilibrium field theory. *Phys. Rev. D*, 63:025012, 2001.

[123] Gert Aarts and Jürgen Berges. Classical aspects of quantum fields far from equilibrium. *Phys. Rev. Lett.*, 88:041603, 2002.

[124] Gert Aarts, Nathan Laurie, and Anders Tranberg. Effective convergence of the 2PI-1/N expansion for nonequilibrium quantum fields. *Phys. Rev. D*, 78:125028, 2008.

[125] Hendrik van Hees and Joern Knoll. Renormalization in selfconsistent approximations schemes at finite temperature. 1. Theory. *Phys. Rev. D*, 65:025010, 2002.

[126] Hendrik Van Hees and Joern Knoll. Renormalization of selfconsistent approximation schemes. 2. Applications to the sunset diagram. *Phys. Rev. D*, 65:105005, 2002.

[127] John C. Collins. *Renormalization: An Introduction to Renormalization, The Renormalization Group, and the Operator Product Expansion*, volume 26 of *Cambridge Monographs on Mathematical Physics*. Cambridge University Press, Cambridge, 1986.

[128] Anthony Duncan. *The Conceptual Framework of Quantum Field Theory*. Oxford University Press, 8 2012.

[129] Hendrik van Hees and Joern Knoll. Renormalization in selfconsistent approximation schemes at finite temperature. 3. Global symmetries. *Phys. Rev. D*, 66:025028, 2002.

[130] Jean-Paul Blaizot, Edmond Iancu, and Urko Reinosa. Renormalizability of Φ-derivable approximations in scalar φ^4 theory. *Phys. Lett. B*, 568:160–166, 2003.

[131] Jean-Paul Blaizot, Edmond Iancu, and Urko Reinosa. Renormalization of Phi derivable approximations in scalar field theories. *Nucl. Phys. A*, 736:149–200, 2004.

[132] Jürgen Berges, Szabolcs Borsanyi, Urko Reinosa, and Julien Serreau. Renormalized thermodynamics from the 2PI effective action. *Phys. Rev. D*, 71:105004, 2005.

[133] Jürgen Berges, Szabolcs Borsanyi, Urko Reinosa, and Julien Serreau. Nonperturbative renormalization for 2PI effective action techniques. *Annals Phys.*, 320:344–398, 2005.

[134] Urko Reinosa. Nonperturbative renormalization of phi-derivable approximations in theories with fermions. *Nucl. Phys. A*, 772:138–166, 2006.

[135] Urko Reinosa and Julien Serreau. 2PI effective action for gauge theories: Renormalization. *JHEP*, 07:028, 2006.

[136] Urko Reinosa and Julien Serreau. Ward Identities for the 2PI effective action in QED. *JHEP*, 11:097, 2007.

[137] Urko Reinosa and Julien Serreau. 2PI functional techniques for gauge theories: QED. *Annals Phys.*, 325:969–1017, 2010.

[138] Gergely Fejos, Andras Patkos, and Zsolt Szep. Renormalisability of the 2PI-Hartree approximation of multicomponent scalar models in the broken symmetry phase. *Nucl. Phys. A*, 803:115–135, 2008.

[139] Takashi Arai. Renormalization of the 2PI Hartree-Fock approximation on de Sitter background in the broken phase. *Phys. Rev. D*, 86:104064, 2012.

[140] Yu. B. Ivanov, Felix Riek, and Joern Knoll. Gapless Hartree-Fock resummation scheme for the O(N) model. *Phys. Rev. D*, 71:105016, 2005.

[141] Stefan Leupold. Selfconsistent approximations, symmetries and choice of representation. *Phys. Lett. B*, 646:155–164, 2007.

[142] Urko Reinosa. 2PI renormalized effective action for gauge theories. *Nucl. Phys. A*, 785:230–233, 2007.

[143] Szabolcs Borsanyi and Urko Reinosa. The Pressure of QED from the two-loop 2PI effective action. *Phys. Lett. B*, 661:88–94, 2008.

[144] Gergely Fejos and Zsolt Szep. Broken symmetry phase solution of the ϕ^4 model at two-loop level of the Φ-derivable approximation. *Phys. Rev. D*, 84:056001, 2011.

[145] N. K. Nielsen. On the Gauge Dependence of Spontaneous Symmetry Breaking in Gauge Theories. *Nucl. Phys. B*, 101:173–188, 1975.

[146] David H. Lyth and Andrew R. Liddle. *The Primordial Density Perturbation: Cosmology, Inflation and the Origin of Structure*. Cambridge University Press, 2009.

[147] Yashar Akrami et al. Planck 2018 results. X. Constraints on inflation. *Astron. Astrophys.*, 641:A10, 2020.

References

[148] Leonard Parker and David Toms. *Quantum Field Theory in Curved Space-time: Quantized Fields and Gravity*. Cambridge Monographs on Mathematical Physics. Cambridge University Press, 2009.

[149] Matti Herranen, Andreas Hohenegger, Asgeir Osland, and Anders Tranberg. Quantum corrections to inflation: the importance of RG-running and choosing the optimal RG-scale. *Phys. Rev. D*, 95(2):023525, 2017.

[150] Ante Bilandzic and Tomislav Prokopec. Quantum radiative corrections to slow-roll inflation. *Phys. Rev. D*, 76:103507, 2007.

[151] Nicola Bartolo, Sabino Matarrese, Massimo Pietroni, Antonio Riotto, and David Seery. On the Physical Significance of Infra-red Corrections to Inflationary Observables. *JCAP*, 01:015, 2008.

[152] Nicholas C. Tsamis and Richard P. Woodard. Stochastic quantum gravitational inflation. *Nucl. Phys. B*, 724:295–328, 2005.

[153] Florian Gautier and Julien Serreau. Infrared dynamics in de Sitter space from Schwinger-Dyson equations. *Phys. Lett. B*, 727:541–547, 2013.

[154] Florian Gautier and Julien Serreau. Scalar field correlator in de Sitter space at next-to-leading order in a 1/N expansion. *Phys. Rev. D*, 92(10):105035, 2015.

[155] Charles W. Misner, K. S. Thorne, and J. A. Wheeler. *Gravitation*. W. H. Freeman, San Francisco, 1973.

[156] Jai-Chan Hwang. Cosmological perturbations in generalized gravity theories: Formulation. *Class. Quant. Grav.*, 7:1613–1631, 1990.

[157] Jai-Chan Hwang. Cosmological perturbations in generalized gravity theories: Solutions. *Phys. Rev. D*, 42:2601–2606, Oct 1990.

[158] Paul A. M. Dirac. Generalized Hamiltonian dynamics. *Can. J. Math.*, 2:129–148, 1950.

[159] Lotfi Boubekeur and David. H. Lyth. Hilltop inflation. *JCAP*, 07:010, 2005.

[160] Eric Braaten and Robert D. Pisarski. Soft amplitudes in hot gauge theories: A general analysis. *Nuclear Physics B*, 337(3):569–634, 1990.

[161] Matti Herranen, Tommi Markkanen, Sami Nurmi, and Arttu Rajantie. Spacetime curvature and Higgs stability after inflation. *Phys. Rev. Lett.*, 115:241301, 2015.

[162] Meindert van der Meulen and Jan Smit. Classical approximation to quantum cosmological correlations. *JCAP*, 11:023, 2007.

201

[163] Julien Serreau and Renaud Parentani. Nonperturbative resummation of de Sitter infrared logarithms in the large-N limit. *Phys. Rev. D*, 87:085012, 2013.

[164] Takashi Arai. Nonperturbative Infrared Effects for Light Scalar Fields in de Sitter Space. *Class. Quant. Grav.*, 29:215014, 2012.

[165] Diana L. Lopez Nacir, Francisco D. Mazzitelli, and Leonardo G. Trombetta. Hartree approximation in curved spacetimes revisited: The effective potential in de Sitter spacetime. *Phys. Rev. D*, 89:024006, 2014.

[166] Julien Serreau. Renormalization group flow and symmetry restoration in de Sitter space. *Phys. Lett. B*, 730:271–274, 2014.

[167] Martin Beneke and Paul Moch. On "dynamical mass" generation in Euclidean de Sitter space. *Phys. Rev. D*, 87:064018, 2013.

[168] Diana López Nacir, Francisco D. Mazzitelli, and Leonardo G. Trombetta. $O(N)$ model in Euclidean de Sitter space: beyond the leading infrared approximation. *JHEP*, 09:117, 2016.

[169] Dietrich Bödeker. On the effective dynamics of soft non-Abelian gauge fields at finite temperature. *Phys. Lett. B*, 426:351–360, 1998.

[170] Archie Cable and Arttu Rajantie. Free scalar correlators in de Sitter space via the stochastic approach beyond the slow-roll approximation. *Phys. Rev. D*, 104(10):103511, 2021.

[171] Fabio Finelli, Giovanni Marozzi, Alexei A. Starobinsky, Gian Paolo Vacca, and Giovanni Venturi. Generation of fluctuations during inflation: Comparison of stochastic and field-theoretic approaches. *Phys. Rev. D*, 79:044007, 2009.

[172] Björn Garbrecht, Gerasimos Rigopoulos, and Yi Zhu. Infrared correlations in de Sitter space: Field theoretic versus stochastic approach. *Phys. Rev. D*, 89:063506, 2014.

[173] Björn Garbrecht, Florian Gautier, Gerasimos Rigopoulos, and Yi Zhu. Feynman Diagrams for Stochastic Inflation and Quantum Field Theory in de Sitter Space. *Phys. Rev. D*, 91:063520, 2015.

[174] Vakif K. Onemli. Vacuum Fluctuations of a Scalar Field during Inflation: Quantum versus Stochastic Analysis. *Phys. Rev. D*, 91:103537, 2015.

[175] Alexander Yu. Kamenshchik, Alexei A. Starobinsky, and Tereza Vardanyan. Massive scalar field in de Sitter spacetime: a two-loop calculation and a comparison with the stochastic approach. *Eur. Phys. J. C*, 82(4):345, 2022.

[176] Clifford P. Burgess, Richard Holman, and Gianmassimo Tasinato. Open EFTs, IR effects \& late-time resummations: systematic corrections in stochastic inflation. *JHEP*, 01:153, 2016.

References

[177] Hael Collins, Richard Holman, and Tereza Vardanyan. The quantum Fokker-Planck equation of stochastic inflation. *JHEP*, 11:065, 2017.

[178] Matthew Baumgart and Raman Sundrum. De Sitter Diagrammar and the Resummation of Time. *JHEP*, 07:119, 2020.

[179] G. Karakaya and Vakif K. Onemli. Quantum effects of mass on scalar field correlations, power spectrum, and fluctuations during inflation. *Phys. Rev. D*, 97(12):123531, 2018.

[180] Julien Grain and Vincent Vennin. Stochastic inflation in phase space: Is slow roll a stochastic attractor? *JCAP*, 05:045, 2017.

[181] Junsei Tokuda and Takahiro Tanaka. Statistical nature of infrared dynamics on de Sitter background. *JCAP*, 02:014, 2018.

[182] Timothy Cohen, Daniel Green, Akhil Premkumar, and Alexander Ridgway. Stochastic Inflation at NNLO. *JHEP*, 09:159, 2021.

[183] Chris Pattison, Vincent Vennin, Hooshyar Assadullahi, and David Wands. Stochastic inflation beyond slow roll. *JCAP*, 07:031, 2019.

[184] Hiroyuki Kitamoto. Infrared resummation for derivative interactions in de Sitter space. *Phys. Rev. D*, 100(2):025020, 2019.

[185] Masahiro Morikawa. Dissipation and Fluctuation of Quantum Fields in Expanding Universes. *Phys. Rev. D*, 42:1027–1034, 1990.

[186] Sabino Matarrese, Marcello A. Musso, and Antonio Riotto. Influence of superhorizon scales on cosmological observables generated during inflation. *JCAP*, 05:008, 2004.

[187] Kari Enqvist, Rose N. Lerner, Olli Taanila, and Anders Tranberg. Spectator field dynamics in de Sitter and curvaton initial conditions. *JCAP*, 10:052, 2012.

[188] Robert J. Hardwick, Vincent Vennin, Christian T. Byrnes, Jesús Torrado, and David Wands. The stochastic spectator. *JCAP*, 10:018, 2017.

[189] Tomislav Prokopec and Ewald Puchwein. Photon mass generation during inflation: de Sitter invariant case. *JCAP*, 04:007, 2004.

[190] Tomas Janssen and Tomislav Prokopec. A Graviton propagator for inflation. *Class. Quant. Grav.*, 25:055007, 2008.

[191] Ian Moss and Gerasimos Rigopoulos. Effective long wavelength scalar dynamics in de Sitter. *JCAP*, 05:009, 2017.

[192] Kuang-chao Chou, Zhao-bin Su, Bai-lin Hao, and Lu Yu. Equilibrium and Nonequilibrium Formalisms Made Unified. *Phys. Rept.*, 118:1–131, 1985.

[193] Esteban Calzetta and Bei-Lok Hu. Closed Time Path Functional Formalism in Curved Space-Time: Application to Cosmological Back Reaction Problems. *Phys. Rev. D*, 35:495, 1987.

[194] Laurence Perreault Levasseur. Lagrangian formulation of stochastic inflation: Langevin equations, one-loop corrections and a proposed recursive approach. *Phys. Rev. D*, 88(8):083537, 2013.

[195] Sergei Winitzki and Alexander Vilenkin. Effective noise in stochastic description of inflation. *Phys. Rev. D*, 61:084008, 2000.

[196] Izrail S. Gradshteyn and Iosif M. Ryzhik. *Table of integrals, series, and products*. Elsevier/Academic Press, Amsterdam, seventh edition, 2007.

[197] Ruslan L. Stratonovich. On a Method of Calculating Quantum Distribution Functions. *Soviet Physics Doklady*, 2:416, July 1957.

[198] John Hubbard. Calculation of partition functions. *Phys. Rev. Lett.*, 3:77–80, 1959.

[199] Bei-Lok Hu, Juan Pablo Paz, and Yuhong Zhang. Quantum origin of noise and fluctuations in cosmology. In *The Origin of Structure in the Universe*, 1992.

[200] Horacio Casini, Rafael Montemayor, and Pablo Sisterna. Stochastic approach to inflation. 2. Classicality, coarse graining and noises. *Phys. Rev. D*, 59:063512, 1999.

[201] Michele Liguori, Sabino Matarrese, Marcello Musso, and Antonio Riotto. Stochastic inflation and the lower multipoles in the CMB anisotropies. *JCAP*, 08:011, 2004.

[202] Alejandro Arrizabalaga, Jan Smit, and Anders Tranberg. Equilibration in phi**4 theory in 3+1 dimensions. *Phys. Rev. D*, 72:025014, 2005.

[203] Gert Aarts and Anders Tranberg. Particle creation and warm inflation. *Phys. Lett. B*, 650:65–71, 2007.

[204] Fred Cooper, John F. Dawson, and Bogdan Mihaila. Quantum dynamics of phase transitions in broken symmetry lambda phi**4 field theory. *Phys. Rev. D*, 67:056003, 2003.

[205] Mark Alford, Jürgen Berges, and Jack M. Cheyne. Critical phenomena from the two particle irreducible 1/N expansion. *Phys. Rev. D*, 70:125002, 2004.

[206] Alejandro Arrizabalaga and Urko Reinosa. Renormalized finite temperature ϕ^4 theory from the 2pi effective action. *Nuclear Physics A*, 785(1):234–237, 2007. Proceedings of the 7th International Conference on Strong and Electroweak Matter 2006.

[207] Gergely Markó, Urko Reinosa, and Zsolt Szép. Broken phase effective potential in the two-loop Φ-derivable approximation and nature of the phase transition in a scalar theory. *Phys. Rev. D*, 86:085031, Oct 2012.

[208] Jean-Paul Blaizot, Edmond Iancu, and Anton Rebhan. Entropy of the qcd plasma. *Phys. Rev. Lett.*, 83:2906–2909, Oct 1999.

[209] Jean-Paul Blaizot, Edmond Iancu, and Anton Rebhan. Approximately self-consistent resummations for the thermodynamics of the quark gluon plasma. 1. Entropy and density. *Phys. Rev. D*, 63:065003, 2001.

[210] Eric Braaten and Emmanuel Petitgirard. Solution to the three loop Phi derivable approximation for massless scalar thermodynamics. *Phys. Rev. D*, 65:085039, 2002.

[211] Gert Aarts and Jose M. Martinez Resco. Transport coefficients from the 2PI effective action. *Phys. Rev. D*, 68:085009, 2003.

[212] Gert Aarts and Jose M. Martinez Resco. Shear viscosity in the O(N) model. *JHEP*, 02:061, 2004.

[213] Margaret E. Carrington and E. Kovalchuk. QED electrical conductivity using the 2PI effective action. *Phys. Rev. D*, 76:045019, 2007.

[214] Jürgen Berges, Szabolcs Borsanyi, and Christof Wetterich. Isotropization far from equilibrium. *Nucl. Phys. B*, 727:244–263, 2005.

[215] Thomas Gasenzer, Jürgen Berges, Michael G. Schmidt, and Marcos Seco. Non-perturbative dynamical many-body theory of a Bose-Einstein condensate. *Phys. Rev. A*, 72:063604, 2005.

[216] Jürgen Berges and Thomas Gasenzer. Quantum versus classical statistical dynamics of an ultracold Bose gas. *Phys. Rev. A*, 76:033604, 2007.

[217] Jürgen Berges. Controlled nonperturbative dynamics of quantum fields out-of-equilibrium. *Nucl. Phys. A*, 699:847–886, 2002.

[218] Jürgen Berges, Szabolcs Borsányi, Urko Reinosa, and Julien Serreau. Renormalized thermodynamics from the two-particle irreducible effective action. *Phys. Rev. D*, 71:105004, May 2005.

[219] Mark C. Abraao York and Guy D. Moore. 2PI resummation in 3D SU(N) Higgs theory. *JHEP*, 10:105, 2014.

[220] Jens O. Andersen and Michael Strickland. Three-loop Φ-derivable approximation in QED. *Phys. Rev. D*, 71:025011, 2005.

[221] Jean-Paul Blaizot, Edmond Iancu, and Anton Rebhan. Selfconsistent hard thermal loop thermodynamics for the quark gluon plasma. *Phys. Lett. B*, 470:181–188, 1999.

[222] Jean-Paul Blaizot, Edmond Iancu, and Anton Rebhan. Approximately self-consistent resummations for the thermodynamics of the quark-gluon plasma: Entropy and density. *Phys. Rev. D*, 63:065003, Feb 2001.

[223] Jan Ambjørn, T. Askgaard, H. Porter, and Mikhail E. Shaposhnikov. Sphaleron transitions and baryon asymmetry: A Numerical real time analysis. *Nucl. Phys. B*, 353:346–378, 1991.

[224] Arttu Rajantie, Paul M. Saffin, and Edmund J. Copeland. Electroweak pre-heating on a lattice. *Phys. Rev. D*, 63:123512, 2001.

[225] Kenneth G. Wilson. Confinement of Quarks. *Phys. Rev. D*, 10:2445–2459, 1974.

[226] John B. Kogut and Leonard Susskind. Hamiltonian Formulation of Wilson's Lattice Gauge Theories. *Phys. Rev. D*, 11:395–408, 1975.

[227] Jan Smit and Anders Tranberg. Chern-Simons number asymmetry from CP violation at electroweak tachyonic preheating. *JHEP*, 12:020, 2002.

[228] Anders Tranberg and Jan Smit. Baryon asymmetry from electroweak tachyonic preheating. *JHEP*, 11:016, 2003.

[229] Vittoria Demozzi, Andrei Linde, and Viatcheslav Mukhanov. Supercurvaton. *JCAP*, 04:013, 2011.

[230] Shun-Pei Miao, Nicholas C. Tsamis, and Richard P. Woodard. Summing inflationary logarithms in nonlinear sigma models. *JHEP*, 03:069, 2022.

[231] Iacopo Carusotto, Serena Fagnocchi, Alessio Recati, Roberto Balbinot, and Alessandro Fabbri. Numerical observation of Hawking radiation from acoustic black holes in atomic BECs. *New J. Phys.*, 10:103001, 2008.